EXPERIMENTAL INVESTIGATIONS ON DI CI ENGINE USING MIXED CULTURE MICROALGAE BIOMASS AS AN ADDITIVE IN COCONUT AND KARANJA BIODIESEL FUELS

Submitted in partial fulfillment of the requirements
for the award of the degree of

DOCTOR OF PHILOSOPHY

in

MECHANICAL ENGINEERING

by

Mr. KATAM GANESH BABU

(Roll No. 701413)

Under the Supervision of

Dr. A. VEERESH BABU

Associate Professor

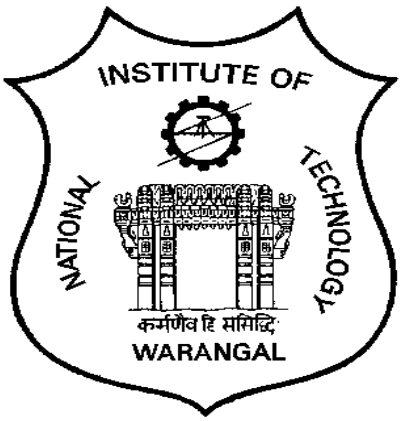

DEPARTMENT OF MECHANICAL ENGINEERING

NATIONAL INSTITUTE OF TECHNOLOGY

WARANGAL-506 004, TELANGANA,

INDIA

JUNE 2019

Dedicated
To
My Parents
&
Friends

NATIONAL INSTITUTE OF TECHNOLOGY
WARANGAL

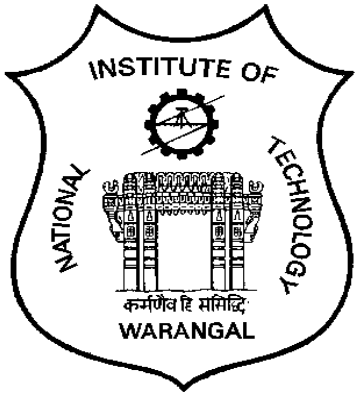

CERTIFICATE

This is to certify that the thesis entitled "**Experimental Investigations on DI CI Engine using Mixed Culture Microalgae Biomass as an Additive in Coconut and Karanja Biodiesel Fuels"** being submitted by **Katam Ganesh Babu** for the award of the degree of Doctor of Philosophy in Mechanical Engineering to the National Institute of Technology, Warangal, India is a record of the bonafide research work carried out by him under my supervision. The thesis has fulfilled the requirements according to the regulations of this Institute and in my opinion has reached the standards for submission. The results embodied in the thesis have not been submitted to any other University or Institute for the award of any degree or diploma.

Date:

Dr. A. Veeresh Babu
Associate Professor
Department of Mechanical Engg.,
National Institute of Technology,
Warangal.

DECLARATION

This is to certify that the work presented in the thesis entitled **"Experimental Investigations on DI CI Engine using Mixed Culture Microalgae Biomass as an Additive in Coconut and Karanja Biodiesel Fuels"** is a bonafide work done by me under the supervision of **Dr. A. Veeresh Babu**, Associate professor, Department of Mechanical Engineering and was not submitted elsewhere for award of any degree.

I declare that this written submission represents my ideas in my own words and where others ideas or words have not been included I have adequately cited and referenced the sources. I also declare that I have adhered to all principles of academic honesty and integrity and have not misrepresented or fabricated or falsified any idea/data/fact/source in my submission. I understand that any violation of the above will be a cause for disciplinary action by the Institute and can also evoke a penal response from the sources which have thus not been appropriately cited or from whom proper permission has not been taken when needed.

Date:

Place: NIT Warangal

Katam Ganesh Babu

Roll No. 701413

ACKNOWLEDGEMENT

It is my pleasure to give my heartfelt thanks to my supervisor **Dr. A. Veeresh Babu** because he cultivated a research attitude in my mind for applying learning approach in my research as well as in the individual life. His important thoughts are given me immense support to complete my research work. His positive and daring attitude in different aspects trained me to handle the situations with enthusiasm. His suggestions helped a lot to make myself stronger in all differing circumstances. His brilliant support made me to sustain and develop knowledge and be close to my home life.

I wish to sincerely thank university authorities, **Prof. N.V. Ramana Rao,** Director, National Institute of Technology, Warangal and other top officials who gave me an opportunity to carry out research work.

I sincerely thank **Dr. P. Bangaru Babu,** Head, Mechanical Engineering Department, National Institute of Technology, Warangal for his continuous support towards carrying out research work.

I wish to express my sincere and wholehearted thanks and gratitude to my doctoral scrutiny committee (DSC) members **Dr. K. Madhu Murthy** Professor Department of Mechanical Engineering, **Dr. P. Ravi Kumar** Professor Department of Mechanical Engineering, **Dr. Y. Pydi Setty** Professor Chemical Engineering Department, National Institute of Technology, Warangal for their kind help, encouragement and valuable suggestions for successful completion of research work.

I express my heartfelt thanks and gratitude to my fellow research scholars **Karthikeya Sharma K, Vijay Kumar M, Ganesh S Warkhade**, and **M Vinod Babu** etc., and faculty members in NIT Warangal for their valuable support in struggles.

I am also thankful to all the supporting and technical staff of the Department of Mechanical Engineering who has directly/indirectly helped during my work. Last but not the least; I would like to thank my parents, wife and my daughter, son, who are undoubtedly the happiest to see me complete this endeavor. To them, I owe all my accomplishments.

KATAM GANESH BABU

Abstract

The global depleting fossil fuels reserves, increasing population insisted on looking into new energy sources. In India, increasing Urban ization by cause of development in the Industrial and Transportation sectors is leading to a search for new alternative sources. As observed from the literature the biofuels are the best alternative energy sources to fulfill Diesel fuel demand by reducing environmental issues.

Among all biofuels, the biodiesel was the best alternative fuel to meet Diesel fuel demand. Because of the lower maintenance cost, the Compression Ignition (CI) engines are playing a vital role in Industrial and transportation sectors. The researchers, scientists, have produced biodiesel from first, second and third generation biodiesel sources. Among all lipid sources, the Microalgae were the most quickly growing, higher oil yielding one.

The by-products while algae to biodiesel conversion process are most valuable than others. The practice of Biodiesel or Diesel in CI engines is leading to increasing NOx emissions. Among all emissions, the Oxides of Nitrogen (NOx) and Particulate Matter (PM) are the most harmful emissions to human and environment. To reduce emissions from the diesel engine, the use of additives in Diesel, biodiesel and their blends is very well practicing fuel modification technique. The higher cost of phenol, amine-based antioxidants is causing to increase CI engine operating cost.

The study involves improving the performance of Coconut oil (of high saturated fatty acids) and Karanja oil (of high unsaturated fatty acids) with the influence of additives. These oils have different physicochemical properties, eg. Coconut had higher Oxygen, Cetane number, and lower Calorific value, density than Karanja biodiesel fuel. To investigate an unmodified diesel engine characteristics, the very finely grounded mixed culture Microalgae (MCM) biomass particles emulsified in neat Coconut, Karanja biodiesel fuels. The Triton X-100 surfactant used to prepare stable blends preparation for avoiding MCM particles sedimentation. Initially, the test runs on the engine carried out by using base fuels (Diesel, neat Coconut, Karanja biodiesels), all MCM particles based blends and Lauric acid contained blends at standard operating parameters (SOPs).

The blending of MCM particles in different proportions (CB+1gAP, CB+2gAP, and CB+3gAP) in Coconut biodiesel has experimentally proved the reduction of NOx

emissions. However, about this reduction, there are two different opinions by Doctoral scrutiny committee (DSC) members. Firstly, this could be because of the presence of Lauric acid in CB, and secondly, this could be because of MCM particles blending in the same biodiesel. Therefore, the author has selected KB, which is free from Lauric acid composition. The author experimented with different proportions of Lauric acid, and MCM particles separately in KB fuel.

The Kinematic viscosity of biodiesel blends increases with either the increase in MCM particles addition or with Lauric acid volume. The author has observed an increase in Brake thermal efficiency by cause of the multilevel micro-explosion of MCM particles. The reduction in NOx emissions is due to the absorption of heat by MCM particles from the combustion chamber. The properties described above are influenced to increase CO, HC, and Smoke emissions though there was an increase in BTE and decrease in NOx emissions than CB, KB fuels.

To overcome the above issues as per the literature is concerned the increase in injection pressure was the predominantly influencing factor. In the final stage of the experimental investigation, the author applied 190, 210, 230 and 250 bar injection pressures on each fuel. In this approach, the increase in brake thermal efficiency, NOx emissions, and the decrease in CO, HC, and smoke emissions have observed. Finally, the reduction in NOx emissions has observed with blends of Lauric acid in KB than MCM particles contained blends, but there was a reduction in Brake thermal efficiency.

At engine, SOPs 3.28% higher ICP (In-cylinder pressure) observed with CB+3gAP blend than KB+3gAP blend. The 28.02, 26.32% highest BTE observed with CB+1gAP blend (@ 250 bar IP) and KB+1gAP blend (@ 210 bar IP) respectively. The highest 14.2% NOx emissions reduction observed with KB+30gLA blend at 210 bar IP. The present investigation revealed that the lower level (1g) addition of MCM particles is improved the engine performance with a slight penalty in NOx emissions. The higher level addition (3g) of MCM particles has reduced NOx emissions with a slight compromise in performance. Overall the MCM particles blends have attained more performance than Lauric acid blends.

Keywords: Biodiesel, blend, compression ratio, combustion, diesel, engine, emissions, injection pressure, microalgae, performance.

TABLE OF CONTENTS

ABSTRACT I

TABLE OF CONTENTS III

LIST OF FIGURES VII

LIST OF TABLES X

NOMENCLATURE XI

CHAPTER 1 1

INTRODUCTION 1

1.1 GENERAL 1

1.2 AVAILABILITY OF FEEDSTOCK'S FOR BIODIESEL PRODUCTION 2

1.3 IMPORTANCE OF MICROALGAE FOR FUELS PRODUCTION 2

1.4 CONSIDERABLE FACTORS FOR BIODIESEL PRODUCTION 4

1.4.1 Fatty acid composition of Oils 5

1.4.2 Effect of Free Fatty Acid (FFA) percentage on Biodiesel conversion 8

1.4.3 Effect of Molar ratio on Biodiesel conversion 8

1.4.4 Effect of type Catalyst on biodiesel conversion 9

1.5 EFFECT OF MICROALGAE ON DIESEL ENGINE OPERATION 10

1.6 THE AIM OF PRESENT WORK 12

1.7 ORGANIZATION OF THESIS 13

CHAPTER 2 15

LITERATURE REVIEW 15

2.1 GENERAL 15

2.2 THEORY ON DIESEL ENGINES 15

2.2.1 Working of DI & IDI CI engines: 16

2.2.2 Working of 2-stroke DI CI engine: 16

2.2.3 Working of 4-stroke DI CI engine: 17

2.3 COMBUSTION PROCESS IN COMPRESSION IGNITION ENGINES: 18

2.4 EFFECT OF OPERATING PARAMETERS ON ENGINE CHARACTERISTICS: 19

2.5 EFFECT OF BIODIESEL COMPOSITION ON ENGINE CHARACTERISTICS 22

2.6 SCOPE TO USE SOLID FUELS IN DIESEL ENGINES 24

2.6.1 Coal & Charcoal based fuels for Diesel engine operation 24

2.6.2 Carbon black based fuels for Diesel engine operation 27

2.6.3 Solid fuel from other sources to apply on Diesel engine 28

2.7 FORMATION OF NOX AND ITS REDUCTION METHODS 30

2.8 OBSERVATIONS FROM THE LITERATURE 32
2.9 OBJECTIVES AND SCOPE OF PRESENT RESEARCH WORK 33

CHAPTER 3 34

FUELS PRODUCTION, BLENDS PREPARATION AND CHARACTERIZATION 34

3.1 GENERAL 34
3.2 MATERIALS FOR BIODIESEL FUEL PRODUCTION 34
3.3 THE TITRATION TEST PROCEDURE 36
3.3.1 Base Transesterification process for Coconut Biodiesel production 37
3.3.2 Acid, base Transesterification process for Karanja Biodiesel production 39
3.3.2.1 Acid treatment for Karanja fatty esters production: 39
3.3.2.2 Base Transesterification for Karanja Biodiesel conversion 40
3.4 MCM PARTICLES PREPARATION PROCEDURE 41
3.5 PREPARATION OF MCM PARTICLES MIXED CB, KB FUELS BLENDS 43
3.6 PREPARATION OF LAURIC ACID MIXED KARANJA BIODIESEL BLENDS 44
3.7 CHARACTERIZATION OF ALL PREPARED FUELS SAMPLES 45

CHAPTER 4 47

EXPERIMENTAL SETUP AND METHODOLOGY 47

4.1 GENERAL 47
4.2 TEST SETUP AND ITS SPECIFICATIONS 47
4.3 SPECIFICATIONS OF DATA LOGGING INSTRUMENTS 49
4.4 SPECIFICATIONS OF EMISSION ANALYZERS 53
4.5 EXPERIMENTAL METHODOLOGY 54
4.1.1 Investigations on Base fuels 54
4.1.2 Investigations on MCM particles blended biodiesel blends 54
4.1.3 Investigations on Lauric acid blended Karanja biodiesel blends 55
4.6 METHOD APPLIED TO VARY NOZZLE OPENING PRESSURE 55

CHAPTER 5 56

RESULTS AND DISCUSSIONS 56

5.1 GENERAL 56

MODULE - 1 58

5.2 COMBUSTION ANALYSIS ON ALL FUELS AT SOPS, 100% LOAD 58
5.2.1 In cylinder pressure (bar) vs. Crank angle (Θ) 58
5.2.2 Cumulative Heat Release (kJ) vs. Crank angle (Θ) 60
5.2.3 Net heat release rate (J/Θ) vs. Crank angle (Θ) 62

5.2.4 Rate of Pressure Rise (dP/dΘ) vs. Crank angle (Θ): 64

5.3 PERFORMANCE ANALYSIS ON ALL FUELS AT SOPS, BY LOAD VARIATION 66

5.3.1 Brake thermal efficiency (%) vs. % Full load 66

5.3.2 Brake specific Energy consumption (MJ/kW-hr) vs. % Full load 68

5.3.3 The Exhaust Gas Temperature (˚C) vs. % Full load 70

5.4 EMISSIONS ANALYSIS ON ALL FUELS AT SOPS, BY LOAD VARIATION 72

5.4.1 Carbon monoxide (% vol) vs. % Full load 72

5.4.2 Unburned Hydrocarbons (ppm) vs. % Full load 74

5.4.3 Oxides of Nitrogen (ppm) vs. % Full load 76

5.4.4 Smoke opacity (%) vs. % Full load 78

MODULE - 2 80

5.5 COMBUSTION ANALYSIS ON CB+MCM BLENDS @ FULL LOAD, 17.5 CR, 1500RPM 80

5.5.1 In cylinder pressure (bar) vs. Crank angle (Θ), IP 80

5.5.2 Cumulative Heat Release (kJ) vs. Crank angle (Θ), IP 83

5.5.3 Net heat release rate (J/Θ) vs. Crank angle (Θ), IP 85

5.5.4 Rate of Pressure Rise vs. Crank angle (Θ), IP 87

5.6 PERFORMANCE ANALYSIS ON CB+MCM BLENDS@ % FULL LOAD, 17.5 CR, 1500RPM 89

5.6.1 Brake thermal efficiency (%) vs. % Full load, IP 89

5.6.2 BSEC (MJ/kW-hr) vs. % Full load, IP 91

5.6.3 Exhaust gas temperature (ºC) vs. % Full load, IP 91

5.7 THE EMISSIONS ANALYSIS VS. % FULL LOAD, IP ON CB+MCM BLENDS @ 17.5 CR, 1500RPM 94

5.7.1 Carbon monoxide (% vol) vs. % Full load, IP 94

5.7.2 Unburned Hydrocarbons (ppm) vs. % Full load, IP 96

5.7.3 Oxides of Nitrogen (ppm) vs. % Full load, IP 98

5.7.4 Smoke opacity (%) vs. % Full load, IP 100

MODULE - 3 102

5.8 COMBUSTION ANALYSIS ON KB+LA BLENDS @ FULL LOAD, 17.5 CR, 1500 RPM 102

5.8.1 Incylinder pressure (bar) vs. Crank angle (Θ), IP 102

5.8.2 Cumulative heat release (kJ)vs. Crank angle (Θ), IP 104

5.8.3 Net heat release rate (J/Θ) vs. Crank angle (Θ), IP 106

5.8.4 Rate of pressure rise (dp/dΘ) vs. Crank angle (Θ), IP 108

5.9 PERFORMANCE ANALYSIS ON KB+LA BLENDS @ % FULL LOAD, 17.5 CR, 1500 RPM 110

5.9.1 Brake thermal efficiency (%) vs. % Full load, IP 110

5.9.2 BSEC (MJ/kW-hr) vs. % Full load, IP 110

5.9.3 Exhaust gas temperature (ºC) vs. % Full load, IP 113

5.10 EMISSION ANALYSIS VS. % FULL LOAD, IP ON KB+LA BLENDS @ 17.5 CR, 1500RPM 115

5.10.1 Carbon monoxide (% vol) vs. % Full load, IP 115

5.10.2 Unburned Hydrocarbons (ppm) vs. % Full load, IP *117*

5.10.3 Oxides of Nitrogen (ppm) vs. % Full load & IP *119*

5.10.4 Smoke opacity (%) vs. % Full load, IP *121*

MODULE - 4 **123**

5.11 COMBUSTION ANALYSIS ON KB+MCM BLENDS @ FULL LOAD, 17.5 CR, 1500RPM 123

5.11.1 Incylinder pressure (bar) vs. Crank angle (Ɵ), IP *123*

5.11.2 Cumulative heat release (kJ) vs. Crank angle (Ɵ), IP *125*

5.11.3 Net heat release rate (J/Ɵ) vs. Crank angle (Ɵ), IP *127*

5.11.4 Rate of pressure rise (dp/dƟ) vs. Crank angle (Ɵ), IP *129*

5.12 PERFORMANCE ANALYSIS ON KB+MCM BLENDS @ % LOAD, 17.5 CR, 1500 RPM 131

5.12.1 Brake thermal efficiency (%) vs. % Full load, IP *131*

5.12.2 Brake specific Energy consumption (MJ/kW-hr) vs. % Full load, IP *133*

5.12.3 Exhaust gas temperature (ºC) vs. % Full load, IP *135*

5.13 EMISSION ANALYSIS ON KB+MCM BLENDS @ % FULL LOAD, 17.5 CR, 1500RPM 137

5.13.1 Carbon monoxide (% vol) vs. % Full load, IP *137*

5.13.2 Unburned Hydrocarbons (ppm) vs. % Full load, IP *139*

5.13.3 Oxides of Nitrogen (ppm) vs. % Full load, IP *141*

5.13.4 Smoke opacity (%) vs. % Full load, IP *143*

CHAPTER 6 **145**

CONCLUSIONS **145**

6.1 GENERAL 145

6.2 THE EFFECT OF MCM PARTICLES ON ENGINE CHARACTERISTICS @ 100% LOAD, SOPS 145

6.3 THE EFFECT OF IP ON ENGINE CHARACTERISTICS WITH CB+MCM, KB+MCM BLENDS @ 100% LOAD, 17.5 CR, & 1500 RPM 146

6.4 THE EFFECT OF LAURIC ACID ON ENGINE CHARACTERISTICS @ 100% LOAD & SOPS 148

6.5 OVERALL CONCLUSIONS 148

6.6 THE SCOPE OF FUTURE WORK 149

6.7 LIST OF PUBLICATIONS 149

6.8 REFERENCES: 151

APPENDIX – A **170**

UNCERTAINTY ANALYSIS OF INSTRUMENTS USED IN EXPERIMENTAL SETUP: 170

DETERMINED PHYSICOCHEMICAL PROPERTIES OF DIESEL FUEL: 171

APPENDIX – B **172**

SAMPLE PERFORMANCE CALCULATIONS ON DIESEL FUEL AT FULL LOAD OPERATION: 172

LIST OF FIGURES

Figure 1.1 Stepwise reactions in the Biodiesel conversion process 4

Figure 2.1 Working DI and IDI Compression Ignition engine 16

Figure 2.2 Working of 2-stroke DI CI engine 17

Figure 2.3 Working of 4-stroke DI CI engine 18

Figure 2.4 Stages of combustion in DI CI engine 18

Figure 2.5 Variation of NOx with flame temperature and excess O_2. 32

Figure 3.1 Flow diagram for two step Transesterification process 35

Figure 3.2 Titration setup 36

Figure 3.3 Methoxide preparation 37

Figure 3.4 Reactor for biodiesel conversion 38

Figure 3.5 Settledbiodiesel sample in a separating funnel 38

Figure 3.6 Unprocessed and processed CB in beakers 38

Figure 3.8 Esterification of Karanja oil in a reactor 39

Figure 3.9 Settled Karanja esters in a separating funnel 40

Figure 3.10 Harvested mixed culture Microalgae biomass 41

Figure 3.11 Coarse size MCM particles 42

Figure 3.12 Stepwise procedure for MCM particles preparation 42

Figure 3.13 Mechanical blending machineforblends preparation 43

Figure 3.14 MCM particles blended CBfuel blends 43

Figure 3.15 MCM particles blendedCBKB fuel blends 43

Figure 3.16 Lauric acid (LA) and LA blends preparation setup 44

Figure 3.17 Lauric acid blended KB fuel blends 45

Figure 4.1 Test engine setup schematic diagram 48

Figure 4.3 Photographic view of the emission analyzers 53

Figure 4.4 Photographic view of fuel injector 55

Figure 5.1 Combustion phenomena of a MCM particle in engine cylinder 57

Figure 5.2$_{a, b, c, \& d}$ ICP (bar)vs. Crank angle (θ) of all fuels @ SOPs 59

Figure 5.3$_{a, b, c, \& d}$ CHR vs. Crank angle(θ) of all fuels @ SOPs 61

Figure 5.4$_{a, b, c, \& d}$ NHRR vs. Crank angle(θ) of all fuels @ SOPs 63

Figure 5.5$_{a, b, c, \& d}$ RPR vs. Crank angle (θ)of all fuels @ SOPs 65

Figure 5.6$_{a, b, c, \& d}$ BTE vs. % Full load of all fuels @ SOPs 67

Figure 5.7$_{a, b, c, \& d}$ BSEC vs. % Full load of KB+AP blends @ SOPs 69

Figure 5.8$_{a, b, c, \& d}$ EGT vs. % Full load of KB+AP blends @ SOPs 71

Figure 5.9$_{a, b, c, \& d}$ CO vs. % Full load of KB+AP blends @ SOPs 73

Figure 5.10$_{a, b, c, \& d}$ HCvs. % Full load of KB+AP blends @ SOPs 75

Figure5.11$_{a, b, c, \& d}$ NOx vs. % Full load of KB+AP blends @ SOPs 77

Figure 5.12$_{a, b, c, \& d}$ Smoke opacity vs. % Full load of KB+AP blends @ SOPs 79

Figure 5.13$_{a, b, c}$ ICP vs.Crank angle (θ)& IP of CB+MCM blends 82

Figure 5.14$_{a, b, c}$ CHR vs. Crank angle (θ) & IP of CB+MCM blends 84

Figure 5.15$_{a, b, c}$ NHRRvs.Crank angle (θ) & IP of CB+MCM blends 86

Figure 5.16$_{a, b, c}$ RPR vs.Crank angle (θ) & IP of CB+MCM blends 88

Figure 5.17 $_{a, b, c}$ BTE vs. % Full load& IP of CB+MCM blends 90

Figure 5.18$_{a, b, c}$ BSEC vs. % Full load, IP of CB+MCMblends 92

Figure 5.19$_{a, b, c}$ EGT vs. % Full load& IP of CB+MCM blends 93

Figure 5.20$_{a, b, c}$ CO vs. % Full load& IP of CB+MCM blends 95

Figure 5.21$_{a, b, c}$ HC vs. % Full load&IP of CB+MCM blends 97

Figure 5.22$_{a, b, c}$ NOx vs. % Full load& IP of CB+MCM blends 99

Figure 5.23$_{a, b, c}$ Smoke opacity (%) vs. % Full load& IP of CB+MCM blends 101

Figure5.24$_{a, b, c}$ ICP (bar) vs. Crank angle (Ɵ)&IP of KB+LAblends 103

Figure 5.25$_{a, b, c}$ CHR (kJ) vs. Crank angle (Ɵ)&IP of KB+LAblends 105

Figure 5.26$_{a, b, c}$ NHRR (J/Ɵ) vs. Crank angle (Ɵ), &IPof KB+LBblends 107

Figure 5.27$_{a, b, c}$ RPR (dP/dƟ) vs. Crank angle (Ɵ)&IPof KB+LAblends 109

Figure5.28$_{a, b, c}$ BTE (%) vs. % Full load&IP of KB+LA blends 111

Figure5.29$_{a, b, c}$ BSEC (MJ/kW-hr) vs. % Full load& IP of KB+LA blends 112

Figure5.30$_{a, b, c}$ EGT (°C) vs.% Full load& IP of KB+LA blends 114

Figure5.31$_{a, b, c}$ CO (%) vs. % Full load& IP of KB+LA blends 116

Figure5.32$_{a, b, c}$ HC(ppm) vs.% Full load& IP of KB+LA blends 118

Figure 5.33$_{a, b, c}$ NO_x (ppm) vs.% Full load& IP of KB+LA blends 120

Figure 5.34$_{a, b, c}$ Smoke opacity (%) vs. % Full load& IP of KB+LA blends 122

Figure 5.35$_{a, b, c}$ ICP (bar) vs. Crank angle (Ɵ)&IP of KB+MCMblends 124

Figure 5.36$_{a, b, c}$ CHR (kJ) vs. Crank angle (Ɵ)&IPof KB+MCMblends 126

Figure 5.37$_{a, b, c}$ NHRR (J/Ɵ) vs. Crank angle (Ɵ)&IPof KB+MCM blends 128

Figure 5.38$_{a, b, c}$ RPR (dP/dƟ) vs. Crank angle (Ɵ)&IPof KB+MCM blends 130

Figure 5.39$_{a, b, c}$ BTE (%) vs.% Full load&IP of KB+MCMblends 132

Figure 5.41$_{a, b, c}$ EGT (°C) vs.% Full load& IP of KB+MCM blends 136

Figure 5.42$_{a, b, c}$ CO (% vol) vs. % Full load&IPof KB+MCM blends 138

Figure 5.43$_{a, b, c}$ HC (ppm) vs.% Full load& IP of KB+MCM blends 140

Figure 5.44$_{a, b, c}$ NO_x (ppm) vs.% Full load& IP of KB+MCM blends 142

Figure 5.45$_{a, b, c}$ Smoke opacity (%) vs. % Full load& IP of KB+MCM blends 144

LIST OF TABLES

Table No	Title
Table 1.1	Comparison of Algal oil yield with some edible, inedible & waste oils
Table 1.2	Comparison of Algal oils fatty acid composition (wt. %) with other oils
Table 1.3	Advantages, disadvantages of widely using catalysts in biodiesel sector
Table 1.4	Comparison of Algal biodiesel physicochemical properties with other
Table 2.1	Comparison of Algal biodiesel (FAME) compositions (wt. %) with other
Table 3.1	Determined Acid values and FFA percentage of Coconut, Karanja oils
Table 3.2	Optimal parametric values to produce KB & CB fuels
Table 3.3	Physicochemical properties of pure form of Lauric acid
Table 3.4	Physicochemical properties of all prepared fuel samples
Table 4.1	Specifications of test engine
Table 4.2	Data logging instruments and their specifications
Table 4.3	Specifications of emissions analyzers
Table 4.4	Configurations of MCM particles blended CB, and KB fuels
Table 4.5	Configurations of Lauric acid blended KB fuel blends

NOMENCLATURE

SYMBOL	DESCRIPTION	UNIT
aTDC	After top dead center	°θ
BSEC	Brake specific energy consumption	MJ/kW-hr
BSFC	Brake specific fuel consumption	Kg/kW-hr
bTDC	Before top dead center	°θ
CA	Crank angle	θ
CB	Coconut biodiesel	-
CHR	Cumulative heat release	kJ
CI	Compression Ignition	-
CO	Carbon monoxide	% vol
CO_2	Carbon dioxide	% vol
CR	Compression ratio	-
DAS	Data acquisition system	kS/s
DI	Direct injection	-
DPF	Diesel particulate filter	-
EGR	Exhaust gas temperature	°C
FAME	Fatty acid methyl ester	-
FFA	Free fatty acid	-
GC FID	Gas chromatography Flame Ionization Detector	-
HC	Unburned Hydrocarbons	ppm
HPLC	High pressure liquid chromatography	-
ICP	In-cylinder pressure	bar
ID	Ignition delay	θ
IDI	Indirect injection	-
IEA	International energy agency	-
KB	Karanja biodiesel	-
LA	Lauric acid	-
MCM/AP	Mixed culture Microalgae	-
NHRR	Net heat release rate	J/θ
NOx	Oxides of Nitrogen	ppm
PCM	Phase change materials	-
PM	Particulate matter	%
Rpm	Revolutions per minute	-
RPR	Rate of pressure rise	bar/θ

CHAPTER 1

Introduction

1.1 General

Globally about 52.5 % of the population lives in urban areas that too in 2050 this may increase by 70%[1]. The 62% oil, 76% coal, and 82% natural gases consumption is mostly from major cities in the world, that to fossil oil sources are majorly using for urban transportation. The population rise in urban areas led to increasing energy demand and leaving the CO_2 footprints into the global environment. The green and sustainability are not possible with Wind, solar and tidal energies by cause of their disadvantages such as low potential, high cost, and technological shortcomings. The primary objective of converting residual agricultural biomass into liquid biofuels is to reduce greenhouse gasses in the environment.

The biomass production involves land, pesticides and time as inputs. However, the emissions from biomass sources are much lower than fossil fuel sources, but they require the tradeoff between Oxides of Nitrogen (NOx) and particulate matter (PM) emissions[2]. The Biofuels broadly classified as Primary and secondary. The primary biofuels such as wood, pellets, and wood chips, are using in unprocessed form majorly for cooking, heating, and power generation purposes.

The secondary biofuels are converting by processing of waste agriculture biomass, into bioethanol, biodiesel, dimethyl and diethyl ethers to utilize in vehicles and industrial applications. The secondary biofuels further divided into three types of first, second and third generation. The first generation is from edible, second from inedible and third is from microorganisms and waste sources[3].

In the case of secondary biofuels, the biodiesel was playing the primary role in the transportation sector to run Diesel engines. The biodiesel considered as ‘‘carbon neutral’’ fuel as it is emitted Carbon dioxide by its combustion in Diesel engine was earlier captured from the environment during its cultivation[4]. The research on Compression Ignition (CI) engines started in the early 18th century. The CI engines are yielding higher efficiency, durability, superior fuel economy and lower maintenance than Spark Ignition (SI) engines. Due to the above reasons almost in all the sectors, these are playing a vital role in light, medium, and heavy-duty applications[5,6]. However, the Diesel engines are emitting the most harmful emissions than Spark

Ignition engines, such as NOx and PM. In general, the in-cylinder and after treatment techniques widely used for diesel engine emissions reduction. In that, Fuel modification, Exhaust Gas Recirculation (EGR), Selective Catalytic Reduction (SCR) converter and Diesel Particulate Filter (DPF) are the most used methods[7].

Among all the above techniques, fuel modification was widely using in-cylinder treatment method to reduce Diesel engine emissions. This approach need not require any engine modifications but may increase the engine operational cost by cause of their high price[8].

1.2 Availability of feedstock's for Biodiesel production

Based on the global statistics, in the year 2017. The United States, Brazil (6, 4.3 billion liters) are the world largest biodiesel producers. By 2025 United states targetted to produce 1 billion gallons to become the world largest producer [9]. The oils sources for biodiesel production categorized as lipid feedstocks and alcohol feedstocks. The lipid feedstocks are vegetable oils, animal fats, and microorganisms like microalgae and Cyanobacteria, usage of any feedstock for biodiesel conversion purely based on their availability.

The Rapeseed oil is widely using in Canada, European countries, Soybean in the United States, Palm in tropical countries like Indonesia and Malaysia, Coconut in a coastal country like the Philippines and Karanja, Jatropha in India[10]. World biodiesel production almost 95% of cases, from edible oil sources such as Rapeseed (84%), Sunflowers (13%), Palm oil (1%) and others (2%). Edible oils are creating food vs. fuel problems and require pesticides during cultivation even though cheaper and readily available[11]. The most viable feedstock's from inedible sources are Jatropha, Karanja, Linseed, and Mahua, but some of them are having higher FFA content[12]. In the year 2012, the Planning Commission of India was tried to fulfill 288 MT of Diesel demand by cultivating and converting biodiesel from Jatropha, Karanja oils[13].

1.3 Importance of Microalgae for fuels production

The First- and second-generation biofuel resources have been insufficient to fulfill immediate biodiesel demand. Biomass production using algae has mostly been for CO_2 fixation, wastewater treatment and to produce co-products such as bio-fertilizers, biopolymers while producing biodiesel. The prices ($52-91) of biofuels from algae sources are higher than those of plant-based bioethanol and biodiesel fuels.

However, it has emerged as a more advantageous energy source than wheat or sugar-beet-based European bioethanol[14].

Based on the source of energy to cultivate microalgae its metabolisms divided into four type's photoautotrophic, heterotrophic, mixotrophic and photo-heterotrophic[15]. The input energies for photoautotroph, heterotrophic, mixotrophic and photo-heterotrophic metabolisms are light, organic compounds, both and organic compounds as well as carbon dioxide respectively[16]. To cultivate photo-heterotrophic metabolism microalgae light is the necessary source for organic compounds consumption[17].

Among all high microalgae metabolisms, photoautotroph is widely using because of light only the source for its cultivation[18]. There is a possibility to produce Renewable fuels from microalgae such as biodiesel, bio-hydrogen, and methane[19]. The Microalgae is the best feedstock for biodiesel conversion due to its growth rate, oil yield, fatty acid composition, and co-products[20]. The Open pond, closed bioreactor, and hybrid are the available methods to produce microalgae in large scale. The open pond, closed bioreactor methods are not appropriate for the genetic engineering approach[21].

To cultivate microalgae light plays an essential role in CO_2 fixation and its growth control. Its productive growth mainly depends on an adequate supply of light, carbon, nitrogen, phosphorus, and micronutrients (manganese, cobalt, sulfur, iron, et cetera)[22,23]. There is an urge for technological developments in commercial scale biofuels production from Microalgae on Cultivation (photo-bioreactors), harvesting (methods), drying (energy consumption), extraction (cell rupture) and conversion (Transesterification)processes[24]. Thorough satellite view 467lakhs of hectares are available wasteland identified in India, but this estimated around 3166lakhs of hectares[25].

It can grow in an environment which is not suitable for other feedstocks such as pure or saline water and fertile or forest lands[26]. The insufficiency of fresh water in India, the cultivation of Microalgae in seawater was the considerable approach[27]. The country like India can put particular attention on biodiesel production from Microalgae by considering the availability of vast wastelands, saline water because of 7500km of the coastal area. India can become self-sustain by utilizing 2-3% of available land for Microalgae cultivation[28].

The microalgae yield 5t/ha per year under full environmental conditions by open ponds, but we can achieve 50-300 t/ha by using photo bioreactor[29]. By changing its composition in growth level, it can yield 25 times more oil than other feed stocks[30]. The FFA value of most Microalgae lipids around 70 wt. percentage based on their storage conditions. It was creating the necessity to adopt Acid (esterification), base (Transesterification) catalyzed Transesterification or advanced processes for Microalgae biodiesel conversion[31].

1.4 Considerable factors for biodiesel production

The higher kinematic viscosity, polyunsaturated characteristics and lower volatility of raw vegetable oils are unacceptable to use in Compression Ignition engines. To overcome the above problem the researchers, scientists are applied many methods like pyrolysis, direct dilution, microemulsion, and Transesterification. Among all the above methods direct dilution, the microemulsion is not preferable due to their higher viscosity and volatility due to the presence of triglycerides in raw oil even process may be simple. The Transesterification is the best and suitable process to convert biodiesel by reducing viscosity, increase volatility by removing Glycerol from Raw oil[32].

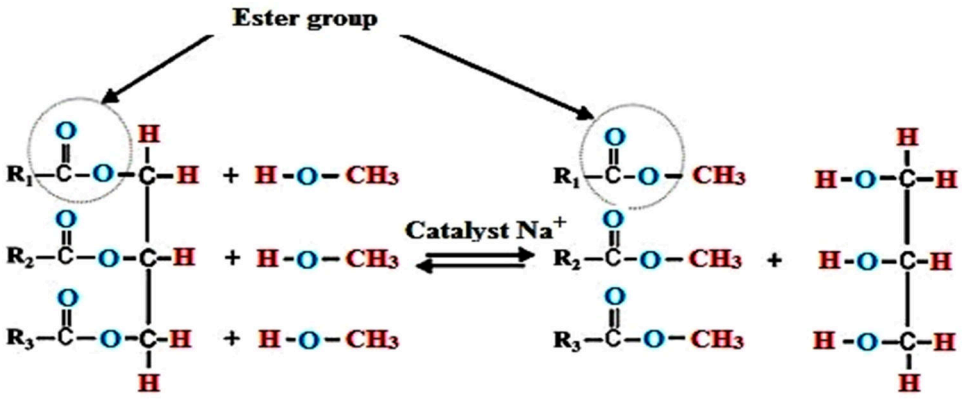

Figure 1.1 Stepwise reactions in the Biodiesel conversion process

The biodiesel fuels are converting from oils/fats by reacting with alcohols such as Methanol, Ethanol, and Butenol in the presence of catalysts usually strong bases, such as Sodium Hydroxide (NaOH) or Potassium Hydroxide (KOH)[33]. As per the literature, more than 350 oil-carrying crops found to produce biodiesel fuels. The cheapest higher oil-bearing plants can reduce 70 - 80 percent of the total biodiesel production cost and also yields higher oil[34]. The biodiesel production cost can be reduced possibly by choosing the better type of catalyst, alcohol to oil molar ratios, optimal reaction temperatures and the fair percentage of free fatty acid content[35].

Table 1.1 Comparison of Algal oil yield with some edible, inedible & waste oils.

Oil source	Feedstock	Oil yield (wt. %)	Oil yield (L/Ha)
Edible	**Coconut**	**63-65**	**2689**
	Palm	30–60	5950
	Groundnut	45-55	1059
	Rapeseed	38-46	1190
	Linseed	40-44	-
	Sunflower	25-35	952
Inedible	**Pongamia pinnata or Karanja**	**30-40**	**225-2250**
	Jatropha carcus	35-40	1892
	Castor	53	1413
	Sea mango	54	-
	Neem	40-50	-
	Mahua	35-42	-
Algal group	**Microalgae Species**	**30-70**	**58,700–36,900**
		Dry wt. %	
Green algae	Botryococcus braunii	25–75	-
	Chlorella Vulgaris	46	-
Heterotrophic	Chlorella protothecoides	55	-
Eustigmatophytes	Nannochloropsis oculata	31–68	-
Wild	**Mixed culture microalgae**	**26.2±06**	**-**

References: [11,36–40].

1.4.1 Fatty acid composition of Oils

The Oils and Fats are essential nutritional substances, metabolites for living organisms as primary energy sources of the body. The Oils are liquid at room temperature due to their lower melting point, but Fats are partially solid at room temperature by cause of their higher melting points. The fats or oils divided into triglycerides, phospholipids, and sterols. The Glycerol found in any Oil or Fat are

mixtures of the alcohol glycerol with various fatty acids. The fatty acids are chain compounds and bonded on to the glycerol. The type of bond between glycerol and fatty acids are influences the compound reactivity and sensitivity of the fat to rancidity. Complex Organic compounds, for example, glyceride is liable to compound changes, and this might be a part by hydrolysis into glycerol and free unattached fatty acids. In general, Fatty Acids (FA) are the constituents of oils or fats. These determined from various chemical analyses, which give specific values such as the Acid value, Saponification value, iodine value, hydroxyl value, and etcetera.

These represented in the form or RCOOH, where R is the Carbon chain. These are composed of Carboxylic acids that are aliphatic and commonly linear, and monocarboxylic acids with long hydrocarbon chains[41].To determine specific saturated or unsaturated fatty acids in any Oil or fat, the gas-liquid chromatography (GLC) is the widely used method. This method is the most informative and accurate technique for specific fatty acid analysis. The Mass spectrometry coupled with Gas Chromatography analysis is the method to know the specific fatty acid of any oil or fat in mass percentage.

The Infrared, Raman spectroscopy's are the most used techniques to detect trans, cis, and isomers of unsaturated fatty acids. Similarly to detect conjugated double bonds in any oil or fat can be determined by Ultra Violet (UV) spectroscopy at 200–400 nm[42].Based on the level of composition fatty acids classified into Saturated and Unsaturated. The saturated fatty acids should not contain double bond along their chain length, but unsaturated fatty acids should contain at least one double bond.

If fatty acid contains one double bond, it's called Monounsaturated fatty acids (MUFA)and more than one double bond as polyunsaturated fatty acids (PUFA) [43]. The previously mentioned fatty acids divided according to their Carbon chain length four types such as short, medium, long and very long. The chain lengths contain even number of carbon atoms are mainly present in lipids of Vegetables and Animals fats.

The 2-4 carbon atoms in a fatty acid chain as short, 6–10 carbon atoms are the medium chain, 12–20 carbon atoms are the long chain and greater than 22 carbon atoms are very long chain[44]. The biodiesel reaction rate increases as the level of unsaturation increase but decrease with the degree of saturation. The optimal reaction temperature increases with an increase in average chain length and decreases when poly-unsaturation bonds decrease[45].

Table 1.2 Comparison of Algal oils fatty acid composition (wt. %) with other oils

Group		Oil	14:0	16:0	18:0	20:0	16:1	18:1	18:2	18:3	Other	Ref.
Edible		Coconut	18	9	3	-	-	6	2	-	A	[46]
		Palm	1	45	4	-	-	39	11	-	-	
		Peanut	0.04	11.2	4.75	1.6	0.1	43.5	35.9	0.04	B	[47]
		Canola	-	4	2	-	-	61	22	10	C	[46]
		Linseed	0.1	6.21	5.63	0.4	-	20.2	14.9	51.2	D	[48]
		Sunflower	-	6	5	1	-	29	58	1	-	[46]
Inedible		Jatropha	3	13.4	3.6	-	-	51.2	28.8	-	-	[49]
		Karanja	-	13.8	6.1	-	-	65.3	11.6	3.2	-	[50]
		Castor	-	1.1	3.1	-	-	4.9	1.3	-	E	[51]
		Neem	-	17.8	16.5	2.4	-	51.2	11.7	-	-	[52]
		Mahua	-	24.5	22.7	1.5	-	37.0	14.3	-	-	[53]
		Sea mango	-	20.2	6.9	-	-	54.2	-	16.3	-	[34]
Waste fats, oils		Chicken fat	1	25	6	-	8	41	18	1	-	[46]
		Beef tallow	4	26	20	-	4	28	3	0	F	
		Lard	1	21.1	11.5	-	1.5	40.1	21.7	1.5	G	[54]
		Yellow grease	1.3	17.4	12.4	0.3	-	54.7	8	0.7	-	[36]
		Waste cooking oil	1	39	4.5	-	-	44.6	10.9	-	-	[50]
Algal group	I	Botryococcus braunii	-	-	4.3	-	4.8	55.7	34.2	0.2	H	[55]
		Chlorella vulgaris	2.3	18.9	0.7	0.1	9.5	19.6	11.2	22.2	I	[56]
	II	Nannochloropsis oculata	5.8	32.2	1	-	29.6	20.1	1.3	-	J	[57]
	III	Chlorella Protothecoides	-	51	2	-	-	39	7	-	K	[51]
		Mixed culture microalgae	1.4	19.3	1.2	0.2	15.1	14.8	15.6	18.1	L	[56]

I-Green algae, II-Diatom, III–Heterotrophic, NF–Not found

Other fatty acids:

A-(6:0 = 1, 8:0 = 7, 10:0 = 7, 12:0 = 47), **B-**(22:0 = 2.32, 20:1 = 0.57), **C-**(20:1 = 1),**D-**(22:0 = 0.222, 24:0 = 0.5), **E-**($18:1_{OH}$ = 89.6), **F-**(12:0 = 1, NF = 14) **G**=2.3, **H-**(17:0 = 0.8), **I-**(16:2 = 0.04, 16:3 = 6.29, 16:4 = 7.62, 20:1 = 0.91, 20:2 = 0.79, 20:4 = 0.01), **J-**(8:0 = 0.2, 12:0 = 0.4,15:0 = 0.5, 17:0 = 0.4, 20:5 = 8.3), **K=**1, **L-**(16:3 = 4.36, 16:4 = 8.94, 18:4 = 0.02, 20:1 = 0.57, 20:2 = 0.67).

1.4.2 Effect of Free Fatty Acid (FFA) percentage on Biodiesel conversion

The FFAs are nothing but fatty acids in the Oils or Fats, but these lost away from the Triglycerides (TGA). The rancidity from any Oil or Fat is an index of free fatty acids. FFA value determines to know the level of Acid value in oil. It is determining by titrating Oil against the conventional alkali catalysts Potassium Hydroxide (KOH) or Sodium Hydroxide (NaOH). The knowing of Oil acidity in percentage is to know the quantity of Alkali catalyst required to convert biodiesel[58].

The conversion of biodiesel from low quality with high free fatty acid (FFA) content is feasible even where it has a harmful effect on catalysts. The Low-quality feedstock's (FFA >1%) have adverse effects on crude biodiesel purification processes during alkaline Transesterification and may lead to Saponification problem. To resolve the above issues with low-quality feedstock's acid-base catalyzed reaction can be a solution, i.e., base Transesterification followed by esterification to bring FFA <0.5%[52].

The Enzymatic (heterogeneous) Transesterification was the most promising process for producing biodiesel from low-quality feedstock's because, by using them, no chance of soap formation and purification, washing, and neutralization problem[59]. Another advantage with enzymatic catalyst reaction can complete at lower temperatures. The presence of high FFA may cause higher reaction rates and can achieve more than 90% biodiesel conversion efficiency. However, there are two significant problems with enzymatic catalysts, one costlier and second is a requirement of more reaction time[59].

1.4.3 Effect of Molar ratio on Biodiesel conversion

The stoichiometric biodiesel reaction requires three moles of Alcohol for one mole of Triglyceride (Oil) to yield 3 moles of Alkyl ester and one mole of Glycerol. Anyhow it requires excess alcohol for higher biodiesel yield and proper phase separation of alkyl esters from Glycerol[60]. The higher biodiesel conversion efficiency with faster reaction rate can attain at higher molar ratios (Methanol to Oil). The higher Peanut Ethyl Ester (PEE) with lower Glycerol obtained at 3:1 than 6:1 molar ratio[61]. The cost and availability of Alcohols, Oils are the most critical materials to produce biodiesel economically.

The primary and secondary monohydric alcohols contained 1 to 8 carbon atoms. The researchers are using many alcohols such as Methanol, Ethanol, Propanol, Butenol,

etc. The optimum molar ratio for Ethanol Transesterification is higher than Methanol Transesterification[62]. The higher chain alcohols are not suitable for Transesterification due to steric interruption, and higher sensitivity to water contamination, than shorter chain alcohol like methanol & ethanol, because of their physicochemical advantages and higher miscibility with NaOH catalyst. The optimum alcohol to oil molar ratio is 6:1 for 98% conversion efficiency and higher biodiesel yield[63].

The too high quantity of alcohol in Transesterification process may lead to increase the reaction mixture polarity, and reduction in biodiesel yield by cause of the reverse reaction, i.e., the solubility of glycerol back to the ester[64]. The Methanolysis process may be cheaper and useful, but it is not Renewable because this derived from Fossil fuels[65]. The lower viscosity, high volatility and Oxygen content of short-chain alcohols are very much recommended to use in Diesel engines[66,67]. The reaction temperature, molar ratio in the Transesterification process ultimately depends on the type of Alcohol used. The boiling and melting points of alcohols are varying with their chain length and molecular weight. The methanolysis process is a bit faster than ethanolysis because Methanol has a lower boiling point than Ethanol even it has lower miscibility with Triglycerides[68].

1.4.4 Effect of type Catalyst on biodiesel conversion

Under normal conditions, the Transesterification reaction has no other inputs than Triglycerides and Alcohols but this reaction proceeds slowly or not at all. To speed up above the reaction the heat source as well as the catalyst is required. These catalysts divided into Alkali (base), Acidic, and Enzyme are again two kinds Homogeneous and Heterogeneous.

Table 1.3 Advantages, disadvantages of widely using catalysts in the biodiesel sector

Catalysts			Advantages	Disadvantages	Ref.
Homogeneous	**Base**	**NaOH, KOH, etc.,**	1. Highly reactive 2. Less time for reaction 3. Cost-effective 4. Benign kinetics 5. Suitable operational conditions	1. Oil FFA must be <1%. 2. Highly hygroscopic 3. Soap formation 4. Huge water wastage 5. Equipment corrosion. 6. Non-recyclable.	[69–71]

	Acid	**H_2SO_4, HCL, H_3PO_4, etc.,**	1. Insensitive to moisture & FFA in Oil 2. Avoid soap formation	2 Fewer reaction rate 3 Long time for reaction 4 Apparatus corrosion 5 High reaction temperature 6 Huge alcohol requirement	[70,71]
Heterogeneous	**Base**	**CaO, MgO, SrO, etc.,**	1. No corrosion problem 2. Environmental friendly 3. Easy separation & Reusable 4. Fewer disposal problems 5. Longer catalyst life	1. Reaction slower than Homogeneous base catalysts 2. Oil FFA must be < 1 wt% 3. Very sensitive to water & FFA 4. Soap formation 5. Complex & costlier production route 6. Expensive catalyst production	[70–73]
	Acid	**ZrO, TiO, ZnO, HPA, and Zeolites**	1. Insensitive to moisture & FFA in Oil 2. Recycle & Reuse, 3. Environment-friendly 4. Non-corrosive to Apparatus	1. Slow reaction rate & time taking 2. The higher reaction temperature & Alcohol are required 3. Weak catalytic action, Lower micro level porosity 4. Diffusion disadvantages 5. Critical & Costlier production path	[70,71]
Enzyme	**Candida Antarctica fraction B, Rhizomucor mieheilipases**		1. Insensitive to moisture & FFA in Oil 2. Avoid soap formation 3. Pollution free & Easy to purify 4. Possibility to recycle and reusable	1. Very slow reaction rate than other catalysts 2. Highly expensive 3. Highly sensitive to alcohol 4. Denaturation of enzyme	[69,71,74]

Among all homogeneous Alkali, catalysts are widely using in Laboratory and commercial scale biodiesel production. By cause of their easy availability, cheaper, and faster reaction rate though these are highly sensitive to moisture & FFA of oil.

1.5 Effect of Microalgae on Diesel engine operation

The level of unsaturation in biodiesel has no evident effect on fuel consumption or brake thermal efficiency. It causes more delayed combustion, higher NOx emissions, and combustion velocity. The fuel borne Oxygen content in biodiesel fuels are causing

to reduce Soot emissions. The lower NOx emissions can be possible with lower Hydrogen to Carbon (H/C) ratio, higher Cetane number fuels[75,76].

Table 1.4 Comparison of Algal biodiesel physicochemical properties with other

Group	FAME		Flash point (°C)	Density @ 15°C (kg/m^3)	Viscosity @ 40°C (mm^2/s)	Calorific value (MJ/kg)	Cetane number	References
Edible	Coconut		136.5	877.1	3.18	36.985	60	[49]
	Palm		188.5	879.3	4.66	39.907	55	
	Peanut		193	886.4	5.25	39.7	54	[77]
	Canola		146	882	3.6	40.1	52.9	[78]
	Linseed		161	865	4.2	40.759	48	[48]
	Sunflower		183	885.6	4.38	39.95	51.6	[77]
Inedible	Jatropha		202.5	883.3	4.81	39.839	51	[49]
	Karanja		196	898	5.46	39.15	57.9	[79]
	Castor		140	886	4.38	39.048	51	[80]
	Neem		110	900	5.5	39.89	55.31	[81]
	Mahua		127	865	5.2	36.9	51	[82]
	Sea mango		138	880	4.5	39.095	-	[83]
Waste fats,oils	Chicken fat		176	876	4.35	39.934	54.8	[84]
	Beef tallow		163	873.2	5.85	38.350	56	[85]
	Lard		159.5	873.2	5.26	39.850	59	[86]
	Yellow grease		-	872.8	5.26	39.817	62.6	[87]
	Waste cooking oil		167	884.2	4.87	39.68	55	[77]
Algal group	I	Botryococcus braunii	140	853	5.52	40.4	55.4	[88]
		Chlorella vulgaris	145	916	5.2	41.2	53	[56]
	II	Nannochloropsis oculata	-	880	4.2	39.8	55	[89]
	III	Chlorella protothecoides	115	864	5.2	41	-	[51]
	Mixed culture microalgae		140	912	4.8	37.2	49	[56]

I - Green algae, II - Diatom, III – Heterotrophic

Blended biodiesels cause low fuel economy in old and new engines because they have less Calorific value than base fuel[90]. It does not appear to make indicated mean effective pressure better, but blending may also improve combustion noise at higher loads and lower engine speeds[91]. The diesel engine was run by using fresh algal oil and observed lower NOx emissions and power outputs and also observed higher brake

Specific fuel consumption (BSFC) and greater particulate matter and CO_2emissions[92]. The slightly lower torque and power outputs found, but lower NOx and higher CO emission values noticed when the engine run with Algal methyl ester[93].

The lower BSFC, HC, CO, and Smoke, but higher NOx emissions noticed by using 10, 15 and 20% blends of algae oil methyl esters on the Single cylinder, water cooled Diesel engine[94]. The higher brake thermal efficiency and lower smoke levels were observed using the B20 blend in an unmodified diesel engine[95]. The 22° bTDC IT is the optimal one to apply B20 algal methyl ester blend. At this injection timing, brake thermal efficiency (BTE) increased, and NOx, CO and smoke emissions reduced. The highest HC reduction at standard injection 23° crank angle (CA) and NOx reduction at 21°CA were observed[96].

The blends of microalgae biodiesel have shown greater combustion characteristics than macroalgae blends. In cylinder pressure and heat release rates were increased in the case of advanced injection and decreased in retarded injection timing. At the full load condition, the combustion characteristics of micro and the macroalgae blends were the same. Finally, B10, B20 macro and microalgae mixtures were found to be better alternatives to diesel fuel[97].

The smoother combustion, lower engine torque, and higher combustion noise observed in an indirect injection (IDI) diesel engine with algae oil methyl ester. These properties can control by controlling the compression ratio and injection timing in the IDI engine[98]. Because of the increasing fuel demands and costs, researchers are trying to run diesel engines in different ways. To avoid the difficulties in biodiesel production, especially from algae the algal biomass has directly emulsified with diesel or biodiesel fuel: the lower NOx and higher CO emissions observed in a DI CI engine[99].

1.6 The aim of present work

From past few decades' researchers, scientists and engine manufacturers are striving to improve engine characteristics, especially emissions to meet stringent emission norms in different approaches. The possible approaches to improve engine characteristics are Fuel/engine side modification techniques. However, the engine side modification is costlier and skill requirement aspects[100,101]. The use of additives in fuel for diesel engine operation was the widely used fuel modification technique

because it will not require any engine modifications. The extensively using additives are CeO_2, Al_2O_3, and MgO as Oxidizers, Polymethyl Acrylate, Methyl Acetoacetate, and Poly alpha-olefin as cold flow improvers Butylated Hydroxytoluene, hydroxyanisole, and polyphenols as Antioxidant additives[102,103].

The accessibility of fuel-borne Oxygen in Biodiesel fuels is required antioxidant additives to stifle NOx formation. The Microalgae biomass could be a great alternative resource to reduce the NOx emissions from diesel engines. This because of naturally available versatile antioxidants than plant-based natural antioxidants[104].Based on the possibilities as mentioned above, an attempt made to improve the single cylinder DI CI engine characteristics by using Mixed culture microalgae (MCM) biomass as an antioxidant additive in Coconut and Karanja biodiesel fuels have been studied by varying blends (1g, 2g and 3g) and by different fuel nozzle opening pressures (190, 210 base, 230 and 250 bar).

1.7 Organization of thesis

Chapter 1 (Introduction)

This chapter explains the essential factors for the selection of vegetable oil from available feedstocks and significant factors for biodiesel preparation. Details on the Diesel engine and working of DI CI engine and combustion phenomena discussed in this chapter. The importance of microalgae in comparison with other feedstock's based on their fatty acid composition, physicochemical properties. The bottlenecks involved in microalgae biodiesel production and their usage, the possible approaches to apply microalgae on DI CI engine.

Chapter 2 (Literature review)

This chapter describes the contribution of earlier researchers who have investigated the Diesel engine by applying solid fuels, towards the development of engine characteristics. The author also made comparison and discussions on the selection of suitable vegetable oils based on their composition and properties for biodiesel production. The author also made a comparison with selected oils and their biodiesels by other available oils by their composition. To define the problem based on identified literature gaps to undertake present work by solid fuels application.

Chapter 3 (Fuels production, blends preparation and characterization)

This chapter illustrates the biodiesel fuels production procedure from selected vegetable oils (Coconut, Karanja) and MCM particles preparation. The preparation procedure to prepare MCM particles based on Coconut biodiesel (CB), Karanja biodiesel (KB) blends. The Lauric acid based Karanja biodiesel blends preparation procedure. The author made discussion on adopted methods to determine required physicochemical properties on all prepared fuel samples.

Chapter 4 (Experimental setup and Methodology)

This chapter describes the description of necessary instruments and their installation in engine setup to log observation data from the experimental setup. The author presented detailed, schematic views of necessary instruments held in the experimental setup. The details of implemented different methodologies and necessary modification implicated on the test engine also discussed in this chapter. The adopted methods to calculate engine characteristics combustion, performance and emissions parameters are discussed. The details of emissions logging instruments and their specifications also discussed in this chapter.

Chapter 5 (Results and Discussions)

This chapter describes the calculation of results from logged observations. The drawing of Graphs from tabulated results, which are calculated and tabulated from, logged observations. The discussions are made on presented graphs with proper justifications.

Chapter 6 (Conclusions)

In this chapter, the presentation of précised conclusions and findings based on results and discussions made in the results and discussions chapter. Mentioning of important conclusions based on the carried out investigations and future scope of present research work.

CHAPTER 2

Literature review

2.1 General

The foremost objective of the literature review is to define a problem for investigations by identifying gaps from the collected research articles in a specific research area. The researchers, engine manufacturers, are attempting hard to improve Performance, combustion characteristics by attaining stringent emission norms. This chapter initially exhibits the essential operational basics of Compression Ignition engine such as fuel spray formation, combustion concepts, and emissions formation.

In this regard, the effect of strategies like Exhaust Gas Recirculation (EGR), after treatment devices, engine geometrical parameters, advanced combustion techniques, and alternative fuels. Further, this chapter also illustrates the characterization and usage of solid fuels (Coal, Charcoal and Algae biomass, etc.) based Diesel or biodiesel slurries to reduce Oxides of nitrogen (NOx), Smoke emissions from the Diesel engine.

2.2 Theory on Diesel engines

The SI engines are mostly using in passenger cars, motor vehicles, while CI engines are using in light, medium and heavy-duty applications. The CI engines are widely using in Transportation, Industrial, Power and Military sectors, due to their higher thermal efficiency, long life and lower maintenance than SI engines. However, there is the availability of advanced technologies such as Electric vehicles, Fuel cell vehicles. The CI engines are the better option for heavy load applications.

Worldwide China has 25% Diesel engines demand Transport and power applications, next to Asia/Pacific, Western Europe, North America, and Other countries are accounts 22%, 23%, 11%, and 19% respectively[105]. The technology towards the increase in CI engines efficiency as well as combustion had become mandatory. Because of globally increasing fuel prices as well as the stringent emission norms[106]. The higher level Oxygen in biodiesel fuel is causing reduce HC, CO, & smoke emissions but this induced to increase in NOx. The moderate turnover of engine modifications, EGR and catalytic reduction techniques are not able to implement completely[107].

2.2.1 Working of DI & IDI CI engines:

Based on the mode of fuel injection into the combustion chamber, the Compression ignition engines divided into Direct Injection (DI) and Indirect Injection (IDI). In DI CI engines the fuel directly sprayed into the main combustion chamber in atomizing form, these sprayed fuel droplets start to ignite once they attain autoignition temperature. In IDI CI engine, the fuel first injected into the pre-combustion chamber in atomizing manner and attained combustion, this combustion flame is entering into the main combustion chamber through a small orifice with high velocity and hits on the piston head.

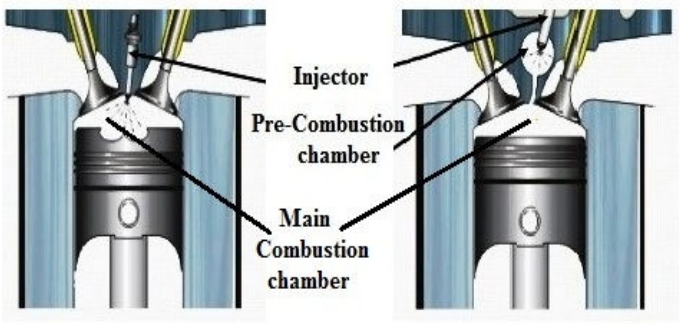

Figure 2.1 Working DI and IDI Compression Ignition engine

Advantages of DI over IDI Diesel engines as follows:

1. The DI CI engines are yielding higher thermal efficiency due to greater fuel efficiency.
2. Lower HC, CO and Soot formation by cause of improved atomization with higher injection pressures
3. Less vibration and noise by cause of single combustion chamber
4. Greater performance at high altitudes because of lower Air density at higher ambient temperatures and lower thrust
5. No cold starting issue by proper atomization
6. More economical than IDI Compression ignition engines[108].

2.2.2 Working of 2-stroke DI CI engine:

An Internal Combustion (IC) engine has to complete the entire conversion process of input heat energy into output Shaft power by undergoing Suction, Compression, Expansion/power, and Exhaust processes. In two-stroke engines, the

ending of the power stroke and the starting of Compression stroke takes place simultaneously, with Suction and Exhaust stroke function occurs at a time.

The one revolution of the crankshaft finishes within one up and down movement of the piston in the cylinder. The two-stroke engines are having higher power density than four-stroke engines because these can develop a power stroke in every crank rotation[109–111].

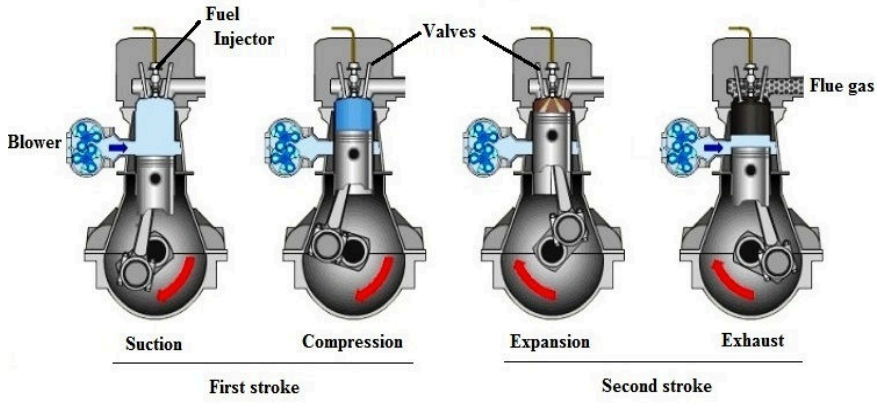

Figure 2.2 Working of 2-stroke DI CI engine

2.2.3 Working of 4-stroke DI CI engine:

A four-stroke engine has to complete the Suction, Compression, Power and Exhaust strokes in every cycle. In each process piston has to move Top Dead Center (TDC) to Bottom Dead Center (BDC) or BDC to TDC as a stroke, i.e., only one Power stroke can attain in 2 revolutions of Crankshaft. In general, the working of CI Engines starts with suction process. The suction of ambient air starts due to the pressure difference, while the inlet valve in opened position as the piston moves from Top dead center (TDC) to Bottom dead center (BDC).

In the Compression process, based on the compression ratio the Temperature and pressure of Air in the cylinder start to rise while the piston moves from BDC to TDC. Just before the end of the compression process, at fixed pressure through the injector, the fuel spray enters into the combustion chamber. In Expansion process/Power stroke, the piston starts to move from TDC to BDC due to the impact of pressure on piston head (i.e., Indicated mean effective pressure) while both valves are in closed position. The Exhaust process starts after the completion of the Expansion process. In this process, the exhaust valve remains open to scavenge flue gases by piston exerted force[112].

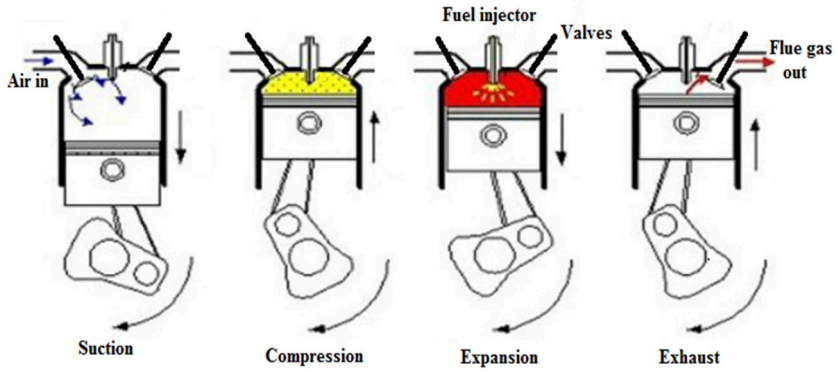

Figure 2.3 Working of 4-stroke DI CI engine

2.3 Combustion process in compression ignition engines:

In CI engine, the Crank angle position from the start of Fuel injection to the end of Expansion/Power stroke called a combustion process. The CI engine combustion efficiency exclusively depends on fuel characteristics, engine geometry, and operating parameters. Based on the importance and influence on engine characteristics, these divided into Primary and Secondary factors.

Primary factors: The type of fuel (conventional, nonconventional), the mass of Induced air (temperature, pressure), and mass of Fuel injected (Atomization, penetration, and characteristics) are the essential primary factors.

Secondary factors: The most influencing secondary factors are Compression ratio, Injection pressure, Geometry of the nozzle hole, and Valve configuration.

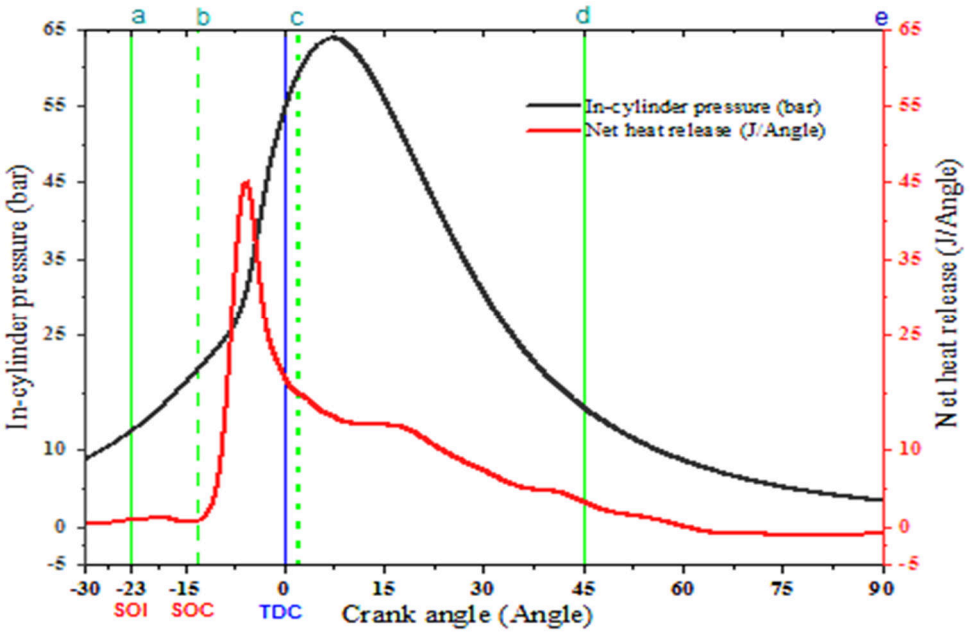

Figure 2.4 Stages of combustion in DI CI engine

The combustion in DI CI engine divided into three stages first one is Ignition delay, the second premixed phase of combustion and third Diffusion combustion. This Diffusion combustion again subdivided into Mixing controlled combustion and late combustion.

Ignition delay (a-b): It is the time interval between the start of injection (SOI) of fuel into the cylinder to the start of combustion (SOC). The ignition delay (ID) progressively occurs in two stages one is Physical delay and second is the Chemical delay. The Physical delay is the time to occur atomization, vaporization of fuel and proper mixing of Air, fuel. The Chemical delay is the aspect of pre-combustion reactions. The Cetane number is the most important property to predict the combustion efficiency in a Diesel engine. The higher Cetane number fuels combust in lower ignition delay vice versa.

Premixed phase of Combustion (b-c): The duration of this combustion phase mainly depends on the quantity of combustible air/fuel mixture formed in Ignition delay (ID) phase. The higher quantity of combustible mixture formation in the ID phase influence rapid combustion in the higher peak in the premixed phase. The Oxygenated fuels are the main influencing fuels for NOx formation also to improve thermal efficiency.

Mixing or rate controlled Combustion (c-d): The combustion in this phase is a very controlled manner and slow. The fuel whichever left to combust in premixed phase is combusting in the diffusion phase of combustion (i.e., mixing or rate controlled combustion and late combustion). In this phase, the locally available Oxygen will reduce the Hydrocarbons (HC), Carbon monoxide (CO) and Particulate matter (PM) emissions at engine tailpipe but this may not influence to improve thermal efficiency.

Late combustion (d-e): The unreacted fuel in earlier stages undergo combustion based on the availability of Oxygen. The reduction of temperature, the pressure in this phase is because of the degradation of chemical reactions by the unavailability of Oxygen. The DI CI engine must complete the above stages in every cycle of operation. These stages are the most deciding factors to increase/decrease engine characteristics. The higher premixed phase peak improves BTE, but this also increases NOx [113].

2.4 Effect of operating parameters on engine characteristics:

The Compression ratio, injection pressure, and injection timing are the extensively used engine operating parameters to improve Diesel engine characteristics. The widely used methods to vary the Compression ratio in Diesel engines are 1 Moving

cylinder head, 2 Changing axis of Crankshaft, 3 Changing the connecting rod geometry, 4 Moving piston crown relative to piston pin axis, 5 Dual pistons, 6 Gear based mechanisms and 7 Tilting head mechanism[114]. The variation in a nozzle opening pressure of Diesel fuel injector is attaining by adjusting the set screw of nozzle spring or by placing or removing the shims under nozzle spring[115,116]. The advancement or Retardation of fuel Injection timing is attaining by placing or removing the required number of shims between the fuel pump and engine[117].

Nanthagopal et al.[118] has investigated the neat Pongamia (Karanja) methyl ester, and its blends with Diesel on a single cylinder and water-cooled four-stroke DI CI engine. He concluded that the neat Karanja biodiesel engine and its blends could run the engine without any modifications. The increase in biodiesel blend ratio is reducing Ignition delay but increasing SFC due to decreasing lower calorific value as the blend increases. The increase in blend ratio increases the NOx emissions but, CO and HC emissions are decreasing.

Gonca et al.[119] studied the effect of the bore to stroke ratio of the piston, CR, equivalence ratio, a variation of percentage load, operating speed and mean piston speed also modifications biodiesel blend percentage, friction coefficient on DI CI engine. The author analyzed the engine through theoretical and experimental investigations to know engine performance, energy losses. The CR, biodiesel blend percentage was the positively affecting parameters on engine performance. The efficiency decreases at constant stroke length but increasing at constant engine speed. The energy losses are classified as friction, heat transfer, exhaust losses and also incomplete combustion losses about compression ratio. At constant cycle temperature ratio and equivalence ratio, and friction losses are constant though there is increase CR, incomplete combustion losses are increasing. On the above conditions, the author observed the increase in heat transfer losses and a decrease in exhaust losses.

Santhosh, and Padmanaban [120] investigated the effect of compression ratios (i.e., 18, 19, 20, 21 and 22) on single cylinder water cooled 4stroke Eddy current dynamometer loaded Direct injection diesel engine with neat Cottonseed methyl ester and its Diesel blends. The better BTE, BSFC and lower Exhaust gas temperature (EGT) found with the increase in compression ratio.

Chavan et al.[121] investigated the single cylinder DI CI engine by varying compression ratio and load. The increase in load and compression ratio is increased the

engine performance as well as decreasing the CO and HC emissions from the engine tailpipe.

Datta, Mandal [122] performed a test on a single cylinder and water cooling four-stroke direct injection 3.5 kW and eddy current dynamometer loaded DI CI engine by using neat Palm biodiesel as fuel. He has observed that the Brake thermal efficiency (BTE), peak cylinder pressure, 50% NOx, and 18% CO_2 increase as the increase in Compression ratio but not a much more significant increase in Heat release rate (HRR) than Diesel fuel.

Jindal et al.[123] investigated the single cylinder water cooled small sized direct injection diesel engine having 3.5 kW with neat Pongamia methyl ester as fuel by varying Injection pressure (IP) and Compression ratio (CR). He justified that the improvement in Brake thermal efficiency (BTE) and reduction in Brake specific fuel consumption (BSFC) by a combined increase of IP & CR. The optimal Compression ratio (CR) and Injection pressure (IP) are 18 and 250 bar respectively.

Ganapathy et al. [117] investigated air cooled single cylinder 5.59kW power naturally aspirated DI CI engine using Jatropha biodiesel by varying IT 340, 345 (base) and 350 Crank angle degree (CAD). The lower BSFC, CO, HC and Smoke and higher BTE, ICP, HRR peaks but higher NOx at early IT from engine ratings. The 340 CAD (retarded) IT influenced significantly @ torque 15 N-m, 1800 rpm to reduce 5.1%BSFC, 2.5% CO, 1.2% HC and 1.5% Smoke and to increase 5.3% BTE, 1.8% Pmax, 26% HRRmax and 20% NOx emissions. The 340 CAD IT was optimal for better engine characteristics.

Pandian et al. [124] achieved lower BSEC, CO, HC, and Smoke with higher BTE, NOx at 225 bar IP, 2.5mm nozzle tip protrusion (NTP), and 30˚BTDC IT. The lower NOx and higher performance achieved at 225 bar IP, 21˚ bTDC IT and 2.5 mm nozzle tip penetration with neat Pongamia biodiesel in RSM optimization approach.

Channapattana et al. [125] Investigated Single cylinder water cooled DI CI engine at rated operating parameters by varying IP of 30 bar above and 30 bar below of rated (210 bar) Injection pressure. The BSFC of neat Honne oil biodiesel at 240 bar IP, 18CR, and 23˚ bTDC IT attributed to 0.042 Kg/kW-hr higher with reasonable lower emissions than Diesel fuel. The increase in NOx emissions observed with increase in IP and blend.

2.5 Effect of Biodiesel composition on engine characteristics

As discussed in the section 1.4.1 the compositions of clean biodiesel fuels influenced by the composition of parent oil. The Transesterification was a widely used the method to remove Glycerol from parent oil[126]. The oil selection was a significant factor to produce biodiesel fuel and to fulfill demand in the market. In 1991 Australia followed DIN51606 most popular German standard, later EN14214 standards for European countries[127]. The biodiesel fuels are the great Diesel fuel alternative because these are renewable, biodegradable and cost effective[128].

Table 2.1 Comparison of Algal biodiesel (FAME) compositions (wt. %) with other

Group		FAME	14:0	16:0	18:0	20:0	16:1	18:1	18:2	18:3	Other	Ref.,
Edible		Coconut	17.4	11.3	3.8	0.2	0.2	9.2	3	-	a	[46]
		Palm	1	38.1	4.1	0.4	0.2	44.2	11	0.3	b	
		Peanut	-	17.2	2.7	0.9	-	40.5	36.6	0.5	c	[47]
		Canola	-	4.2	2.1	0.7	-	64.7	18.6	8.3	d	[46]
		Linseed	-	5.2	3.2	-	-	14.5	15.3	61.9	-	[48]
		Sunflower	-	4.9	2.3	-	-	32.6	59.4	-	e	[46]
Inedible		Jatropha	0.1	14.1	7.6	0.2	0.6	44.1	31.5	0.3	f	[49]
		Karanja	-	13.8	6.1	-	-	65.3	11.6	3.2	-	[50]
		Castor	-	1.3	1.3	0.1	-	3.8	5.3	0.8	g	[51]
		Neem	-	10.8	9.2	-	0.1	18.2	61.3	0.5	-	[52]
		Mahua	0.2	20.8	25.2	-	-	36.4	15.8	0.3	h	[53]
		Sea mango	-	24.7	6.06	-	0.8	53.4	7.70	-	-	[34]
Waste fats, oils		Chicken fat	0.7	20.9	5.6	-	5.4	40.9	20.5	-	i	[46]
		Beef tallow	3.2	23.8	12.7	-	4.7	47.2	2.6	0.8	j	[129]
		Lard	1.3	23.5	13.5	-	2.6	41.7	10.7	-	k	[54]
		Yellow grease	2.4	22.8	12.0	0.2	3.8	45.0	7.8	0.8	l	[36]
		Waste cooking oil	1.5	27.3	4.9	-	-	36.1	25.7	1.9	m	[50]
Algal group	I	Botryococcus braunii	-	28.8	-	-	3.8	48.0	11.7	7.8	-	[55]
		Chlorella vulgaris	2.3	6	10.3	-	-	20.3	-	2.3	n	[56]
	II	Nannochloropsis oculata	7.7	35.4	2.5	-	27.6	8.6	5.2	-	o	[57]
	III	Chlorella protothecoides	-	4.7	2	1.9	-	65.2	15.5	6.9	p	[51]
		Mixed culture microalgae	5.0	26.7	5.8	2.4	8.9	23.5	14.0	9.8	q	[56]

I-Green algae, **II**-Diatom, **III**–Heterotrophic, **NF**–Not found

Other fatty acids: a-(6:0=0.3, 8:0=6.5, 10:0=6, 12:0=42.1), **b**-(12:0=0.3, 20:1=0.2, 22:0=0.1), **c**-(22:0=1.5), **d**-(20:1=1.2, 22:1=0.3), **e**-(22:0=0.5), **f**-(12:0=0.1, 20:1=0.1, 22:0=0.1, 22:1=0.1, 24:0=0.5), **g**-($18:1_{OH}$=87.10, 20:1=0.4, 22:0=0.01, 22:1=0.01), **h**=1.3**, i**-(14:1=0.1), **j**-(14:1=1.3, 15:0=0.5, 17:0=1.1), **k**-(17:0=0.4), **l**-(15:0=0.36, 17:0=1.0), **m**-(12:0=1.6), **n**-(14:1n9c=0.6, 16:1n9c=6.1, 16:1n9t=10.3, 18:1n9t=6.2, 18:3n6=18.6**),o** - (20:4=2.5, 20:5=8.3, 22:6=2.2), **p**-**(**24:0=0.6).**q**-(12:0=1.3, 15:0=0.6, 17:0=2.0).

The fatty acid composition is the most influencing factor on biodiesel properties, engine characteristics. This composition determined by gas chromatography-flame ionization detector (GC – FID), gas chromatography-mass spectrometry (GC-MS), and also with high-performance liquid chromatography (HPLC)[130]. Biodiesel possesses poor cold flow properties if this composed saturated fatty acid composition also high viscous than unsaturated fatty acids because of their higher melting points.

Similarly, the highly unsaturated fatty acids are having higher Oxygen composition and viscosity than saturated fatty acid biodiesel, and it may lead to lower Oxidation stability. The above two effects may influence on fuel spray pattern and NOx emissions from the engine tails pipe because of their higher viscosity and Oxygen composition respectively[131].

Pinzi et al. [132] developed a statistical prediction and correlations by considering the physical and chemical properties of biodiesel fuels to know the most impacting fatty acid composition on NOx and Soot emissions from a Diesel engine. The depicted conclusion from this study was, the higher carbon chain length of highly unsaturated fatty acids contained biodiesel fuels are lead to increase NOx emissions as well as HC, CO and Soot emissions from engine tailpipe.

The lower chain saturated fatty acids contained biodiesel fuels are preferable to reduce NOx and Soot emissions from a Diesel engine, for example, Coconut biodiesel is highly composed of Lauric acid which is having a carbon chain length 12. If any biodiesel having highly Linolenic acid (i.e., C18:3 poly unsaturation) in it leads to increase NOx emissions as well as poorer oxidation stability than saturated fatty acids composed biodiesel fuels.

Gopinath et al. [133] conducted a series of tests on Single cylinder DI CI engine at 1500rpm to know the impact of biodiesel fuel unsaturation on its physicochemical properties and engine characteristics. They concluded that the increase in level biodiesel fuels unsaturation would lead to reducing Kinematic viscosity with higher Density as well as with Calorific value, Cetane number and thermal efficiency than saturated fatty acids. The high-level unsaturation may also increase NOx, in-cylinder temperatures than saturated fatty acid biodiesel. however, they reduce HC, CO, and Smoke emissions.

2.6 Scope to use solid fuels in Diesel engines

From the past few decades, solid fuels are using to produce heat for daily human needs such as cooking, boiling water, and power production in power plants. Based on their origin the solid fuels are of various types such as Coal, coke, biological wastes from agriculture, Industrial sources. As per the International energy agency (IEA) statistics worldwide 41% of naturally available fossil coal is using to fire in furnaces for steam generation in steam power plants for electricity generation.

To avoid GHG emissions from waste biomass sources while recovering heat energy through their direct combustion. The scientists and researchers introduced and developed many methods like Gasification, Pyrolysis, anaerobic digestion, and fermentation. The Pyrolysis is the thermochemical process to produce gas, solid fuels (Biochar) by decomposing of biological solid wastes in the absence of Oxygen. The Anaerobic digestion is the process to produce liquid and gaseous fuels from waste biomass materials in the absence of Oxygen.

The Gasification is the process to produce gaseous fuel from organic waste biomass. It is not in use due to the emission of ash particles into the environment. The processes mentioned above are widely using to produce Solid, liquid and gaseous fuels for various heat generation applications but the liquid and gaseous fuels are only using in IC engine applications in various approaches. The researchers are trying to convert and utilize bio-char, conventional coal, and coke into water or liquid fuel based slurries in Diesel engines by slight fuel injection system modification [134].

2.6.1 Coal & Charcoal based fuels for Diesel engine operation

Urban et al. in 1988 [135] investigated an EMD-567B engine at rated operating parameters with Coal water slurry (CWS) fuel and observed slight diameter enlargement in fuel injector nozzle hole. The NOx emissions observed not more than half of type 2 Diesel fuel, but smoke emissions are higher with CWS fuel. The above result obtained by without considering optimized parameters to run the engine with CWS fuel. The optimization required in the area of injection, which must include fuel atomization, structure, the start of injection, and its duration between main and pilot injections.

The CWS attains higher ignition delay due to the slow rate of combustion by cause of lower Cetane number and higher droplet size. To improve the rate of combustion in the engine, it requires higher combustion chamber temperature before

injection of fuel. The literature on combustion bomb experiments revealed that it requires 727°C pre-combustion temperature for higher combustion efficiency with CWS fuel on EMD-567B engine.

There are two conventional ways to increase the pre-combustion temperature one is by heating intake air and another by increasing the compression ratio. The other less conventional methods for increasing pre-combustion temperature is by insulating the combustion chamber and by optimizing in-cylinder air motion. By doing all the above modifications engine can run with commercially acceptable coal slurry as potential fuel for commercial utilization.

Ryan [136] have investigated the modified Ricardo swirl chamber diesel engine with Water, Diesel and Methanol as carrier fluids to prepare 50 wt.% Based on Coal powder slurries. To run the Diesel engine with the fuels mentioned above samples author has modified the jerk pump fuel system. The primary motive of this work is to attain possible performance improvement by coal/water based slurry than regular Diesel fuel. This specially designed engine to run with Coal/Water based slurry by increasing inline air temperature and glow plug arrangement to attain autoignition temperature.

The Coal/Diesel slurry fuels require higher temperatures to combust because of poorer coal combustion in the pre-combustion phase caused to decrease pre-combustion peak. The Coal/Water and Coal/Diesel fuels slurries are having slower combustion rate if pilot injection used with Diesel fuel. At 38°C inline air temperature and glow plug arrangement with the Coal water slurry attained thermal efficiency almost equal to regular Diesel fuel. Additionally, the adiabatic combustion approach can generate even more heat energy but need to compromise for extra fuel consumption.

Yuchi et al. [137] studied the 16 types of Chinese coals characteristics to know the effect on coal water slurry properties. The author concluded that the grindability index and slurry ability increases as the Carbon content increases in the coal. He also correlated that ash content, dissolvable ions, shown a better effect on coal water stability but inertinite (highly oxygenated) has a negative impact.

Zhangqiang et al. [138] investigated an 8kW, 1500 rpm gen set engine with an electronic control unit. This engine fuelled with Coal based Diesel and Water slurries. The test results revealed that the electronically controlled unit require a control strategy to limit the generating unit frequency, speed, and output voltage. As per author advise this generating unit capable of acting as a mobile power plant because it can be usable in small capacity electricity production purposes eg., mining, rural and forest areas,

town side, small hotels and restaurants. The Coal based Diesel or Water slurries fuelled Genset engine could be capable of producing general performance, at a rated output voltage, and frequency, and should accomplish the durable, reliable operation.

Patton et al. [139] reported that the Coal based slurries are causing to higher abrasion problems than Charcoal based water slurries that to Charcoal is naturally cleaner and environmentally friendly. The running of Diesel engines with the Charcoal-water slurries is the practically suitable idea because Charcoal water slurries are cheaper and can consume >75% than diesel fuel.

Soloiu et al. [140] described the fuel preparation and characterization of charcoal water slurry as fuel for Yanmar NF-19, single cylinder, air-cooled, direct injection, 1200rpm speed, 7.8 bmep, and the GƆ-type combustion chamber diesel engine. This study aims to determine the essential performance, emission characteristics, and durability issues by using Charcoal water slurries as fuel. The lower heating value of slurry fueled to 4.8% higher brake specific fuel consumption than Diesel fuel but the presence of fuel-borne Oxygen in Charcoal slurry the lower smoke Bosch number observed.

The 30% higher NOx emissions than Diesel fuel has observed with Charcoal slurry but the lower NOx emissions observed with retarded injection timing. The Injector choking, needle sticking observed at every load per hour operation of an engine. The reason for the decrease in efficiency with the increase in load was by cause of the mitigation of particles at the needle upper part to valve stem clearance and at the needle seat and sac.

The design of injector is required to deal with higher size particles, but these are offering cooling effect at the injector's needle and stable efficiency at 50% load for 90min operation without injector sticking. Further investigations are required to understand the wear effect by Charcoal, water slurry fuel as fuel for Diesel engine operation.

Qiang and Lan-zhu [141] was carried investigations on the single cylinder, air-cooled, at 1200rpm Diesel engine by Coal water slurry blends with variously advanced injection timings. This study revealed that a 20% decrease in brake-specific fuel consumption and thermal efficiency increased with the increase in fuel injection timing from 171CA to 181CA. The combustion duration was found shortest at 181CA fuel injection advancement.

The advancement of fuel injection timing shown a more significant effect on engine emissions reduction. The exhaust smoke decreased, but Unburned Hydrocarbons increased. The NOxdecreasedat lowered loads and increased at higher loads, but the Carbon monoxide emissions increased at lower loads and decreased at full load.

2.6.2 Carbon black based fuels for Diesel engine operation

Wamankar and Murugan [142] carried out investigations on single cylinder DI diesel engine without any significant modifications by using carbon black–water–diesel blend as fuel for combustion and emissions analysis. At full load operation the in-cylinder pressure, heat release rate for all the fuel samples reported 3.9–4.4% and 2.5–3% lower respectively. Here NOx emissions 16–42% lower for all blends than Diesel. This effect was due to poor air, fuel mixture formation and the less calorific value of the blended fuel than Diesel.

Wamankar and Murugan [143] performed test runs for engine characteristics (combustion, performance, and emission) analysis by using Carbon blank based Diesel fuel in an unmodified 4.4 kW power rated, four strokes, single cylinder, DI CI engine at 1500rpm. The reported in-cylinder pressures, heat release rate for Carbodiesels are 1.5– 9.7% and 1.4–5.3% respectively than Diesel fuel at full load operation.

The longer ignition delay for Carbodiesels was due to lower Cetane number and higher density than that of Diesel fuel. The higher Density and Viscosity of Carbodiesels caused by improper atomization and air-fuel mixing in the combustion chamber. At full load operation, 3.7 – 9.4% lower brake thermal efficiency of Carbodiesels is due to less calorific value than Diesel fuel. Based on this analysis the author suggested that the engine can run with Carbodiesels without any significant engine modifications.

Wamankar and Murugan [144] experimented with the same engine fueled with the CBWD10 blend fuel with minor engine modification. Author's earlier investigation revealed that CBWD10 was the optimum blend based on better performance and emissions at full load. The author investigated the effect of IT, IP on the combustion process, performance and exhaust emissions in a diesel engine. The author achieved HRRmax of 57.7 J/CA with the CBWD10 blend at 220bar with 26°bTDC, which was higher about 5.38% than Diesel at full load. The 4% of higher BTE noticed by blend operation at 26° bTDC IT, 220 bar IP because of fine droplet size due to improvement

in atomization. The obtained results are signifying that the CBWD10 blend exhibited 16– 42% lower NOx emissions at all IT and IP than Diesel.

2.6.3 Solid fuel from other sources to apply on Diesel engine

Piriou et al. [145] review include the possibilities to run reciprocating engines with solid biomass-based Diesel/biodiesel fuels. The usage of coal powder in a dry/slurry form created wear, ignition control and fuel handling problems. The earlier studies performed in this approach revealed that the usage of finely grounded biomass particles to run Diesel engines is an unusual approach than Coal.

The combustion of biomass particles in a Diesel engine can take place quicker with less wear than coal dust or its slurries. The supply and metering of coal-based fuels into the engine combustion chamber is the primary bottleneck especially in powder form, but it can overcome by using computerized controlled injection system. The usage of finely grounded solid biomass contained fuels in diesel engines is a potential approach, but it requires advancements in pulverization techniques to grind the coal dust into tiny size for Diesel/biodiesel slurries preparation.

Purushothaman and Nagarajan [146] Investigated the effect of injection pressure on the combustion and exhaust emission characteristics of the single cylinder, air-cooled, DI CI engine which can produce 4.4 kW power at 1500 rpm with Orange skin powder based Diesel Solution (OSPDS). Author's earlier investigation on mentioned unmodified engine revealed that the 30% ofOSPDS was optimum for optimal performance, emission characteristics at full load operation. In this study, the engine (combustion, performance, and emissions) characteristics were studied and compared with Diesel fuel by varying the injection pressures 215bar, 235bar, and 255bar with 30% OSPDS.

After drawing all the results from logged data on the mentioned engine operating conditions, the author reported that the higher in-cylinder pressure obtained at 235barfuel injection pressure than diesel fuel. However the highest ignition delay and 1.1% higher brake thermal efficiency found at 235 bar injection pressure (IP)with 30% OSPDS, but it is lower than Diesel fuel. The 26% higher NOx emissions, 66% lower Hydrocarbon emissions and 39% lower Carbon monoxide (CO) emissions found with 30% OSPDS at 235bar IP than Diesel fuel at engine full load operation. The author concluded that 235bar IP was optimal for better combustion, performance and emission characteristics than other injection pressures.

Rohith and Vinay [147] performed test runs on single cylinder DI CI engine which can produce 3.7kW power at 1500rpm with 20% & 30% Orange peel powder based Diesel fuel blends for performance and emission characteristics analysis. The CO_2 emissions were 13.3% lower at 20% load and 16.1% lower at 80% load for both 20% and 30% OPPDS than that of diesel. The 53.3% lower HC and 16.7% lower CO emissions found with 30% OPPDS than Diesel fuel, but lower NOx emissions found at all loads of engine operation.

Vigneshwaran and Suresh [148] performed the test on an unmodified four stroke, single cylinder DI CI engine using the 45microns sized pulverized Coconut shell powder based Diesel fuel blends up to 30% weight basis with each 5% blend (i.e., 10, 15, 20, 25%). The blends preparation was limited to 25% because the viscosity of blends was increasing with increasing the blend ratio. It is possible to apply higher blends by preheating the slurry fuel or by preparing a chemically stable blend and also by bypassing the fuel from the fuel filter.

The author reported lower BSFC and higher BTE with all blends than Diesel fuel. The author also concluded that the running of the unmodified diesel engine by using lower blends of Coconut shell powder based diesel fuel is a potential approach. Further studies with advanced techniques are required to overcome the injector hole erosion problems with the higher blends of Coconut shell power based Diesel fuels.

Vinukumar et al. [149]performed test runs by using Diesel as the base fuel for comparison, B20 blend of Pongamia pinnata methyl ester and Coconut shell particles (CSP) based blend of 20%BD+80%DF+CSP fuel on an unmodified four-stroke single cylinder DI CI engine can produce 3.5kW power at 1500rpm. The particle size of Coconut shell power reduced to 20nm by running 5h at 300rpm ofFritcsh planetary mono mill machine.

The 18.56% reduction of NOx emissions than Diesel fuel has observed with the 20%BD+80%DF+CSP fuel sample at full load operation. At the all loads engine operation the reduction in CO, CO_2 emissions and the improvement in BTE and BSFC were observed with 20%BD+80%DF+CSP fuel sample than Diesel fuel. Author justified that the engine can run with 20%BD+80%DF+CSP fuel sample without any modifications.

Scragg et al. [99] carried out investigations on four stroke, single cylinder DI CI engine by using Diesel, Rapeseed methyl ester (B100) and 5 – 10 μm sized unicellular

Chlorella Vulgaris algal particles contained Rapeseed methyl ester slurry. The lower NOx and higher CO emissions and higher brake thermal efficiency observed with 20% algal particles contained Rapeseed methyl ester slurry than Diesel fuel.

Xu et al. [150] used Chlorella sorokiniana species microalgae contained diesel fuel to apply on ω shaped piston bowl type single cylinder, water cooling DI CI engine for analysis. The 0.44g of Span80, 0.30g of CTAB, 0.49g of Butanol, and 0.45g of Water (i.e., 1.68g) are used to prepare stable blend which is at 6.6% wt/wt basis. All of the wet Chlorella sorokiniana species based Diesel slurry blends emitted lower NOx (ppm) and Particulate matter (%)and higher Carbon monoxide (%) emissions observed than Diesel fuel.

2.7 Formation of NOx and its reduction methods

The NOx formation is taking place mainly in three ways, 1st Thermal NOx, 2nd Fuel NOx, and 3rd Prompt NOx. Among all, thermal NOx is the most contributing phenomena from Diesel engines. Thermal NOx formation is due to the highest temperature in the engine cylinder when Nitrogen and Oxygen combine [151]. The In cylinder and after treatment techniques are the widely used methods to reduce NOx emissions.

The water/steam injection into the induction line, water emulsion with fuel, fuel modification by adding antioxidant additive and Exhaust gas recirculation (E.G.R.) are widely using in cylinder NOx treatment methods[152] and coming to after treatment techniques Selective Catalytic Reduction (SCR), Selective Non-Catalytic Reduction (SNCR), Solid Selective Catalytic Reduction (SSCR) and Lean NOx Trap (LNT) are the widely used techniques. Among all Urea SCR was extensively using proven methods for NOx reduction[153].

By using Ammonia (NH_3) in Urea SCR, 96-99% conversion efficiency can be achievable at temperature range 200°C to 400°C. The conversion efficiency of SNCR is 50% only because its effectiveness depends on NH_3/NOx ratio. The LNT technique was the costlier technique than others because of these catalysts based on ceramic substrates and layered porous plug and more expensive precious metals (eg., Platinum, Palladium and Rhodium)[154].

Among all the above techniques the after treatment techniques are required with somewhat engine modifications. The user must carefully deal with precious, costlier and hazardous catalytic materials. The fuel modification technique (antioxidant) it

seems to be cheaper, the easiest method to reduce NOx from the engine. This auto-oxidation reaction undergoes by three stages first initiation, second Propagation and third terminations (i.e., RH +I*→ R* + IH).

In the initiation process, the radicals (I*) reacts with FAME substrate (RH) and Hydrogen is attracted a fatty acid carbon molecule to form (R*) carbon less radical. The formation of initiation radicals undergoes different mechanisms (ROOH → RO* + OH*) at elevated temperature hydroperoxides (ROOH) retain as an impurity. In storage conditions, metals (M) present in the fuels is acts as contamination, and these initiates fatty acid esters decomposition as a catalytic reaction ($ROO+M_2+ \rightarrow RO^*+OH^*+M_3$). There is a chance to under photo-oxidation when fuels directly exposed to light [155].

In general antioxidant additives are three types 1. Phenolic, 2. Amines and 3. Thiophenols. The phenolic antioxidant additives are similar to natural polyphenolic additives. The easy availability, cost, and performance point of view, phenolic additives are mostly using for diesel engine operation with oxygenated fuels. The widely used phenolic antioxidant additives are butylated hydroxytoluene (BHT), butylated hydroxyanisole (BHA), and tertiary-butylhydroquinone (TBHQ) with biodiesel and their blends application.

By adding phenolic based additives (BHA, BHT) in biodiesel fuels are improved engine performance, NOx emissions but increased CO, HC and Smoke emissions [156,157]. The natural polyphenolic antioxidant additives are widely present in some plant materials, and these are acting as natural antioxidants to improve the Oxidation stability (eg., polyphenols, tocopherols, chlorophylls, tocotrienols, ascorbates, carotenoids and lignin).

These natural antioxidants in vegetable oils are destroyed in the transesterification or at the time of the biodiesel refining process[158,159]. The aromatic amines antioxidant is very much appropriate to apply in Biodiesel fuels than phenolic and polyphenolic additives due to its better resistance to heat, corrosion, oxidation stability and inbuilt ‘N’ molecule reducing NOx emissions[160,161].

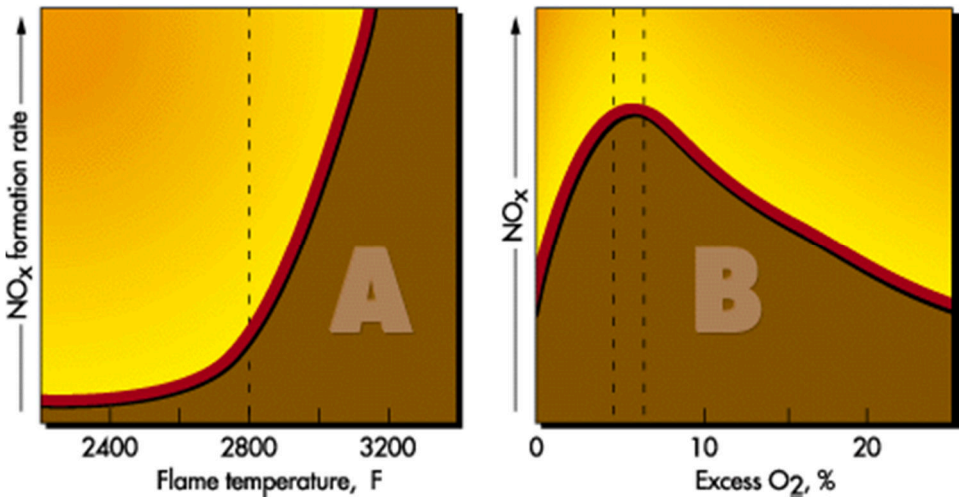

Figure 2.5 Variation of NOx with flame temperature and excess O_2.

At starting, the fuel jet penetrates from the tip of the nozzle to the combustion chamber. The compressed high temperature, pressure Air in the combustion chamber can enter into the fuel spray and tries to evaporate up to some length is known as the liquid length. This fuel and air mixture seeks to prepare rich fuel level in the Ignition delay period and starts to combust rapidly in the premixed phase of combustion.

The products of combustion from the rich premixed phase try to diffuse radially towards the flame surface and coming to contact with the cylinder gases. Once the stoichiometric mixture formed along the above region, the diffusion flame formed. This flame tries to extend up to the tip of the nozzle, i.e., towards the upstream of the fuel jet.

The distance from the start of diffusion to the tip of the nozzle is the lift of length. The available Oxygen, Nitrogen in fuel, at the highest temperatures caused to NOx formation(John dec, 1997). As shown in Figure 2.5 the improvement in combustion leads to above 1538˚C in cylinder temperature and below 5% exhaust Oxygen. The improper combustion leads more than 5% of exhaust Oxygen and below 1538˚C in cylinder temperature [162].

2.8 Observations from the Literature

The cultivation of microalgae is the greater solution to capture CO_2 from the environment and wastewater treatment. However, the cultivation of particular species of microalgae and its application on diesel engines is the cost involving aspect.

The direct usage of Algae biomass as a solid fuel in diesel engines is the potential approach to avoid difficulties in Oil extraction and biodiesel production. In particular,

the mixed culture microalgae are the more significant source to naturally available antioxidants than vegetable oil feedstocks.

This can use to reduce the NOx emission than other costlier and harmful antioxidants. Even the high viscous Algal oil or clean biodiesel fuels application on the diesel engine is increasing BSFC, PM and CO_2 emissions. As per Indian geographical, environmental conditions, the Coconut, Karanja oils are the quickly growing and higher oil yielding feedstocks.

According to **Ashraful et al.** [163] the Karanja was the best Nitrogen fixing tree. The favorable properties of Karanja biodiesel are much appropriate to apply for Diesel engines. The increase in Kinematic viscosity with Algal biomass blend ratio in Water/Diesel/Biodiesel influencing to increase BSFC, PM, CO, and HC, etc. through the reduction in NOx emissions. The smaller droplet size with the increase in IP helps to improve BTE, BSFC.

2.9 Objectives and scope of present research work

1. To synthesize the Biodiesel fuels from Coconut and Karanja oils.
2. To collect the mixed culture microalgae (MCM) biomass for the preparation of the required quantity and size of particles.
3. To prepare the MCM particles based Coconut, Karanja biodiesel fuels.
4. To determine the physicochemical properties of prepared fuel samples.
5. To investigate the engine characteristics by using all prepared fuel samples.
6. To study the influence of additives in improving the performance of Coconut and Karanja biodiesel fuels.
7. To reduce NOx, Particulate matter emissions from the diesel engine

CHAPTER 3

Fuels production, blends preparation and characterization

3.1 General

In the present work, the biodiesel fuels produced from two different oils such as Coconut and Karanja. These oils are higher oil yielding feedstocks from edible and inedible sources. The Coconut oil is highly composed of saturated fatty acid in particular Lauric acid > 70%, and the Karanja oil has higher unsaturated fatty acids mainly Oleic acid > 70%. By applying Transesterification process, the neat biodiesel fuels produced from selected oils. The Diesel, neat CB, KB considered as base fuels in this study. The coarse size dried MCM particles grounded in the planetary ball-milling machine to allow < 0.28mm size nozzle hole. The wet grounded fine MCM particles blended in CB, KB biodiesel fuels separately.

The MCM particles contained biodiesel blends 1g, 2g and 3g per (i.e., 0.1, 0.2, 0.3 w/v ratio) liter are prepared with each neat biodiesel separately. The Triton-X100 used as a surfactant to prepare stable MCM particles merged Coconut and Karanja biodiesel fuels separately. The baseline fuels, their microalgae particle blends physicochemical properties determined in the Mechanical engineering fuels laboratory at NIT Warangal. This chapter emphasized the procedure to synthesize biodiesel fuels, preparation of microalgae particles, their blends preparation, and determination of physicochemical properties of prepared fuel samples.

3.2 Materials for Biodiesel fuel production

The oil yielding capacity of various oils from different sources and the selected (Coconut & Karanja) oils fatty acid composition and their biodiesel fuels properties presented in Table 1.1, Table-1.2, and Table-1.4. The chemicals Methanol, Sulfuric acid (H_2SO_4), Sodium hydroxide (NaOH), Phenolphthalein indicator ($C_{20}H_{14}O_4$), 0.1N NaOH/KOH solution, Isopropyl alcohol (C_3H_8O) and distilled water for biodiesel water washing. The glassware 250ml conical flasks, two 500ml flat bottom flasks with condensers, submersible pump to circulate water into the condenser, and three 2lts and one 1lt capacity separating funnels. The thermometers for temperature measurement,

Magnetic beads, and Hotplate magnetic stirrer and 3liter capacity three-necked biodiesel reactors with condensers.

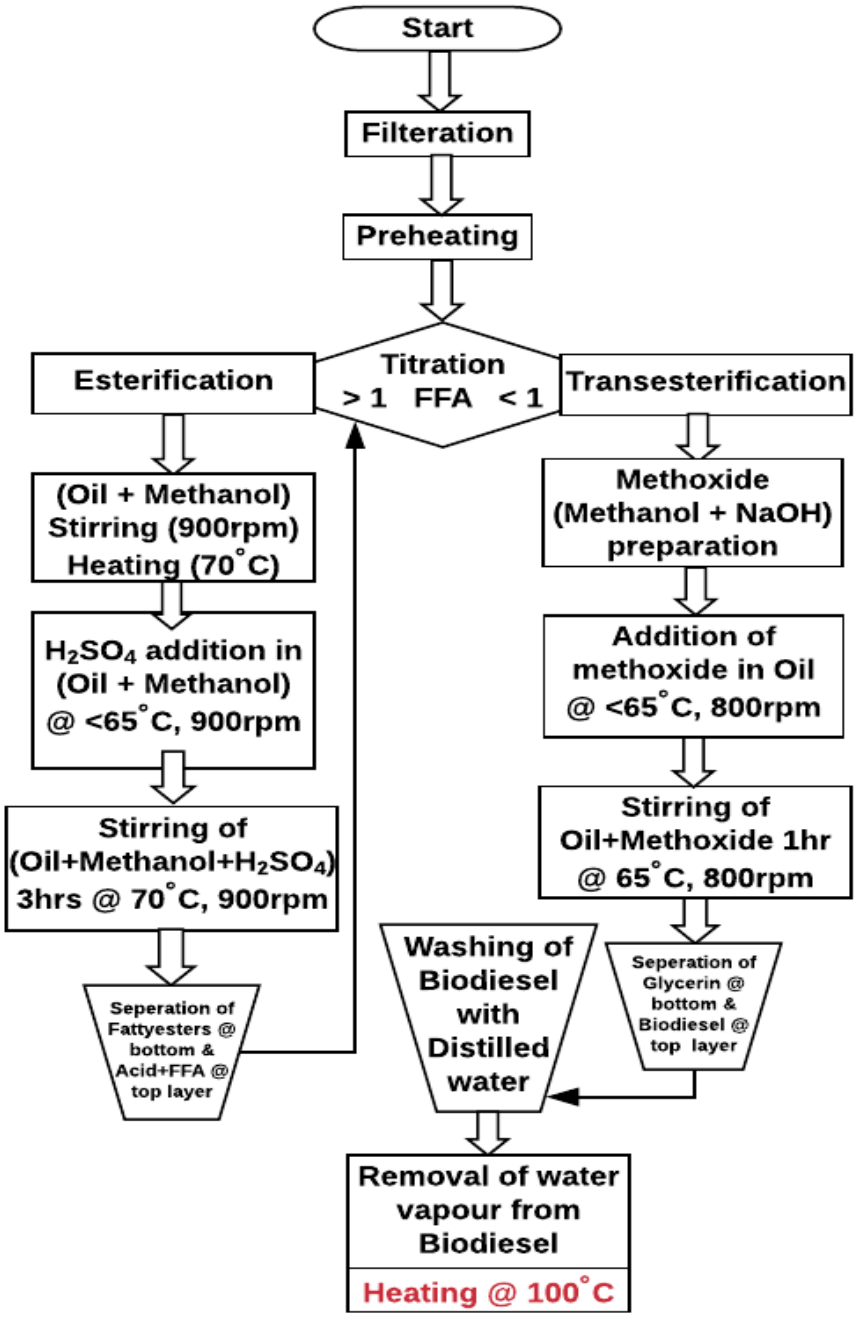

Figure 3.1 Flow diagram for two-step Transesterification process

4 Before undergoing the titration process, the filtration, preheating methods are the necessary steps to remove solid particles and moisture from oil.

5 The titration was the process to determine the free fatty acid (FFA) value of any oil/fat, to know the required quantity of base catalyst and to decide suitable biodiesel conversion (Transesterification) process.

6 To convert biodiesel from any oil/fat the determination of FFA value necessary to opt biodiesel conversion process. If oil/fat has >1% FFA the two-step (i.e., Acid, base) Transesterification process or if <1% the single step (base) Transesterification process has to opt for biodiesel conversion from any oil/fat.

7 In the present work, the easy availability and low cost of Methanol and NaOH used as Alcohol and catalyst for the production of Coconut and Karanja biodiesel fuels.

3.3 The titration test procedure

1. Firstly, weight the 10g of oil/fat in an Erlenmeyer flask to pour 20ml of 95% Methanol and apply phenolphthalein 0.5 ml/lt and mix until Oil and Methanol dissolve correctly.
2. Start the titration by dropping NaOH 0.1 N solution until the color changes in pink, and it has to retain at least 30sec.

Figure 3.2 Titration setup

3. Apply all the obtained values in the below equation to get FFA in percentage.

$$Acid\ \text{value (AV)} = \left(\frac{(MW_{BC} \times 10)}{MW_{FA}} \right) \times \%\ FFA$$

$$\%\ \text{FFA} = \left(\frac{(N \times MW_{BC} \times V \times 100)}{(1000 \times \text{Oil}_{W})} \right)$$

Where: V = Volume of NaOH/KOH solution consumed in ml.

N = Normality of NaOH/KOH solution (eg. 0.1 Normality).

MW_{FA}= Molecular weight of highest Fatty acid (eg. Oleic acid = 282.47, Lauric acid = 200.32 g/mol).

MW_{BC} =Molecular weight of Base catalyst (eg. NaOH = 39.997, KOH = 56.1g/mol)

$Oil_{Wt.}$ = Weight of Oil/Fat in grams.

The highest mass percentage occupied fatty acid molar mass in an Oil/Fat should be taken as $MW_{FA}$to determine accurate results of the Free fatty acid percentage (FFA%)[164].

Table 3.1 Determined Acid values and FFA percentage of Coconut, Karanja oils

TERM	COCONUT OIL	KARANJA OIL
V	11	29
N	0.1	
MW_{FA}	200.32	282.47
MW_{BC}	40	
Oil_W	10	
AV	0.88	1.643
% FFA	0.44	1.16

To produce biodiesel, based on the obtained oil FFA percentage the single step Base Transesterification process applied for Coconut oil and Acid, base (Two-step) Transesterification process for Karanja oil.

3.3.1 Base Transesterification process for Coconut Biodiesel production

Preheating: The1-liter volume of filtered, preheated Coconut oil has0.44% free fatty acid poured in a three-necked glass reactor by using a funnel.

Meth-oxide preparation: The 7g of NaOH pellets added to 160ml of Methanol in a 250ml of conical flask, stirred on a magnetic stirrer until it thoroughly dissolves.

Figure 3.3 Methoxide preparation

Meth-oxide addition in Oil: The prepared meth-oxide slowly added in one liter of Coconut oil after attaining temperature 65˚C.

Reaction: The reaction between Meth-oxide and oil continued 1hour by maintaining speed 800rpm and temperature 65˚C.

Figure 3.4 Reactor for biodiesel conversion

Settling: The reacted sample poured in 2-liter capacity separating funnel and left it for 12hr for settling. The biodiesel floats in the upper layer and glycerin in the bottom layer.

Figure 3.5 Settledbiodiesel sample in a separating funnel

Glycerin removal: In a beaker, the bottom settled glycerin removed from separating funnel to carry out water washing in the next step.

Water washing: The above 65˚C temperature hot distilled water poured in the crude biodiesel sample to remove excess alcohol, NaOH and Glycerin.

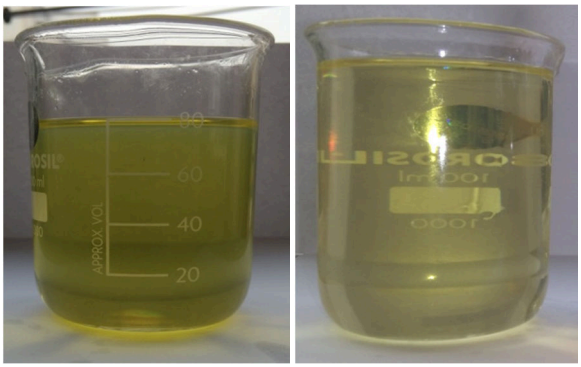

Figure 3.6 Unprocessed and processed CB in beakers

Acid treatment: The water washed biodiesel neutralized by titration process with 0.1N aqua based Phosphoric acid.

Moisture removal: The Phosphoric acid treated biodiesel sample heated at 100˚C for removing distilled water droplets.

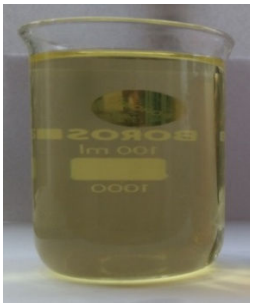

Figure 3.7 Moisture removed water washed biodiesel

Filtration: The Grade1 Whatman filter paper used to remove solid particles from moisture removed biodiesel.

3.3.2 Acid, base Transesterification process for Karanja Biodiesel production

The biodiesel produced from >1% FFA Karanja oil by applying Base Transesterification followed by Acid treatment (i.e., Esterification).

3.3.2.1 Acid treatment for Karanja fatty esters production:

The < 1.16 percentage FFA contained filtered and preheated Karanja oil taken in a three-necked glass reactor and mixed with 25% methanol on an oil volume basis. The Methanol mixed Karanja oil sample mixed thoroughly in the reactor by maintaining speed 900rpm, and temperature ≤ 70˚C.

The 3 to 4ml of Sulfuric acid (H_2SO_4) added in methanol mixed Karanja oil at65˚Ctemperature and stirred the sample 3 hours by maintaining speed940rpm.

Figure 3.8 Esterification of Karanja oil in a reactor

The acid treated sample (Oil+methanol+H_2SO_4) taken into separating funnel and allowed 12hr for settling.As shown in Figure 3.9 the fatty esters are settled in the bottom layer and excess methanol, H_2SO_4 & moisture in the upper layer.

Figure 3.9 Settled Karanja esters in a separating funnel

The settled fatty esters collected in a beaker and taken 10g of ester sample to determined FFA percentage by titration process. The single step base Transesterification can apply if the collected ester sample FFA% is < 1% if not repeat the esterification process until to get fatty esters FFA% <1.

3.3.2.2 Base Transesterification for Karanja Biodiesel conversion

The moisture was removed, and FFA reduced to <1% by applying (Esterification) acid treatment process to apply base Transesterification process on Karanja oil.

Methoxide preparation: The 8.5 grams of NaOH pellets added to 160ml of Methanol in a 250ml of the conical flask and stirred on a magnetic stirrer to dissolve in methanol.

Methoxide addition in Oil: After attaining oil temperature 65˚C the prepared methoxide slowly added in Karanja oil ester.

Reaction: This continued 1hr by maintaining speed800rpm and temperature 65˚C.

Settling: The reacted sample collected in the separating funnel and it allowed 12hr to settle down glycerol in the bottom layer and biodiesel in the upper layer.

Glycerin removal: The bottom settled glycerol removed to apply water washing on biodiesel in separating funnel.

Water washing: The water washing is necessary to remove excess alcohol, NaOH and glycerin from crude biodiesel sample. The distilled water heated ≤ 65˚C to wash the crude biodiesel sample in separating funnel. The larger volume of distilled water is required to remove glycerol from high FFA contained oil based biodiesel.

Acid treatment: The acid (Phosphoric acid) treatment is necessary to step to neutralize the biodiesel and to remove excess NaOH and methanol.

Moisture removal: the acid treated biodiesel collected in a beaker, kept on hotplate magnetic stirrer and heated above 100˚C for moisture removal.

Filtration: This filtration is to avoid choking of tiny particles in the injector nozzle hole (0.28mm diameter). The Whatman Grade1 filter paper used to remove tiny particles from CB & KB biodiesel.

Table 3.2 Optimal parametric values to produce KB & CB fuels

Parameter	Karanja (FFA 1.16)		Coconut (FFA 0.44)
	Esterification	Transesterification	Transesterification
Methanol (ml)	250	160	150
H_2SO_4 (ml)	4	-	-
NaOH (wt. % of oil)	-	0.75	0.75
Stirring speed (rpm)	950	800	800
Temperature (°C)	75	65	65
Time (hr)	3	1	1
Yield	96.5		98.4

3.4 MCM particles preparation procedure

The water washing was done in a separating funnel to remove contaminants from harvested MCM biomass and collect in a beaker as shown in the below figure.

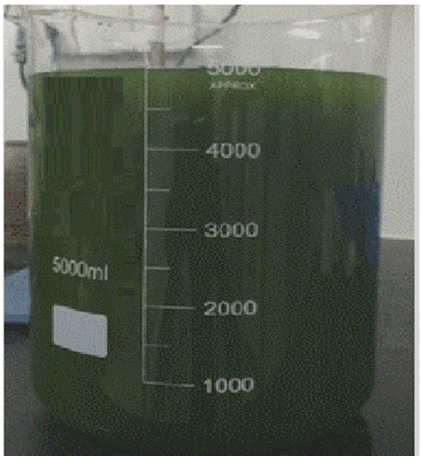

Figure 3.10 Harvested mixed culture Microalgae biomass

The harvested biomass dried under direct sunlight for moisture removal and to reduce the input energy expenses in the drying process. To convert coarse size MCM biomass particles initially the dry MCM biomass grounded in a domestic mixer grinder.

Figure 3.11 Coarse size MCM particles

The five grams of coarse-sized particles mixed with 50ml of methanol for the grinding process. This mixture was taken into a jar of the planetary ball milling machine to reduce the coarse size particles into fine particles (i.e., <0.28mm). These MCM particles (AP) emulsified with neat Coconut, Karanja biodiesel fuels in 1g, 2g and 3g per liter as blends.

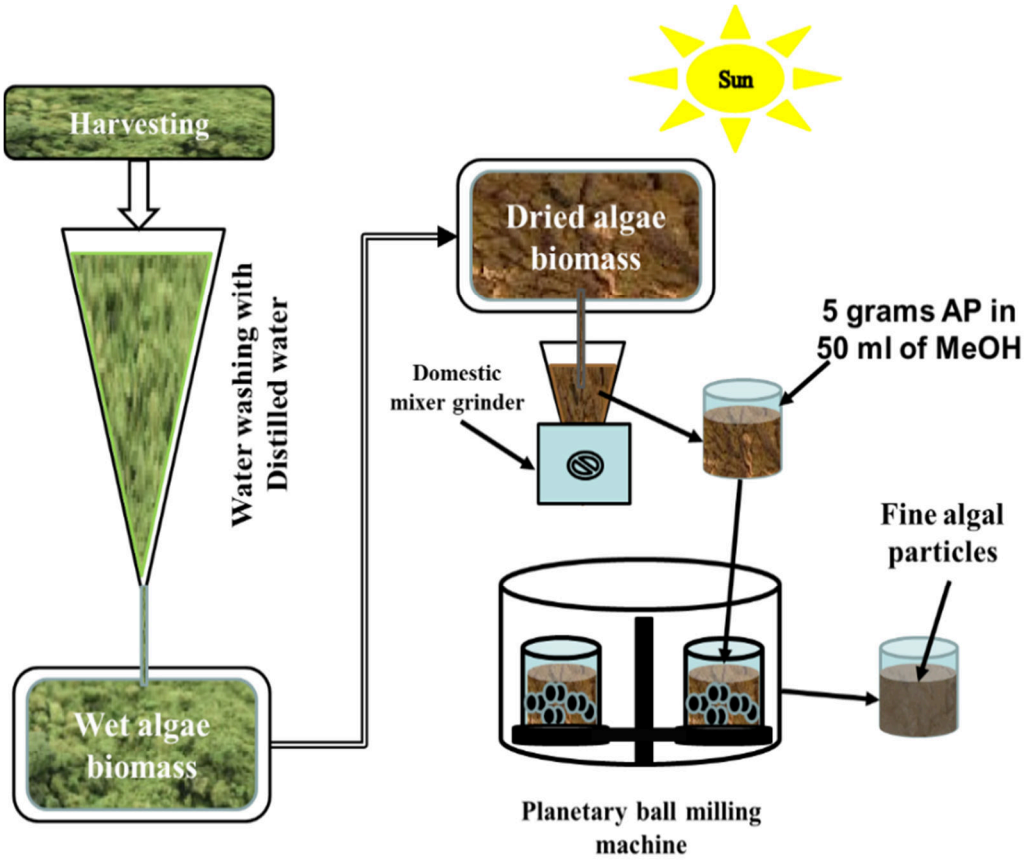

Figure 3.12 Stepwise procedure for MCM particles preparation

3.5 Preparation of MCM particles mixed CB, KB fuels blends

The fine wet grounded 1g, 2g & 3g of MCM particles emulsified separately in the 1-liter volume of CB & KB fuels. These mixtures blended in mechanical emulsifier, which is available in NIT Warangal fuels laboratory.

Figure 3.13 Mechanical blending machine for blends preparation

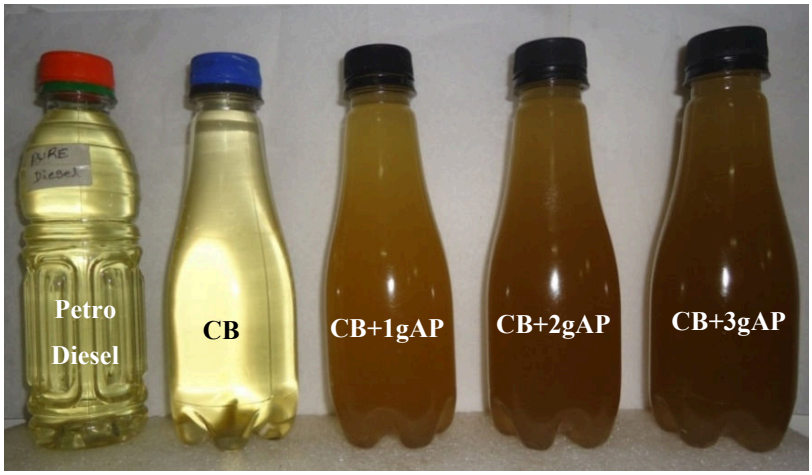

Figure 3.14 MCM particles blended CB fuel blends

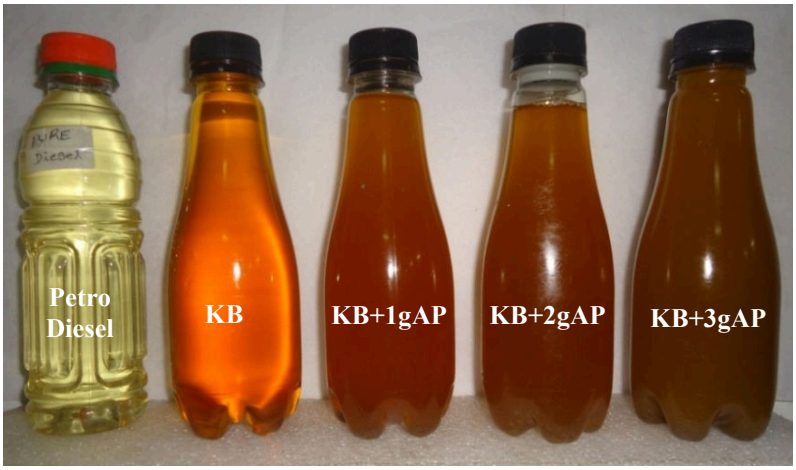

Figure 3.15 MCM particles blended CB, KB fuel blends

3.6 Preparation of Lauric acid mixed Karanja biodiesel blends

The literature reviews revealed that the neat Coconut biodiesel composed with the highest percentage of saturated fatty acid that is Lauric acid. This is semisolid at room temperature, due to its higher melting point. In the present work, the author used Lauric acid based Karanja biodiesel, to confirm the significant reason for the reduction of NOx emissions and improvement in performance of microalgae-based Coconut biodiesel on a Diesel engine. Table 3.3 describes the physicochemical properties of the pure form of Lauric acid.

Table 3.3 Physicochemical properties of the pure form of Lauric acid

Property (unit)	Value	Ref
Density (kg/m^3)	868	[165]
Viscosity (mPa.sec @ 50 °C)	7.3	
Flashpoint (°C)	112.8	
Boiling point (°C)	225	
Melting point (°C)	43. 9	
Molecular weight (g/mol)	200.3	
Vapour Pressure (@ 760 mm Hg)	571˚F (299˚C)	
Colour	White crystal	

Figure 3.16 Lauric acid (LA) and LA blends preparation setup

The above shown Lauric acid white crystals are emulsified 10g, 20g & 30g per liter of neat Karanja biodiesel fuel while heating above 55°C temperature at stirring speed 2000rpm under mechanical stirrer. The above three blends prepared in the mechanical blender (Figure 3.13) which is used to blend MCM particles with Coconut and Karanja biodiesel fuels. These emulsified fuel samples experimentally investigated on single cylinder four strokes DI CI engine characteristics analysis by varying percentage full load, and IPs 190, 210, and 230 bar. The photographic view of Lauric acid blended samples presented in Figure 3.17.

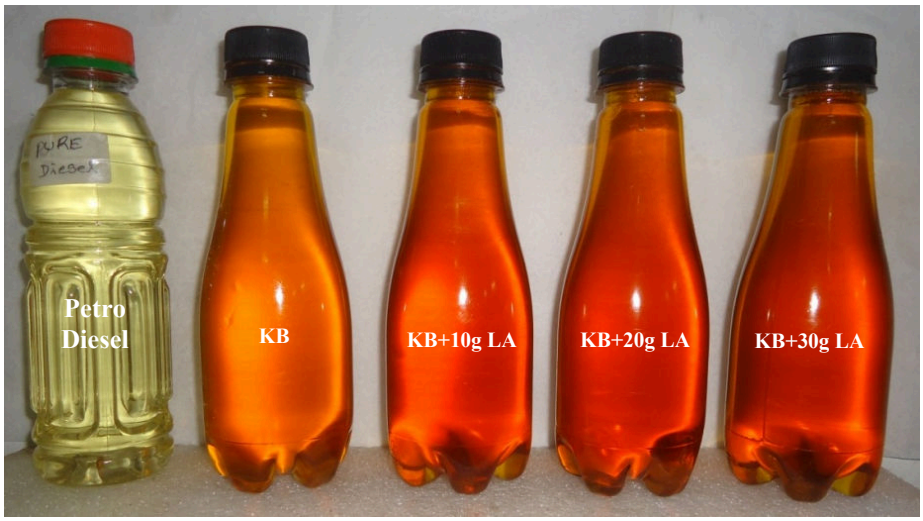

Figure 3.17 Lauric acid blended KB fuel blends

3.7 Characterization of all prepared fuels samples

The characterization of above all produced fuel samples, i.e., some essential physicochemical properties determined in fuels laboratory, Mechanical engineering department, of the National Institute of technology Warangal. The Hydrometer used to determine the Density of all the fuel mentioned above samples at 30°C. The Kinematic viscosity of all produced fuel samples was determined on Redwood viscometer-1.

The Calorific value determined by using SPAN automated Bomb calorimeter. The flash and fire points of all fuels determined by using Pensky martin's apparatus in closed cup mode. The elemental composition (i.e., CHO) of prepared MCM particles are getting tested in Sophisticated Test & Instrumentation Centre Cochin University of Science and Technology which is accredited by NABL laboratories. The previously mentioned physicochemical properties of all fuel samples presented in the Table-3.4.

Table 3.4 Physicochemical properties of all prepared fuel samples

Fuel type	Density @ 30 ˚C (kg/m^3)	Calorific value (kJ/kg)	Kinematic viscosity (mm^2/sec)	Flash Point (˚C)	Fire Point (˚C)
Diesel	832	43712	2.82	53	57
CB	871	38250	3.24	143	149
CB+1g AP	872	38067	3.85	146	152
CB+2g AP	873	37926	4.23	149	154
CB+3g AP	874	37740	4.87	152	159
KB	881	38821	4.78	162	167
KB+ 1g AP	882	38537	5.23	164	169
KB+ 2g AP	883	38392	5.73	167	173
KB+ 3g AP	884	38162	6.34	171	176
KB+10g LA	883	38534	4.92	154	157
KB+20g LA	884	38363	5.15	152	156
KB+30g LA	885	38095	5.37	149	153
	Carbon	**Hydrogen**	**Oxygen**	**Formula**	**References**
MCM particles	76.12	11.31	12.57	-	-
Lauric acid	71.95	12.08	15.97	$C_{12}H_{24}O_2$	[166]
Diesel	85.2	14.8	-	$C_{7.1}H_{14.68}$	[167]
KB	76.1	12.2	11.7	$C_{6.34}H_{12.1}O_{0.73}$	
CB	73.68	12.28	14.04	-	[168]

In the present work Diesel, Coconut biodiesel (CB or CB) and Karanja biodiesel (KB or KB) used as base fuels to analyze the DI CI engine characteristics. Among all base fuels, the Diesel fuel has the lowest Density, Kinematic viscosity, and highest Calorific value. Among all base fuels samples, the clean Coconut biodiesel fuel has the highest Oxygen after Lauric acid, Hydrogen, and lowest Carbon composition. The 3g of Algal particles based Karanja biodiesel has the highest Kinematic viscosity, flash and fire points than all other fuel samples.

CHAPTER 4

Experimental setup and Methodology

4.1 General

To conclude the research works in an experimental approach. The researcher needs to build an experimental test setup by acquiring knowledge of the required instruments. After that, the researcher requires to log the observation data from the experimental setup by using appropriate data logging instruments. This chapter describes the specifications of each user data logging instrument, software, pressure transducer, and crank angle encoder. This chapter also described the specifications of the test setup, emission analyzers and applied a methodology for Direct Injection Compression Ignition (DI CI) engine characteristics analysis.

4.2 Test setup and its specifications

In this study, the single cylinder, 4-stroke, water cooled Kirloskar make AV_1 model DI CI engine, which is capable of producing 3.5kW power at 1500rpm, was used for analysis. The schematic diagram of the experimental test setup conferred in Figure4.1 and photograph of this experimental setup portrayed in Figure 4.2. The complete specifications of the test engine setup presented in Table-4.1.

To apply required load on Engine is equipped with Eddy current type dynamometer by rotating loading wheel, which held on Panel box for Brake power calculation. The base fuels Diesel, biodiesel fuels Coconut and Karanja stored in fuel tanks. The valves held in a fuel line to allow these fuels into burette from two different fuel tanks. To measure fuel flow at burette, the fuel line optical sensors used to give the signal to the Data acquisition system (DAS).

The fuel consumption starts to measure as the counter time start by clicking on an Icon of software in laptop and fuel consumption ends as the counter time stops (i.e., 60sec). This fuel consumption data send to software on a volume basis by DAS. The fuel injected into the combustion chamber through the existing fuel injector at 210 bar standard injector opening pressure.

The air enters into the combustion chamber via intake manifold after passing through the air box. This airflow measured by the airflow sensor, which mounted at the

entry of the Airbox. The applied methodology to analyze DI CI engine characteristics clearly explained at every module of operation.

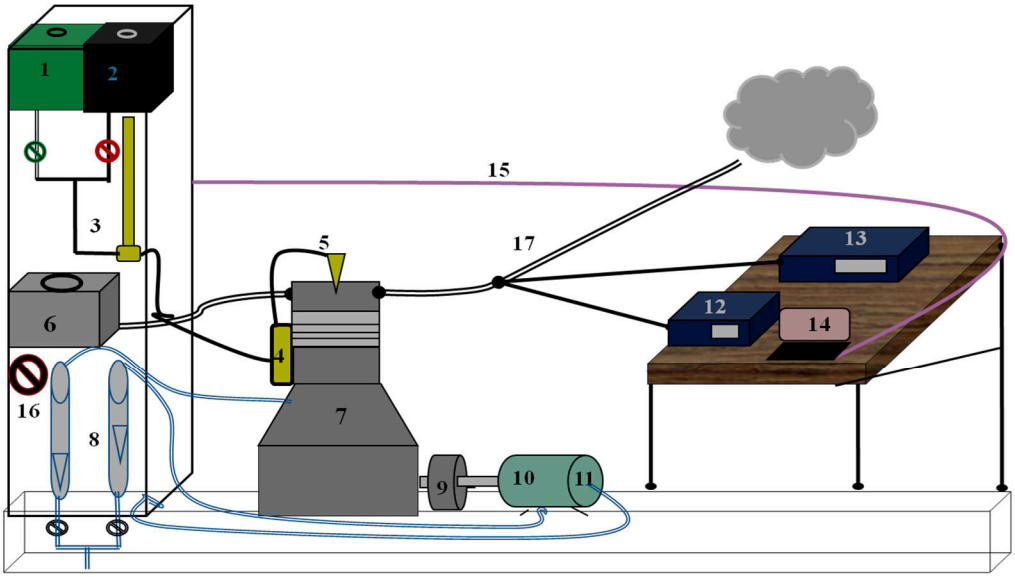

1, 2 – Biodiesel, Diesel tanks, **3** – Burette, **4** – Fuel pump, **5** – Fuel injector, **6** – Air box, **7** – Engine, **8** – Water flow meters, **9** – Fly wheel, **10** – Eddy current Dynamometer, **11** – Crank angle encoder, **12** – Emission analyser, **13** – Smoke meter, **14** – Laptop for data acquisition, **15** – Cable to connect laptop, **16** – Loading wheel, **17** – Exhaust line.

Figure 4.1 Test engine setup schematic diagram

Figure 4.2 Photographic view of test engine setup

Table 4.1 Specifications of a test engine

Name of the description	Details/value
Manufacturer	Kirloskar (AV_1)
Operating principle	4 stroke DI CI
Cooling system	Water cooling
Number of cylinders	One
Bore x stroke	87.5 x 110mm
Compression ratio (range)	17.5:1 (12 - 18)
Volume	661.45 cm^3
Fuel injection pressure (range)	210 bar (170-290)
Brake power @ speed	3.5kW @ 1500rpm
Dynamometer type	Eddy current
Dynamometer load range	0 – 50kg
Dynamometer arm length	185mm

4.3 Specifications of data logging instruments

Above engine was built with essential instruments like Crank angle encoder to capture crank angle data. The Piezoelectric pressure transducers to track pressure data for the corresponding crank angle from the combustion chamber and at fuel line. The Airflow transmitter at the entry of Airbox and Fuel flow transmitter at burette to log Air, fuel consumption. The temperature sensors/ transmitters such as resistance temperature detectors (RTDs)/thermocouples to capture the temperature data at each required location of engine setup.

To apply required load on an engine the instruments like Eddy current dynamometer, Load cell, and loading wheel the and to log load data from engine setup. To interface above all instruments, the US based National Instruments (NI) make USB-6210 model 16-bit Data acquisition device used to capture 250-kilo samples data per second (kS/s). The ICEngineSoft software used to analyze engine Performance and Combustion characteristics based on captured observations data with some input values of fuel physicochemical properties — the photographic views &specifications of the above each instrument described below.

Table 4.2 Data logging instruments and their specifications

Sl. No.	Name (Model)	Details/value
1	Crank angle encoder (8.KIS40.1361.0360)	German based Kubler company make, 1-degree Resolution, the 5500rpm speed with TDC pulse
2	Piezo sensors (S111A22)	USA based PCB Piezotronics company make 5000psi (344.75 bar) pressure range Piezo sensors at Combustion chamber and Fuel inline.
3	Data acquisition device	United States based NI make USB-6210, 16bit, 250kS/s
4	Software	National Instruments developed LabVIEW based ICEngineSoft software
5	ECU	Make PE USA, Model PE3
6	Temperature sensor	Make Radix, Type RTD, PT100, and Thermocouple, Type K
7	Temperature transmitter	Make ABUSTEK USA, Type 2 wire, Input RTD/Thermocouple, Output 4 - 20mA
8	Load cell	Make VPG Sensotronics, Load cell, S Type strain gauge
9	Fuel flow transmitter	Make Yokogawa Japan, DP transmitter, Range 0-500mmWC
10	Air flow transmitter	Make Wika Germany, Pressure transmitter, Range 0-250mmWC

1. Crank angle Encoder (8.KIS40.1361.0360):

Order code Shaft version	8.KIS40 Type	.	1 a	X b	X c	X d	.	XXXX e

	.	1	3	6	1	.	0	3	6	0
Type		**a**	**b**	**c**	**d**		**e**			

The above table represents the shaft order code for Kubler make Incremental type Rotary Encoder (8. KIS40):

a – The number **1** denotes that 40mm diameter synchronous Flange for clamping

b – The number **3** denotes that 6mm diameter 12.5mm length flat shaft

c – The number **6** denotes that 5 Volts DC input supply RS422 with the inverted signal

d – The number **1** denotes that 2 meters PVC axial cable

e – The number **0360** denotes pulse rate

The IP64, Logic level: RS422; Supply= 5VDC Incr/turn: 360 PPR

2. Piezo sensors (S111A22):

The 6gram weight Pizeo sensor with Stainless Steel housing with 344.75 bar has maximum pressure measurement range, 0.00145 sensitivity, 0.001 Hz low-frequency response and >=400kHz Resonant frequency and 10-32 Coaxial jack.

3. Technical specifications of PE make Electronic control unitPE3:

Size	:	11 x 12 x 3 centimetres
Weight	:	0.4 kgf of aluminium &potted waterproof enclosures
Operational voltage:		6 – 22v DC supply
Operational temperature:		-30°C to 75°C depends on loading
Active voltages	:	3.25v (High) & 2.0v (Low)

The Maximum continuous supplied voltage for Digital system: 22v

4. Specifications of Data acquisition device:

This model USB6210 made in United States of America (USA) by National Instruments (NI). The ADC resolution is 16bits with sample rate 250-kilo samples per second (kS/s). The range of Operational current -16mA (high) & 16mA (low). The lowest & highest digital input voltages are 0 to 5.25. The DC input coupling with timing accuracy 50ppm of sample rate and resolution 50 ns.

5. The specifications of Load cell:

The VPG Sensotronics Company make 60001 Model S beam type 50kg Capacity load cell manufactured with high-quality alloy steel with nickel coated plate presented above.

6. Differential pressure Fuel transmitter (Model-EJA110E-JMS5J):

Model EJA110E – JMS5J suffix codes and description:

J-stands for **Output signal** range**-** 4 to 20mA Direct Current (DC) with digital communication (HART 5/HART 7 protocols)

M-stands for **Measurement span** (capsule) range**-** 1 to 100kPa (4 to 400 inH_2O)

S-stands for **Wetted parts material** *of Cover flange, process connector:* ASTM CF-8M *Capsule:* Hastelloy Diaphragm C-276[4]; F316L SST, 316 L SST Capsule gaskets*:* Teflon-coated316L SST*Vent/Drain plug* 316 SST

5-stands for **process connections** without process connector (1/4 NPT female on the cover flanges)

J-stands for **bolts, nuts materials** made with B7carbon steel.

7. ICEngineSoft:

The National instruments developed LabVIEW based ICEngineSoft software to analyze Performance, Combustion characteristics using logged observation data from test setup and by some input fuel properties.

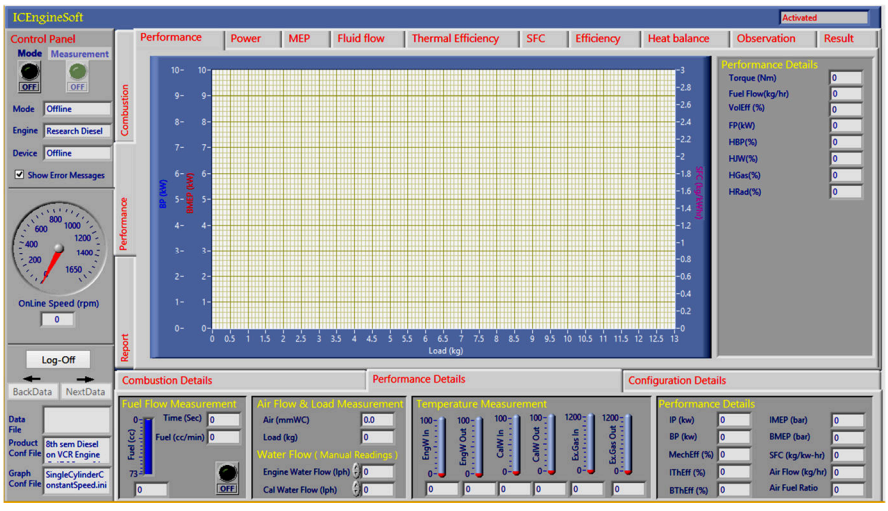

8. Temperature transmitter:

The USA based ABUSTEK company make 2 wire, Input Resistance Temperature Detector (RTD) or Thermocouple with Output of 4 - 20mA.

9. Airflow transmitter (SL-1-A-MQA):

The WIKA CompanymakesAirflow transmitter SL-1-A-MQA model 4-20mA output current and zero to 10bar pressure range.

4.4 Specifications of emission analyzers

In the present work, the DI CI engine tailpipe emissions are Carbon monoxide (CO), Carbon dioxide (CO_2), Unburned Hydrocarbons (HC), Oxygen (O_2) and NOx measured by using Indus make PEA 205N model 5 gas analyzer. The Smoke emissions measured by using NETEL make NPM-SM-111B model Smoke Meter. The detailed specifications of the above 5 gas analyzer and Smoke meter given in Table 4.4 and their photographic views presented in Figure 4.3. The Co, HC, & CO_2 measured by Nondispersive Infrared Detector and NOx, O_2 measured by Electrochemical sensor.

Table 4.3 Specifications of emissions analyzers

INDUS 5 gas analyzer, Model: PEA 205N					
Emission	**Measurement principle**	**Unit**	**Range**	**Resolution**	**Accuracy**
CO	NDIR	% vol	0 - 15	0.001	±0.02
HC	NDIR	ppm	0-30000	1	±4
CO_2	NDIR	% vol	0 - 20	0.01	±0.5
O_2	Electrochemical sensor	% vol	0 - 25	0.01	±0.02
NO_x	Electrochemical sensor	ppm	0-5000	1	±5
NETEL Smoke meter Model: NPM-SM-111B					
Emissions		Unit		Range	Resolution
Smoke density(K)		m^{-1}		0 - 9.99	0.01
Smoke opacity(%/HSU)		%		0-99.99	0.01

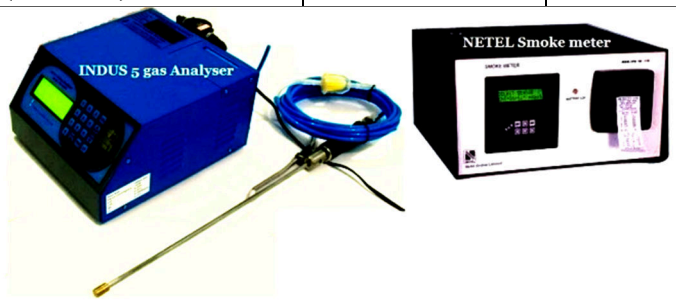

Figure 4.3 Photographic view of the emission analyzers

4.5 Experimental methodology

This section describes the adopted methodologies to investigate the engine characteristics such as Performance, Combustion, and Emissions with or without modification of engine and fuel. The observations logged from the engine using data acquisition system (DAS) by varying engine input variables and fuel blends. The engine side input variables, the percentage full load (0 to 100% step of 20%) in kgs, and injector opening pressures 190, 210, 230 and 250 bar.

The fuel blends prepared by emulsifying microalgae particles 1g, 2g & 3g in CB, KB biodiesel fuels and also blends of Lauric acid with KB. The Observation data was logged for every input variable after entering the values of fuel properties like Density, Calorific value as inputs to ICEngineSoft software.

4.5.1 Investigations on Base fuels

The Performance, combustion and emission characteristics analyzed by using the Diesel, neat Coconut, and Karanja biodiesel fuels as base fuels at standard engine operating parameters such as Compression ratio 17.5, Injection pressure 210 bar and by varying load on the engine from 0 to 100% with 20% increment.

4.5.2 Investigations on MCM particles blended biodiesel blends

In the present study, the MCM particles based Coconut and Karanja biodiesel fuels are prepared and applied on the engine to investigate the performance, combustion and emission characteristics. These prepared MCM particles based biodiesel blends configurations presented in the below Table 4.4.

Table 4.4 Configurations of MCM particles blended CB, and KB fuels

Sl. No.	Base fuel	The quantity of Microalgae particles/liter		
		1g	2g	3g
1	**CB**	CB+1gAP	CB+2gAP	CB+3gAP
2	**KB**	KB+1gAP	KB+2gAP	KB+3gAP

In the above Table 4.4the CB and KB stands for Coconut and Karanja biodiesel fuels and AP represents mixed culture Microalgae particles. The previous sections 3.4, 3.5 and 3.6 describe the MCM particles preparation, their blending withCB, KB fuels, and characterization.

4.5.3 Investigations on Lauric acid blended Karanja biodiesel blends

As per the literature is concerned the highest composition of Lauric acid in Coconut oil and its higher melting point the Coconut oil is semi-solid at room temperature. Because of the above reasons, the pure form of Lauric acid was widely used substance in the phase change material (PCM) applications. To know the right reason for NOx emission reduction with Microalgae particles contained Coconut biodiesel, the author applied Lauric acid based Karanja biodiesel on the same engine for characteristics analysis.

Table 4.5 Configurations of Lauric acid blended KB fuel blends

Sl. No.	Base fuel	The quantity of Lauric acid/liter KB		
		10g	20g	30g
1	**KB**	KB+10gLA	KB+20gLA	KB+30gLA

4.6 Method applied to vary nozzle opening pressure

To attain required IP the tension of tension spring in the injector has adjusted by the rotating injection pressure setting screw (2). The fuel IP checked in the fuel IP setting setup which is available in the IC engine laboratory of Mechanical Engg., Dept in NIT Warangal. The testing engine performed by using 4 injectors after setting fuel IPs 190, 210, 230 and 250 bar. The baseline fuels Diesel, CB, KB baseline data has logged at 210bar (rated) IP. The testing done on engine setup by applying above all IP's on each MCM particles; Lauric acid blended fuel blends.

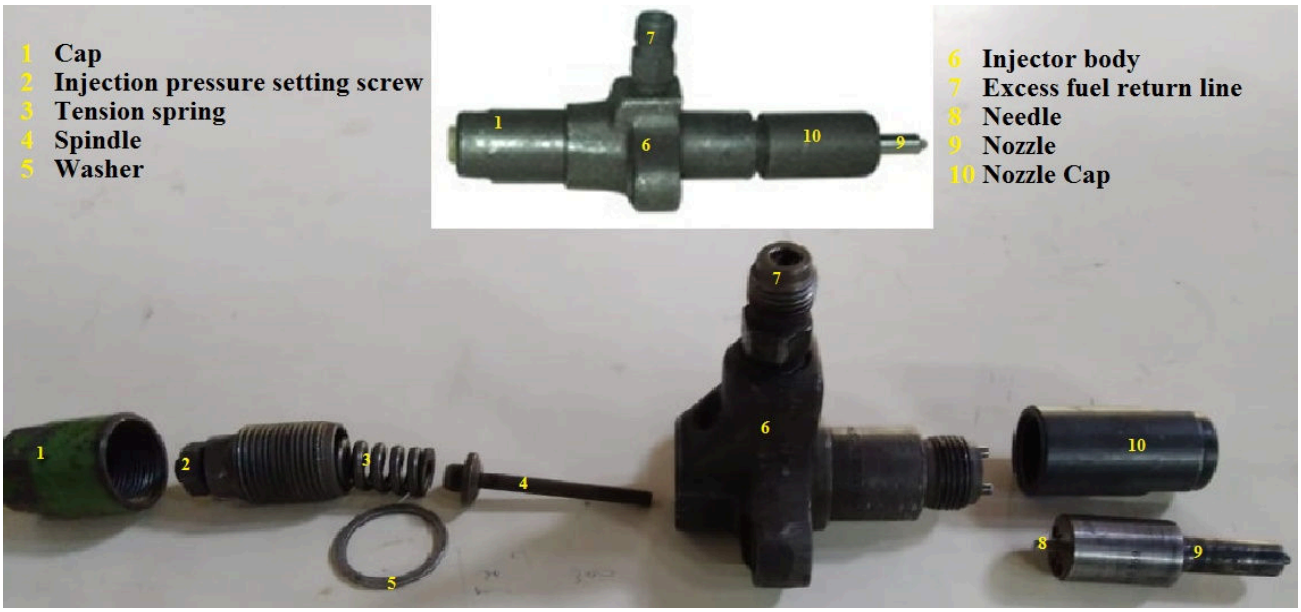

Figure 4.4 Photographic view of fuel injector

CHAPTER 5

Results and Discussions

5.1 General

The blending of MCM particles in different proportions in Coconut biodiesel has experimentally conformed the reduction of NOx. However, about this reduction, there are two different opinions by Doctoral scrutiny committee (DSC) members. Firstly, this could be because of the presence of Lauric acid in CB, and secondly, this could be because of MCM particles blending in the same biodiesel. Therefore, the author has selected KB, which is free from Lauric acid composition. The author experimented with different proportions of LA, MCM particles separately in KB fuel.

In Module -1 author presented results on engine (combustion, performance, and emissions) characteristics at engine standard operating parameters (SOPs). The combustion characteristics in the form of Graphs at 100% full load operation with Crank angle (CA) variation. The Performance and emissions characteristics in the form of Graphs by varying, load 0 to 100% full load with 20 % variation.

Configurations for first module experimentation at SOPs:

a. Load (0, 20, 30, 40, 60, 80, and 100%)
b. Diesel, CB, and KB as base fuels
c. CB+1gAP, CB+2gAP and CB+3gAP (1 g, 2 g and 3 g MCM particles)
d. KB+10gLA, KB+20gLA, and KB+30gLA (10 g, 20 g and 30 g Lauric acid)
e. KB+1gAP, KB+2gAP, and KB+3gAP (1 g, 2 g and 3 g MCM particles)

In Module -2 authors presented results in the form of Graphs on 1 g, 2 g, and 3 g MCM particles blends with CB fuel. The combustion results presented at engine full load operation on above blends by varying injection pressures (IP) 190, 210, 230 and 250 bar and Crank angle. The performance, emissions results also presented on the same blends by varying load 0 to 100% full load with 20 % variation and IP 190, 210, 230 and 250 bar.

Configurations for the second module of experimentation:

a. Load (0, 20, 30, 40, 60, 80, and 100%)
b. Injection pressures (190, 210, 230 and 250 bar)
c. CB+1gAP, CB+2gAP and CB+3gAP (1 g, 2 g and 3 g MCM particles)

In Module -3 author presented results in the form of Graphs on 10 g, 20 g and 30 g Lauric acid blends with KB fuel. The combustion results presented at engine full load operation on above blends by varying injection pressures (IP) 190, 210, 230 bar and Crank angle. The performance and emissions result also presented on the same blends by varying load 0 to 100% full load with 20 % variation and IP 190, 210, 230 bar.

Configurations for second module experimentation:

a. Load (0, 20, 30, 40, 60, 80, and 100%)
b. Injection pressures (190, 210, 230 and 250 bar)
c. KB+10g/LA, KB+2gLA, &KB+30gLA (1 g, 2 g and 3 g MCM particles)

In Module -4 author presented results in the form of Graphs on 1 g, 2 g, and 3 g MCM particles blends with KB fuel. The combustion results presented at engine full load operation on above blends by varying injection pressures (IP) 190, 210, 230 and 250 bar and Crank angle. The performance and emissions results also presented on the same blends by varying load 0 to 100% full load with 20 % variation and IP 190, 210, 230 and 250 bar.

Configurations for the second module of experimentation:

a. Load (0, 20, 30, 40, 60, 80, and 100%)
b. Injection pressures (190, 210, 230 and 250 bar
c. KB+1gAP, KB+2gAP, and KB+3gAP (1 g, 2 g and 3 g MCM particles)

The Combustion, performance results on the above modules generated with ICEngineSoft software with required inputs and graphs plotted by using Origin software. The logged emission data from emission analyzers tabulated and portrayed in the form of Graphs by using Origin software.

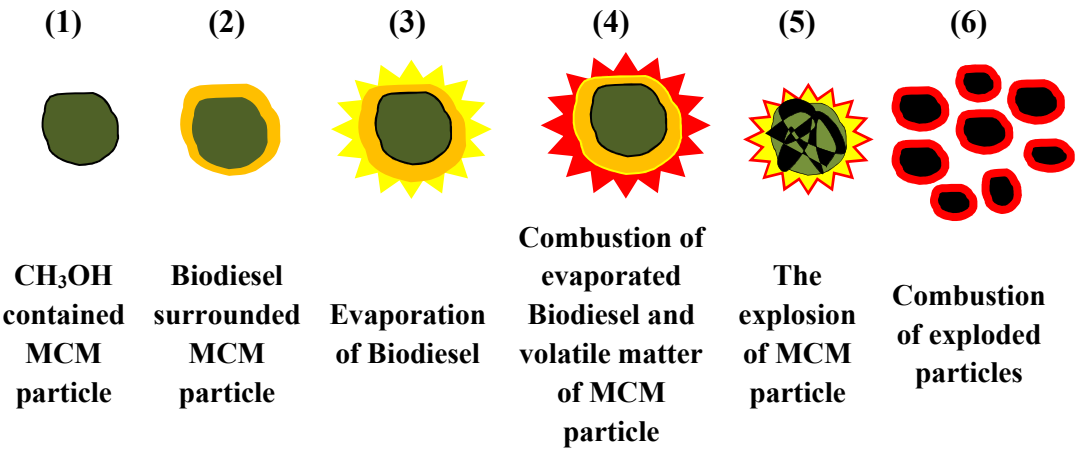

Figure 5.1 Combustion phenomena of an MCM particle in the engine cylinder

Module - 1

5.2 Combustion analysis on all fuels at SOPs, 100% load

5.2.1 In cylinder pressure (bar) vs. Crank angle (θ)

The in-cylinder pressure (ICP) peak in the premixed phase of combustion mostly depends on the amount of combustible mixture formation and rate of combustion in the ignition delay (ID) period [169]. The neat biodiesel fuels ID is less due to the presence of Oxygen, higher Cetane number though these are highly viscous and less volatile than Diesel fuel[170]. **Figure 5.2$_a$** illustrates the KB fuel has attained higher ICP peak than CB and Diesel fuels. The ICP peaks for Diesel, CB, and KB are 63.87, 64.13 and **66.32** respectively. Author Balamurugan et al.[171]described the higher peak of Karanja biodiesel is due to the lower Cetane number, higher Calorific value than CB. The higher ID of KB caused to accumulate more combustible mixture formation than CB.

In **Figure 5.2$_b$**, the higher ICP peak **72.99 bar** with CB+3gAP emulsion. This is because of higher fuel accumulation in the longer ID. The increase in MCM particles quantity in CB fuel caused to increasing fuel Kinematic viscosity, Density and decreased Cetane value, over-all Oxygen composition. The lower ICP peaks attained with the increase in LA quantity in KB fuel. This can observe in **Figure 5.2$_c$**. The literature revealed that the Lauric acid is widely using PCM material, as of its high heat absorption and storage capacity. The above capacities are the majorly influencing factors to decrease ICP peaks. These peaks are even lower than Diesel fuel.

The ICP peaks for Diesel, KB, KB+10gLA, KB+20gLA, and KB+30gLA, are 63.87, **66.32**, 60.12, 49.74, and 47.76 bar respectively. In **Figure 5.2$_d$**, the higher ICP peak with KB+3gAP is**69.74**. The KB+1gAP, KB+3gAP blends are attained higher peaks than KB+2gAP blend. This is because of multilevel micro-explosion of MCM particles and increased ID than KB fuel. Similarly, the higher fuel accumulation of KB+3gAP blend is because of higher ID. Among all fuel samples, the higher ICP peaks are achieved with MCM particles contained CB+3gAP, KB+3gAP, blends and lowest ICP peak with KB+30gLA blend.

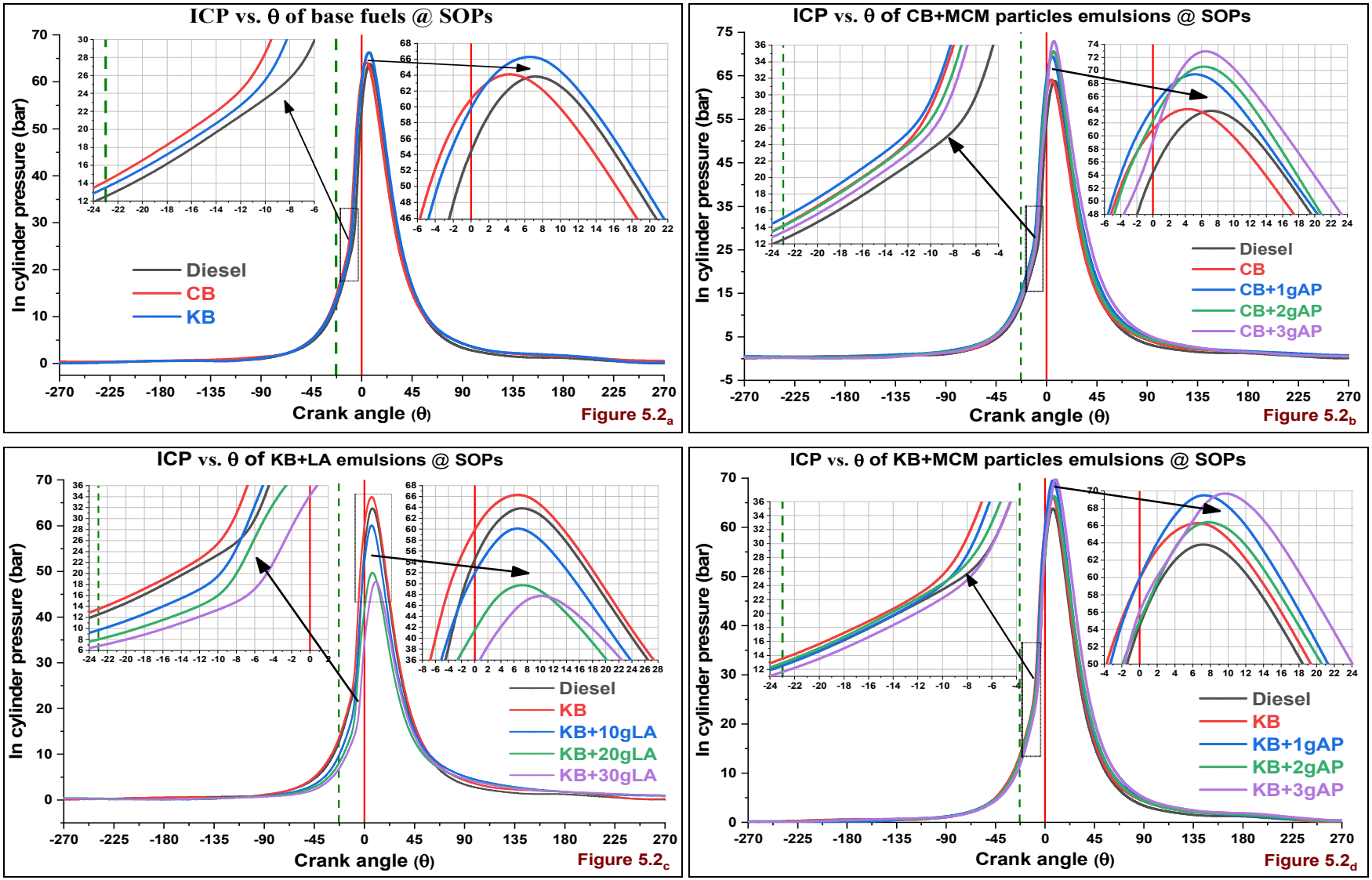

Figure 5.2a, b, c, &d ICP (bar) vs. Crank angle (θ) of all fuels @ SOPs

5.2.2 Cumulative Heat Release (kJ) vs. Crank angle (θ)

The Cumulative heat release is nothing but the aggregate sum of combustion ability of the fuel in the combustion chamber. The increase and decrease CHR of any fuel mainly depends on the fuel characteristics such as Density, viscosity, ID, and volatility, also on engine operating parameters[172]. The higher percentage of combustion at constant volume also the reason to increase CHR peak[173]. The Kinematic viscosity of biodiesel blends increases with either the increase in MCM particles addition or with Lauric acid volume.

In **Figure 5.3$_a$**the higher CHR peak of 1.02 kJ for KB fuel. The higher accumulation of KB fuel is because of higher ID, kinematic viscosity and density. The higher Cetane number of CB fuel led to less ID period and less fuel accumulation. This caused to attain diffusion combustion because of the availability of Oxygen.

In **Figure 5.3$_b$**, the higher CHR peak with CB+3gAPblendis 1.26 kJ. This is because of the explosion of particles after attaining autoignition. The CB fuel higher volatility, Cetane number, and lower kinematic viscosity and density led to lower CHR peak than MCM particles based CB blends. The lack of Oxygen in Diesel fuel led to lower CHR peak though it has the lowest Kinematic viscosity, density with higher Calorific value.

In **Figure5.3$_c$**, the 1.13 kJ CHR peak attained with KB+10gLAblend.The less quantity of Lauric acid in KB fuel induced to less reduction of calorific value. This caused to slight increase in Kinematic viscosity. Due to this reason, the CHR peak led to attain too much away from TDC even after 90ºCA.

In the **Figure 5.3$_d$**the CHR peaks for Diesel, KB, KB+1gAP, KB+2gAP, &KB+3gAP are 0.92, 1.02, 1.12, 1.07 and 1.25 kJ respectively. Due to the higher delay, Kinematic viscosity and the multilevel explosion of particles are the reasons to attain higher peak for KB+3gAP blend than all other fuel samples.

The max availability of time in ID period caused to prepare the higher amount of combustible mixture for attaining higher premixed phase peak. The diffusion combustion attained because of insufficient time to combust the prepared mixture in the premixed phase. The Diesel has lowest CHR peak than all other fuels by cause of its higher ID due to lack of Oxygen composition even though this has higher Calorific value, lower density, and Kinematic viscosity.

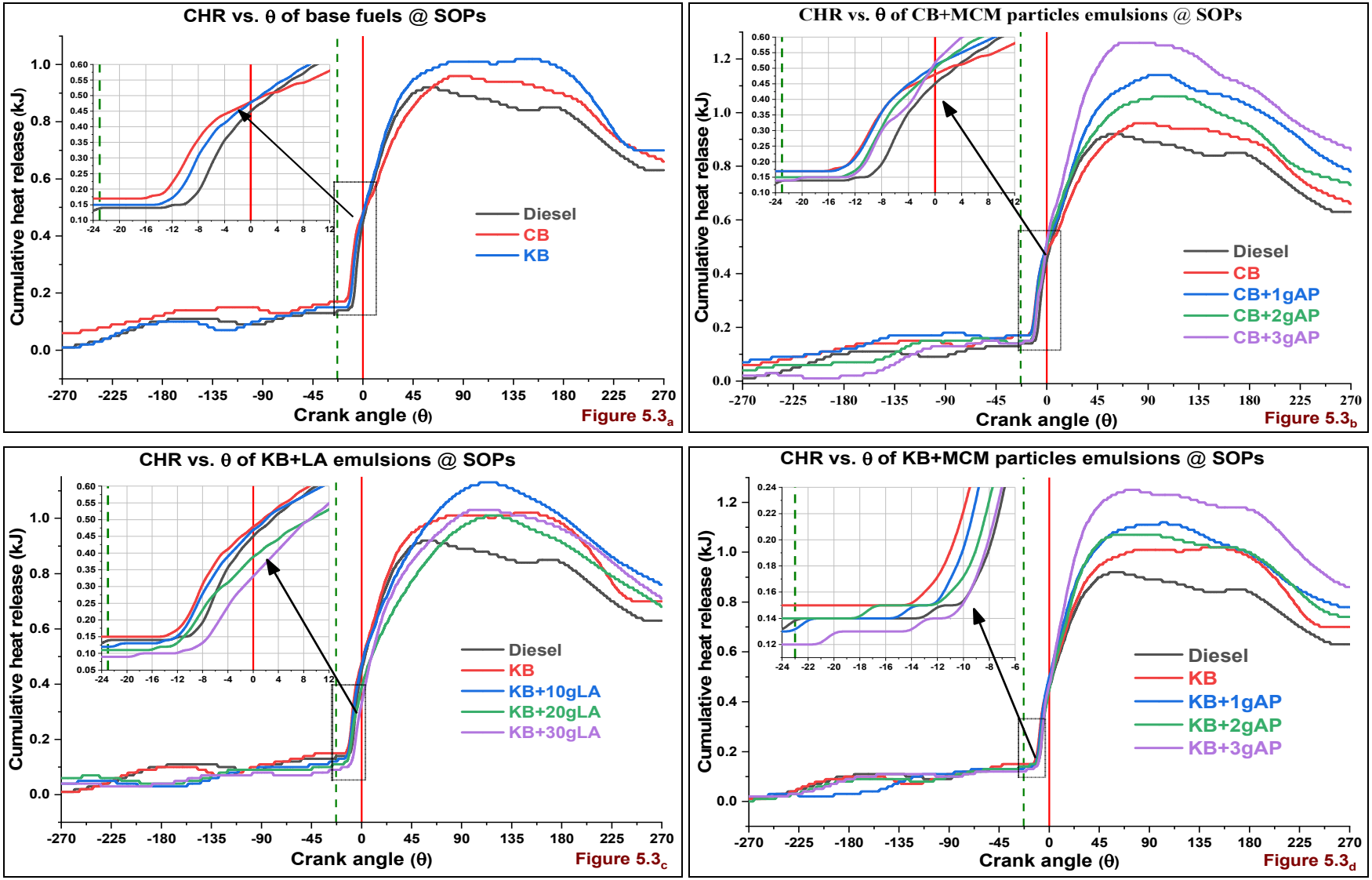

Figure 5.3$_{a, b, c, \& d}$ the CHR vs. Crank angle (θ) of all fuels @ SOPs

5.2.3 Net heat release rate (J/θ) vs. Crank angle (θ)

According to author Breda et al. [174]the higher kinematic viscosity, density, and Oxygen composition, higher bulk modulus, the lower vapor pressure of clean biodiesel fuels are influencing to earlier injection because of rapid propagation of pressure waves from the fuel pump to fuel injector needle.

In **Figure 5.4$_a$**NHRR peaks for Diesel, CB and KB are 46.64, 39.01, and 44.92J/θ respectively. The lower NHRR peaks with biodiesel fuels (CB, KB)due to less ID because of their higher Cetane number and less Calorific value. The Diesel fuel NHRR peak is higher because of its high calorific value and higher ID. The higher depression of CB in Figure 5.4$_a$just after injection of fuel into combustion is due to the presence of higher Lauric acid composition and its higher heat absorption capacity.

In **Figure 5.4$_b$**, NHRR peaks for Diesel, CB, CB+1gAP, CB+2gAP, and CB+3gAP are 46.64, 39.01, 41, 44.5, and 43.64J/θ respectively. By absorption of heat from the combustion chamber, the explosion of algal particles and their multilevel explosion influenced to increase NHRR peak. The increasing MCM particles blend ratio causing to attain multistage peaks in the diffusion combustion.

In **Figure 5.4$_c$** obtained peaks for Diesel, KB, KB+10gLA, KB+20gLA, and CB+30gLA are 46.64, 44.92, 37.97, 31.1, and **30.51J/θ** respectively. The addition of Lauric acid in KB caused to decrease NHRR peaks because of higher heat absorption from the combustion chamber for evaporation.

In **Figure5.4$_d$** NHRR peaks for Diesel, KB, KB+1gAP, KB+2gAP, & KB+3gAP are 46.64, 44.92, 46.91, 41.88, and **48.31J/θ** respectively. The accumulation of a higher quantity of fuel in ID period caused to attain higher NHRR peaks and induced to early diffusion combustion though they have lower Cetane number, Calorific value.

Among all fuel samples at standard engine operating parameter 210 bar IP &17.5 CR, the KB+3gAP blend has attained 48.31J/θ NHRR peak and KB+30gLA has attained 30.51J/θ lowest NHRR peak.

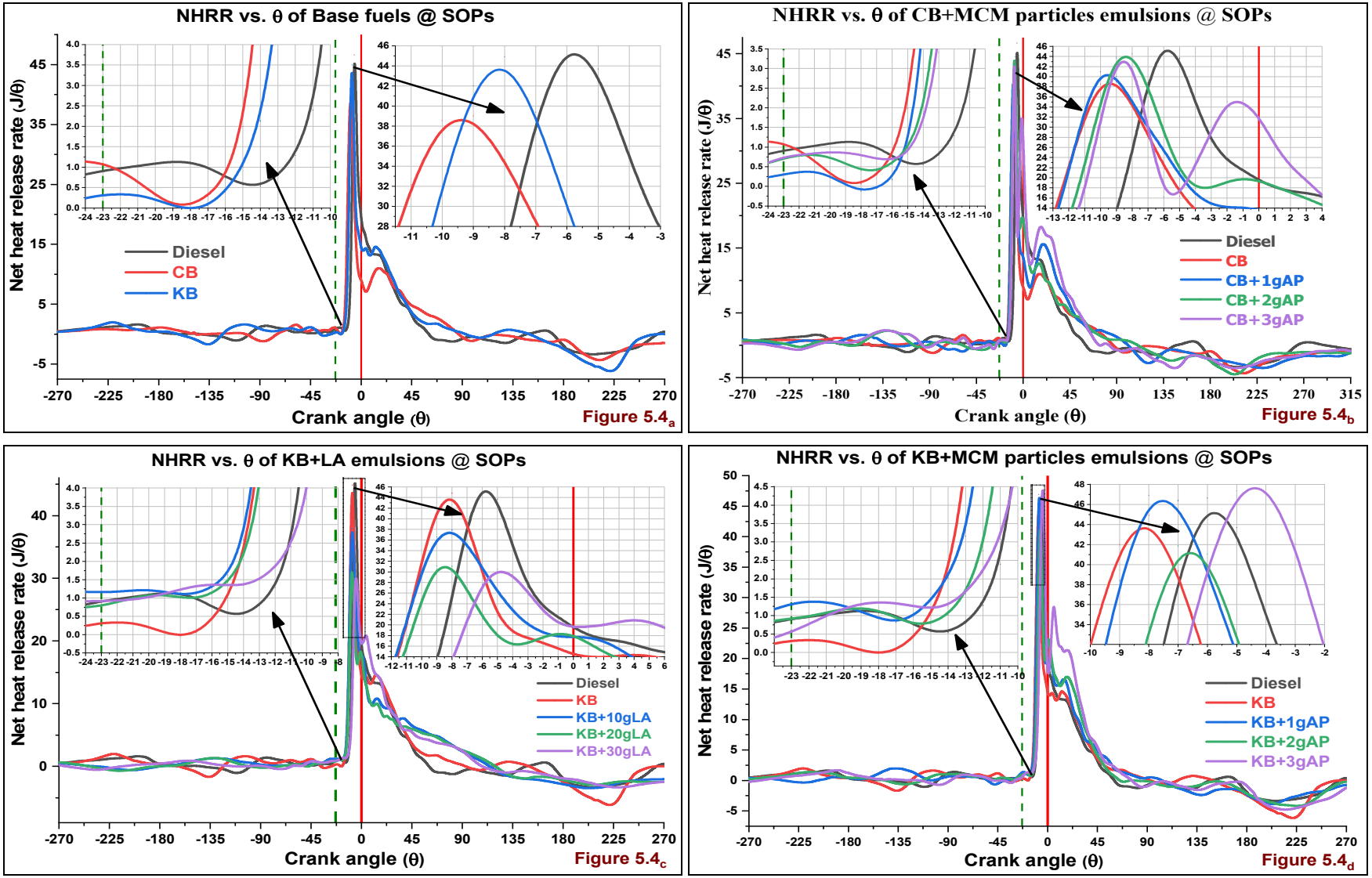

Figure 5.4$_{a, b, c, \& d}$ NHRR **vs.** Crank angle (θ) of all fuels @ SOPs

5.2.4 The rate of Pressure Rise (dP/dθ) vs. Crank angle (θ):

The behavior of MCM particles contained CB, KB fuels and also Lauric acid contained KB fuel blends Rate of pressure rise (RPR) with Crank angle (Ɵ) at 210bar Injection pressure (IP) & 17.5 Compressions ratio (CR) was portrayed in the below Figures 5.5_a to 5.5_d. As per the author Murat et al. statement[175], the rate of pressure rise increases with lower Cetane number fuels and it may lead to Knocking problem in the engine.

The observations from **Figure 5.5_a** revealed that the Diesel fuel has the highest RPR than CB, KB because of higher ID and lack of Oxygen for smooth combustion. After Diesel fuel, the KB has attained next higher peak even there are availability Oxygen and Cetane number because of its higher Kinematic viscosity and Density. The CB RPR peak was lower than the other two base fuels because of higher Oxygen, Cetane number with lower Kinematic viscosity and density than KB fuel.

Figure 5.4_b depicts the RPR variation with Crank angle of DI CI engine by blends of MCM particles in CB. The RPR peaks for Diesel, CB, CB+1gAP, CB+2gAP and CB+3gAP are 5.19, 4.59, 4.71, 5.11and 4.93bar/θ respectively. After Diesel fuel, the CB+2gAP blend has got highest RPR than CB+1gAP, and CB+3gAP blends may be due to its lower Cetane number and slightly increased viscosity and density.

The observations from **Figure 5.5_c** revealed that the Lauric acid contained KB+30gLA blend achieved lowest RPR peak than all other blends. The peak decreased as blend quantity increases in neat KB. This may be because of cool combustion due to the blend of the large quantity of Lauric acid in neat KB helped to absorb more heat from the combustion chamber.

The observations from **Figure 5.5_d** revealed that the MCM particles contained KB blends attained the highest RPR peak than Diesel &KB except for KB+2gAP blend. Among all Karanja consists of MCM particle blends, the KB+3gAP blend has reached the highest RPR peak, because of increase Viscosity, density, and lowest Calorific value, Cetane number. Among all fuel samples, the KB+3gAP blend hit the highest peak and the KB+30gLA blend achieved lowest RPR peak than all other blends.

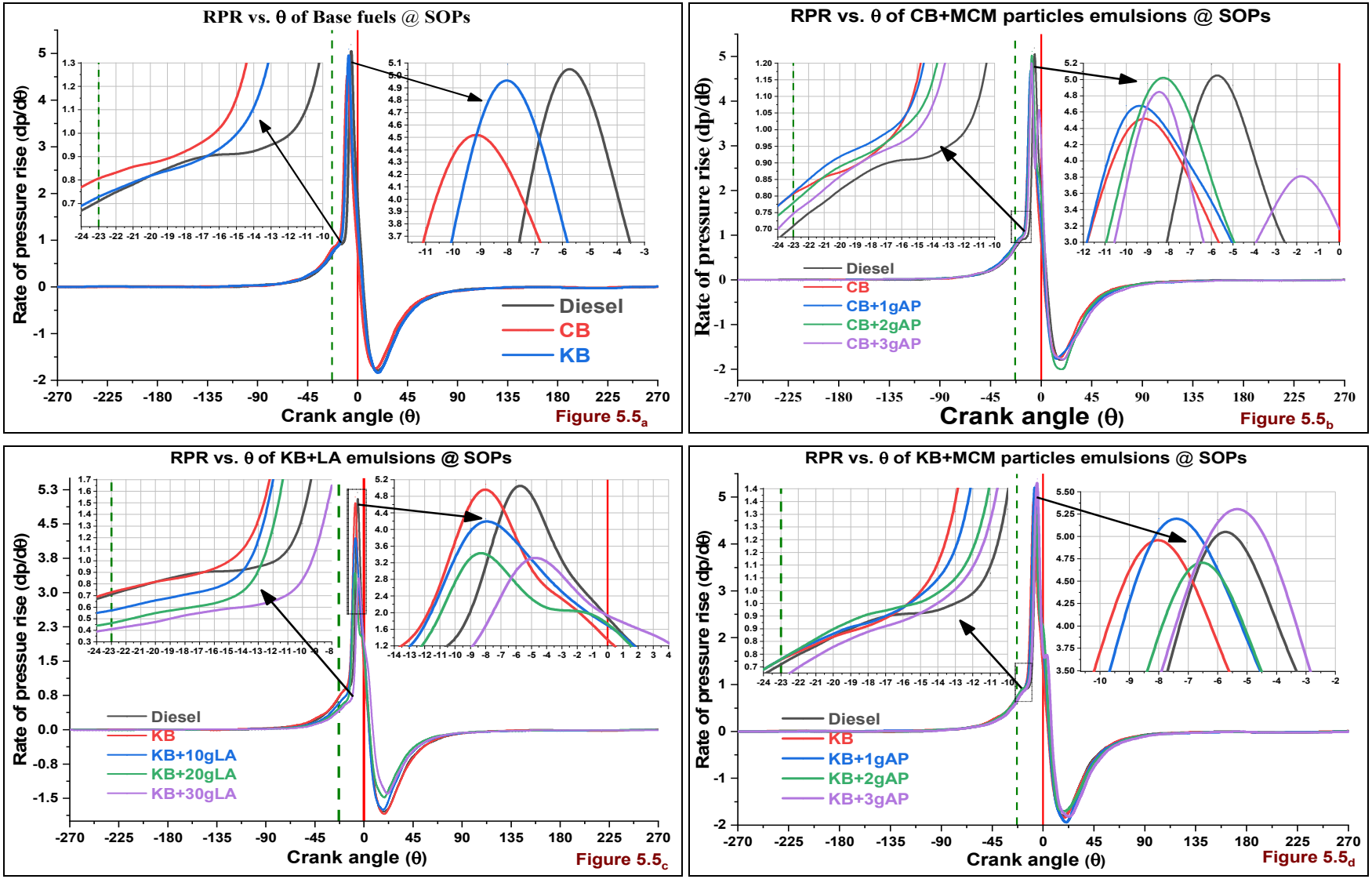

Figure 5.5a, b, c, & d RPR (dp/dθ) **vs.** Crank angle (θ) of all fuels @ SOPs

5.3 Performance analysis on all fuels at SOPs, by load variation

5.3.1 Brake thermal efficiency (%) vs. % Full load

The author An et al.[176]statement, the increase or decrease of Calorific value of any fuel mainly depends on their Hydrogen, Oxygen and Sulfur composition. The lower BTE with biodiesel fuels because of less energy content due to less Hydrogen and higher Oxygen composition.

The higher viscosity, density of biodiesel fuels reduces the Air-fuel mixing process in the combustion chamber[101]. The less BTE with higher Cetane number biodiesels fuels due to increased compression work because of much earlier combustion[177]. The higher Cetane number in CB& KB fuels caused to lower BTE in **Figure 5.6$_a$**.

The MCM particles contained CB blends BTE decreasing with increasing blend ratio by cause of increasing viscosity and density. At all loads, these blends are achieved higher BTE than CB fuel but lower than Diesel fuel because Diesel has a lower density, viscosity and has higher Calorific value. The multi-level explosion of MCM particles in premixed phase combustion caused to increase BTE this can observe in **Figure 5.6$_b$**.

Figure 5.6$_c$ describes the variation of BTE with % full load at 210 bar IP and 17.5 CR. As the LA blend ratio increases in KB fuel, the heat absorption capacity of the blends is also increasing. The higher viscosity, the density of Lauric acid based KB blends induced to absorb more heat from the combustion chamber. This heat absorption is not leading to attaining combustion because of fuel volatility problem.

In **Figure 5.6$_d$**the KB+2gAP blend has the lowest BTE than MCM particles contained KB blends because of the lower peak than KB+1gAP and KB+3gAP blends. The increased viscosity, density of MCM particles merged KB blends has lower BTE at 0% load by cause of improper atomization.

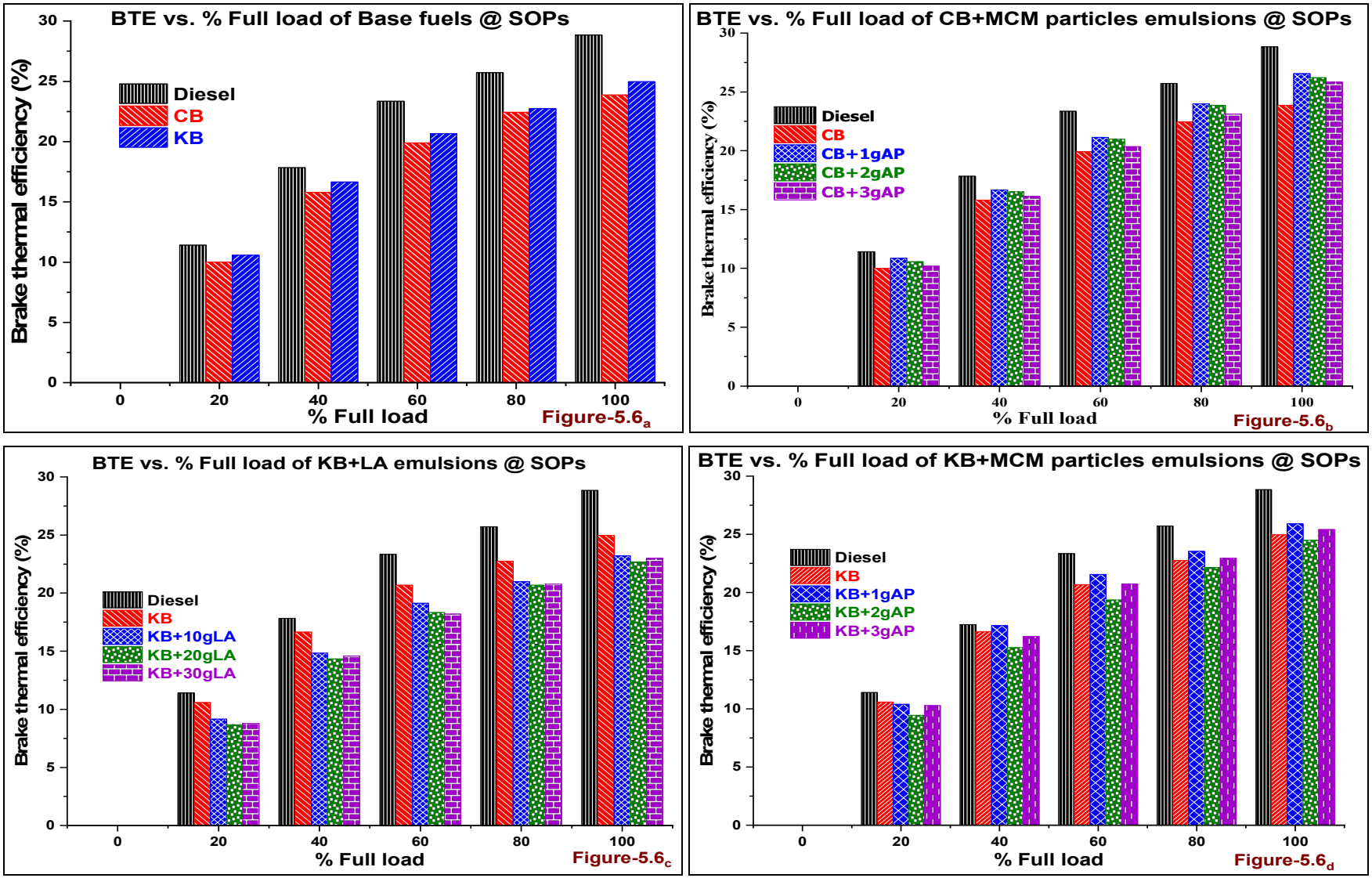

Figure 5.6$_{a, b, c, \& d}$ BTE vs. % Full load of all fuels @ SOPs

5.3.2 Brake specific Energy consumption (MJ/kW-hr) vs. % Full load

The change in Brake specific Energy consumption (BSEC) with % Full load of base fuels at 210bar IP& 17.5CRwas accessible from the Figures 5.7$_a$ to 5.7$_d$.The BSEC was the vital parameter to justify the effect of fuels which are having nearby viscosity, density and energy content, else better to present parameter BSFC for justification[172].

Figure 5.7$_a$ explores the behavior of base fuels. The Diesel fuel BSEC was lower than CB&KB by cause of its lowest Density, Kinematic viscosity, and higher Calorific value. The CB fuel has the highest BSEC then Diesel and KB because it has the lowest calorific value. The BSEC for MCM particles mixed CB blends are portrayed in the **Figure 5.7$_b$**describes the BSEC variation with % full load of CB+1gAP, CB+2gAP & CB+3gAP blends. The BSEC is for the above fuels are decreasing with increasing blend because of decreasing the lower calorific value of blends. The increasing viscosity, density, and ID also playing a major role in BSEC variation with these blends even there is slight availability of Oxygen composition.

The Lauric acid contained KB blends has highest BSEC than KB fuel by cause of the decrease in Calorific value as well as increasing Kinematic viscosity and density; this can observe in **Figure 5.7$_c$**. These blends have highest BSEC than other fuel samples due to heat absorbed by Lauric acid from combustion chamber for evaporation. This effect influenced the decrease in ICP peaks and NHRR peaks.

The variation of BTE with % full load of MCM particles blends presented in **Figure 5.7$_d$**. Here the KB+2gAP blend has highest BSEC than other blends may be because of its lower peak and increased delay and viscosity. The lower peak of the above blend is by cause of less available time for proper mixture formation than KB+3gAP blend. This hindered to attain a combustible range of MCM particles in KB+2gAP blend. The increase in particles percentage in KB fuels reasoned to increase the turbulence in the combustion due to the increased velocity of droplets[140].

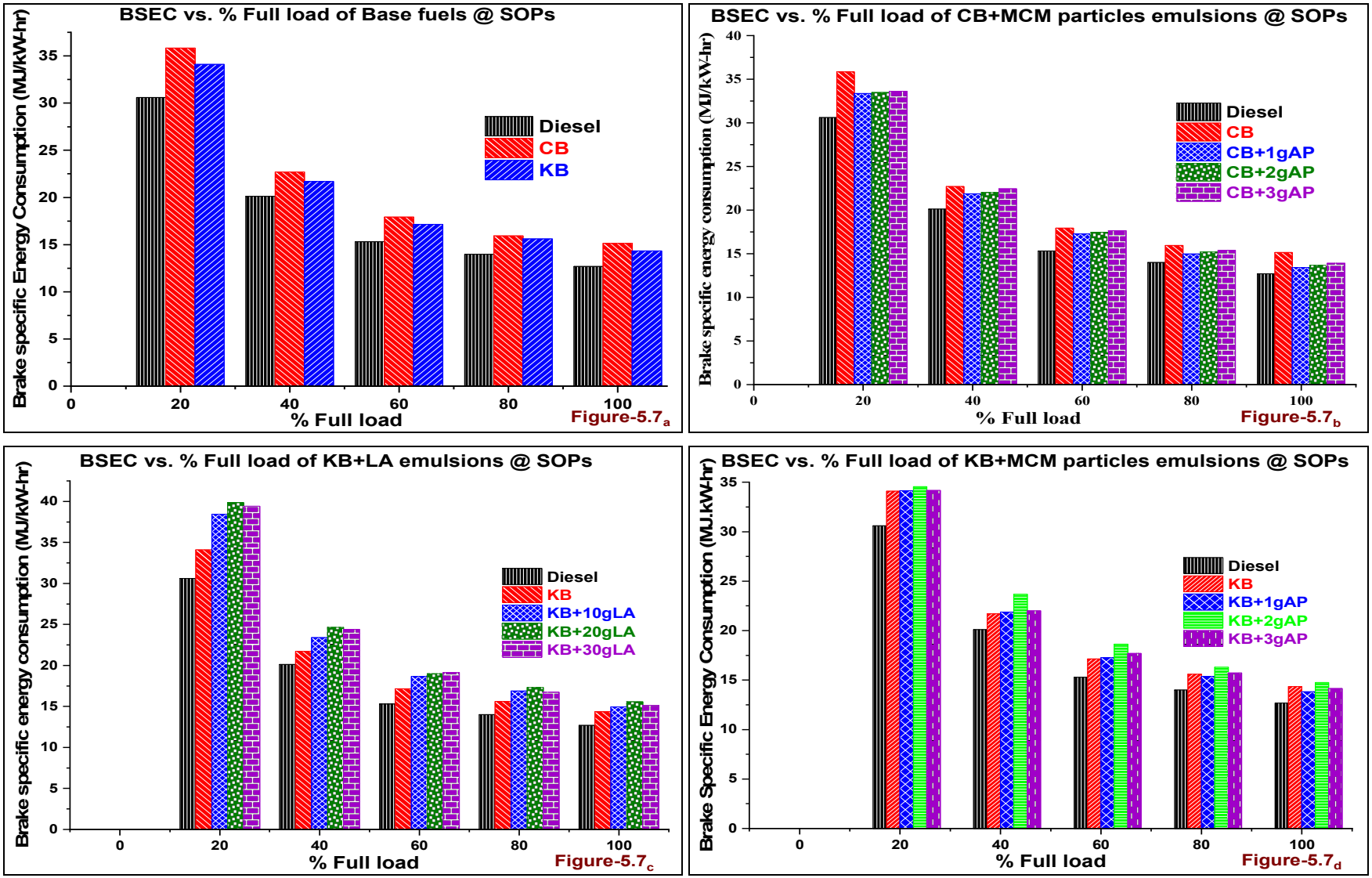

Figure 5.7$_{a, b, c, \& d}$ BSEC **vs.** % Full load of KB+AP blends @ SOPs

5.3.3 The Exhaust Gas Temperature (˚C) vs. % Full load

In **Figure 5.8$_a$** at all loads, to compensate for their less Calorific value higher quantity of biodiesel fuel needs to increase. The presence of Oxygen in biodiesels leads to reduce Calorific value. The increasing trend of EGT is due to the increase in combustion temperature by cause of availability of Oxygen. The lack of Oxygen in Diesel fuel engenders to lowest EGT than CB&KB biodiesel fuels. The higher flash, fire points and lower volatility of KB have achieved nearly the same EGT at lower loads. At all loads the KB fuel EGT higher than Diesel and CB fuels. The higher accumulation of KB fuel is due to its higher ID, viscosity, and density than CB fuel. The presence of the highest percentage of Lauric acid, Cetane number in CB fuel led to cool combustion.

In **Figure 5.8$_b$** the increasing ID and increase in fuel quantity of MCM particles included CB blends caused to decrease in the percentage of EGT concerning load. This because of the absorption of heat by MCM particles as well as the presence of inbuilt Lauric acid in CB+3gAP blends. This reduction in EGT thanCB+1gAP, CB+2gAP blends. The EGT of MCM particles contained CB blends is lower due to higher viscosity, density, and lower heating value.

In **Figure 5.8$_c$** the EGT decreases with the increase in Lauric acid quantity in KB fuel though there is an increase in ID period. The higher heat absorption and storage capacity and higher kinematic viscosity, density, less calorific value induced above effect.

Figure 5.8$_d$ describes the behavior of EGT with MCM particles emulsified KB fuel. The increasing MCM particles in KB fuel are increasing the viscosity, density, and reduction in Calorific value. The reduction of EGT with the increase in MCM particles emulsion quantity in KB fuel.

The EGT of CB+3gAP, KB+20gLA, and KB+2gAP blends are having 332.94, 351.52 and 362.69 respectively at full load. The MCM particles emulsified CB fuel blends has lowest EGT because of inbuilt Lauric acid CB and Particles.

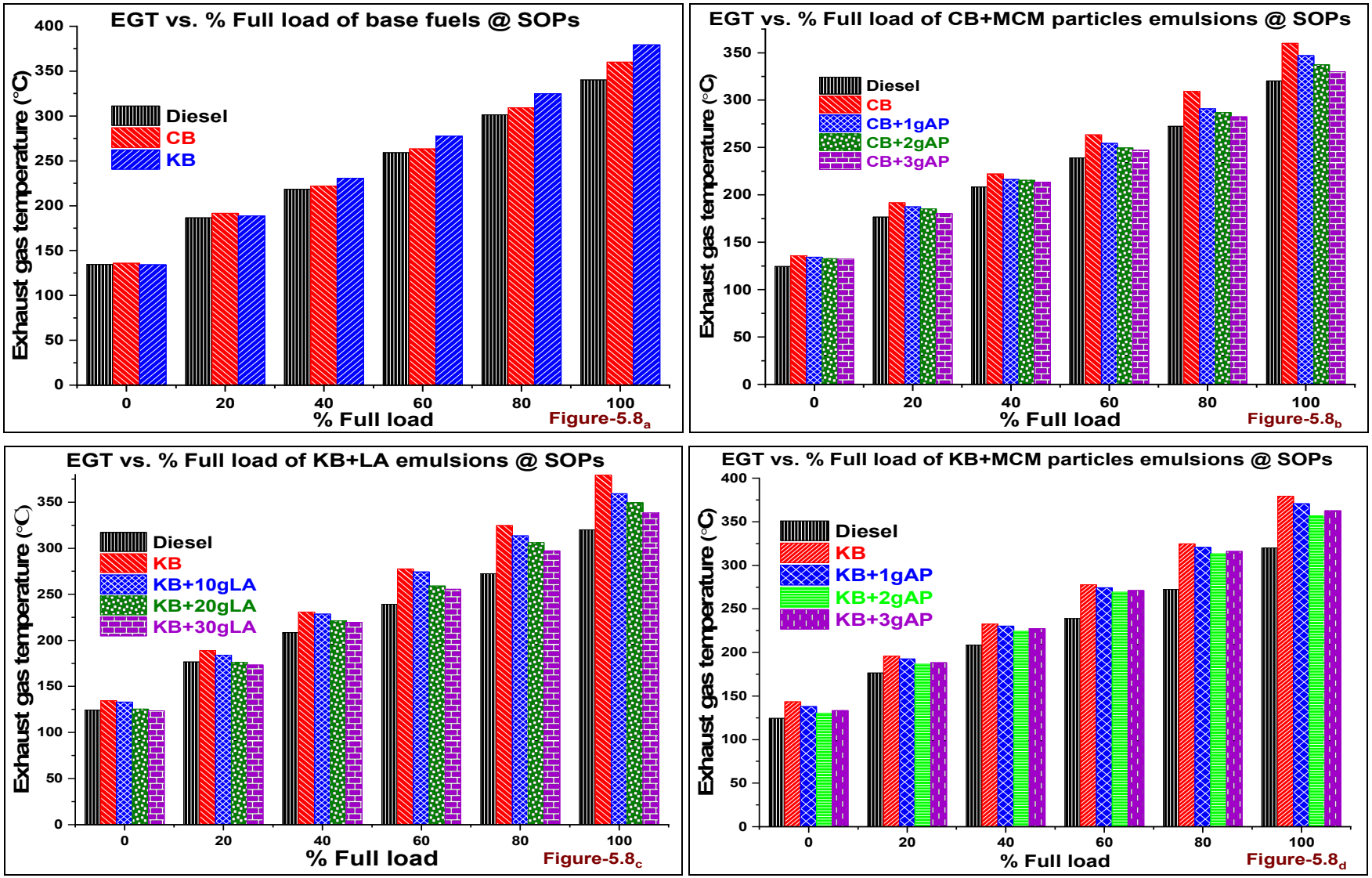

Figure 5.8$_{a, b, c, \& d}$ EGT **vs.** % Full load of KB+AP blends @ SOPs

5.4 Emissions analysis on all fuels at SOPs, by load variation

5.4.1 Carbon monoxide (% vol) vs. % Full load

In the **Figures 5.9$_a$ to 5.9$_d$**, the lowest CO emissions attained at 60% load because of availability time for mixture formation and temperature for combustion at that injected fuel quantity. The higher CO emissions from DI CI engine was the significance of incomplete combustion[5]. The CO emission for the CB fuel is lower than Diesel; KB fuels because of the higher percentage of fuel contained Oxygen, lower viscosity, and Density than KB can observe in Figure 5.9$_b$.

The slightly increased ID of KB than CB fuel, its higher viscosity, density, slightly deteriorated atomization, and less Oxygen composition influenced to fuel rich zones which increase CO emissions[178]. The CO emissions for all fuels from DI CI Engine were high at low & full load. At lower load the lack of insufficient combustion temperature, Lack of time for mixture formation at full load intended to above effect the CO emissions for Diesel fuel higher at all loads due to lack of Oxygen. Similarly, the higher viscosity, density and flash point of KB have higher CO emissions than CB fuel.

In **Figure 5.9$_b$** the MCM particles included CB fuels blends are also following a similar trend with base fuels, but these are higher than CB lower than Diesel fuel. The increased viscosity, density, and decreased calorific value induced to above effect. The MCM particles contained CB blends ID period increasing with increasing particles quantity. Because of less fuel Cetane number and calorific value but ID period less than Diesel fuel.

In **Figure 5.9$_c$** the CO emissions of KB+20gLA blend have higher CO emission than KB+30gLA blend. The ID of KB+10gLA has the highest peak and less ID than the other two blends because of lowest LA composition and higher calorific value than the other two blends.

In **Figure 5.9$_d$** the less CO with KB+3gAP blend because of higher mixture formation and improved diffusion combustion. The CO emissions are higher with the other two blends by cause of their lower peaks and higher droplet size due to higher viscosity, density, and lower calorific value.

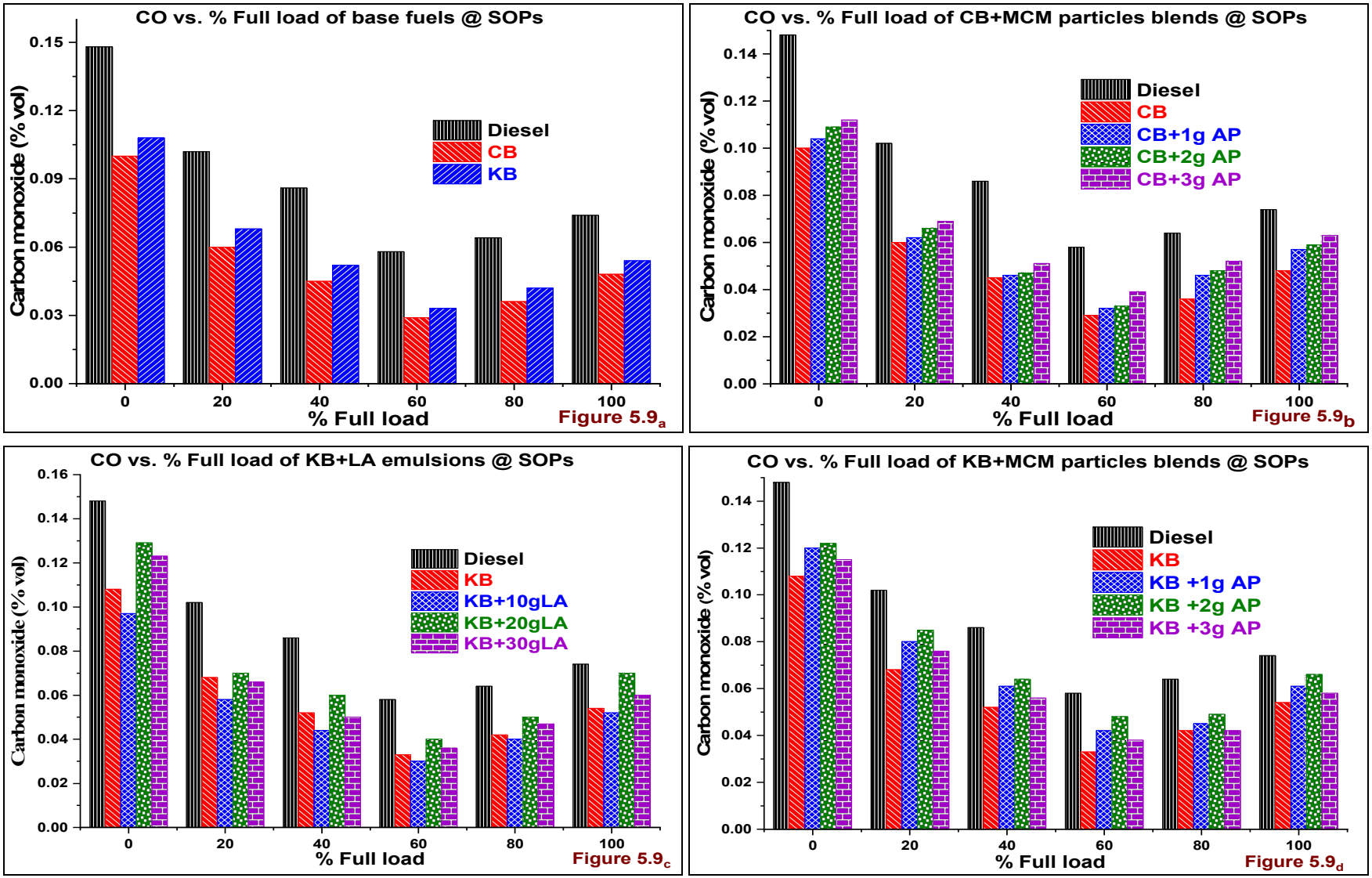

Figure 5.9$_{a, b, c, \& d}$ CO vs. % Full load of KB+AP blends @ SOPs

5.4.2 Unburned Hydrocarbons (ppm) vs. % Full load

Figure 5.10a to 5.10$_d$ interpret the variation of Unburned Hydrocarbons (HC) with % Full load of all fuels at 210 bar IP, 17.5 CR and 1500rpm. The presence of a higher percentage of Oxygen in CB fuel the HC emission was much lower than Diesel &KB fuel. The HC emission for Diesel fuels is higher by cause of lack of Oxygen even it has lower Density and higher Calorific value than CB&KB fuels. The HC emissions for KB were higher than CB due to its higher Kinematic viscosity, Density even it has Oxygen composition.

Authors Higgins et al. [179]and Genzale et al. [180]stated the increased density, viscosity, and decreased volatility, calorific value of these blends are caused to increase penetration length. In **Figure 5.10$_b$** the HC is higher for CB+3gAP blend due to its higher viscosity, density and lower calorific value than other MCM particles emulsified CB blends. These properties may be increased penetration length and to impinge on the piston head. It led to crevice formation on the piston head. The above reasons are causing to generate HC emissions with increasing blend ratio.

The trend of HC emissions with percentage Full load of DI CI engine by using Lauric acid included KB fuel bends presented in **Figure 5.10$_c$**. As the increase in the percentage of LA in KB blend leading to decrease peak even increase in ID. Due to absorption of heat from the combustion chamber even there is a time to the higher forms of a mixture in the combustion chamber. The KB+20gLA blend has the highest peak than the other two blends because of lower heat formation in the combustion chamber due to the higher melting point of LA, i.e., 43.2ºC and boiling point 298.9ºC.

The KB+2gAP blend has reached the lowest peak because of less availability of time at that viscosity & density and its lower heat value. The viscosity, density and lower heat value of KB+3gAP blend have led to increasing higher ID. The formation of higher mixture affected to attain sharp combustion peak. The prepared fuel mass did not combust in the premixed phase is attained to combust in mixing controlled combustion phase. This excess mixture attaining combustion in diffusion phase heat utilized for reaction this led to decrease combustion temperature @ 270 CA in **Figure 5.10$_d$**.

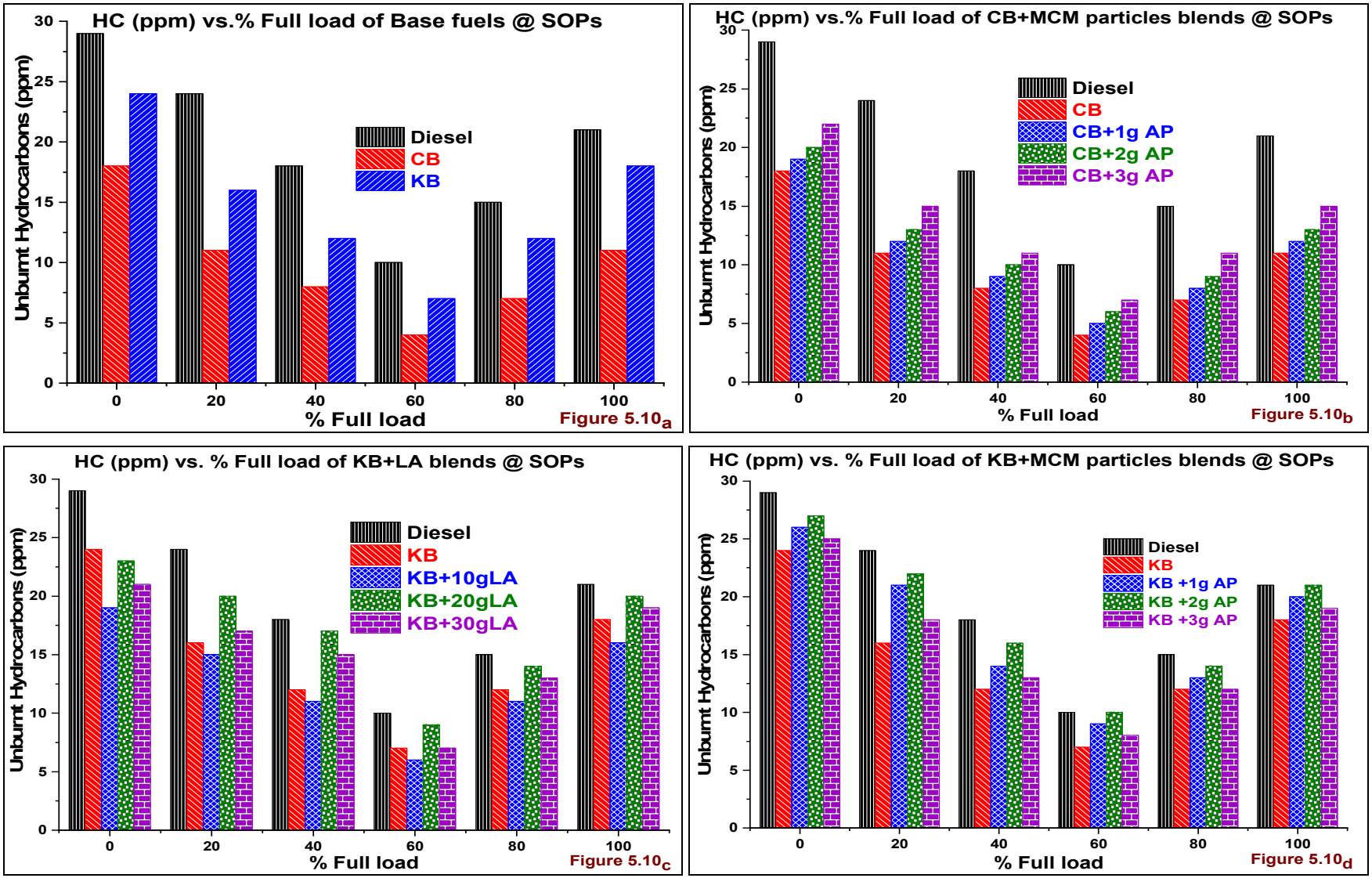

Figure 5.10$_{a, b, c, \& d}$ HC **vs.** % Full load of KB+AP blends @ SOPs

5.4.3 Oxides of Nitrogen (ppm) vs. % Full load

The NO, N_2O, and NO_2 called Oxides of Nitrogen (NOx). The Oxides of Nitrogen formed when the Nitrogen triple bond breaks at above 2200K in-cylinder temperature[181]. According to Muzio et al. [182] the availability of fuel-borne Oxygen, Nitrogen at higher combustion temperatures are the main influencing factors for NOx formation in Diesel engines. The increase in IP at fixed Injection timing (IT) with CB, KB fuels induced to increase in NOx emissions at all loads[183].

In **Figure 5.11$_a$** the KB fuel NOx emissions are higher than Diesel &CB fuels. The slightly increased ID period with calorific value and Oxygen in case of KB influenced to increase fuel accumulation and its sudden combustion in premixed phase. This occurrence led to increasing combustion temperature than Diesel and CB fuel. The higher ID lack of Oxygen in Diesel fuel led to decrease NOx though it has lower viscosity, density, and higher heating value.

In **Figure 5.11$_b$** the less Calorific value, inbuilt Lauric acid and increasing viscosity of these particles contained blends are influencing to absorb more heat for attaining evaporation before an explosion. These exploded particles are absorbing heat from the combustion chamber, i.e., in the diffusion phase of combustion, this can observe in Figure 5.4$_b$ at 315 CA.

In **Figure 5.11$_c$** the reduction in NOx emissions with percentage Full load of Lauric acid blends lower than all fuels but higher than Diesel fuel. The increase in LA blend quantity was influencing to decrease combustion temperature due to an increase in viscosity, density, and higher heat absorption capacity.

In **Figure 5.11$_d$** the KB+2gAP blend NOx reduction higher than other two MCM particles blends because of lower peak and less ID. This less ID may be due to slightly improved Cetane number at better air/fuel mixture proportion. This led to less fuel accumulation and less peak.

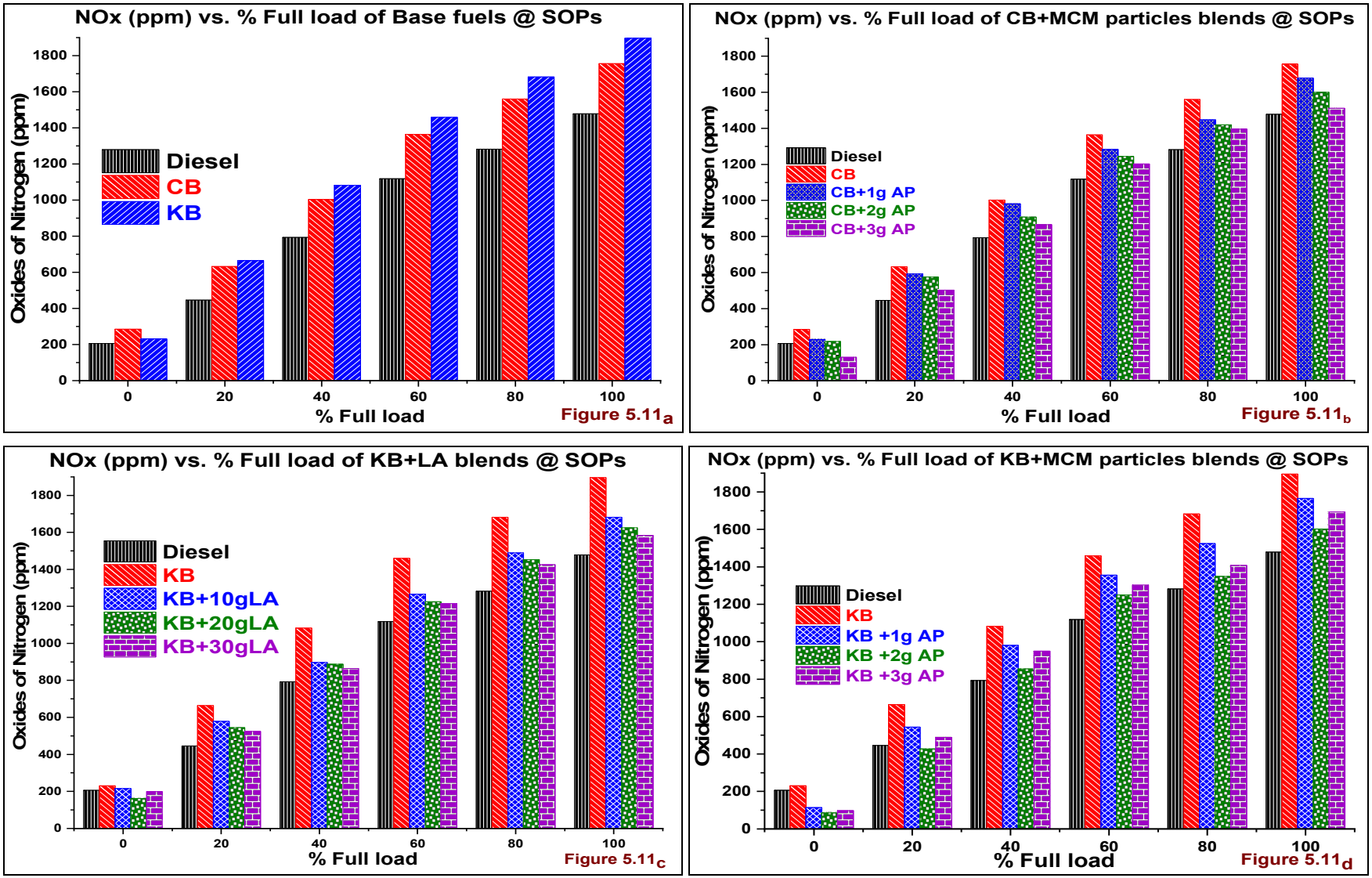

Figure5.11$_{a, b, c, \& d}$ NOx **vs.** % Full load of KB+AP blends @ SOPs

5.4.4 Smoke opacity (%) vs. % Full load

According to Medipally et al. [184]as the load increases the Smoke opacity (%) also increases by cause of the increase in fuel consumption with the load. Below the engine rated load condition, the neat biodiesel fuel Smoke opacity will be lower due to the improvement in mixing controlled combustion by cause of availability of Oxygen[187]. The smoke opacity increasing with the load under free radicals delayed Oxidation rate with hydroxyl group[186]. In **Figures 5.11$_a$** to **5.11$_d$**, the Diesel Smoke opacity was too high than CB&KB because of the presence of aromatics, ring, branched structures, thermal stability &lack of Oxygen. The KB fuel Smoke opacity is higher than CB is due to the improper atomization by cause of higher Kinematic viscosity, Density and also lower Oxygen composition. The CB fuel lower viscosity, density, ID and higher fuel carried Oxygen than KB fuel reasoned for highest Smoke reduction.

In **Figure 5.11$_b$** the reduction in Smoke opacity with the increase in MCM particles with CB and KB fuels due to the increased surface area to volume ratio of particles and their turbulence. This effect will lead to the early start of Diffusion combustion and multiple peaks with higher blends. The presences of Oxygen in the MCM particles after surrounded biodiesel combustion causing the explosion in the diffusion phase of combustion. The traces of Oxygen in the MCM particles because of the addition of methanol in the preparation level[187].

The observations from **Figure 5.11$_c$** revealed that the Lauric acid emulsified fuels viscosity, density increases with increasing LA blend quantity. This led to increase the fuel droplet size. The ID for KB+30gLA fuel was even higher than Diesel fuel. This result because of Lauric acid higher melting point, higher heat absorption for evaporation.

In **Figure 5.11$_d$** the increased quantity of MCM particles let to increase their surface area to volume ratio. The enhanced air/fuel mixing in the combustion chamber. Here the lower size particles are attained combustion in premixed phase, and higher size particles are exploding in the Diffusion phase of combustion. The KB+2gAP sample has higher Smoke than other two blends due to less accumulation of fuel in the less ID period.

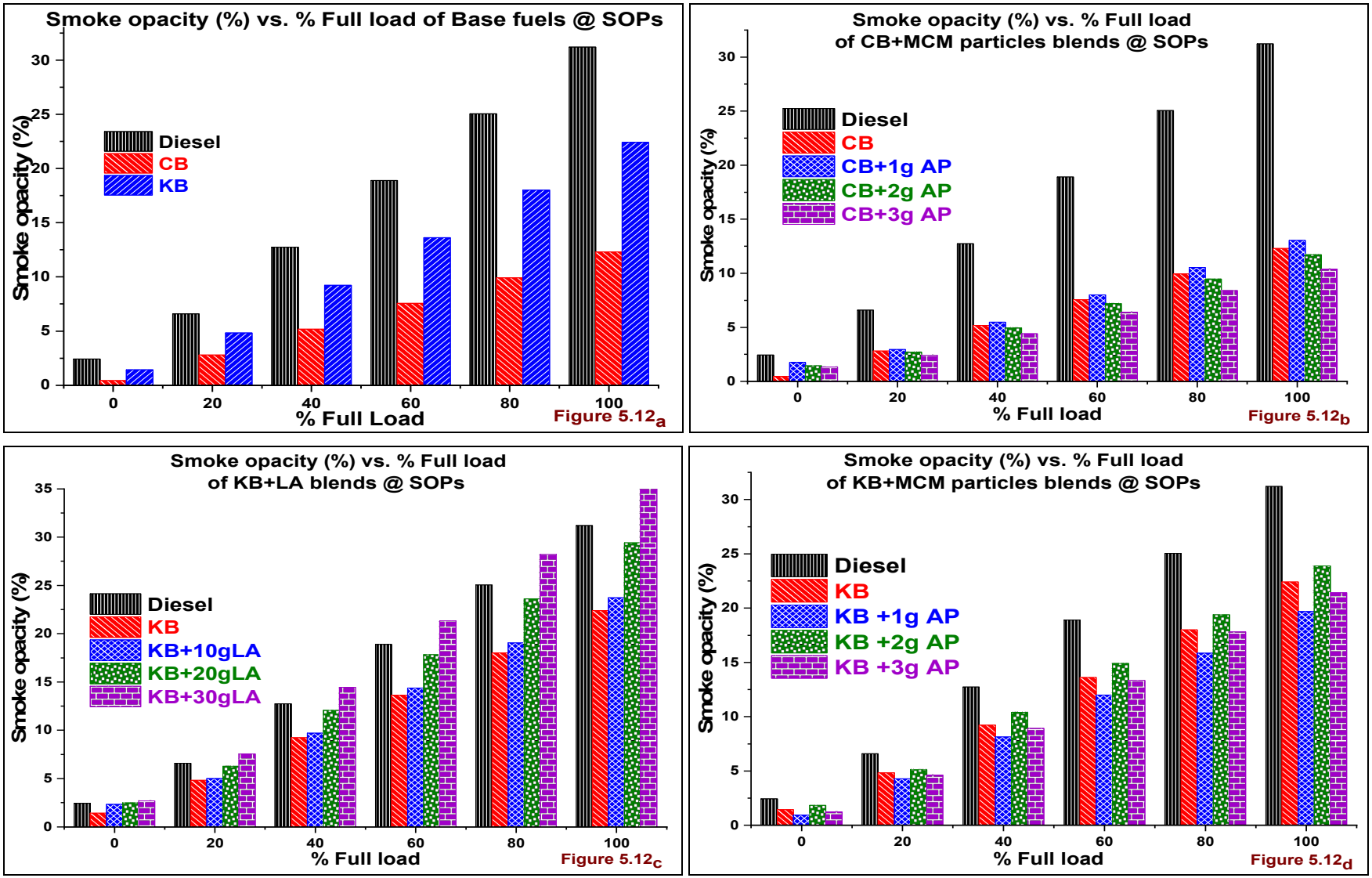

Figure 5.12a, b, c, & d Smoke opacity **vs.** % Full load of KB+AP blends @ SOPs

Module - 2

In this module, the author tested DI CI engine by varying Injection pressures on each blend. To reduce the impact of the higher viscosity of MCM particles included CB blends with the increase in blend ratio. This viscosity increase of blends has badly influenced higher CO and HC emissions formation in DI CI engine. To compensate these issues, the author applied the injection pressure variation between 190 to 250 bar with the 20bar interval. The injection pressures on DI CI engine varied by adjusting nut in the injector and ensured the injection pressure with the injection pressure testing setup.

5.5 Combustion analysis on CB+MCM blends @ Full load, 17.5 CR, 1500rpm

5.5.1 In cylinder pressure (bar) vs. Crank angle (θ), IP

As per the discussions made in the earlier section 5.2.1, the increasing MCM particles quantity leading to increasing fuel droplet size because of increased kinematic viscosity and density. The observations from **Figure 5.13a** revealed similarity results of authors Enweremadu et al.[188] & Tewari et al. [189]. The increase in MCM particles quantity helped to increase surface area to volume ratio and to improvements in the mixing process. The ICP peaks in Figure 5.13a increased with the increase in Injection pressure of CB+1gAP blend at 17.5 CR and 1500rpm.

At injection pressure 210, 230 and 250 bar the ID period for CB+1gAP fuel lower than CB fuel. Because of the decrease in droplet size, greater evaporation due to atomization, and flame spread the entire combustion chamber by cause of proper air, fuel mixing[190].In the Figure 5.13athe obtained peaks at IPs 190, 210, 230, and 250 bar of CB+1gAP blend are 67.64, 69.49, 68.93, and 69.64bar respectively. The obtained peaks for CB+1gAP blend were higher than base fuels, i.e., and this has attained higher 69.64bar peak at 250 bar IP.

Here the increased IP helping to attain higher combustible mixture formation with less ID because of atomization. At higher IP the turbulence is occurred due to the increase in the surface area to volume ratio. **Figure 5.13b** depicts the similar outcomes of Figure 5.13a, but the increase in MCM particles quantity, i.e. CB+2gAP fuel the surface area to volume ratio is becoming higher than CB+1gAP blend. The higher injection pressure CB+2gAP fuel particularly at a full load of operation the fuel quantity is increased and causing to fuel penetration[100].

In **Figure 5.13$_c$** the CB+3gAP fuel has the higher kinematic viscosity, density and also reduction in Calorific value. These are the significant properties are influencing to decrease in ICP peaks of this blend due to increased penetration. The higher kinematic viscosity and density led to an increase in droplet size. This higher diameter droplet takes more time for evaporation it leads to increase ID than other blends. The higher bulk modulus and higher viscosity of biodiesel fuels are increasing the inline pressure of the fuel.

This higher inline fuel pressure leads to increasing penetration of spray, and this may be causing to impingement of fuel on cylinder walls as well as on piston head. Because of the higher surface tension, the viscosity increased the liquid length and decreased Weber number of CB+3gAP blend[178]. Based on the above factors the ID is decreasing with the increase in IP on the same fuel (CB+3gAP) blend and also leads to decrease ICP with an increase in IP. This phenomenon can observe in Figure 5.13$_c$.

The observations from Figure 5.13$_a$, 5.13$_b$, and 5.13$_c$are obtained higher ICP peak ofCB+1gAPfuel at 250 bar IP, the CB+2gAP fuel at 230 bar IP and the CB+3gAP fuel at 210 bar IP respectively. Among all fuels, the higher ICP peak attained with CB+3gAP fuel 72.99 at 210 bar IP. The sufficient ID, higher surface area to volume ratio and the multilevel explosion of MCM particles are the reasons to increase ICP peak.

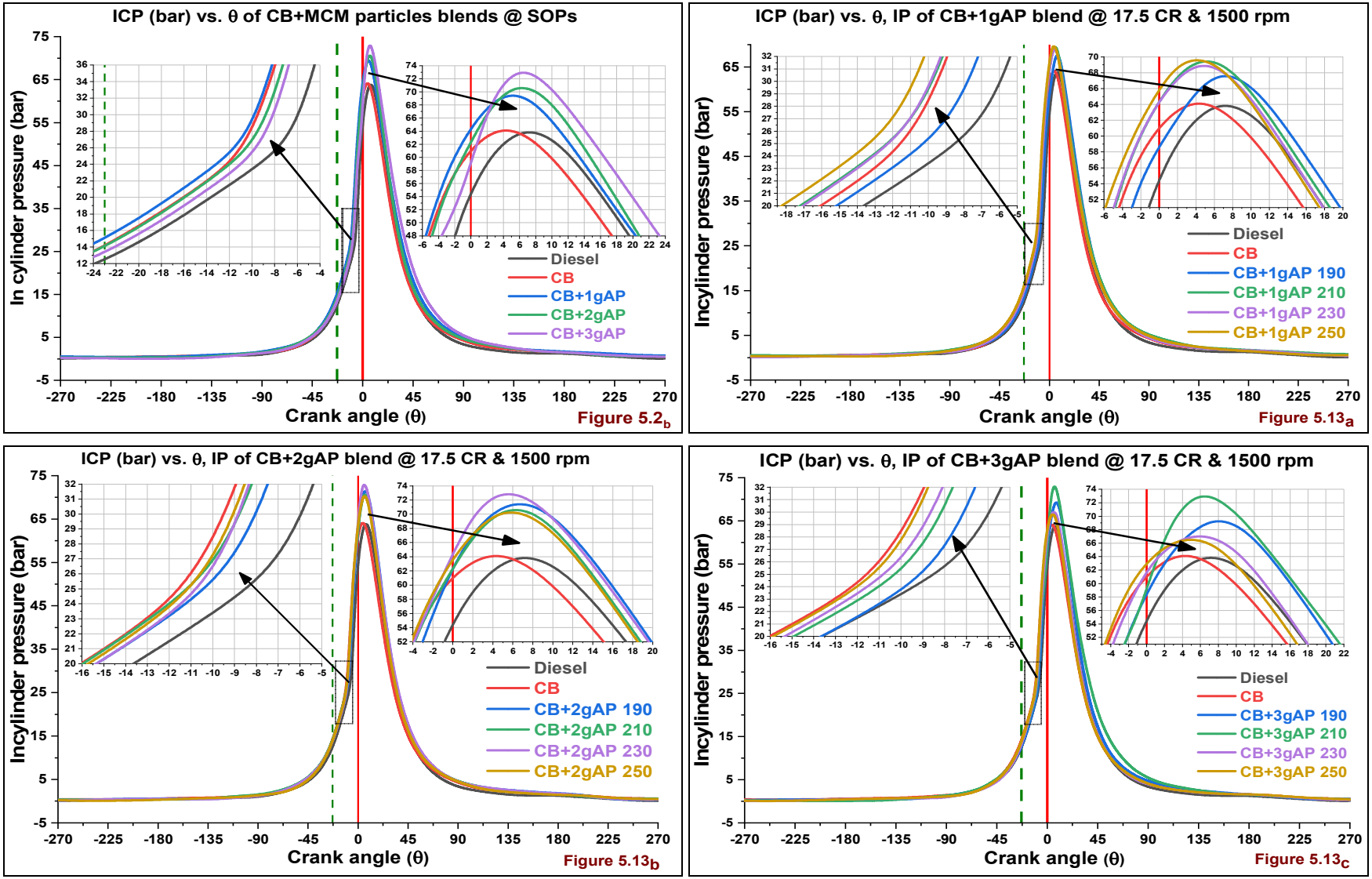

Figure 5.13$_{a, b, c}$ ICP **vs.** Crank angle (θ) & IP of CB+MCM blends

5.5.2 Cumulative Heat Release (kJ) vs. Crank angle (θ), IP

The significant increase in surface area to volume ratio and the more extended ID period of CB+3gAP blend induced to proper air/fuel mixing. At this point, the combustion improved because of the multilevel explosion of MCM particles and this induced to attain early CHR peak, i.e., 1.26kJ at 210 bar IP.

The findings from this **Figure 5.14$_a$** illustrates that the highest CHR peak obtained at 250 bar IP after 190 bar IP. The highest CHR peak is 1.20kJ at 190 bar IP because of a higher ID. The maximum particles accumulated in the combustible mixture formation. The explosion of MCM particles reasoned to increase CHR peak. Coming to the second highest CHR peak 1.19kJ at 250 bar IP because of proper atomization influenced to increase the combustible mixture formation even there is less ID than CB.

In **Figure 5.14$_b$**the CB+2gAP fuel attained highest CHR peak 1.11kJ at 230 bar IP. Due to the impingement of fuel jet to the cylinder walls at 250 bar IP. At 250 bar IP the CHR peak even though lower, i.e., 1.08kJ but this peak attained earlier than 230 bar IP. The CHR peak at 190 bar IP 1.09kJ may be higher than 250 bar IP, but CHR peak delayed this portrayed in Figure 5.14$_b$.

As per the discussion made in section 5.2.2, the ID is increasing with increasing blend ratio at standard IP 210 bar. The same thing can observe in **Figure 5.14$_c$**, i.e., as the increase in IP increasing penetration this induced to impingement of fuel jet with cylinder walls and on the piston head. The highest peak appeared at 210 bar IP with CB+3gAP fuel due to increase delay for attaining higher combustible mixture.

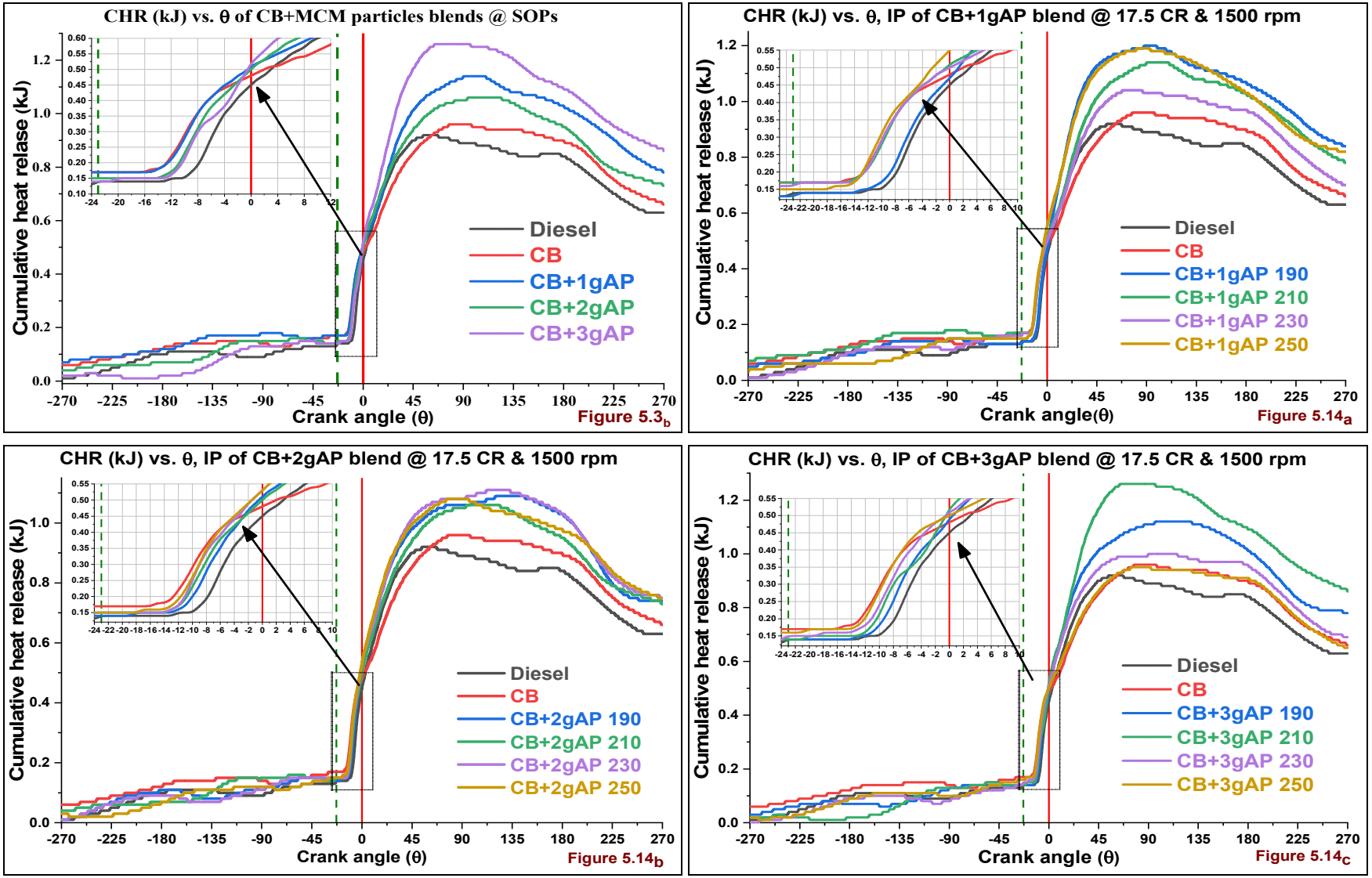

Figure 5.14$_{a, b, c}$ CHR **vs.** Crank angle (θ) & IP of CB+MCM blends

5.5.3 Net heat release rate (J/θ) vs. Crank angle (θ), IP

The discussions on Figure 5.4$_b$ presented in the earlier section 5.2.3. In **Figure 5.15$_a$**, the ID rose with increasing blend ratio. The combustion of minimal size MCM particles led to higher NHRR attainment in premixed phase combustion. The higher size particles are combusting in the mixing controlled combustion phase. The peaks in this phase are due to explosion and combustion of higher size particles after attaining evaporation.

This effect was higher in case of higher blends of MCM particles in the CB fuel at 210 bar IP. The author Piriou et al.[145]presented a similar justification in his article. In the **Figure 5.15$_b$** the higher NHRR peak 49.13 (J/θ) for CB+2gAP fuel at 230 bar IP because of sufficient ID period for combustible mixture formation and proper fuel dispersion. The CB+2gAP blend at 250 bar IP has induced to lower peak than 230 bar IP.

By cause of impingement of fuel jet on the cylinder wall and Piston head. In **Figure 5.15$_c$** the NHRR peak higher for CB+3gAP blend at 250 bar IP, but it is lower than 190 bar. At 250 bar, IP the CB+3gAP blend underwent proper atomization with less ID though it has high viscosity. At lower IPs 210, 230 bar the CB+3gAP blend led to improper mixing may be due to increased droplet size by cause of higher viscosity and density.

The NHRR peak was higher at 190 bar due to the increase in ID period, the viscosity for higher fuel accumulation. Among all fuel samples, the CB+2gAP fuel attained the higher peak of 49.13 (J/θ) at 230 bar IP. At this IP the CB+2gAP fuel undergoes sufficient time for required fuel accumulation for proper combustion in the combustion chamber.

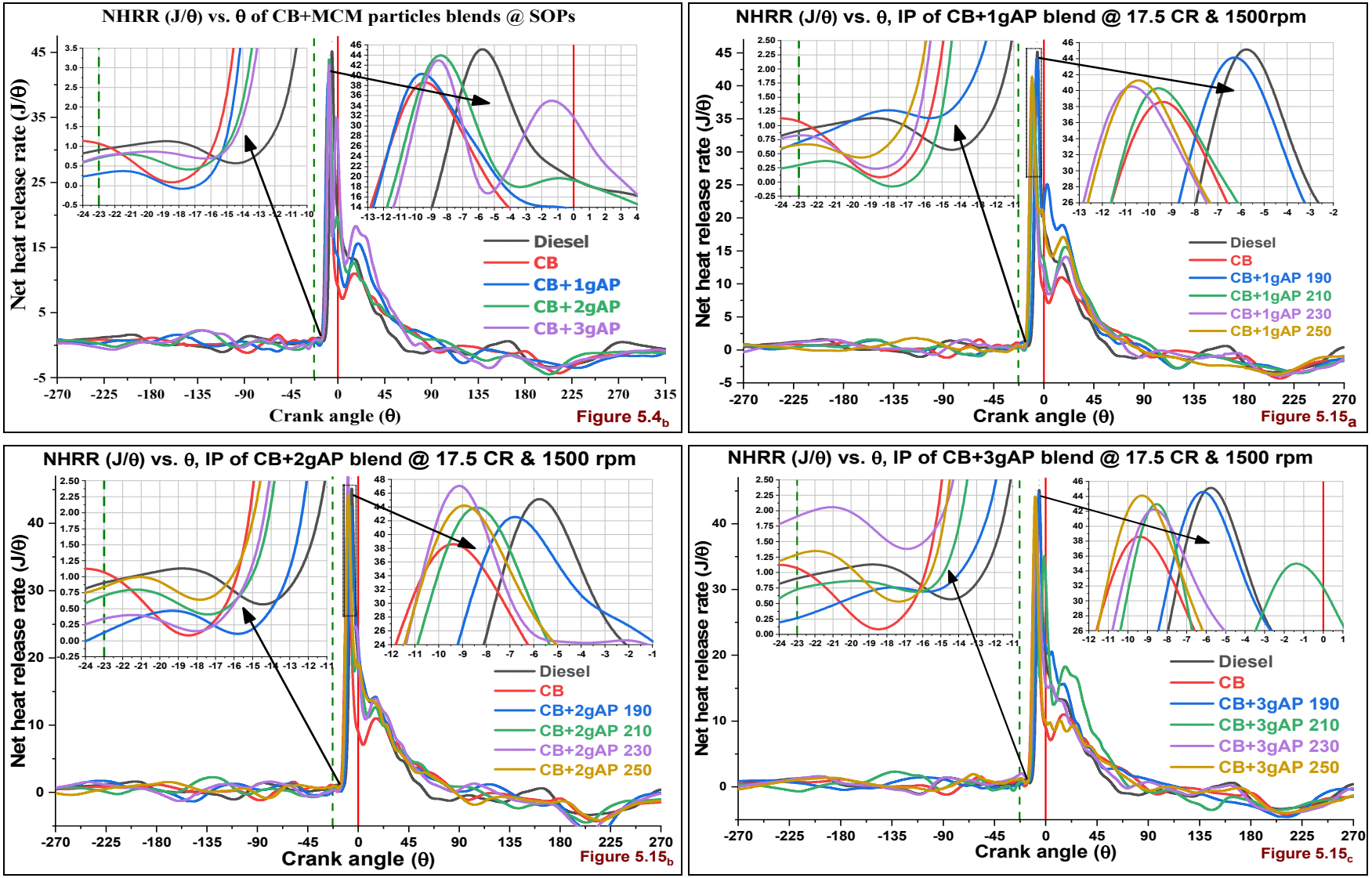

Figure 5.15a, b, c NHRR vs. Crank angle (θ) & IP of CB+MCM blends

5.5.4 Rate of Pressure Rise vs. Crank angle (θ), IP

The **Figures 5.16$_a$** to **5.16$_c$** explains the behavior of MCM particles emulsified CB samples on DI CI engine Rate of pressure rise (RPR). The increased ID period leads to an increase in the rate of pressure rise, and this leads to knocking. In the case of neat biodiesel fuels due to higher Cetane number the less ID and lower RPR[191]. In **Figure 5.16$_a$** the RPR is higher for 190 bar IP because of the higher ID period.

As we discussed above the RPR has been higher for higher ID period. After the Diesel fuel the RPR peak 5.19 at 210 bar IP then the higher RPR peak 4.82bar for CB+1gAP fuel at 190 bar IP because of the higher ID period. In **Figure 5.16$_b$** the higher RPR of CB+2gAP fuel at 230 bar IP. The increased fuel viscosity, density of fuel led to increasing fuel penetration. This RPR peak even more than Diesel fuel through the fuel contains Oxygen.

The higher RPR peak of 5.42 at 230 bar IP attained due to the accumulation of more fuel in less ID period and its sudden combustion. In **Figure 5.16$_c$** the higher RPR of CB+3gAP fuel are 5.16, 4.93, 4.88, and 5.11 at 190, 210, 230 and 250 bar respectively. The higher peak at 190 bar IP because of the higher ID period and due to increased penetration. The higher RPR peak also can observe in Figure 5.16$_c$ at 250 bar IP.

This because of the proper mixing of CB+3gAP fuel in the combustion chamber though there are less ID period and its rapid combustion. The higher RPR peaks for CB+1gAP fuel at 190 bar, CB+2gAP at 230 bar and CB+3gAP at 190 bar. The present work has shown the similar RPR results of the author Lahane et al. [191]. The higher RPR peak with MCM particles emulsified CB fuel sample is attained mostly at lower IP, i.e., 190 bar. At this IP the ID period higher than all other IPs.

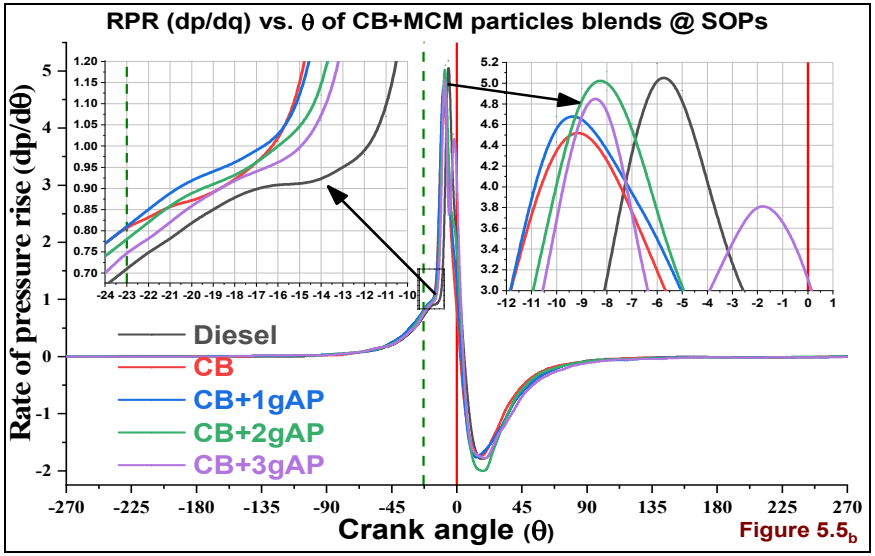

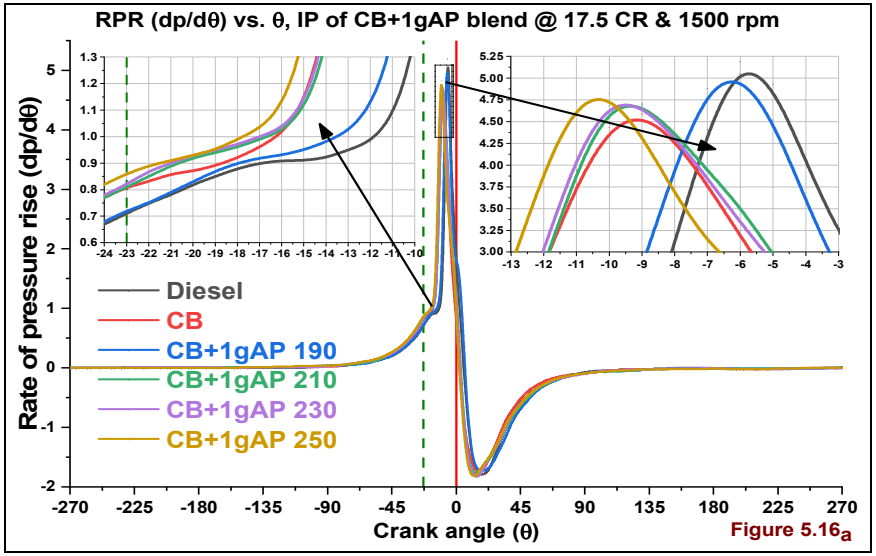

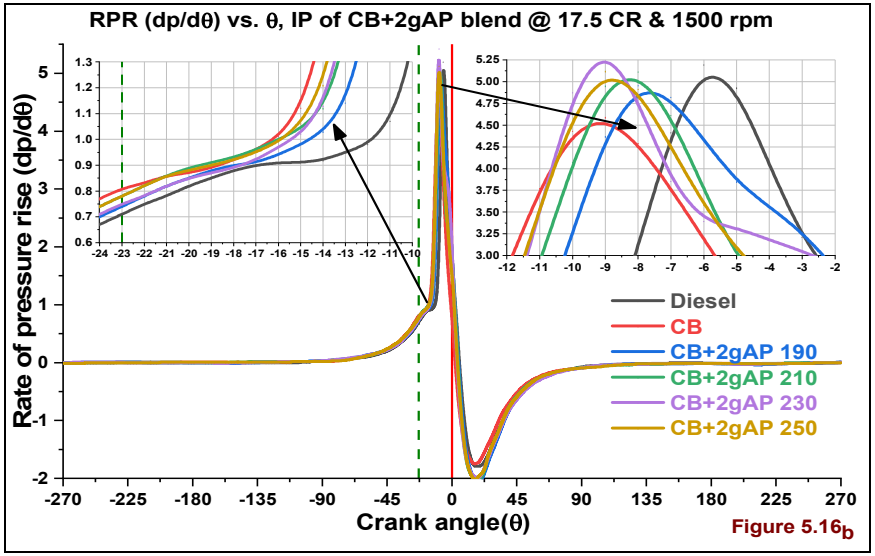

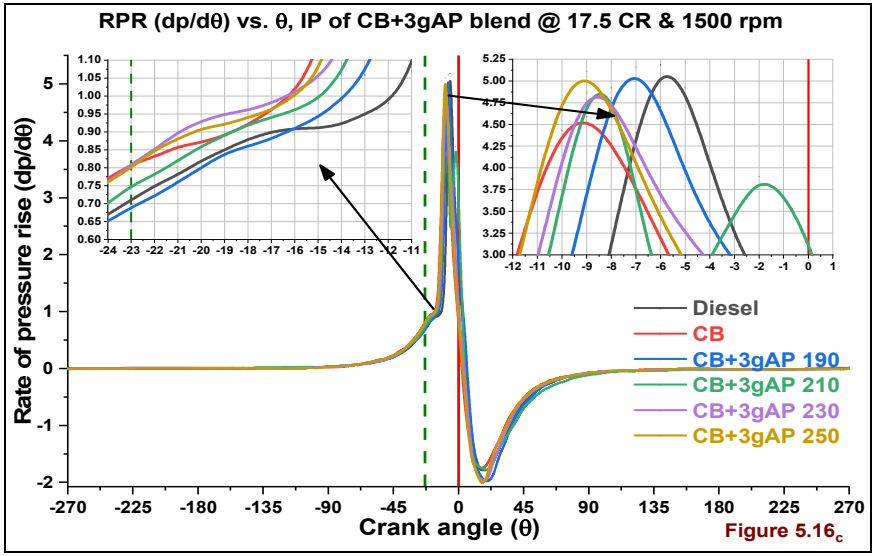

Figure 5.16a, b, c RPR vs. Crank angle (θ) & IP of CB+MCM blends

5.6 Performance analysis on CB+MCM blends@ % Full load, 17.5 CR, 1500rpm

5.6.1 Brake thermal efficiency (%) vs. % Full load, IP

The higher calorific value of pure diesel fuel caused to increase BTE than all fuels at all loads. The micro level explosion of MCM particles into tiny particles and their combustion are caused to increase BTE than CB. The viscosity of emulsified fuels is increasing with increase in MCM particles quantity in CB. The main objective to increase IP is to atomize the fuel for faster evaporation in ID period.

In **Figure 5.17$_a$** the Brake thermal efficiency (BTE) of CB+1gAP fuel increasing with increasing IPs. This is because of proper atomization within the less ID period. The observations from Figure 5.13$_a$ revealed that the ICP peak near to TDC at 250 bar IP but at 190 bar IP the ICP peak away from the TDC. That is at lower IP 190 bar due to improper atomization the droplet size may increased due to which the ID also increased. At this increased ID period, the maximum amount of fuel accumulated for combustion. The presence of MCM particles in fuel blends increasing surface area to volume ratio. This led to increasing the mixing process as well as BTE.

The observations on **Figure 5.17$_b$** illustrates that the increased IP has shown an adverse effect on BTE i.e., the higher BTE observed at 230 bar IP than 250 bar. This is because of a slight improvement in viscosity and reduction in calorific value of CB+2gAP fuel. This increased viscosity and increased particles quantity caused to the increased surface area to volume ratio of MCM particles. This influenced fuel penetration, over mixing and air entrainment.

In **Figure 5.17$_c$** the BTE increased with the increase in IP though there is an increase in viscosity and reduction in CB+3gAP fuel Calorific value. Here the improvement in air-fuel mixing at 250 bar IP in combustion chamber let to increase BTE through the CB+3gAP fuel is viscous. In Figure 5.13$_c$ the ICP peak may be higher at 190, 210 bar IPs but at 250 bar IP peak near to TDC. This led to improving the BTE of CB+3gAP fuel at 250 bar IP than 210 and 230 bar IP.

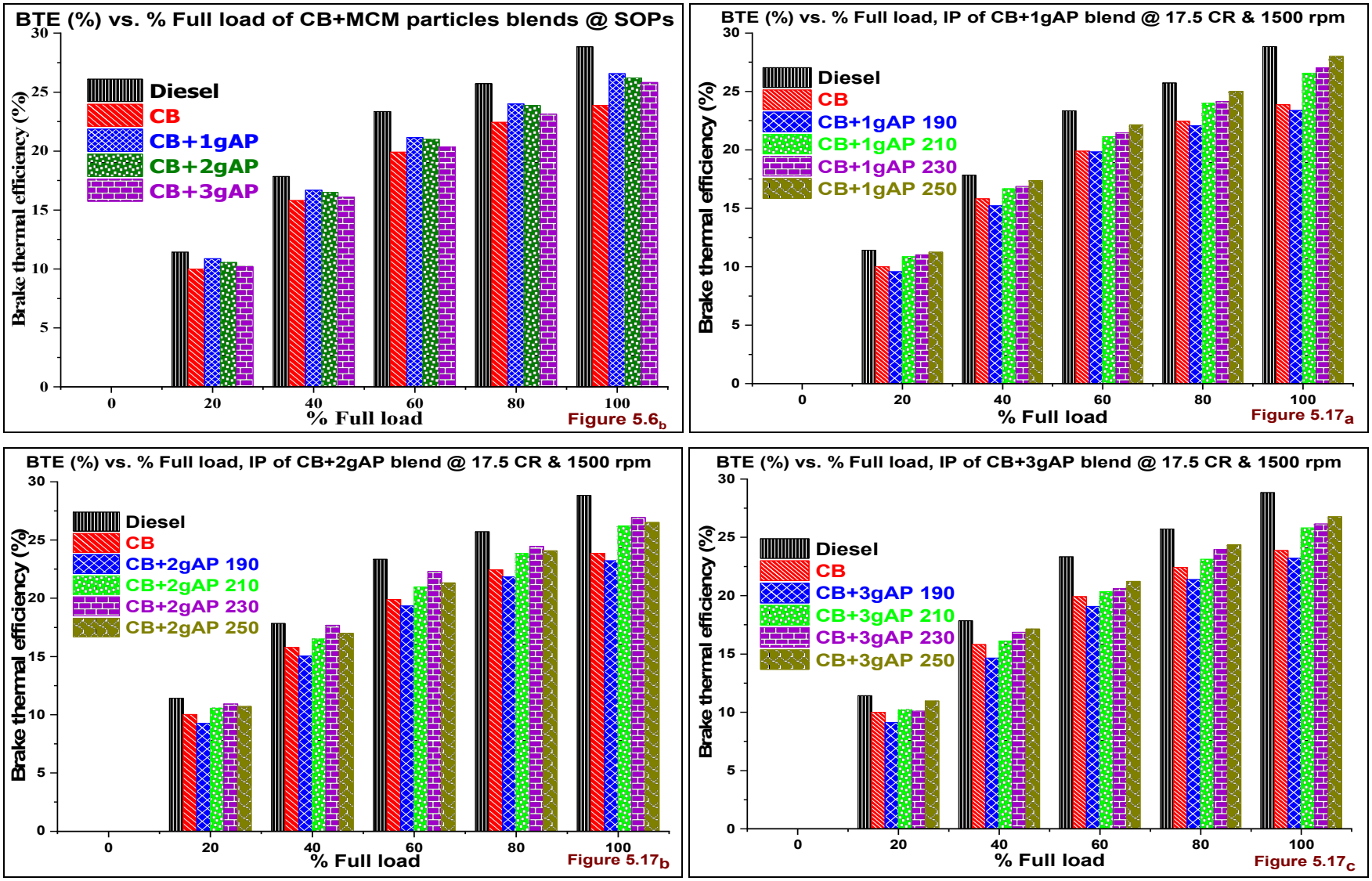

Figure 5.17 a, b, c BTE vs. % Full load & IP of CB+MCM blends

5.6.2 BSEC (MJ/kW-hr) vs. % Full load, IP

The BSEC increasing with neat biodiesel fuels even there is an improvement in combustion. The biodiesel fuels combustion improvement due to the presence of fuel-borne Oxygen. This Oxygen presence is led to decrease in their calorific value because of reduction in Hydrogen composition. In particular, the more fuel needed to inject into the combustion chamber to compensate for the less calorific value and to attain required shaft power. As the biodiesel fuel viscosity may be caused to increase the droplet size. The implementation of a variation of CR and IP are the best methods to attain improvement in BSEC. The variation in IP and CR can improve the fuel atomization, evaporation rate and flame spread in the combustion chamber[192].In **Figure 5.18$_b$** the BSEC increase at 190 bar IP because of improper atomization due to increased viscosity of CB+2gAP fuel led to an increase in droplet size. The improvement in BSEC at 230 bar IP because of improvement in the injection process and appropriate ID period. The BSEC slightly less at 250 bar IP with CB+2gAP as of the increase in surface area/volume ratio, penetration caused over mixing of fuel. In **Figure 5.18$_c$** the BSEC improvement observed at 250 bar IP. This is because of increased viscosity of CB+3gAP fuel due to increase in MCM particles quantity. At 190 bar IP, the CB+3gAP fuels have the highest BSEC than all other MCM particles contained CB fuel. This because of higher viscosity and Density of CB+3gAP fuel ID period has prolonged due to increased droplet size.

5.6.3 Exhaust gas temperature (ºC) vs. % Full load, IP

In **Figure 5.19$_a$** the higher Exhaust gas temperature (EGT) with CB at 210 bar IP is due to the presence of Oxygen and lack of particles to absorb heat. The available Oxygen in the clean fuel improved the combustion rate and EGT. In **Figure 5.19$_b$** max EGT due to ID than CB+1gAP sample. The increase in fuel droplet size because of high viscosity, the density of CB+2gAP blend. At lower IP 190 bar the quantity of fuel injected more into the combustion chamber to compensate less energy content in CB+2gAP fuel. In **Figure 5.19$_c$** the EGT at 190 bar IP was lower than other blends. At same IP the increase in heat absorption rate of MCM particles from the combustion chamber for evaporation and explosion. The observations from Figure 5.19$_{a, b, c}$

revealed that the highest EGT attained at 190 bar IP for all blends. The highest EGT of CB+2gAP fuel by cause of higher peak and maximum fuel retention time in the combustion chamber. The EGT is increasing as the IP increases at above 210 bar IP. The improvement in fuel atomization, evaporation rate has led to increasing EGT.

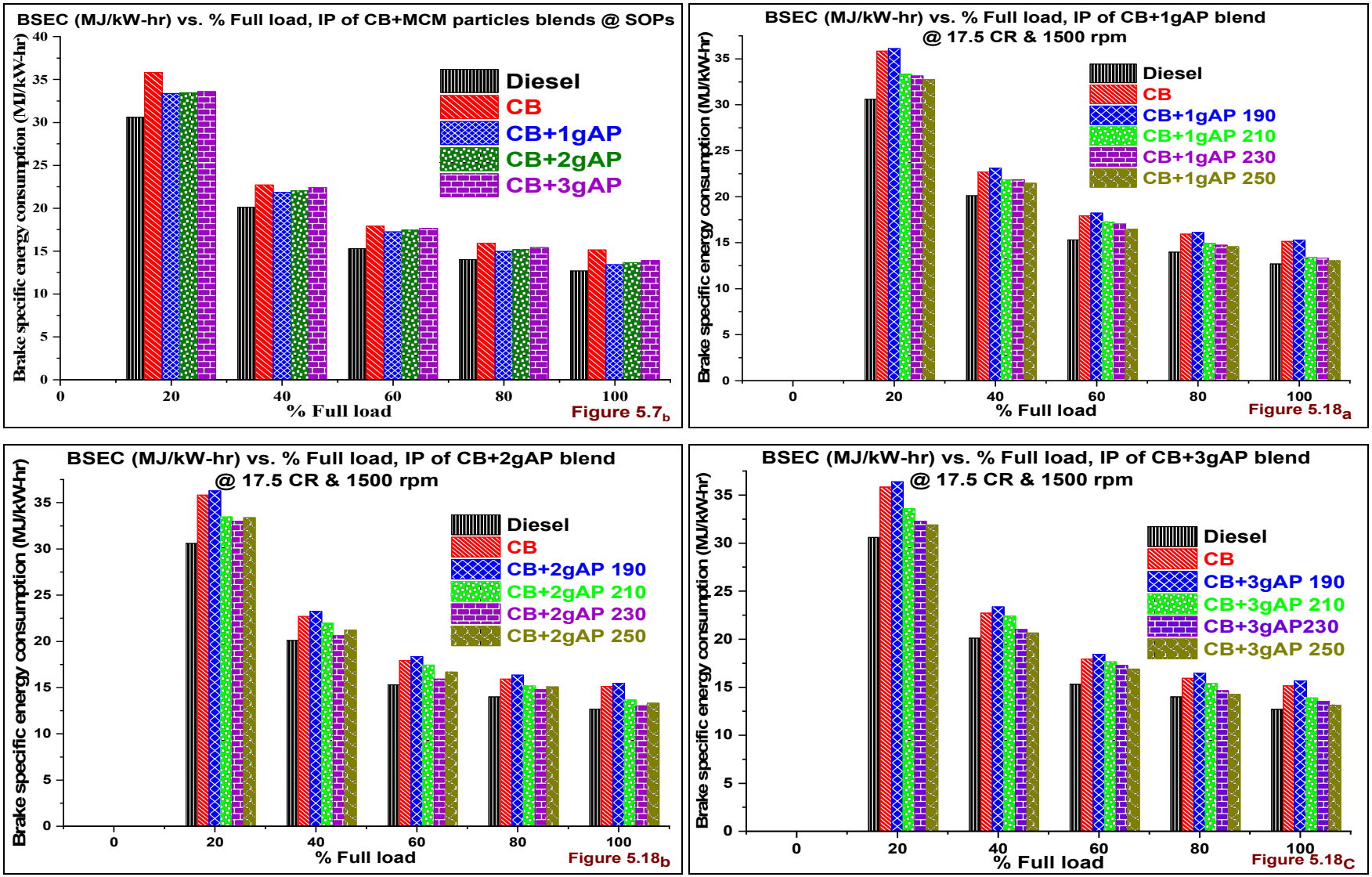

Figure 5.18a, b, c BSEC vs. % Full load, IP of CB+MCM blends

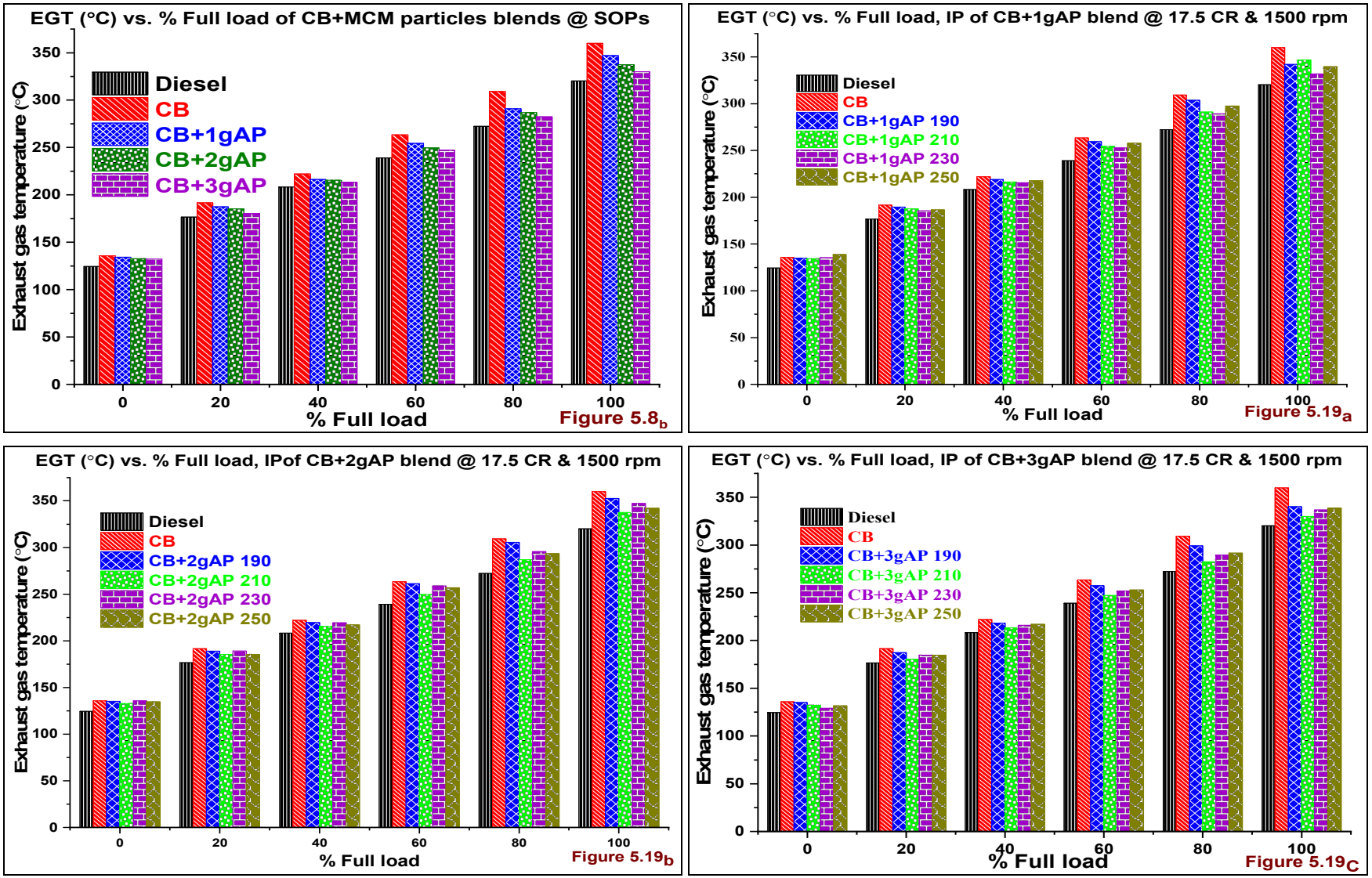

Figure 5.19$_{a, b, c}$ EGT vs. % Full load & IP of CB+MCM blends

5.7 The Emissions analysis vs. % Full load, IP on CB+MCM blends @ 17.5 CR, 1500rpm

5.7.1 Carbon monoxide (% vol) vs. % Full load, IP

The discussions presented on Figure 5.9_b in the previous section 5.4.1. The similar trend of Figure 5.9_b can observe in the below portrayed Figure 5.20_a, 5.20_b, &5.20_c but here the CO emissions are decreasing with increasing IP. In the above figures at 190 bar IP, the CO emissions are higher for MCM particles contained CB after Diesel at 210 bar IP. The increase in IP is helping to improve the fuel atomization, quick evaporation and proper flame spread in the combustion chamber. These effects are effectively influencing combustion phenomena to achieve the required temperature for CO reduction. In **Figure 5.20_a** the CO emissions of CB+1gAP fuel higher at 190 bar and lower emissions are attained at 250 bar IP.

The increase of CO emissions at 190 bar IP is due to improper fuel atomization and increased droplet size. The increased droplet size at 190 bar IP is causing to take maximum evaporation time. This influenced to form fuel rich zones and to increase CO emissions at 190 bar IP though there is an availability of Oxygen. The CO emissions are higher with CB+2gAP blend because of slightly increased Kinematic viscosity, density, Carbon composition, and less Calorific value. In the portrayed **Figure 5.20_b** the increased MCM particles quantity caused to over mixing at 250 bar IP and impinging jet on Cylinder walls. Based on the above reason the lower CO emissions are attained at 230 bar IP of CB+2gAP sample after CB at 210 bar IP.

The CO emissions increased at 250 bar IP because of fuel over penetration, piston head impingement and quenching problem in the combustion chamber[193].In **Figure 5.20_c** the lower CO emissions are attained with CB+3gAP blend at 250 bar IP. The CB+3gAP blend has higher Kinematic viscosity, Density, and less Calorific value than CB+1gAP and CB+2gAP blends. At this IP the CB+3gAP blend gets atomize and tend to improve evaporation rate. Because of uniform flame spread the increase in combustion chamber temperature at 250 bar IP.

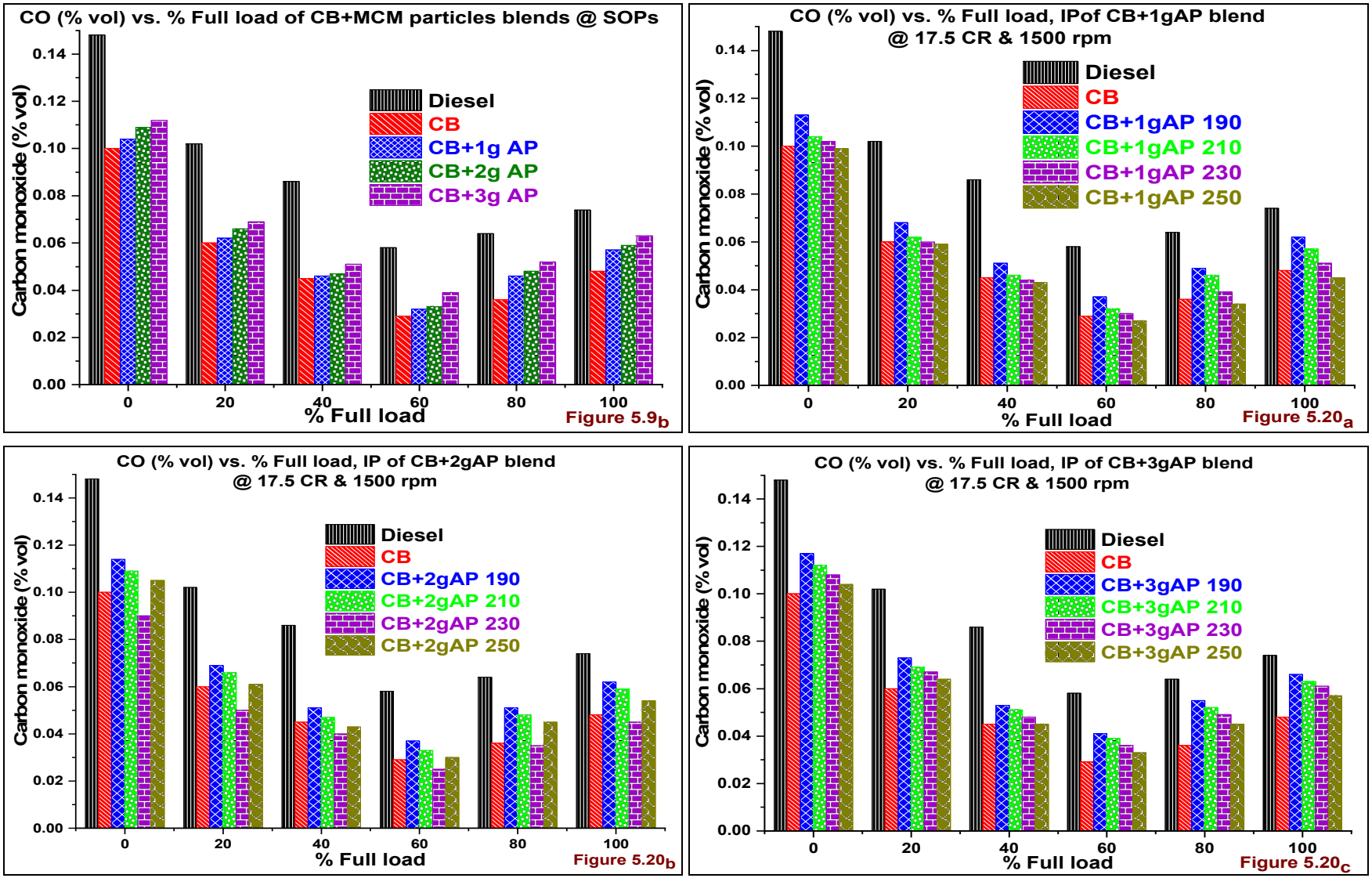

Figure 5.20$_{a, b, c}$ CO vs. % Full load & IP of CB+MCM blends

5.7.2 Unburned Hydrocarbons (ppm) vs. % Full load, IP

The HC emissions are increased with the increase of MCM particles quantity in CB and decreasing with the increase of IP. This can observe in Figure 5.10_b, Figure 5.21_a, 5.21_b, and 5.21_c. In all the cases the HC emissions are higher in Diesel fuel than all other fuels because of lack of fuel-borne Oxygen though fuel is less viscous and dense. In **Figure 5.21_a** the lower HC emissions are observed at 250 bar IP because of proper atomization, flame spread and attainment of reaction temperature in the combustion chamber.

In **Figure 5.21_b** the HC emissions are lower than CB fuel at 230 bar IP. The increased 1g MCM particles in CB+2gAP fuel increased surface volume ratio and helped to increase the mixing process in the combustion process. At 250 bar IP the fuel jet impinging on piston because the piston is very close to TDC and fuel jet which leads to piston head impingement and heat absorption from piston head[193]. The Figures 5.15_b, 5.16_b depicts this phenomenon in the left size zoom window.

In **Figure 5.21_c** the UCH emissions for CB+3gAP fuel increased than CB+1gAP, CB+2gAP fuel samples. The increase in MCM particle quantity may be helping to increase the mixing process, but there is an increase in fuel viscosity and density. Due to this reason, the proper mixing and flame spread in the combustion chamber attained at 250 bar IP.

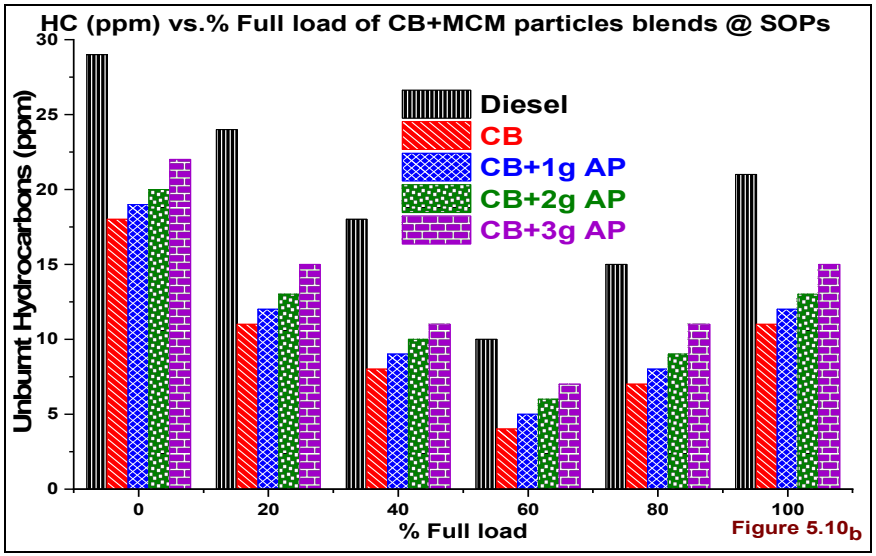

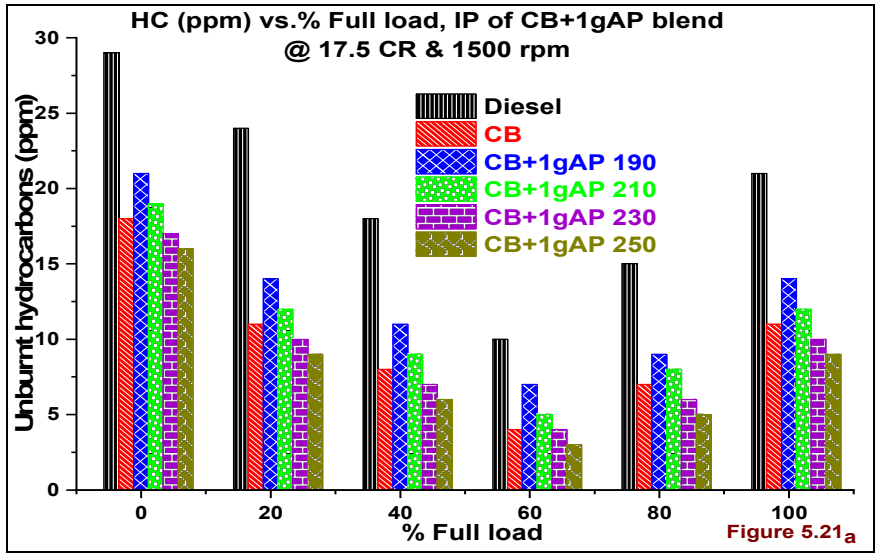

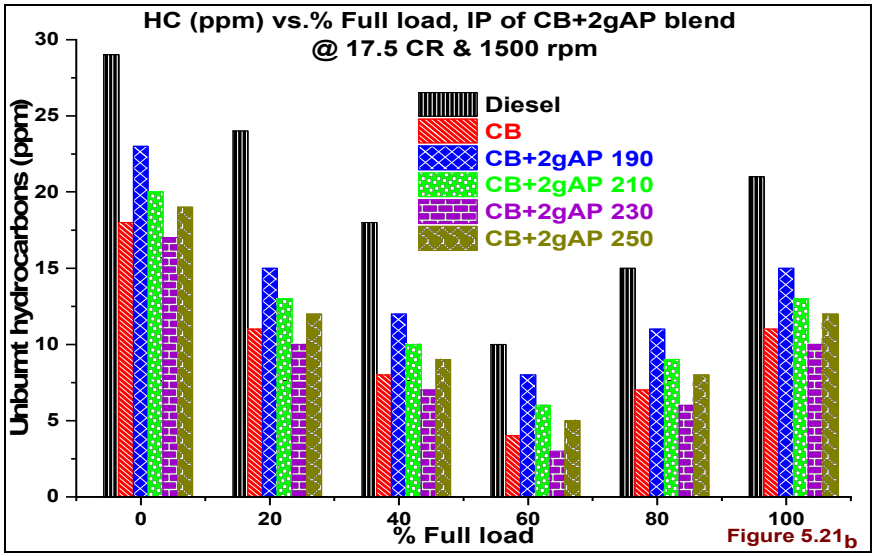

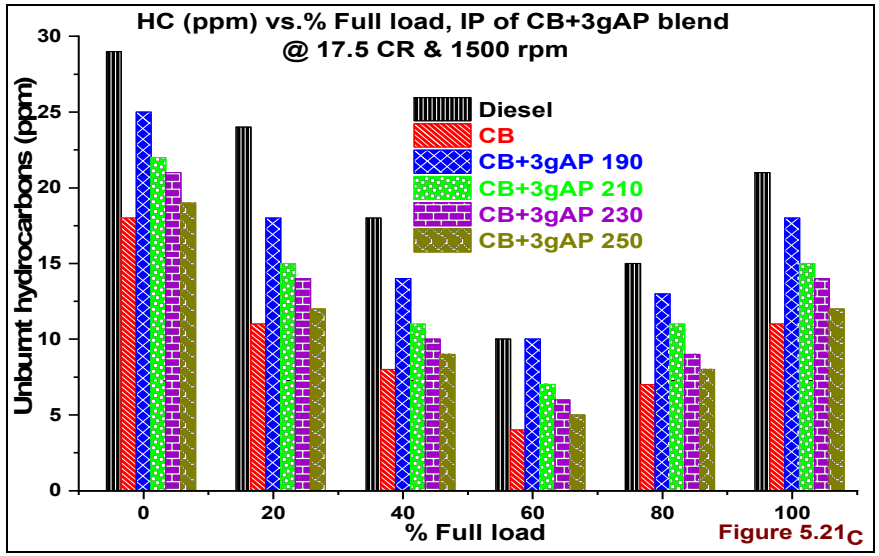

Figure 5.21$_{a, b, c}$ HC vs. % Full load & IP of CB+MCM blends

5.7.3 Oxides of Nitrogen (ppm) vs. % Full load, IP

In **Figure 5.22$_a$**, the NOx emissions are higher for clean Coconut biodiesel fuel and lower for Diesel fuel. The NOx emissions are increasing with an increase in the IP, but NOx, emissions are higher at 190 bar IP with CB+1gAP blend. The increase ID caused to accumulate more fuel for combustion and its sudden combustion causing higher ICP peak this portrayed in Figure 5.13$_b$.

The higher peak retention causes to form NOx at 190 bar IP. The ICP peaks are higher 210, 230 and 250 bar IPs but less retention time. The NOx is higher at 250 bar though fuel has less Oxygen composition than neat CB. The explosion of MCM particles helped to proper flame spread in the combustion chamber and tended to NOx formation.

In **Figure 5.22$_b$** after clean CB fuel, the NOx emissions are higher at 230 bar IP. At this IP the increase in MCM particles quantity motivated to increase surface area to volume ratio and improvement in proper air/fuel mixing. The proper flame spread caused to fever combustion temperature and affected to increase NOx. The lower energy content in CB+2gAP blend led to lower BTE than neat CB but this CB also lower than Diesel.

In **Figure 5.22$_c$** the NOx emissions are higher in case of 190 and 210 bar IPs. At these Injection pressures the higher ID due to increased droplet size because of higher Kinematic viscosity, density, and lower calorific value. The higher viscosity and density CB+3gAP blend accumulated higher fuel quantity in ID period. The accumulated fuel gets rapid combustion in premixed phase.

The increased MCM particles quantity in CB+3gAP blend projected to increase Kinematic viscosity, density. However, the droplet size is higher at lower IPs with CB+3gAP blend have shown a positive effect on air/fuel mixing. At higher IPs, this higher viscous fuel signified to increase penetration length and over mixing.

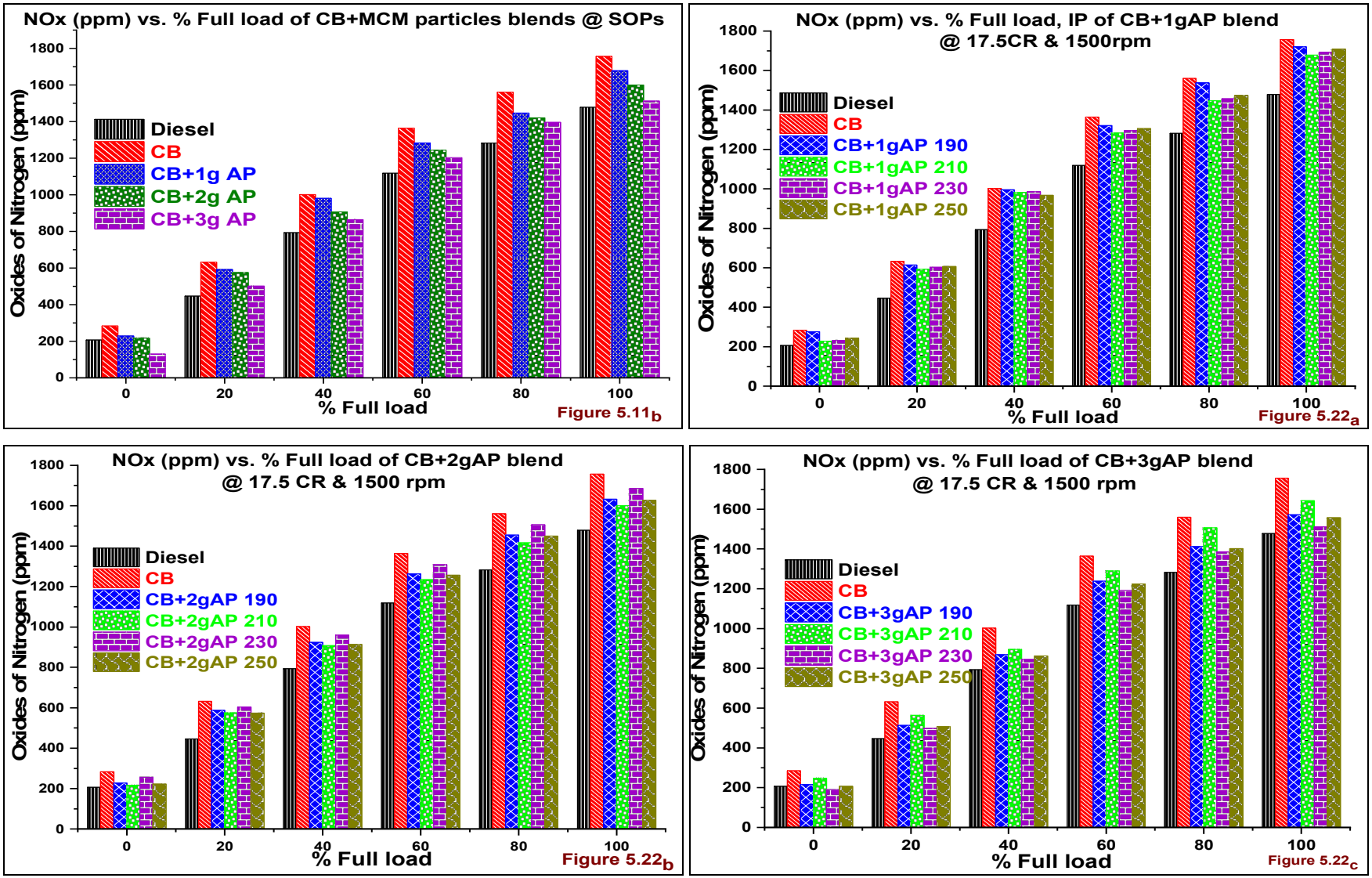

Figure 5.22$_{a, b, c}$ NOx vs. % Full load & IP of CB+MCM blends

5.7.4 Smoke opacity (%) vs. % Full load, IP

The enhancement in the mixing process with CM particles blends because of improvement in surface area to volume ratio. This effect depicted in Figure 5.12_b. In **Figure 5.23_a** the highest smoke emissions at 190 bar IP because of improper atomization and increased droplet size. The increased CB+1gAP fuel droplets size due to MCM particles addition caused to increase ID. At lower injection pressure 190, 210 bar the mixing process deteriorated by cause of higher fuel droplet size.

In Figure 5.23_b the behavior of CB+2gAP blend has provoked the mixing process. In **Figure 5.12_b** the Smoke is decreasing with the increase in MCM particles blend quantity. At this MCM particles blend quantity the combustion is improved at 210, 230 bar IP except at 190, 250 bar IP can observe in the Figure 5.13_b, 5.14_b, &5.15_b.

The increased MCM particles quantity improved mixing controlled combustion. In **Figure 5.23_c** the increase in Smoke opacity of CB+3gAP fuel at 190, 210 bar IPs because of high viscosity, density and ID. The increased ID induced to the higher quantity of fuel accumulated to promote rapid premixed phase of combustion. The Diffusion peaks occurred at this IPs because of higher size fuel droplets are not entirely combust in the premixed phase.

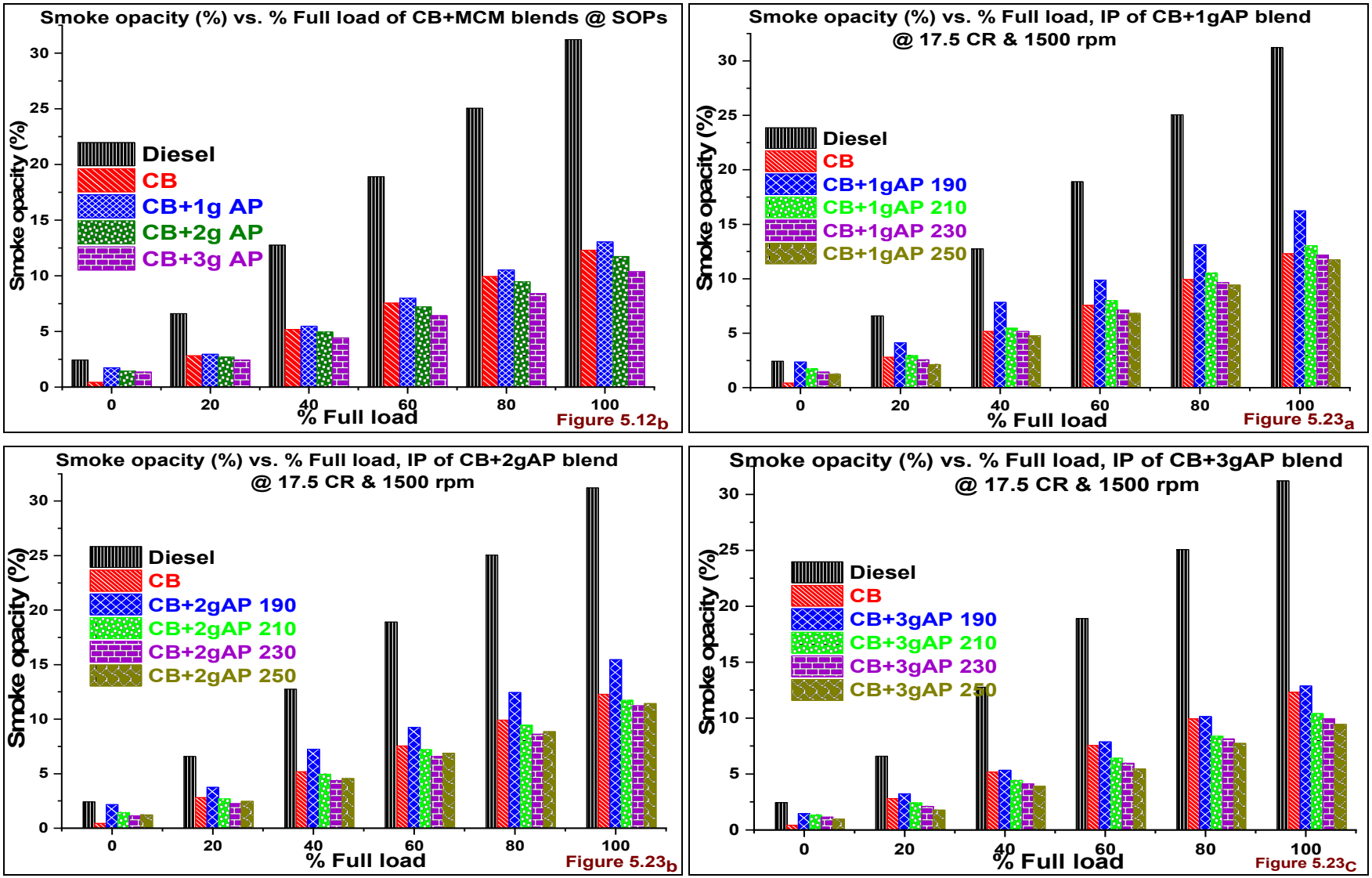

Figure 5.23$_{a, b, c}$ Smoke opacity (%) vs. % Full load& IP of CB+MCM blends

Module - 3

5.8 Combustion analysis on KB+LA blends @ Full load, 17.5 CR, 1500 rpm

5.8.1 Incylinder pressure (bar) vs. Crank angle (θ), IP

The discussions on **Figure 5.3c** presented in section 5.2.1. The LA higher heat absorption and storage capacity majorly influenced engine characteristics. The increase in IP increased the fuel atomization as well as evaporation rate and portrayed in **Figure 5.24a**. The ICP peaks for Diesel, KB, at 210 bar IP and KB+10gLA blend at 190, 210 and 230 bar are 63.87, 66.32, 49.39, 60.12, and 64.23bar respectively. The blend obtained at 230 bar IP. The KB+10gLA blend has attained higher ICP peak because of fewer droplet size, required temperature for its evaporation in a shorter ID period. The higher size droplet requires a longer time to evaporate at 190 bar IP. These obtained peaks with IP variation are much lower than KB fuel but higher than Diesel fuel.

In **Figure 5.24b** the ICP peaks for KB+20gLA at 190, 210 and 230 bar IPs are 50.42, 47.76, and 49.87bar. At 190 bar IP, the 50.42 was the highest ICP peak after KB fuel. At 190 bar IP increase in droplet size because of an increase in LA blend quantity. In Figure 5.24a the increase in IP caused to increase ICP peak because of less quantity of LA. There is no more significant variation of ICP peak with KB+20gLA blend. At this quantity of LA blend, the ID slightly increased due to the increase in droplet size.

In **Figure 5.24c** the ICP peak for KB+30gLA at 190, 210 and 230 bar IPs are 47.21, 49.74, 52.39bar. The increase in LA quantity, i.e., 30g blend influenced to reduce ID than KB+20gLA blend because of the increase in Cetane number (CN). The higher ICP peak with KB+30gLA blend at 230 bar IP is because of improvement in fuel atomization. At lower IP 190 bar the improper atomization increased the droplet size and increased ICP peak.

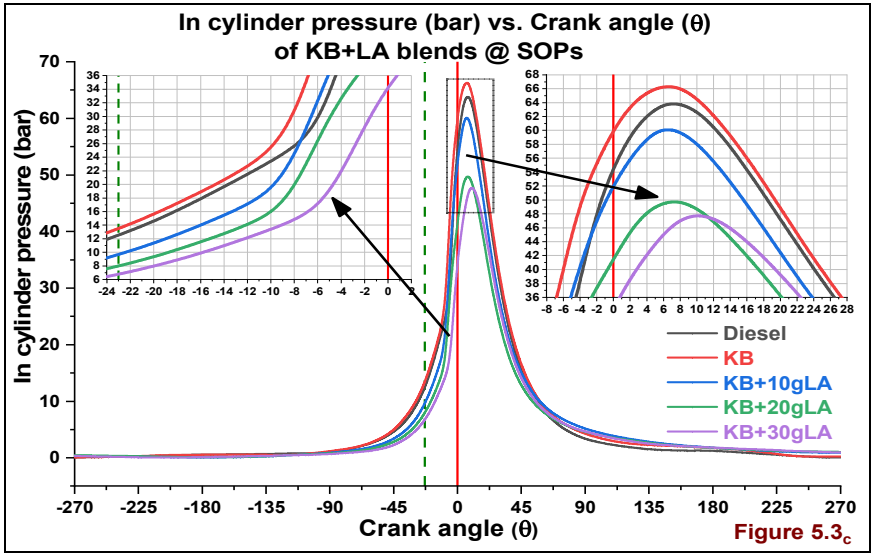

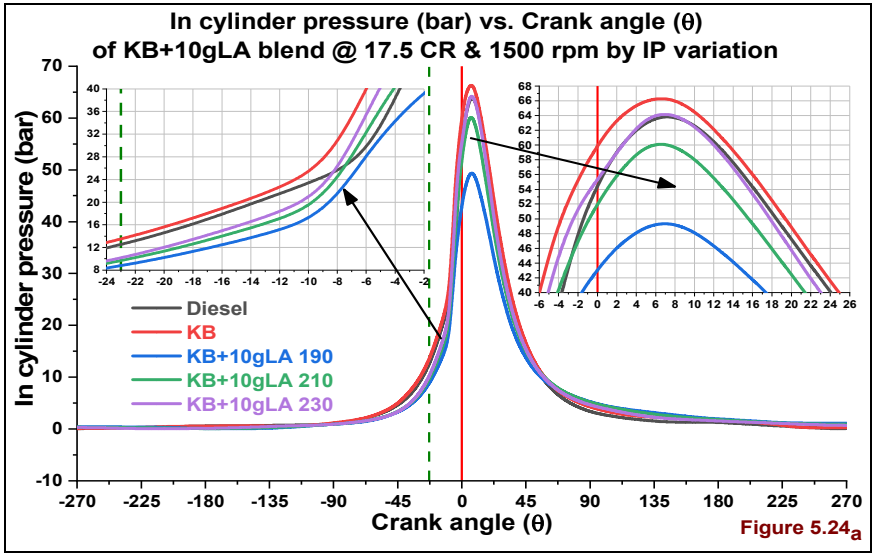

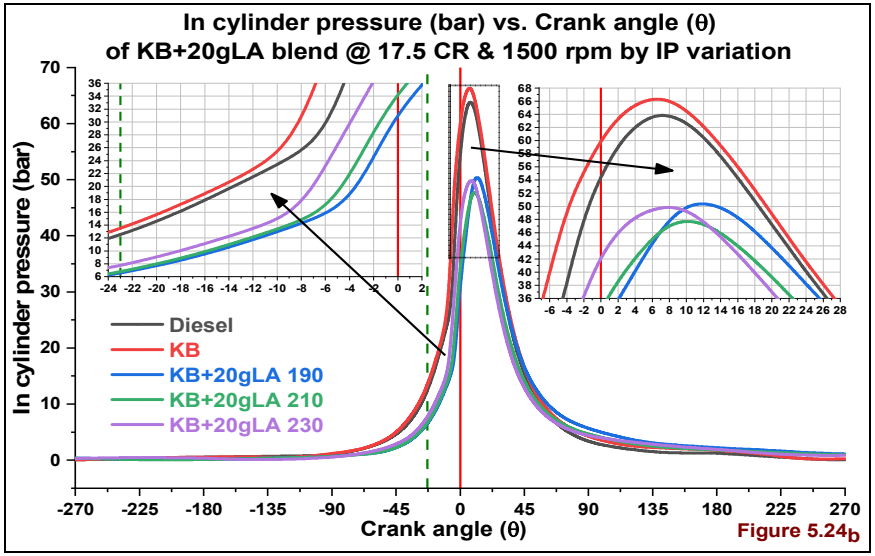

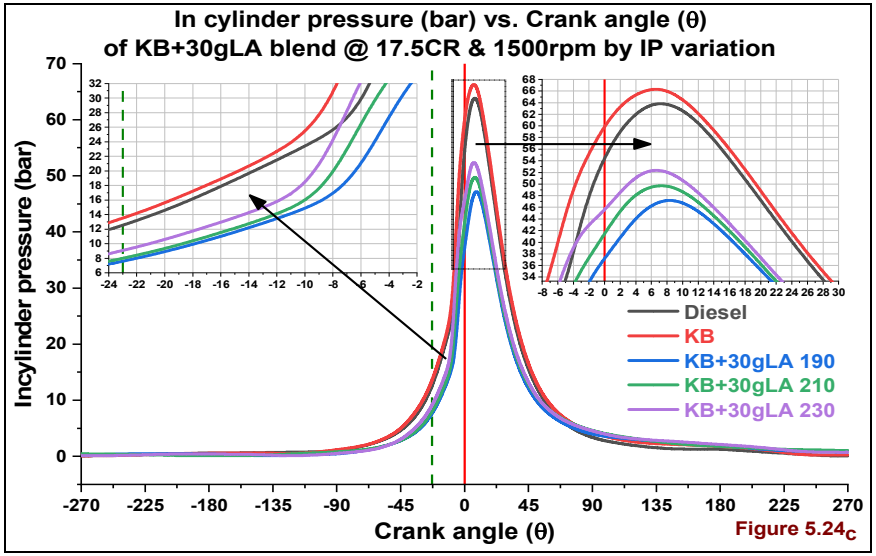

Figure5.24$_{a, b, c}$ ICP (bar) vs. Crank angle (Θ) & IP of KB+LA blends

5.8.2 Cumulative heat release (kJ)vs. Crank angle (θ), IP

The discussions on Figure5.4c made in Section 5.4.20. In **Figure 5.25$_a$** the CHR peaks for KB+10gLA are 1.1, 1.13, and 1.08 kJ at 190, 210, and 230 bar respectively. The higher CHR peak obtained at 210 bar IP because of attainment of sufficient fuel accumulation in the required ID period. At 230 bar IP the CHR peak is lower because the proper fuel atomization occurred but lack of time in the ID period less fuel accumulated. At 190 bar IP, the CHR peak was higher than 230bar because of available time to mixture formation though droplet size higher.

In **Figure 5.25$_b$** the CHR peaks are 1.2, 1.034, and 1.03kJ at 190, 210, and 230 bar IPs. The higher peak at 190 bar IP because of improper atomization the droplet size increased and induced higher ID. This longer ID influenced to accumulate more fuel in this period. The higher quantity of accumulated fuel gets combust in premixed combustion phase. The less quantity of fuel accumulated at 230 bar IP because of the lower ID period. The less CHR peak at 230 bar IP because the mass, which not gets combust in premixed phase, combust in mixing controlled combustion phase.

In the **Figure 5.25$_c$** the CHR peaks are 0.96, 1.01 and 1.04 kJ at 190, 210 and 230 bar IP. The increase in fuel Kinematic viscosity lead to higher ID because of an increase in droplet size. The more fuel accumulation in ID period lead to the rapid combustion in premixed phase. It can be possible when the fuel has sufficient Oxygen, Calorific value, and Cetane number. The highest CHR peak at 230 bar IP but this is away from TDC than 210 and 190 bar IPs. In this case, the availability of time for mixture preparation has played a significant role to attain higher CHR peak than IP. The highest CHR peaks for KB+10gLA, KB+20gLA, and KB+30gLA are at 210, 190, & 230 bar IPs. The highest peak at 190 bar IP with KB+20gLA blend because of sufficient ID period required fuel accumulation.

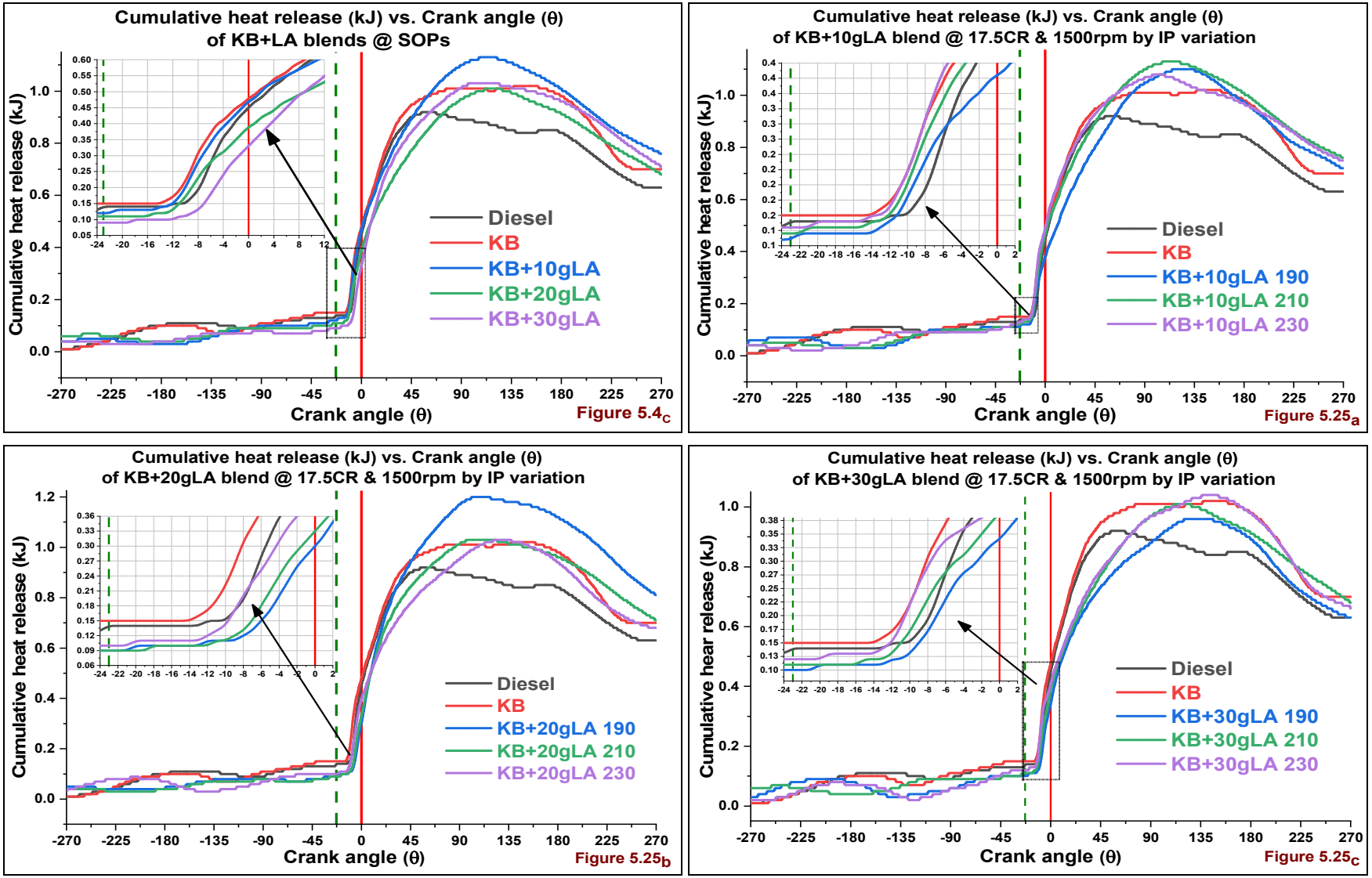

Figure 5.25$_{a, b, c}$ CHR (kJ) vs. Crank angle (Θ) & IP of KB+LA blends

5.8.3 Net heat release rate (J/θ) vs. Crank angle (θ), IP

The discussions on Figure 5.4$_c$ presented in section 5.2.3. The NHRR peak is decreasing with increase in Lauric acid quantity by cause of increased viscosity and reducing calorific value than KB fuel. In **Figure 5.26$_a$** the NHRR peaks are30.67, 37.97, and 46.27 J/Ɵ at 190, 210, and 230 bar IPs respectively. The higher NHRR peak attained at 230 bar IP with KB+10gLA blend than KB fuel at 210 bar IP. Because of the increase in fuel atomization, shorter injection timing and proper flame spread in the combustion chamber at decreased ID period than KB fuel. Among all IPs the less ID period for 230 bar IP by cause of early fuel injection and increased atomization. The higher NHRR peak observed with lower Lauric acid blend fuel, i.e., KB+10gLA at 230 bar IP. Because of the reduction in droplet size which induced to improve air/fuel mixing and higher premixed phase of combustion[194].

In **Figure 5.26$_b$** the NHRR peaks are 31.59, 30.51, and 29.49 J/Ɵ at190, 210 &230 bar IPs respectively. The higher NHRR peak attains at 190 bar IP with KB+20gLA blend because of increased fuel accumulation in the sufficient ID period. The less ID period led to less fuel accumulation at 230 bar IP with KB+20gLA blend. The representation of an arrow on Figure 5.26$_b$ depicts the higher peak retention at the 230 bar lead to higher NOx formation than 190, 210 bar IPs.In **Figure 5.26$_c$** the NHRR peaks are 29.61, 31.1, &38.67 J/Ɵ at 190, 210, and 230 bar IPs respectively. The higher NHRR peak attained at 230 bar IP with KB+30gLA blend. The proper atomization because of higher injection led to quick evaporation of droplets in the less ID period than 190, 210 bar IPs.

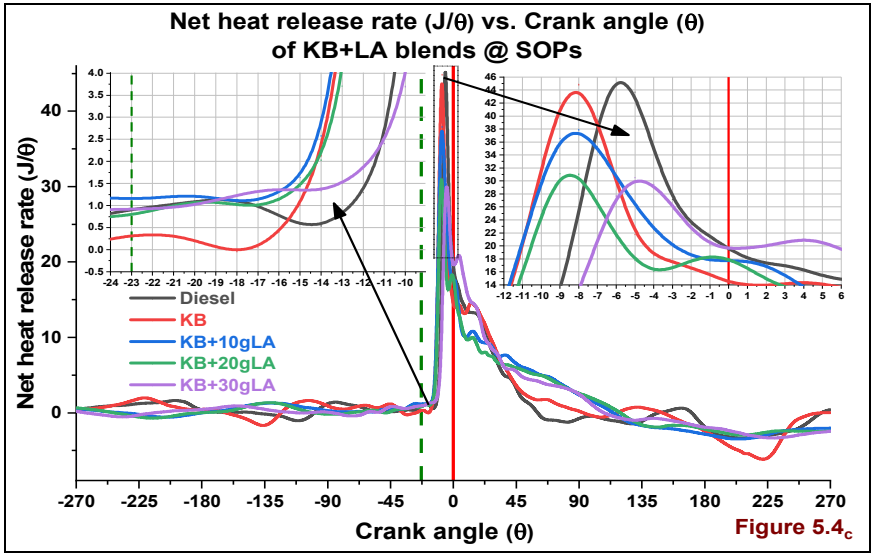

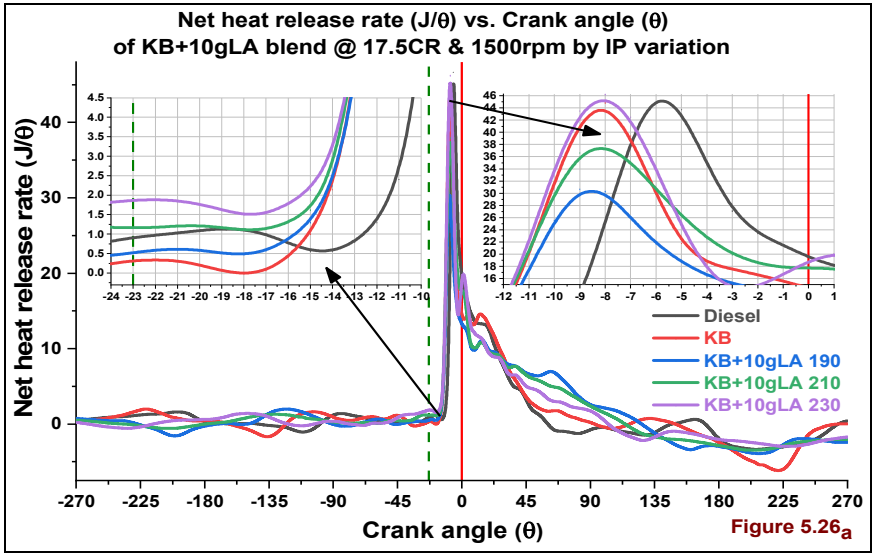

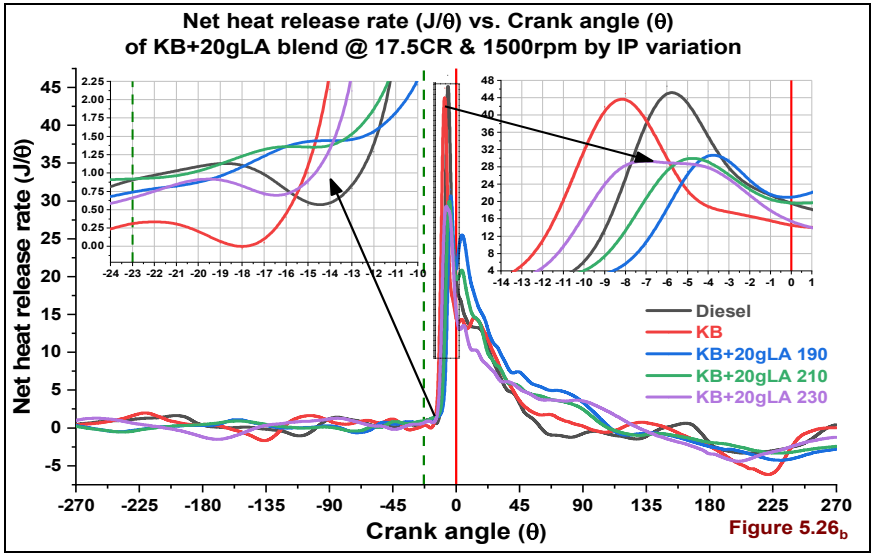

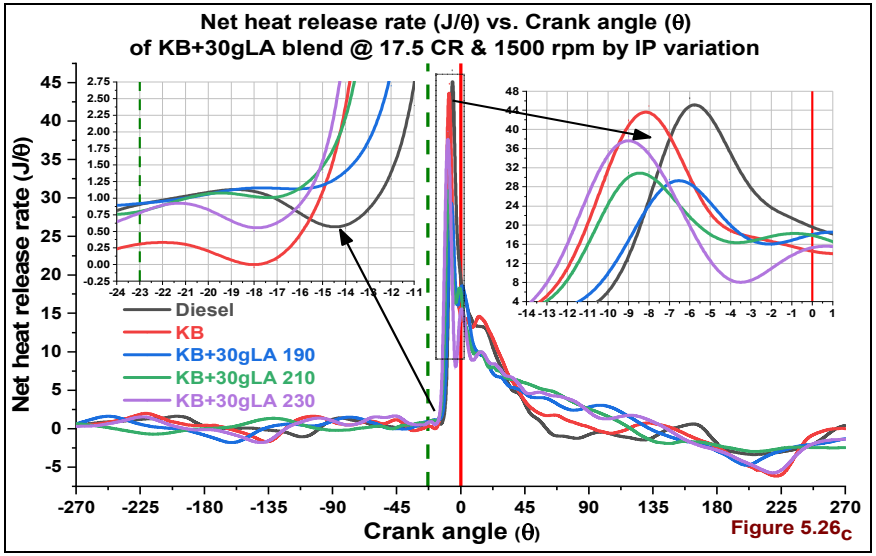

Figure 5.26$_{a, b, c}$ NHRR (J/Θ) vs. Crank angle (Θ), & IP of KB+LB blends

5.8.4 Rate of pressure rise (dp/dθ) vs. Crank angle (θ), IP

The ID is increasing at the same IP with the increase in the Lauric acid blend in KB fuel. This because of the higher heat requirement for initiating combustion and may be due to increasing Kinematic viscosity and density. The increase in IP on the same fuel is causing to increase RPR peak by cause of proper fuel atomization.

The RPR peaks for KB+10gLA blend are 3.46, 4.26, and 5.08bar at 190, 210 and 230 bar IPs respectively. In general, the increase in IP leads to increase in RPR. In the **Figure 5.27$_a$** the RPR peak is higher at 230 bar IP because of rapid combustion in premixed phase due to proper atomization of low viscous KB+10gLA fuel at 230 bar IP in the less ID period[98].

The RPR peaks for KB+20gLA blend are 3.46, 3.37, and 3.34bar at 190, 210 and 230 bar IPs respectively. In Figure 5.27$_a$ the RPR peak is higher at 190 bar IP. At this IP the improper atomization and the higher viscosity, density of KB+20gLA blend induced higher ID period and led to increasing fuel accumulation. This RPR peak at 190 bar of KB+20gLA blend is lower than KB+10gLA blend though there is a delay. This occurrence is because KB+20gLA require more heat to attain combustion, but it has less Calorific value than KB+10gLA.

The Rate of pressure rise (RPR) is higher at 230 bar IP with KB+10gLA blend. This because of improved spray formation induced to grater combustion. With the same fuel at 190 and 210 bar IPs the improper atomization of fuel induced to poor combustion and led to lower RPR[195].

At 230 bar higher IP the lower RPR attributed with KB+20gLA blend in the **Figure 5.27$_b$**. The increase in spray penetration and its impingement on the piston head because of spray tip near to piston head and it caused to absorb heat at constant pressure.

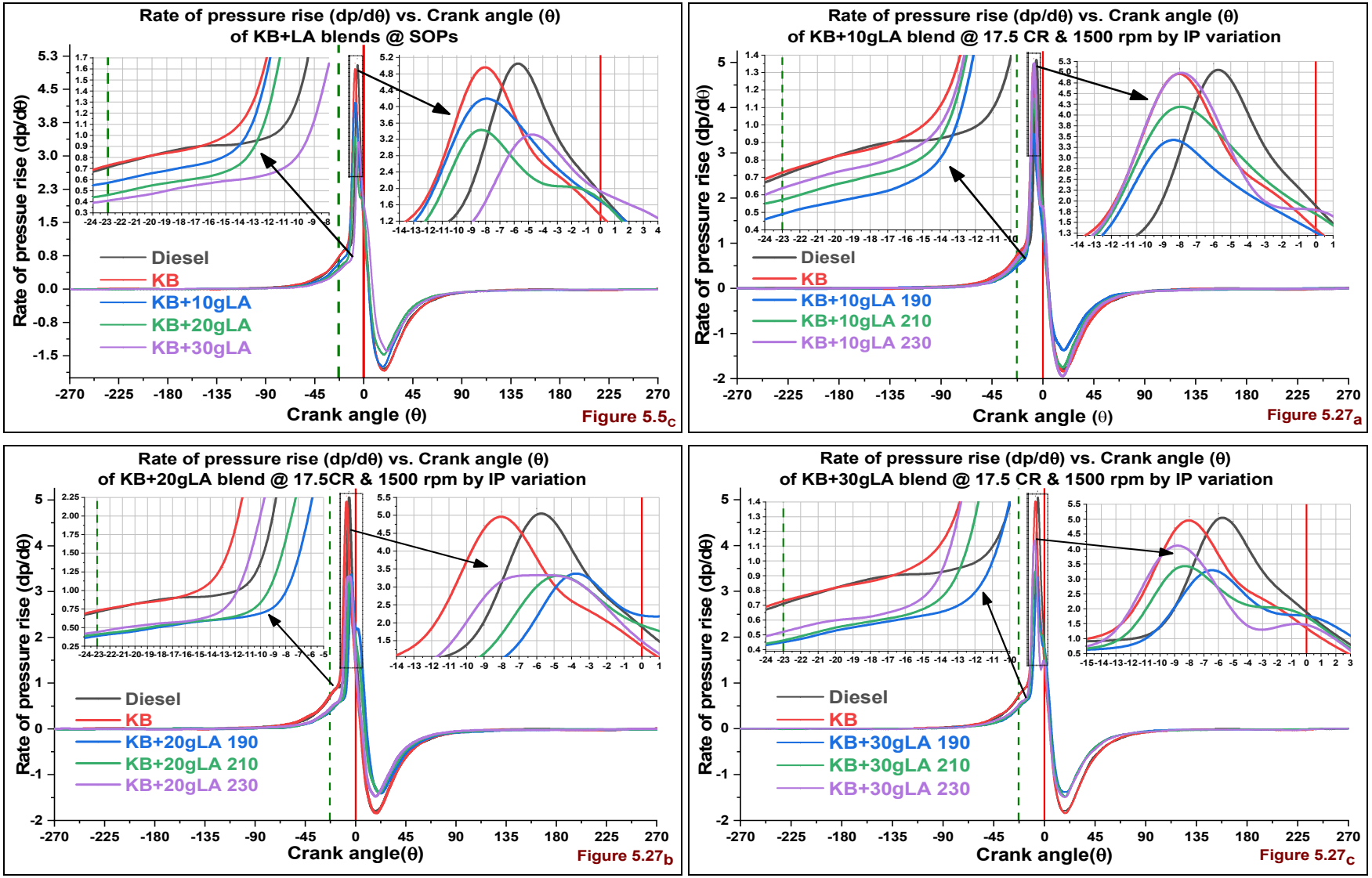

Figure 5.27$_{a, b, c}$ RPR (dP/dΘ) vs. Crank angle (Θ) & IP of KB+LA blends

5.9 Performance analysis on KB+LA blends @ % Full load, 17.5 CR, 1500 rpm

5.9.1 Brake thermal efficiency (%) vs. % Full load, IP

The authors Yehliu et al. and Agarwal et al.[183,196] find that the increase in BTE with the increase in IP by cause of the increase in spray tip penetration with the increase in spray spread at fixed injection timing. In **Figure 5.28$_a$** the BTE is increasing with increase in IP but lower than KB fuel. This because of less Calorific value, increases in viscosity and density of Lauric acid blends than KB fuel[194].

In **Figure 5.28$_{a, b, c}$** the BTE increased with increase in IP because of improvement in air-fuel mixing. This improvement owing to increase premixed phase of combustion and induced to improve combustion characteristics and reduction in emissions except for NOx emissions[197]. The decreasing calorific value with the increase in Lauric acid blend quantity is inducing to decrease BTE can observe in below **Figure 5.6$_c$**.

5.9.2 BSEC (MJ/kW-hr) vs. % Full load, IP

As per Park et al. findings the increase in fuel IP at the same Injection timing (IT) causing to lower BSEC. This because of small droplet size which to improve the air/fuel mixing and thus to increase premixed combustion peak. This result to cause less fuel consumption than higher viscous fuels[198]. The BSEC is increasing with the increasing Lauric acid blend quantity in KB fuel.

By cause of the increase in blends viscosity, density, and reduction in lower calorific value can observe in Figure 5.7$_c$. The BSEC improvement is lowering with the increase Lauric acid blend quantity even with IP increase. In **Figure 5.29$_a$** the BSEC is decreasing with the increase in load on the engine by cause of the increase in fuel injection quantity to attain required brake power. This increased quantity of fuel is inducing to increase heat energy in the combustion chamber.

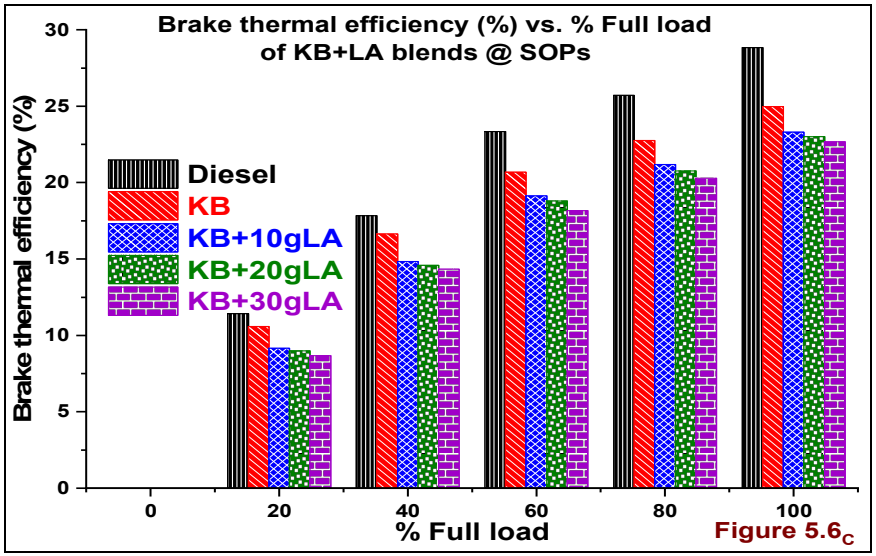

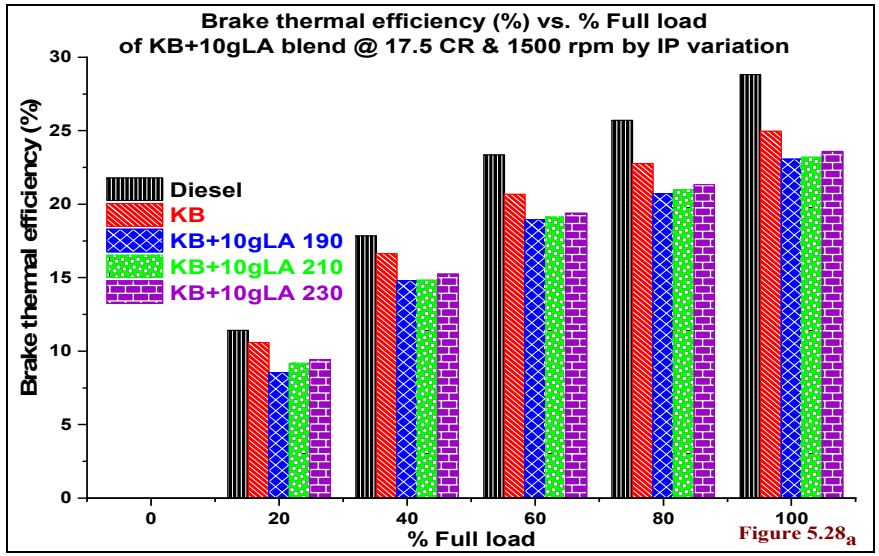

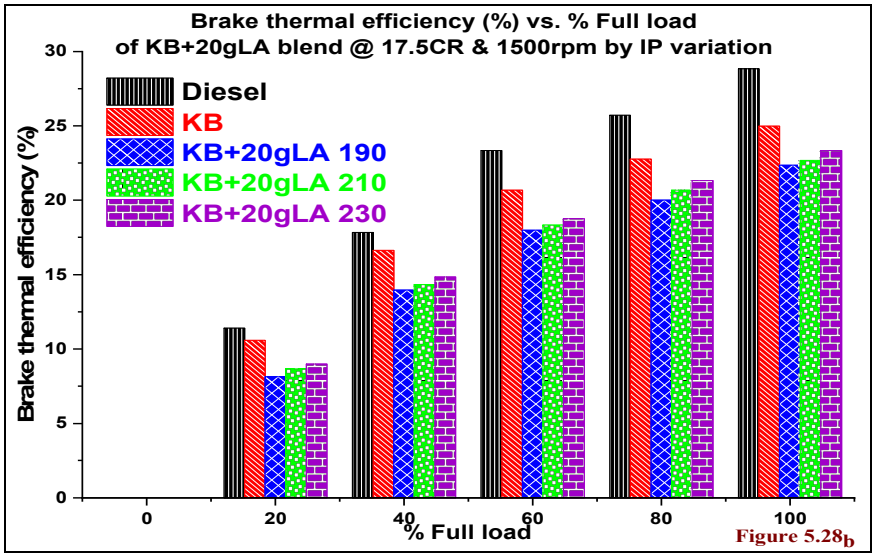

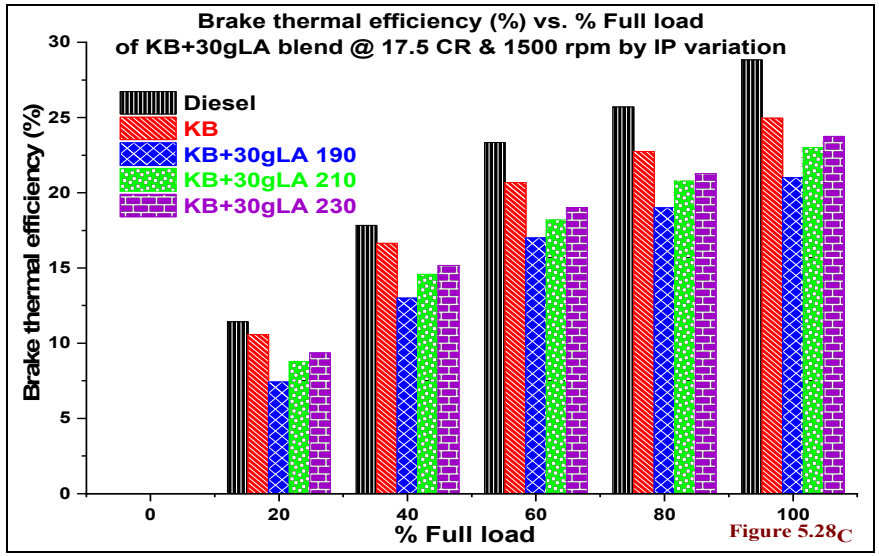

Figure5.28$_{a, b, c}$ BTE (%) vs. % Full load & IP of KB+LA blends

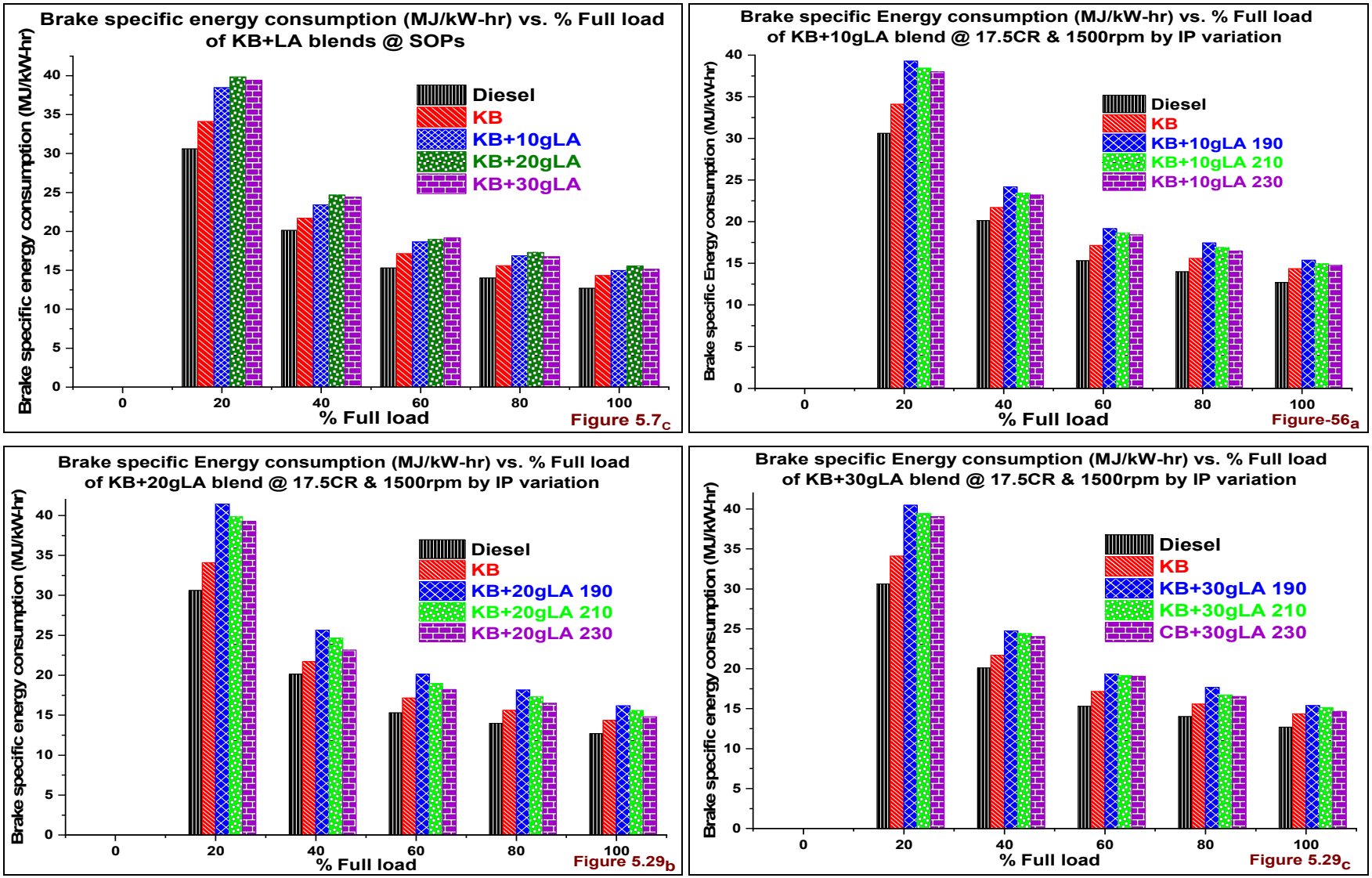

Figure5.29$_{a, b, c}$ BSEC (MJ/kW-hr) vs. % Full load& IP of KB+LA blends

5.9.3 Exhaust gas temperature (ºC) vs. % Full load, IP

The Exhaust gas temperature (EGT) is increasing with the increase in load on Engine. This because of increased heat energy in the combustion chamber with the increased fuel injection quantity at each increased engine load[199]. The author Mohan et al.[115] stated that the EGT is decreasing with the increase in IP but most of the cases the EGT increasing with the increase in IP. There is a slightly increased delay period to rise injector nozzle line pressure for injection. The increased droplet size attributed to decrease EGT because of the retarded injection of fuel into the combustion chamber.

In **Figure 5.30$_a$** the EGT is higher than Diesel but lower than KB fuel because of an increase in Viscosity, density, and slightly less Calorific value and Oxygen composition.

In **Figure 5.30$_b$** the EGT lower at 210 bar IP because of lower ICP and NHRR peaks, this can observe in Figure 5.24$_b$. The EGT higher at 230 bar IP due to increased retention time at peak value this portrayed in Figure 5.26$_b$.

In **Figure 5.30$_c$** the EGT lower at all cases because of increase Lauric acid blend quantity in the KB fuel. This increase led to absorbing more heat for evaporation from the combustion chamber before attaining combustion.

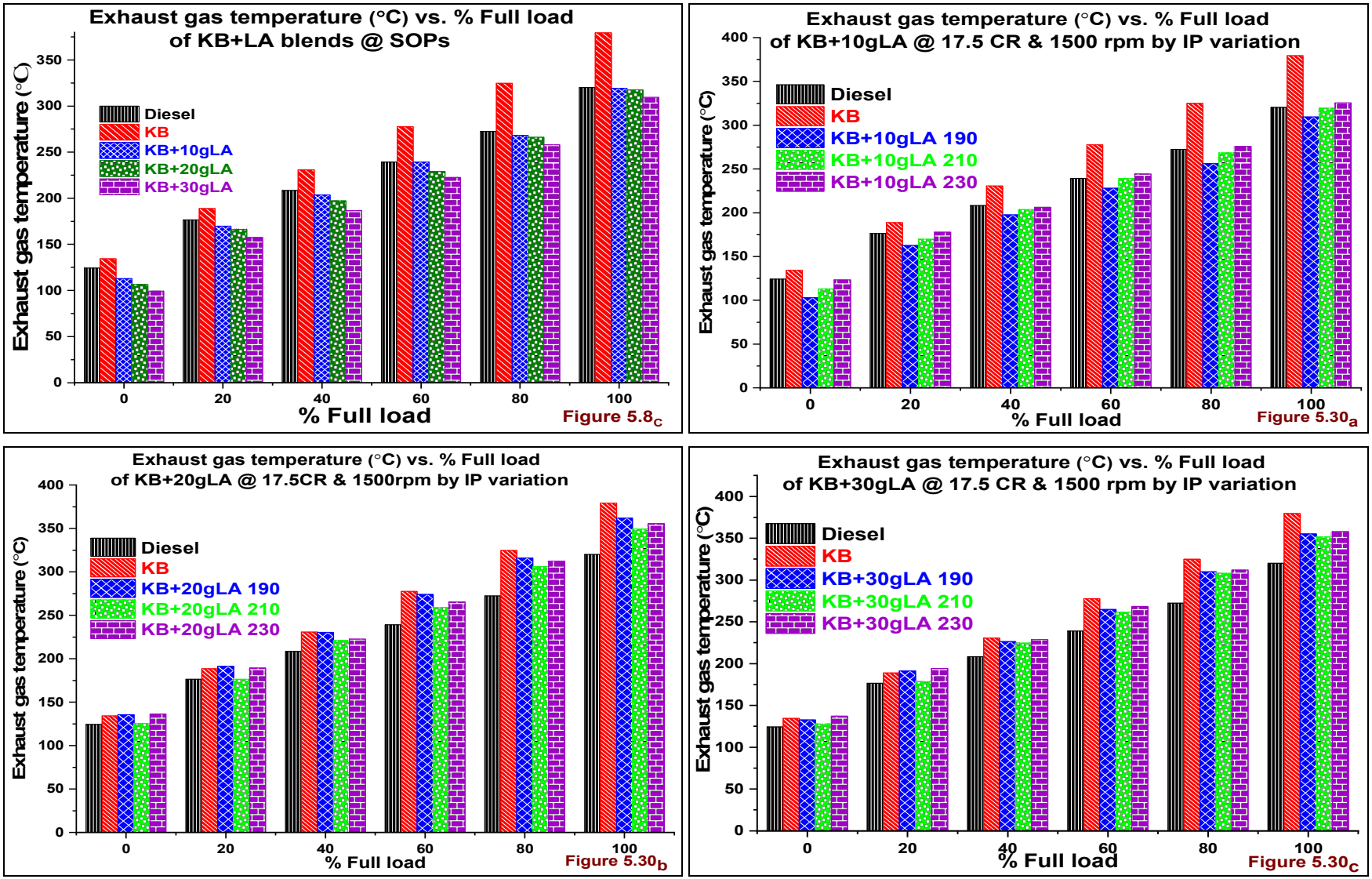

Figure5.30$_{a, b, c}$ EGT (°C) vs. % Full load& IP of KB+LA blends

5.10 Emission analysis vs. % Full load, IP on KB+LA blends @ 17.5 CR, 1500rpm

5.10.1 Carbon monoxide (% vol) vs. % Full load, IP

The CO emissions are decreasing with increase in engine load at constant CR and IP. The combustion temperatures are increasing with increase in engine load. This temperature increase is helping to improve combustion though there is an increase in fuel quantity. This increased fuel quantity was also increasing the available Oxygen for CO emissions reduction in the combustion chamber[200,201]. The increase in IP was also the majorly influencing factor in reducing CO emissions from the engine. The improvement in air/fuel mixing process led to improving combustion[202].

In **Figure 5.31$_a$** the CO emissions at 230 bar IP even lower than KB fuel because of the increase in the mixing process. This improvement is because of slight variation in the increased ICP and NHRR peaks in Figure 5.24$_a$&5.26$_a$. These peaks are decreasing with the increase in Lauric acid blend quantity.

In **Figure 5.31$_b$** the increase in CO emissions because of a reduction in ICP &NHRR peaks. In Figure 5.24$_b$, 5.26$_b$ the composition difference of KB+20gLA fuel influenced to decrease fuel volatility.

In **Figure 5.31$_c$** the CO emissions are higher at 190 bar IP because of improper injection due to increased viscosity and density. The reduction in CO emission because of the slightly increased ICP peaks. The increase in peak and decreased ID period attributed to attaining required temperature. This available temperature may be improved CO emissions for KB+30gLA than KB+20gLA.

In **Figure 5.31$_{a, b, c}$** the CO emissions are increasing with increase in blend ratio because of the increase in Viscosity and Density of Lauric acid blends. In all the portrayed figures the lower CO emissions are observed at 60 % full load because of availability of Oxygen, delay time and temperature for reaction.

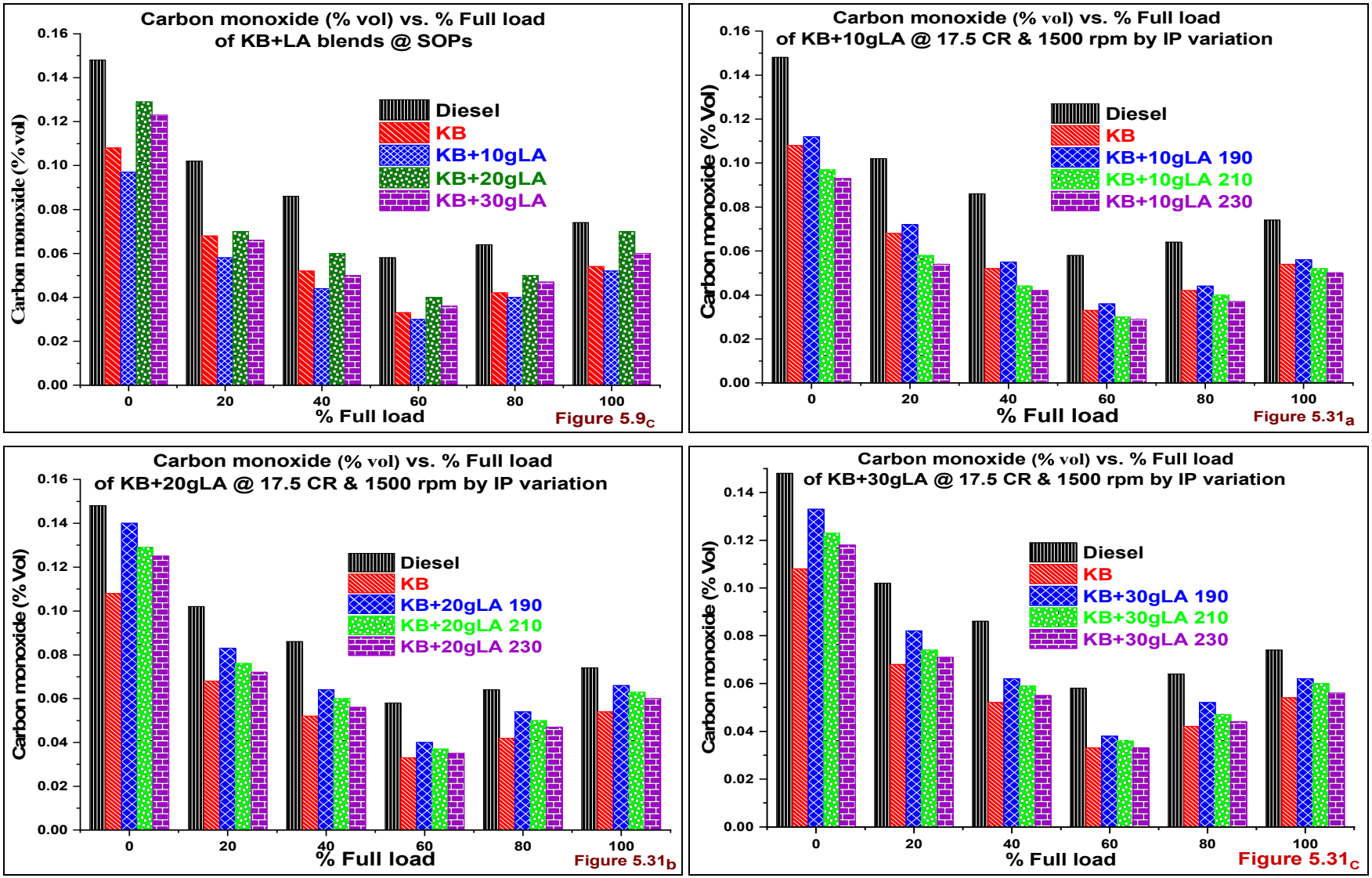

Figure5.31$_{a, b, c}$ CO (%) vs. % Full load& IP of KB+LA blends

5.10.2 Unburned Hydrocarbons (ppm) vs. % Full load, IP

The fuels which are available either naturally or produced fuels must consist of Carbon, Hydrogen, Oxygen, and sometimes Sulfur elements. The element like Oxygen is not available in conventional fuels like petrol, or the petrodiesel. The alternate fuel like biofuels are consists of Oxygen as a central element. The combustion CI or SI engine comes under exothermic reaction, i.e., Oxidation of Unburned Hydrocarbons in the combustion chamber. In the complete combustion, the Unburned Hydrocarbons ends with H_2O &CO_2, but incomplete combustion ends with higher proportions of HC & CO emissions[203].

Author Lakshminarayanan et al.[204]express that the Unburned Hydrocarbons emissions less influencing by the air-fuel equivalence ratio than homogeneously mixed air-fuel ratio. The author Gumus et al. [203] deliberation the increase in IP shows a tremendous effect on HC emissions reduction.

In Figure 5.10_c the HC emissions are higher with KB+20gLA blend because increased viscosity, density, less fuel Calorific value also a compositional difference. In the portrayed **Figures 5.10_c, 5.32_a, 5.32_b**, and **5.32_c**HC emissions are lower at 60 % full load as a result of available time, temperature and proper air entrainment around injected fuel droplets.

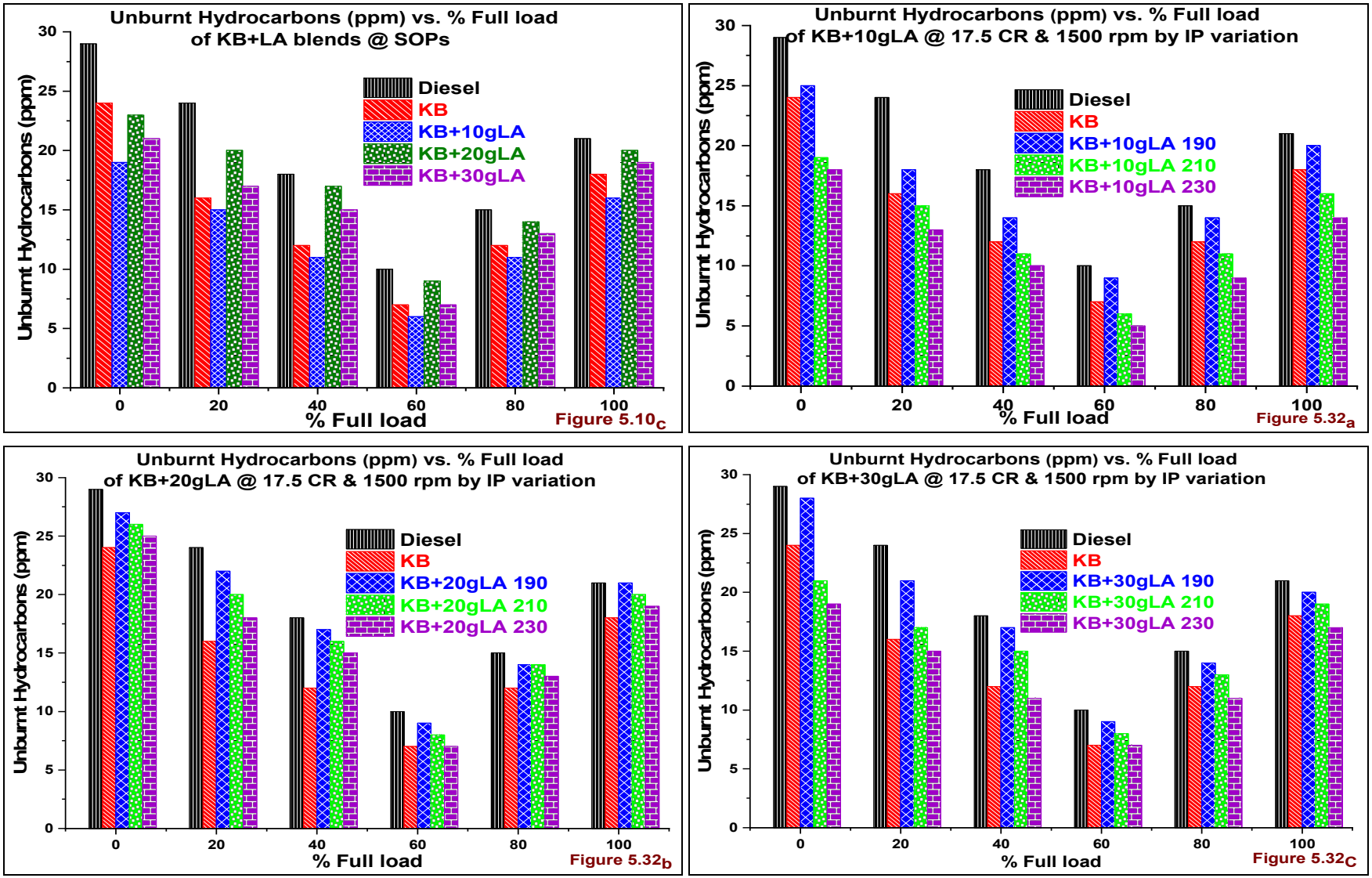

Figure5.32$_{a, b, c}$ HC (ppm) vs. % Full load & IP of KB+LA blends

5.10.3 Oxides of Nitrogen (ppm) vs. % Full load & IP

The air/fuel borne Nitrogen has mono and diatomic molecules. The diatomic molecules are stable at lower temperatures than monatomic molecules. The temperatures above 1200°C the diatomic molecules are vigorously reacting with fuel borne Oxygen and forming Oxides of Nitrogen (NOx) emissions[205]. The variation of IP is the significant input variable to apply high viscous fuels on DI CI engine for better BTE and BSEC through there is an increase in NOx emissions. The increase in NOx emissions because of improvement in air-fuel mixing and proper flame spread in the combustion chamber[206].

In Figure 5.11_c the NOx emissions are decreasing with the increase of Lauric acid blend quantity in KB fuel. At lower blend of Lauric acid in KB fuel, i.e., KB+10gLA higher ICP, NHRR, and RPR peaks are attained at 230bar IP are portrayed in Figure 5.24_a, 5.26_a, and 5.27_a respectively. The author Ogunkoya et al.[207] observed similar results by investigating the DI CI engine using deoxygenated Canola based Lauric acid.

The highest NOx emissions have arrived with KB+10gLA blend than KB+20gLA and KB+30gLA. In Figure 5.2_c and 5.24_a, the higher peak and lower ID with KB+10gLA blend because of improvement in Cetane number. This increased ICP peak with higher retention time reasoned to increase NOx emissions portrayed in Figure 5.33_a.

In **Figure $5.33_{a, b, c}$** the NOx emissions increased with the increase in % full load on the engine but the reduction in NOx emissions with the increase in Lauric acid quantity. The NOx emissions also increased with the increase in IP, but the decreasing trend can perceive in Figure 5.11_c.

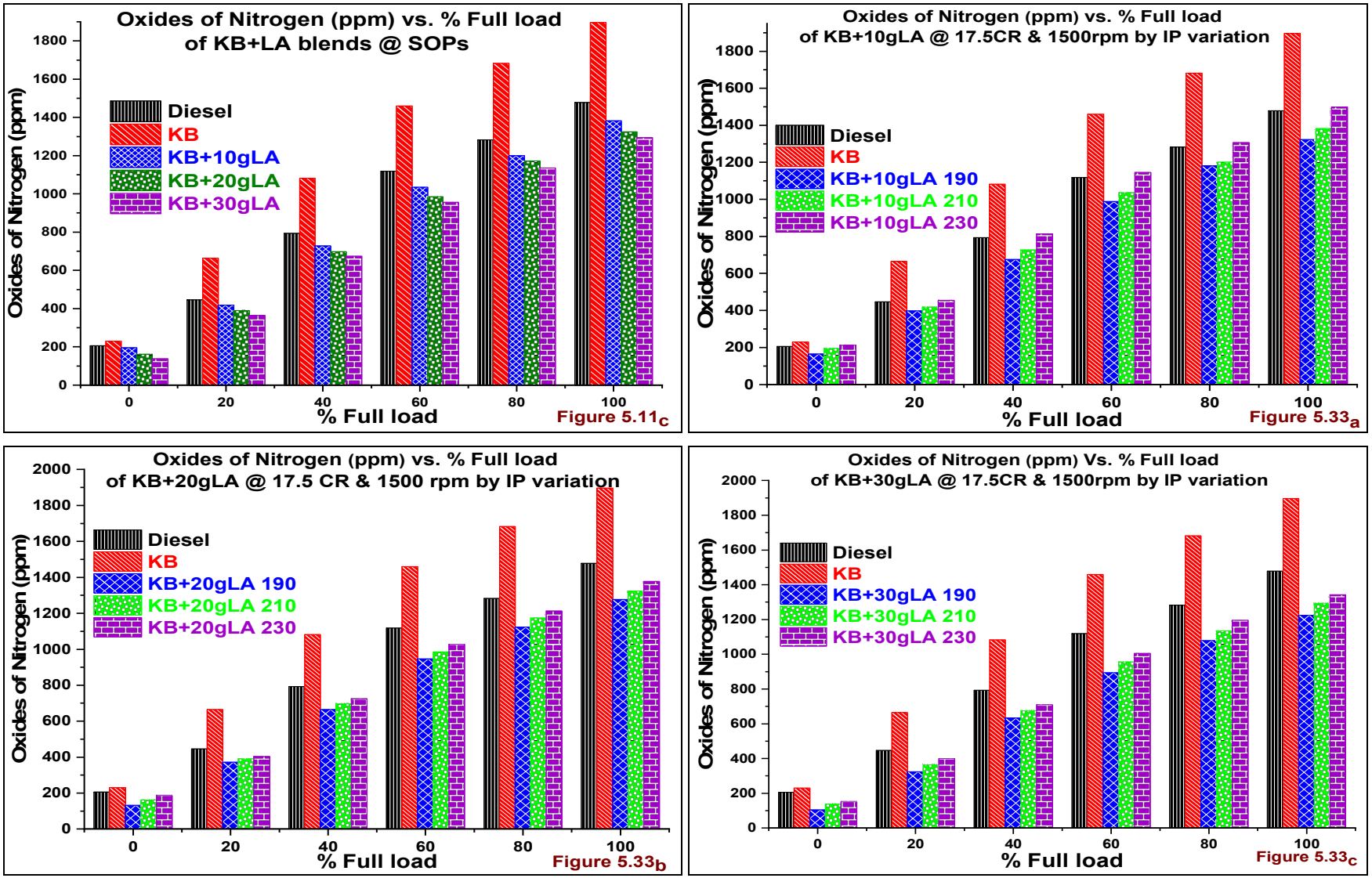

Figure 5.33$_{a, b, c}$ NO_x (ppm) vs. % Full load & IP of KB+LA blends

5.10.4 Smoke opacity (%) vs. % Full load, IP

The literature leveled that the increasing Smoke trend with the increase in load on an engine by cause of increasing fuel quantity with the increased % full load[208]. Author Man et al.[209]reported that the presence of Oxygen in fuel led to reducing Smoke emissions in the diffusion phase of combustion. The lowest Smoke emissions observed with clean KB fuel because of availability of Oxygen composition and slightly high Calorific value than Lauric acid blends.

Authors Ogunkoya et al. and Venkanna et al. [207,210] reported that the aromatics are increasing with the increase in the Lauric acid blend. The increase in aromatics with the blend of Lauric acid is causing to increase Smoke opacity which can observe in Figure 5.12_c. The decrease in Calorific value was the major influencing factor to decrease ICP, NHRR peaks can observe in Figure 5.2_cFigure $5.24_{a, b, c}$.

In Figure 5.12_c the Smoke emissions are increasing with the increase in blend ratio. This increase because of an increase in viscosity, density, less Calorific value, and increase in aromatics.

In **Figure 5.34$_a$** the Smoke opacity decreased with the increase in IP with the KB+10gLA fuel. This decrease because of proper fuel atomization and attainment of the required flame temperature to burn the tiny droplets. Here the Smoke opacity less than Diesel fuel even at 190 bar IP but higher than KB fuel.

In **Figure 5.34$_b$** the Smoke opacity reached higher at 190 bar IP because of the increase in the viscosity, density and less calorific value of KB+20gLA. The increased droplet size because of improper atomization at 190 bar is due to the increase of Lauric acid blend in KB fuel.

The observations from **Figure 5.34$_c$** revealed that the increase in Smoke opacity by cause of loss Calorific value, increased viscosity, density, and aromatic compounds. Here the Smoke opacity at all injection pressures even higher than Diesel fuel.

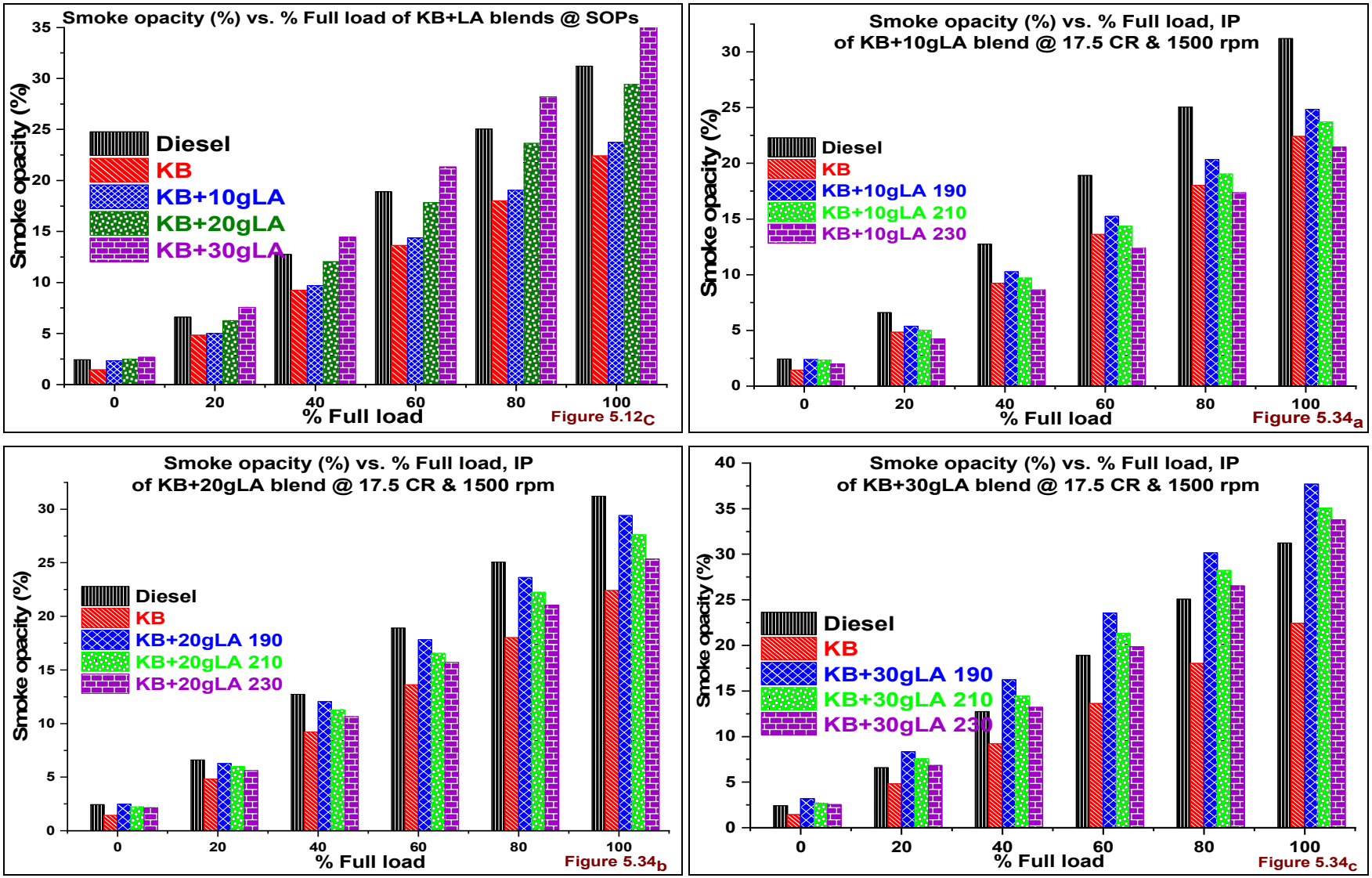

Figure 5.34$_{a, b, c}$ Smoke opacity (%) vs. % Full load& IP of KB+LA blends

Module - 4

5.11 Combustion analysis on KB+MCM blends @ Full load, 17.5 CR, 1500rpm

5.11.1 Incylinder pressure (bar) vs. Crank angle (θ), IP

The In cylinder pressures with MCM particles blend in KB fuel samples at full load operation with IP 210 bar, and at engine speed 1500rpm are Diesel (63.87), KB (66.32), KB+1gAP (69.57), KB+2gAP (66.42), KB+3gAP (69.74). The higher ICPs peaks accomplished at, the lower higher level of the blend. The ICP peak increased with KB+1gAP blend in the combustion chamber.

Because of lower viscosity, density and increased surface area to volume ratio of the MCM particles has induced improvement in the mixing process. The higher viscosity, density and lower Calorific value of KB+3gAP blend led to accumulating more fuel in the increased ID period. The multilevel explosion of MCM particles leads to increasing ICP peak with KB+3gAP than above blend. The author Sadhik et al.[211]observed similar results in his work.

The obtained ICP peaks with KB+1gAP blend are 67.06, 69.57, 67.58 and 68.15 bar at 190, 210, 230 and 250 bar IPs portrayed in the **Figure 5.35$_a$**. The higher IPC peak obtained at 210 bar IP. Because of the available ID period is sufficient to accumulate the required fuel quantity and to attain proper Combustion.

The ICP peaks with KB+2gAP blend are 69.5, 66.42, 70.16, and 66.49 bar at 190, 210, 230, and 250 bar IPs in **Figure 5.35$_b$**. The higher ICP peak at 230 bar IP is because of proper atomization and sufficient spray angle. Another highest ICP peak 69.5 bar reached at 190 bar IP because of higher droplet size due to improper atomization. This increased ID caused to accumulate more fuel for combustion.

The obtained ICP peaks with KB+3gAP blend are 69.63, 69.74, 70.65 and 70.04 bar at 190, 210, 230 and 250 bar IPs. The increased ID caused to accumulate more fuel for the above three blends but higher ICP peak 70.65 bar observed at 230 bar IP. The multilevel micro explosion reasoned to increase ICP peak for all fuel samples depicted in **Figure 5.35$_c$**.

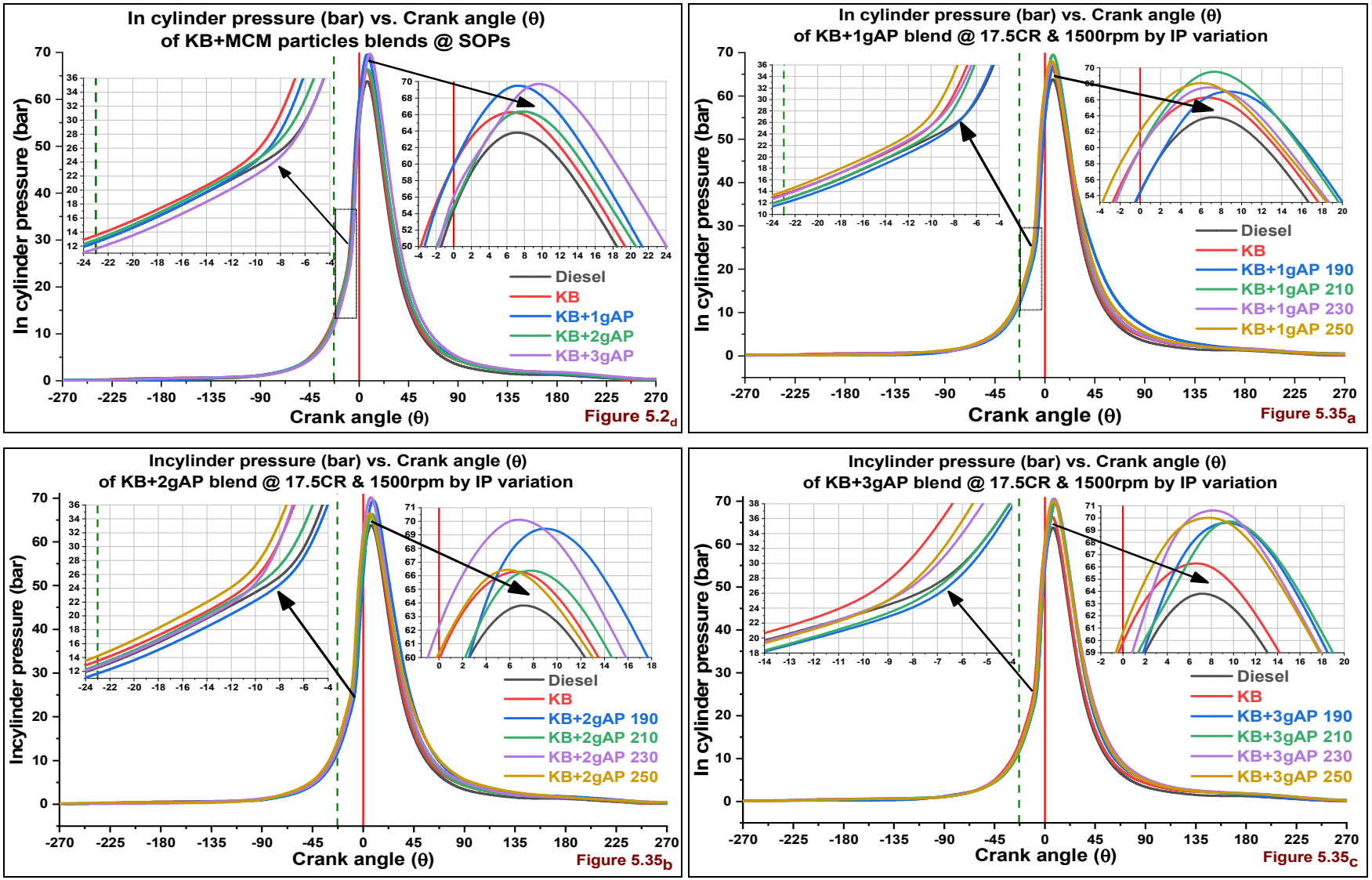

Figure 5.35$_{a, b, c}$ ICP (bar) vs. Crank angle (Θ) & IP of KB+MCM blends

5.11.2 Cumulative heat release (kJ) vs. Crank angle (θ), IP

The increase in IP reduces the injection duration as well as combustion duration because increased spray area with small droplet size. At higher IP unusually high density and viscosity of neat biodiesels attain prior injection by cause of their higher Cetane number, bulk modulus[212].

The maximum CHR peaks are 1.43, 1.12, 1.11 and 1.26 kJ at 190, 210, 230, and 250 bar IP. In **Figure 5.36$_a$** the highest CHR peaks are attained at 190, 250 bar IPs. The improper injection and increased droplet size at 190 bar IP caused higher ID period. At this IP the maximum accumulated fuel caused to rapid combustion in the premixed phase. At 250 bar IP the smaller droplet size by cause of improved atomization led to improving the combustion and flame spread though there is less fuel accumulation in the less ID period.

The CHR peaks are 1.26, 1.07, 1.17, and 1.26 kJ at 190, 210, 230, and 250 bar IPs. In **Figure 5.36$_b$** the higher CHR peaks are obtained at 190, and 250 bar IPs. At 190 bar IP because of poor atomization, the droplet size higher because of increased viscosity, density. The higher ID led to accumulating more fuel and induced to rapid combustion in the premixed phase even though the accumulated fuel underwent partial combustion. This retained mass accomplished combustion in mixing controlled combustion phase because of the availability of Oxygen after particle explosion. The higher peak at 250 bar IP the smaller droplet size because of proper atomization provoked to improved flame spread in the combustion chamber.

In **Figure 5.36$_c$** the max CHR peaks are 1.17, 1.25, 1.22, and 1.33 kJ at 190, 210, 230, and 250 bar IPs. The higher viscosity, density of KB+3gAP blend is bringing to being higher ID than KB+1gAP; KB+2gAP blends. At IP 250 bar the high viscous KB+3gAP blend has attained proper atomization than at 190, 210 and 230 bar IPs. At lower IPs, the higher size droplets have absorbed more heat from the surrounded hot air in the combustion chamber. At 190 bar IP the decrease in the cylinder temperature and motivated to occur maximum combustion in the mixing controlled combustion phase.

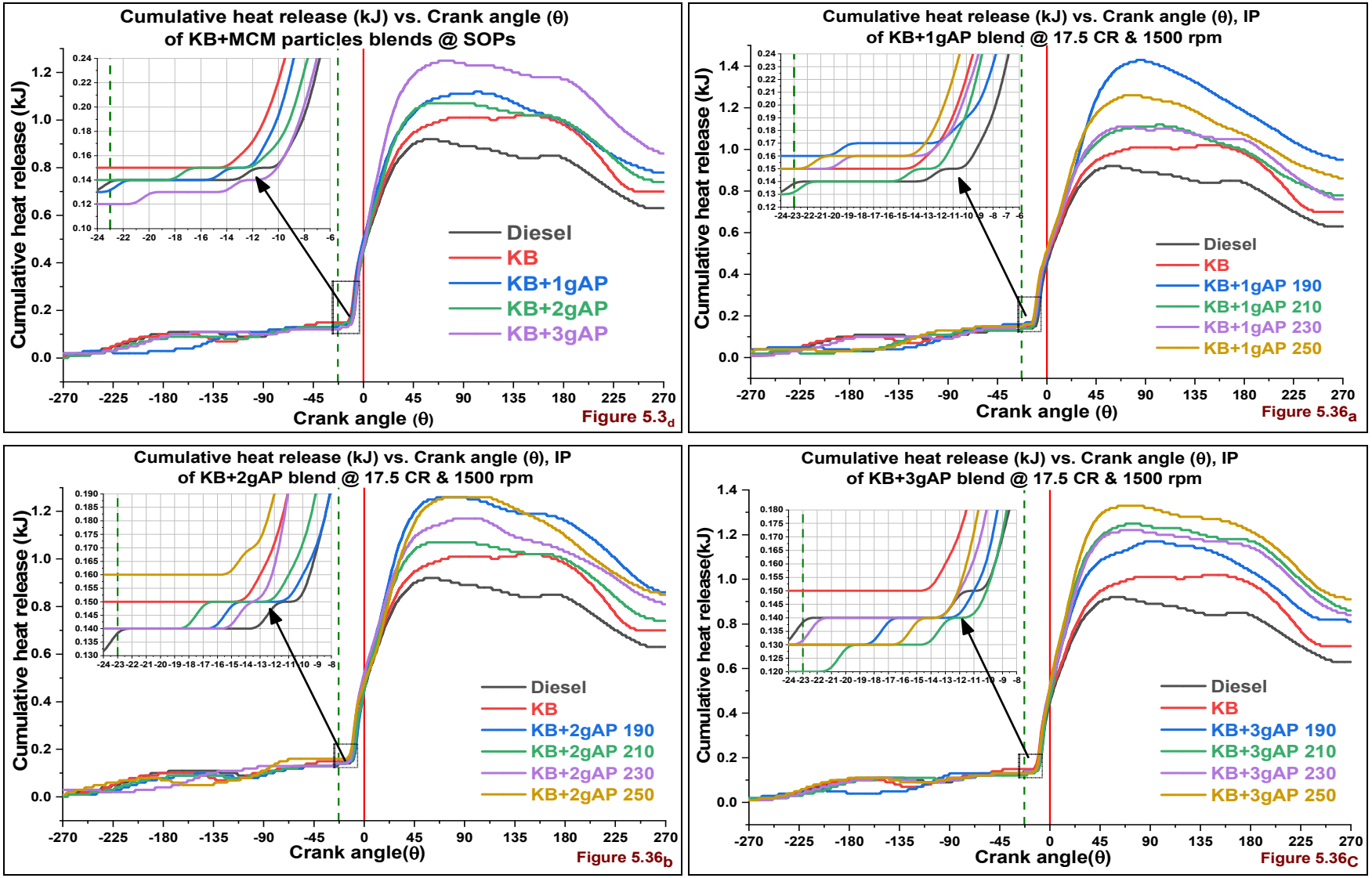

Figure 5.36$_{a, b, c}$ CHR (kJ) vs. Crank angle (Θ) & IP of KB+MCM blends

5.11.3 Net heat release rate (J/θ) vs. Crank angle (θ), IP

In Figure 5.4$_d$ at standard IP (210 bar) the Net heat release rate (NHRR) is higher with KB+1gAP, KB+3gAP blends. The increase in NHRR with KB+3gAP is due to more fuel accumulation in the higher ID period and also multilevel microexplosion of MCM particles.

The increase in IP leading to decreases in the ID period because of improvement in atomization, better dispersion and also earlier fuel injection[48]. The maximum NHRR peaks with KB+1gAP blend are 45.91, 46.91, 42.79 and 44.75J/θ at 190, 210, 230, and 250 bar IPs respectively. The higher NHRR peak at 210 bar IP is because of sufficient time to accumulate more fuel in ID period and to attain rapid combustion in the premixed combustion phase. The less ID at higher IPs is induced to attain combustion in the diffusion combustion phase this can observe in the**Figure 5.37$_a$**.

The viscosity is increasing with the increase in MCM particles blend quantity in KB fuel. The increase in MCM particles blend in KB fuel owes to increased the contact area of particles. The above effect increased the heat absorption rate of particles with hot air in the combustion chamber. The MCM particles explosion also improved mixing process[213].

The NHRR peaks are 41.86, 41.88, 42.29 and 49.27J/θ at 190, 210, 230 and 250 bar IPs respectively. The increase in NHRR at 250 bar IP is because of improved air/fuel mixing because of proper atomization though there is less ID period than other IPs. The too much increase in droplet size at lower 190, 210 bar IPs is influenced to increase the ID period. Due to which the maximum fuel is undergoing combustion in the mixing controlled combustion phase represented in **Figure 5.37$_b$**.

The NHRR peaks are 49.14, 48.31, 45.25 and 50.21J/θ at 190, 210, 230 and 250 bar IPs respectively. The above similar reasons can observe in **Figure 5.37$_c$** at 250 bar IP. The increase in inline pressure and increasing ID period because of the increase in surface tension and viscosity of KB+3gAP blend. Because of increased penetration and impingement of jet on piston head or cylinder walls[178] affected to increase NHRR peak at 190, 210 and 250 bar IPs.

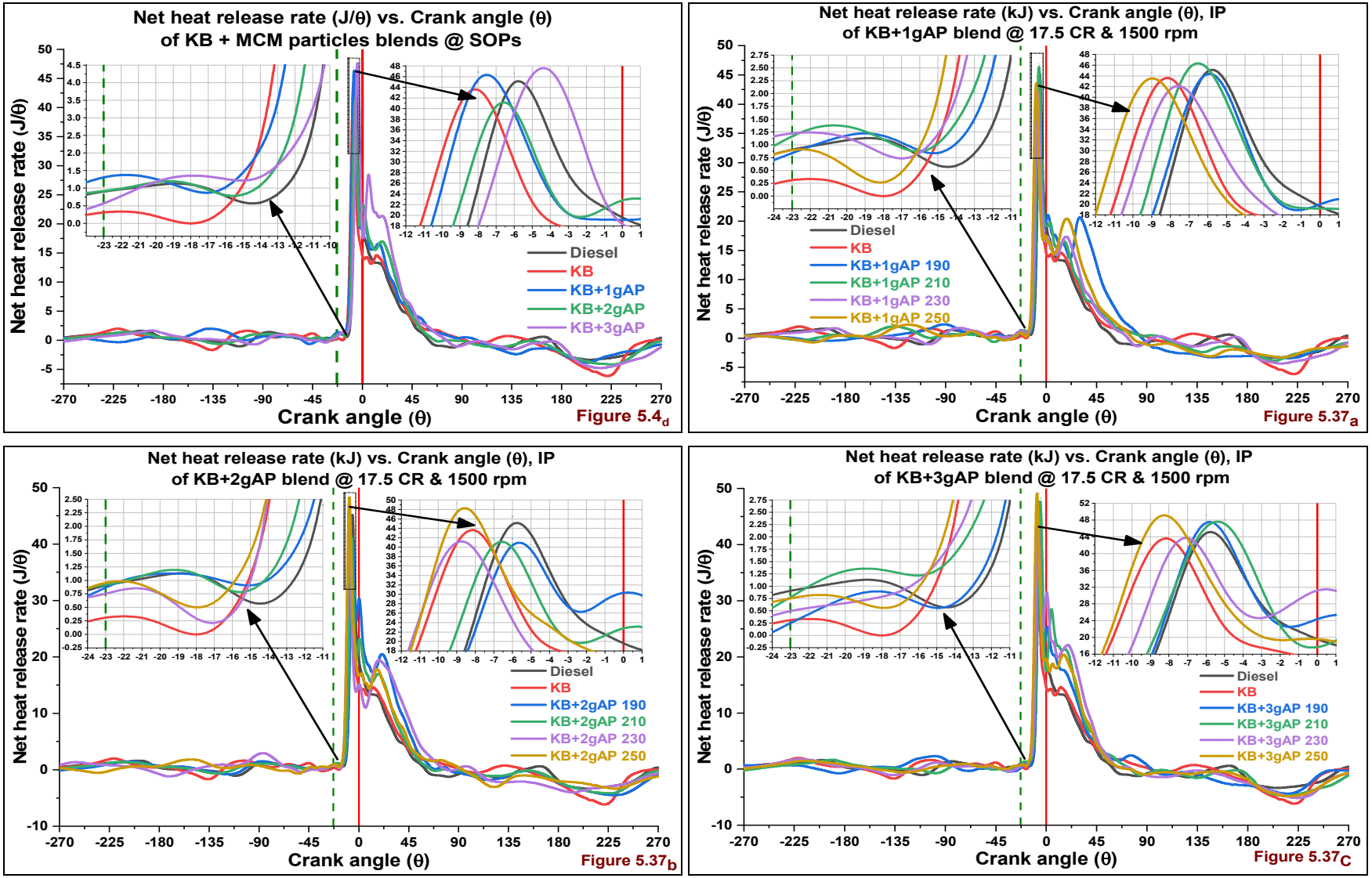

Figure 5.37$_{a, b, c}$ NHRR (J/Θ) vs. Crank angle (Θ) & IP of KB+MCM blends

5.11.4 Rate of pressure rise (dp/dθ) vs. Crank angle (θ), IP

The higher rate of pressure rise (RPR) in DI CI engine is because of less fuel comprised Oxygen, increased viscosity, density, and higher ID due to less Cetane number. All these parameters are the majorly influenced to accumulate more fuel in the ID period and attain rapid premixed combustion led to increasing RPR peak[98,214].

The obtained RPR peaks with KB+1gAP blend are 5.16, 5.25, 4.87, and 5.06 bar at 190, 210, 230 and 250 bar IPs respectively. In the portrayed **Figure 5.38$_a$** the higher RPR peak at 210 bar IP. Because of the accumulation of higher size droplets in the higher ID period. The increased viscosity signified to increase ID period because of improper fuel atomization and less Cetane number of KB+1gAP blend than KB fuel.

The attained RPR peaks with KB+2gAP blend are 4.73, 4.76, 5.38 and 4.82 bar at 190, 210, 230 and 250 bar IPs respectively. In the portrayed **Figure 5.38$_b$** the higher RPR peak attained with KB+2gAP blend at 230 bar IP. Because of an increase in viscosity, density, surface area to volume ratio and less Calorific value than KB+1gAP blend. At lower IPs such as 190, 210 bar IPs the improper atomization is induced to increase droplet size and led to decrease NHRR values. In Figure 5.38$_b$ at 250 bar IP, the less RPR peak by cause of improved atomization due to smaller droplet size as well as improvement in combustion.

In the depicted **Figure 5.38$_c$**, the RPR peaks with KB+3gAP blend are 5.42, 5.39, 5.06 and 5.58 bar at 190, 210, 230, and 250 bar IPs respectively. The KB+3gAP blend higher viscosity, density, surface area/volume ratio and less Oxygen, the Cetane number increased ID period. The factors mentioned above reasoned to higher RPR peaks with KB+3gAP blend than all other blends. The author Yesilyurt et al.[215] reported similar results.

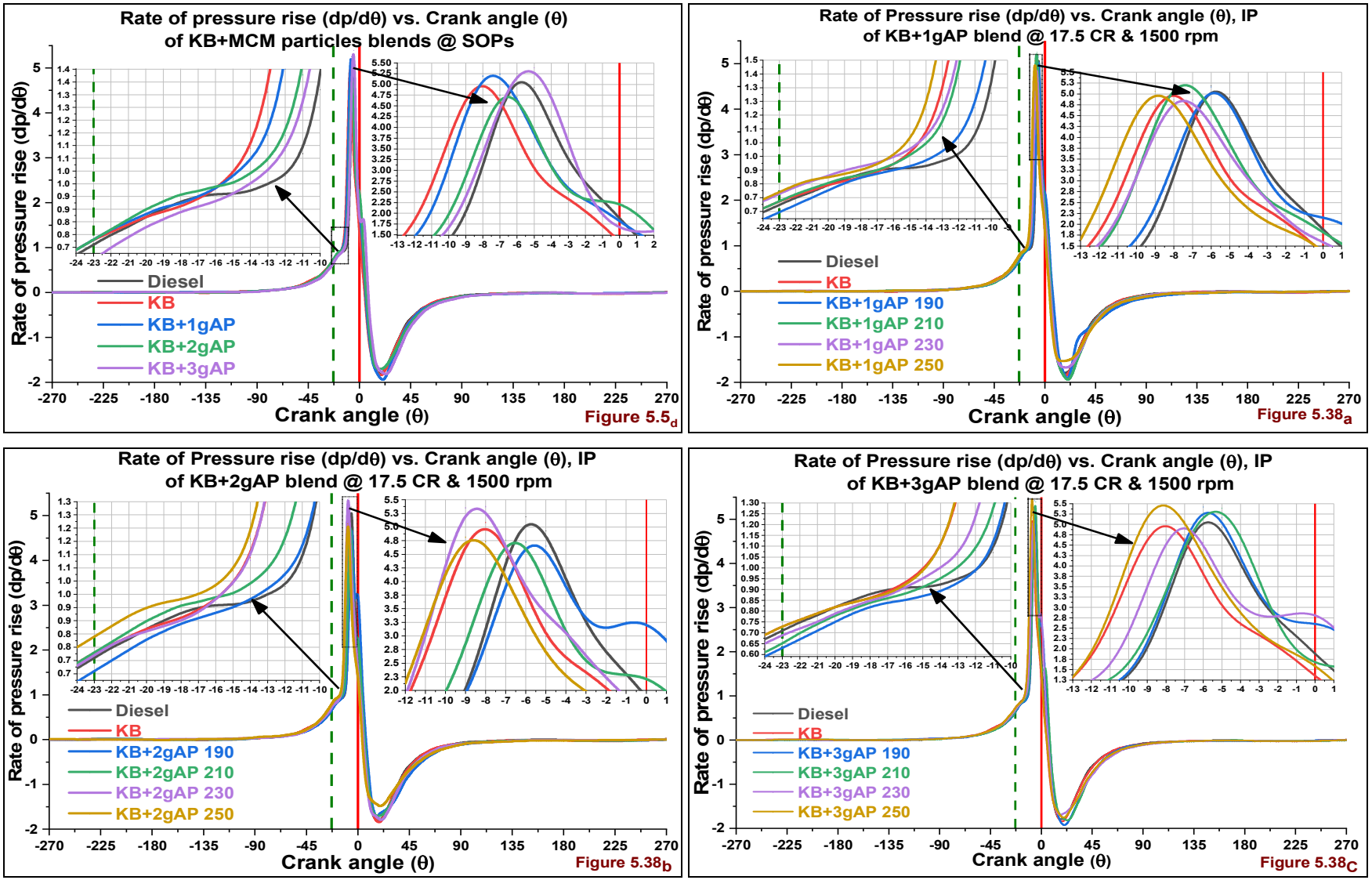

Figure 5.38$_{a, b, c}$ RPR (dP/dΘ) vs. Crank angle (Θ) & IP of KB+MCM blends

5.12 Performance analysis on KB+MCM blends @ % load, 17.5 CR, 1500 rpm

5.12.1 Brake thermal efficiency (%) vs. % Full load, IP

The increase in MCM particles blend in KB fuel is caused to decrease in Brake thermal efficiency (BTE). This because of a reduction in Calorific value and increased viscosity and density of MCM particles blends. The lower BTE with KB+2gAP blend because of compositional difference and lower ICP, CHR, NHRR, and RPR peaks in the Figures 5.2_d, 5.3_d, 5.4_d, and 5.5_d respectively.

In **Figure 5.39$_a$** the higher BTE with KB+1gAP blend at 210 bar IP because of higher ICP, NHRR peaks. In Figure 5.35_a, 5.37_a the higher NHRR peak near to bTDC with higher ICP peak increased BTE. Because of the maximum quantity of fuel droplets accumulation in the necessary ID period.

In **Figure 5.39$_b$** the higher ICP peak arose with KB+2gAP blend at 230 bar IP. In Figure 5.35_b the higher BTE at 230 bar IP because of the occurrence of higher ICP peak near to TDC with higher RPR.

The higher BTE obtained with KB+3gAP blend at 250 bar IP. Because of an increase in fuel atomization and its accumulation in the more extended ID period than KB+1gAP, KB+2gAP fuel blends. The increase in MCM particles quantity in fuel influenced to increase surface area to volume ratio and viscosity. At 250 bar IP the KB+3gAP blend played the leading role in improving BTE however there is an increase in ID period.

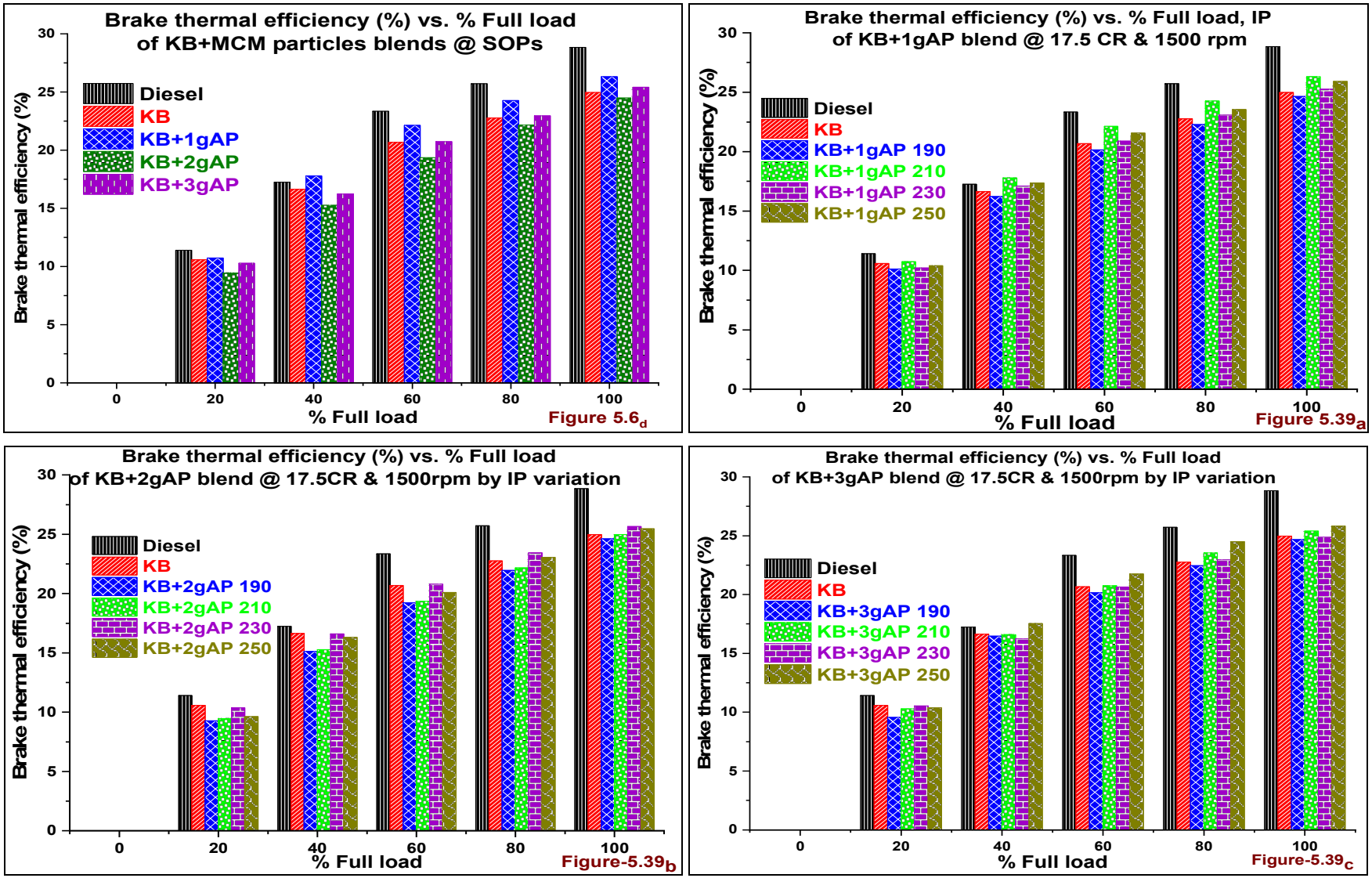

Figure 5.39$_{a, b, c}$ BTE (%) vs.% Full load & IP of KB+MCM blends

5.12.2 Brake specific Energy consumption (MJ/kW-hr) vs. % Full load, IP

The Author Puhan et al. reported that the brake specific fuel consumption (BSFC) is not the preferable parameter. The BSEC is the preferable parameter to compare fuels with different nearby Calorific values, densities, and viscosities. The Brake specific energy consumption (BSEC) is to know the required energy for developing unit power of an IC engine. The BSEC is the dependent variable on each fuel calorific value, density and viscosity together. Sometimes the BSFC may have a more considerable difference with Diesel but BSEC near to diesel because of its lower Viscosity, density with higher Calorific value[216].

In **Figure 5.40$_a$**, **5.40$_b$**and **5.40$_c$**at 190 bar IP the BSEC increased with the increase in MCM particles blend quantity. At this IP the increased MCM blend quantity provokes to increase viscosity this led to increasing fuel injection quantity. The increase in ID period can observe in the portrayed Figures 5.35$_{a, b, \&c}$. The blend Calorific value and Cetane number also decreased with the increase in MCM particles blend. The lower BSEC is with Diesel at 210 bar IP because of its lower density, viscosity, and higher Calorific value.

In **Figures 5.40$_{a, b, \&c}$** the BSEC decreased as the increase in IP on the same blend. This BSEC increased with increase in MCM particles blend quantity in KB fuel though there is an increase in IP. In Figure, 5.40$_a$ the KB+1gAP blend BSEC is lower at 210 bar IP. The NHRR peak 46.91J/θ has attained in Figure 5.40$_c$because of higher ICP peaks in the Figures 5.35$_a$, 5.37$_a$.

In **Figure 5.40$_b$** the BSEC is lower at 250bar IP with KB+2gAP blend because of improved atomization. In the Figures 5.35$_b$, Figure 5.37$_b$ the 70.16 bar high ICP peak, 49.27J/θ high NHRR peak respectively. In Figure 5.40$_c$ the BSEC is lower at 250 bar IP due to improvement in fuel atomization, similarly the higher BSEC at 190 bar IP because of improper atomization. The minimal BSEC variation at all IP in **Figure 5.40$_c$** because of minimal ICP, NHRR peaks variation in Figures 5.35$_c$, 5.37$_c$ respectively.

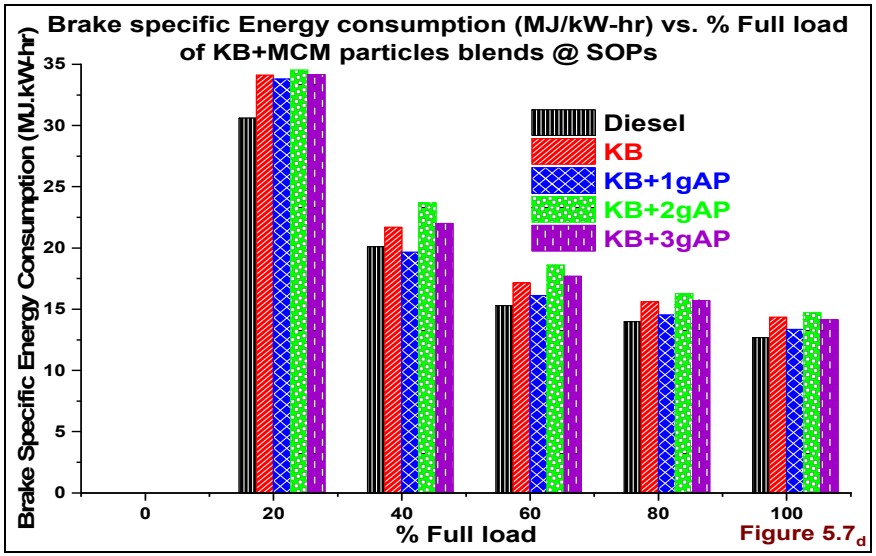

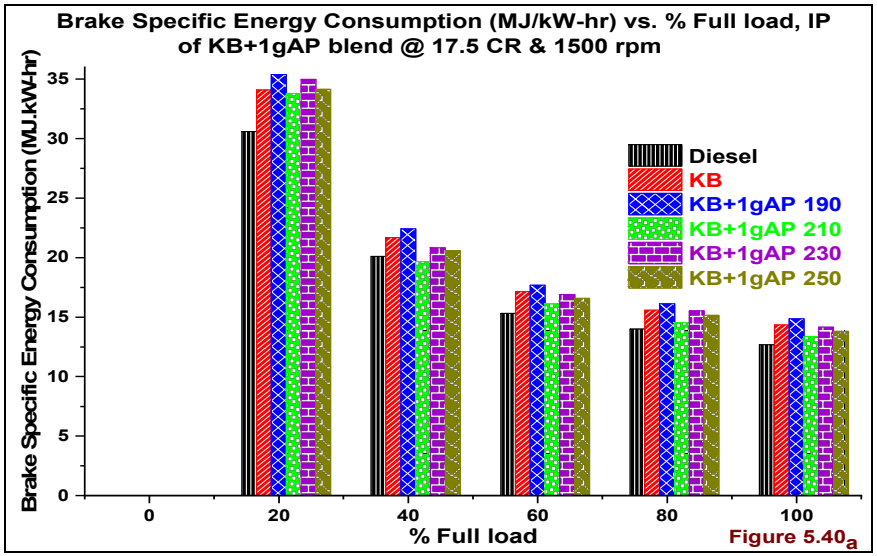

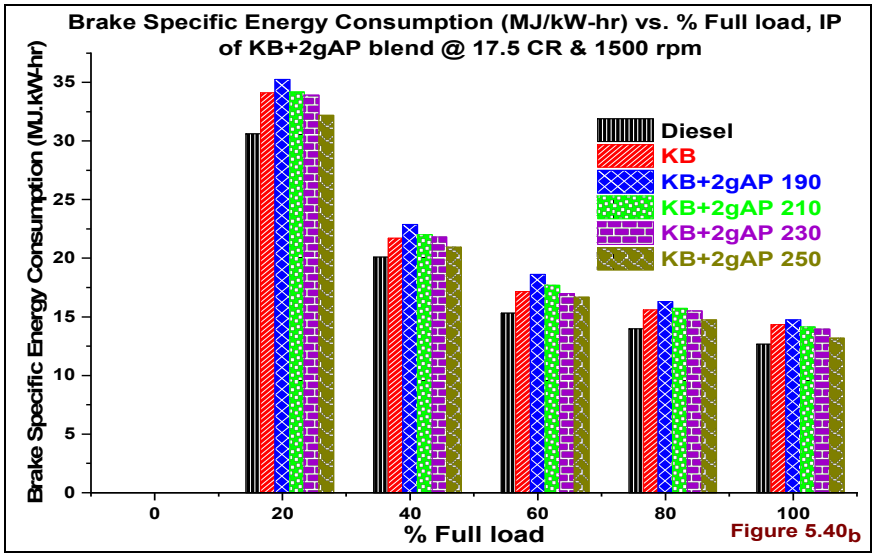

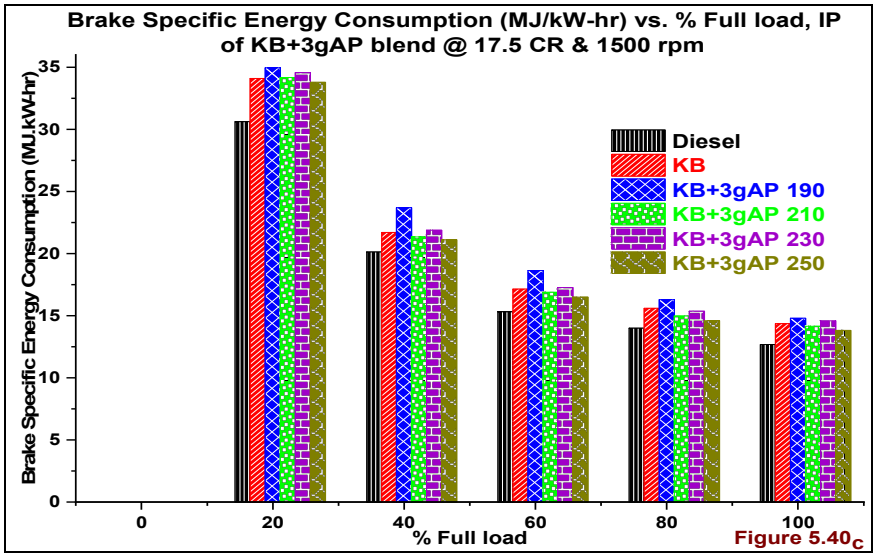

Figure 5.40$_{a, b, c}$ BSEC (MJ/kW-hr) vs. % Full load & IP of KB+MCM blends

5.12.3 Exhaust gas temperature (ºC) vs. % Full load, IP

The Exhaust gas temperature (DGT) is increasing with the increasing load on the engine. An increase in fuel quantity with the load increased in energy release in the combustion chamber. This increased fuel quantity facilitates the availability of Oxygen in fuel and increases in peak though there is a reduction in ID period. Similarly, the increase in fuel IP leading to increasing in EGT. The neat biodiesel bulk modulus caused to occurring prior injection. The increased peak retention time when the ICP peaks are near aTDC, and NHRR peaks are away to bTDC [202].

The attainment of the above situation in the Figures 5.2_{d}, $5.35_{a, b, \&c}$ and also Figures 5.4_{d}, $5.37_{a, b, \&c}$ leads to sharp premixed peak incite to occur the diffusion combustion. In the Figures $5.35_{a, b, \& c}$ the ICP peaks near to aTDC because of occurrence of early injection, increased atomization and decreased fuel droplet size. The incidence of ICP peaks at near to aTDC is leading to increasing the time for fuel combustion in the combustion chamber. In particular, this occurrence initiated diffusion combustion and to increase the BTE, EGT with the increase in IP.

In **Figure 5.41_{a}** the highest EGT at 210 bar IP is because of sufficient time to accumulate more quantity of fuel in the ID period. The multilevel micro explosion started after absorption of heat of MCM particles from the hot air in the combustion chamber. In Figure 5.41_{a} the higher EGT at 210 bar IP with KB+1gAP blend because of higher ICP peak in Figure 5.35.

In **Figure 5.41_{b}, 5.41_{c}** the higher EGT with KB+2gAP, KB+3gAP blends at 250 bar IP because of proper fuel atomization though these are highly viscous and less Calorific value. At this IP the increase in MCM particles surface area to volume ratio improved mixing and initiated the multilevel micro-explosion.

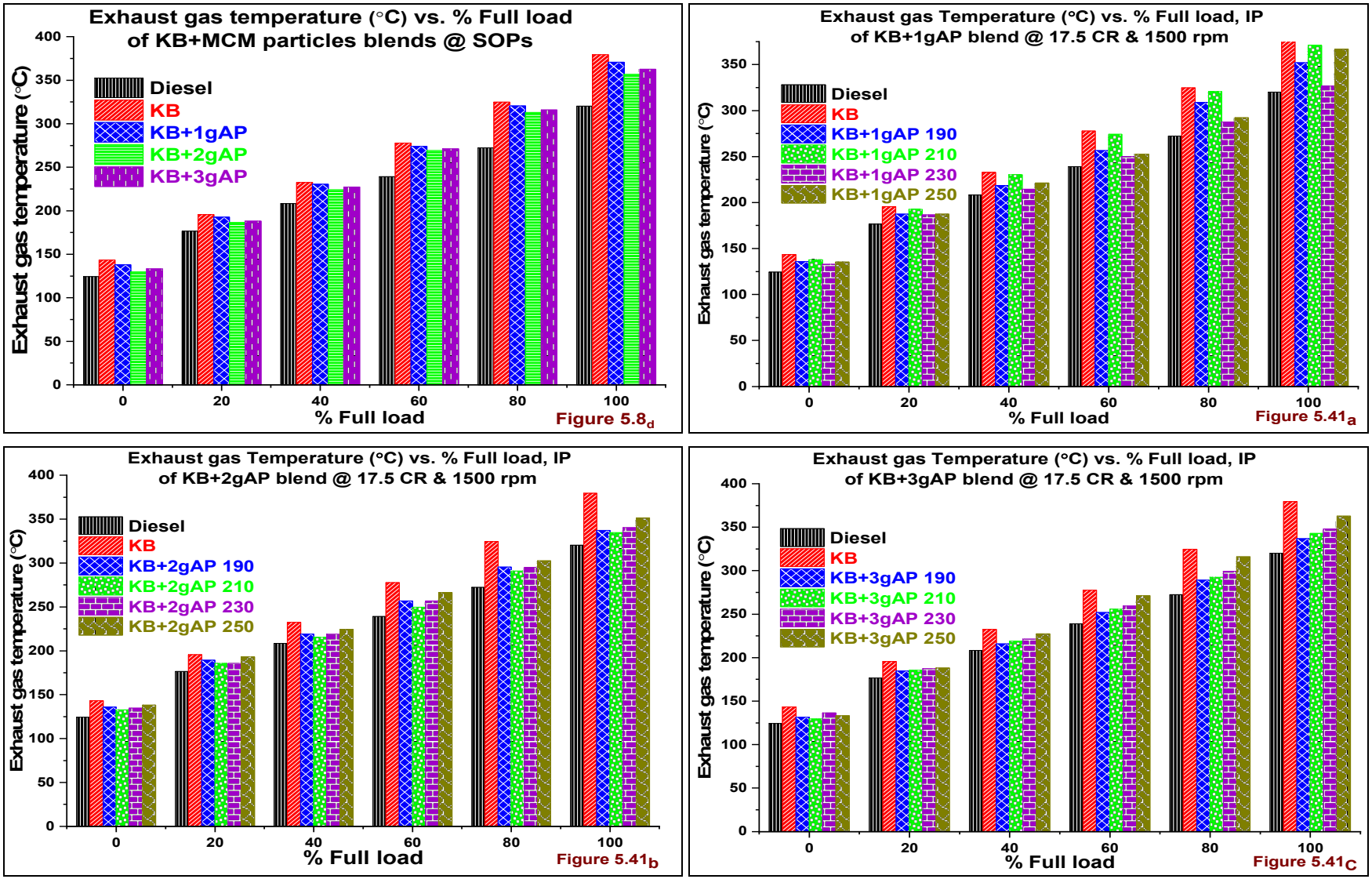

Figure 5.41$_{a, b, c}$ EGT (°C) vs. % Full load & IP of KB+MCM blends

5.13 Emission analysis on KB+MCM blends @ % full load, 17.5 CR, 1500rpm

5.13.1 Carbon monoxide (% vol) vs. % Full load, IP

The CO emissions are lower at 210 bar IP than 230, 250 bar IPs. Because of available time for higher fuel accumulation in the extended ID period. At higher IPs 230 and 250 bar, the injected fuel induced to over air/fuel mixing. This because of the presence of MCM particles with lower viscosity and density than KB+2gAP, KB+3gAP blends. In **Figure 5.42$_a$** the 1g particles in KB+1gAP blend at 210 bar IP facilitate to proper air/fuel mixing directed to lower CO emissions. In Figure 5.42$_a$ at 230, 250 bar IP the over air/fuel mixing of KB+1gAP blend directed to higher CO emissions.

In Figures 5.9$_d$, **5.42$_b$** the higher CO emissions due to the compositional difference, increase in viscosity, a density of KB+2gAP blend than KB+1gAP, KB+3gAP. The CO emissions of KB+2gAP blends lightly higher than KB+1gAP, KB+3gAP blends though it has followed a similar trend. The CO emissions are higher at 190 bar IP with KB+1gAP, KB+2gAP, and KB+3gAP blends.

In **Figure 5.42$_c$**, at 250 bar IP the CO emissions of KB+20gLA blend even lower than KB fuel due to the occurrence of diffusion combustion. The droplet size increased because of an increase in viscosity of the KB+3gAP blend. This viscosity increase provoked too early fuel injection, less ID with superior atomization than 210 bar IP. This accumulated mixture not able to combust completely in the premixed phase. The explosion of particles and release of Oxygen due to particles contained methanol led to diffusion combustion.

The MCM particles contained Karanja biodiesel viscosity increased with the increase in quantity. This increase in viscosity and reduction in calorific value compensated at higher IP 250 bar. The availability of Oxygen in the MCM particle is because of the presence of methanol. The presence of methanol in the MCM particles is because of its usage at the time of wet grinding in the planetary ball mill.

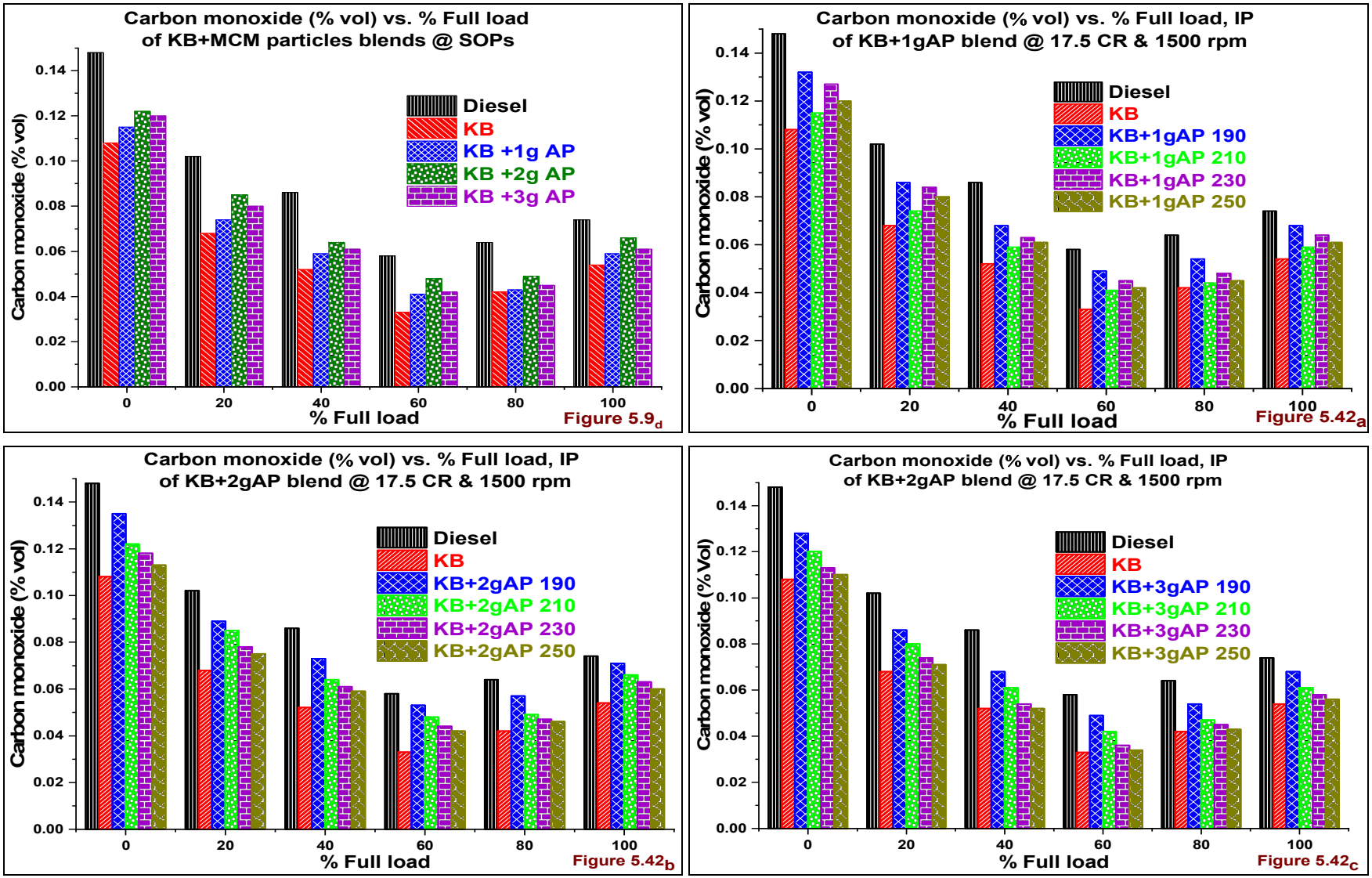

Figure 5.42$_{a, b, c}$ CO (% vol) vs. % Full load & IP of KB+MCM blends

5.13.2 Unburned Hydrocarbons (ppm) vs. % Full load, IP

The improved air/fuel mixing due to the increased surface area to volume ratio with the accumulation of sufficient mixture at 210 bar. In Figure 5.10_b the HC emissions are lower with KB+1gAP blend. The further increase in MCM particle in KB fuel increased viscosity, density, and reduced calorific value. In Figure 5.4_d the occurrence of diffusion combustion with KB+3gAP blend led to a reduction in HC emissions.

In **Figure 5.43_a** the HC emissions are lower at 210 bar IP because of over mixing of air/fuel at higher IPs 230 and 250 bar. At this higher IPs, the crevices formation due to fuel impinged on cylinder walls commenced to cool down the cylinder chamber and deterioration in combustion.

The KB+2gAP blend has attained higher HC emissions in Figure 5.10_b because of increased viscosity, density, and reduction in calorific value. In Figure 5.43_b the HC emissions are lower at 250 bar IP. The high viscous fuel accumulation is higher with higher droplet size increased the delay at lower IPs. This effect can observe in **Figure 5.43_b**, but the HC reduction is not lower than KB+3gAP blend.

In the portrayed Figure 5.37_cat all IPs, the KB+3gAP blend undergone diffusion combustion. The KB+3gAP blends higher viscosity caused to higher fuel accumulation in the less ID period. At 230, 250 bar IPs this high viscous fuel attained to occur early injection. The early injection and reduction in droplet size initiated sufficient mixture formation even in less ID period. The lower HC emissions are because of availability of Oxygen due to the explosion of particles.

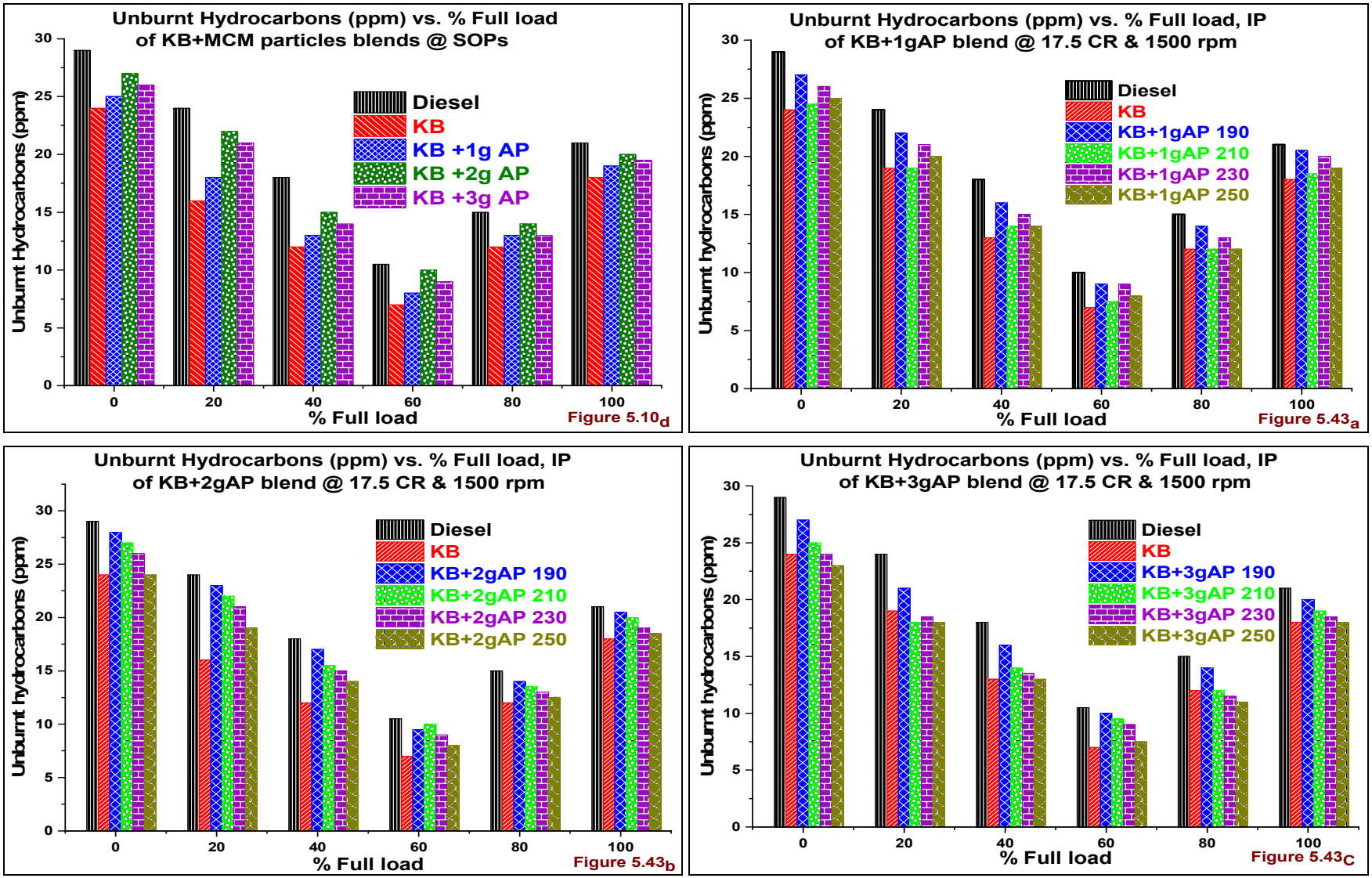

Figure 5.43$_{a, b, c}$ HC (ppm) vs. % Full load & IP of KB+MCM blends

5.13.3 Oxides of Nitrogen (ppm) vs. % Full load, IP

The monatomic molecules are quote unstable and rapidly participating in the reaction with nascent Oxygen to form NOx emissions for stabilization. The following three stages of Zeldovich Mechanism explains the NOx formation in CI engines[129].

1. $N_2 + O \rightarrow NO + [N]$
2. $[N] + O_2 \rightarrow NO + [O]$
3. $[N] + [OH] \rightarrow NO + [H]$

In the Figure 5.11_d the lower NOx emissions observed with KB+2gAP blend because of less available time to form sufficient air/fuel mixture formation at 210 bar IP and less calorific value, slightly increased viscosity, density. The increase in surface area to volume ratio helped to improve air/fuel mixture formation. The NOx emissions slightly increased with KB+3gAP blend. The higher NOx emissions are with KB fuel because of inbuilt Oxygen and higher calorific value. The lower NOx emissions are because of a lack of Oxygen in Diesel than all other fuel blends.

In **Figure 5.44_a** the NOx emissions are lower at 190 bar IP is because of improper air/fuel mixing because of poor fuel atomization. The NOx emissions are higher at 210 bar IP with KB+1gAP blend. Here the presence of 1g of MCM particles in KB+1gAP blend helped to proper air/fuel mixing due to the increase in surface area to volume ratio. At 230 bar IP, the fuel impinged on cylinder walls, and this deteriorated the combustion process. At 250 bar IP the reduction in fuel droplet size and increased penetration influenced to increase NOx emissions than 230 bar IP.

The highest NOx emissions attained with KB+2gAP, KB+3gAP blends at 250 bar IP because of increased above blends atomization though there is an increase in viscosity. At this IPs, the KB+1gAP blend may be causing to deteriorate combustion rate. At the pressure mentioned above the higher viscous KB+2gAP, KB+3gAP blend induced to proper atomization and drove to increase NOx emissions.

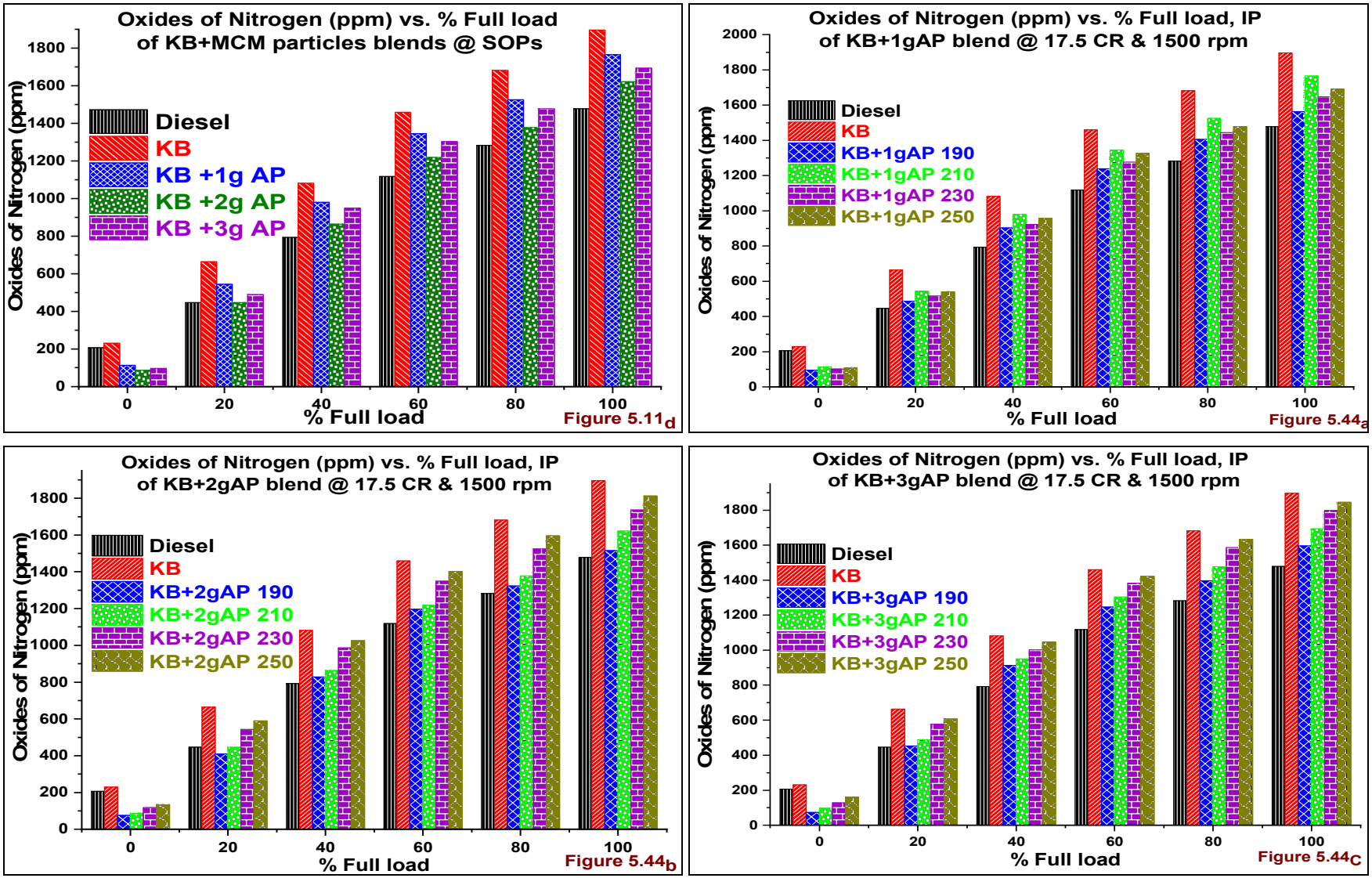

Figure 5.44$_{a, b, c}$ NO_x (ppm) vs. % Full load & IP of KB+MCM blends

5.13.4 Smoke opacity (%) vs. % Full load, IP

The lack of Oxygen, improper air/fuel mixing is because of poor fuel atomization are the majorly influencing factors for the increase in smoke emissions. The MCM particles contained KB fuel, i.e. KB+1gAP and KB+3gAP blends attained lower Smoke emissions. The lower Smoke emissions with KB+1gAP blend are because of attainment of higher ICP peak and available time for fuel combustion. The decrease in smoke emissions with KB+3gAP blend because of the availability of fuel contained Oxygen though there is a higher ID period.

This Oxygen availability is because of higher fuel accumulation by cause of higher ID period. This higher accumulated fuel lead to increase methanol contained MCM particles in the combustion chamber. The Smoke emissions are higher at 190 bar IP for all blends because of increased droplet size by cause of improper atomization. This increased droplet size led to absorbing more heat for evaporation and deteriorated the combustion rate.

In the portrayed **Figure 5.45$_a$** the Smoke emissions are lower at 210 bar IP. At this IP the required fuel gets accumulated in the sufficient ID period. This accumulated fuel also mixed correctly because of the increase in surface area to volume due to the MCM particles blend. At higher IPs 230, 250 bar the fuel got over mixed and accumulated less quantity of fuel in the ID period through smaller in droplet size.

The KB+2gAP, KB+3gAP blends are having a higher viscosity than KB, KB+1gAP blend because of the increase in fuel viscosity, density. The smoke emissions are lower at 250 bar IP with the above fuels. The proper dissolution of fuel at 250 bar IP in the combustion chamber led to uniform flame spread.

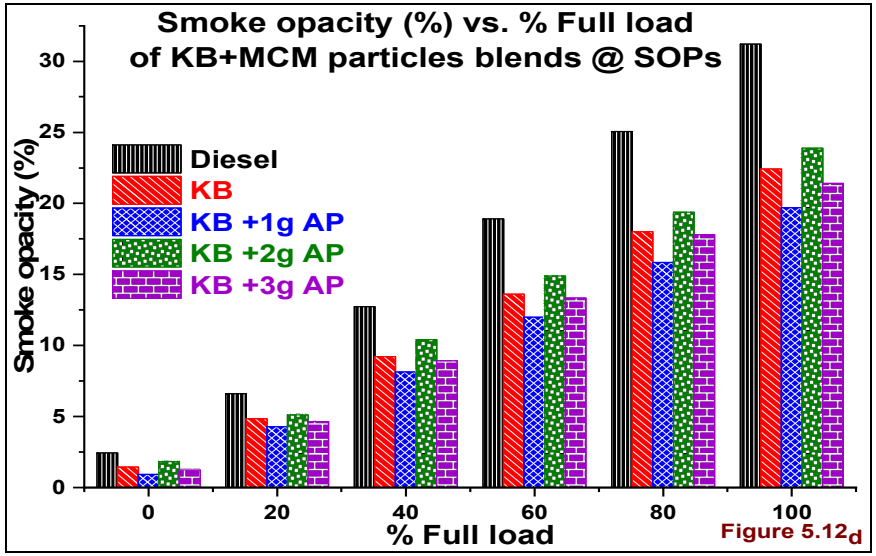

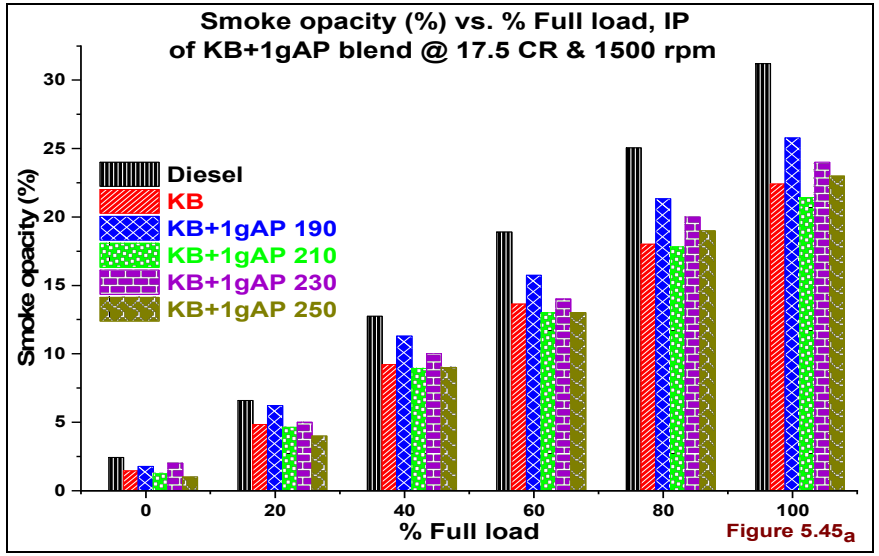

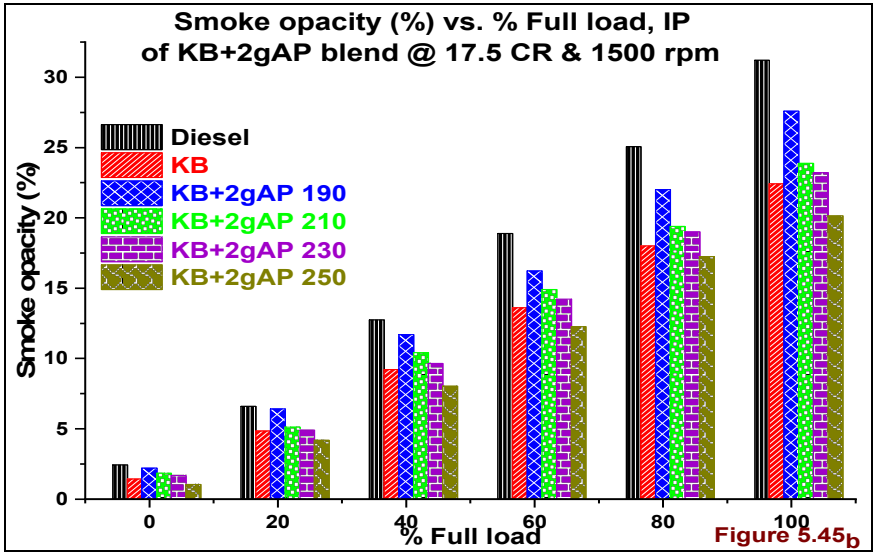

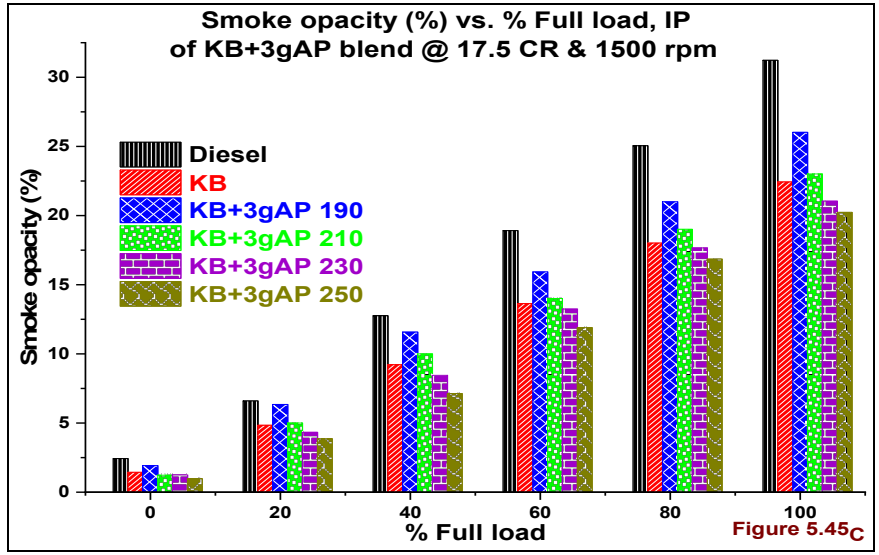

Figure 5.45a, b, c Smoke opacity (%) vs. % Full load & IP of KB+MCM blends

CHAPTER 6

Conclusions

6.1 General

In this experimental study, the test runs carried out on an unmodified DI CI engine using MCM particles blended Coconut & Karanja biodiesel fuels also Lauric acid blended Karanja biodiesel as fuel. The observations logged from the test engine by applying all the fuels mentioned above. Based on the logged data the results calculated and presented in the form of graphs in Chapter 5 as Results and discussions. The conclusions presented in this chapter based on the discussions made in the results and discussions chapter.

6.2 The effect of MCM particles on engine characteristics @ 100% load, SOPs

The methanol mixed wet grounded MCM particles emulsified in the neat Coconut biodiesel in 1 g, 2 g, and 3 g. These blends physicochemical properties are presented in Table 3.4. The percentage increases of CB+3gAP, KB+3gAP blends Density in comparison with Diesel fuel was 4.81, 5.88 respectively.

1. The increasing MCM particles quantity in CB, KB fuels caused to increase viscosity and density of blends.
2. The inclusion of MCM particles in CB, KB fuels has helped to increase surface area to volume ratio and owing to their multilevel micro-explosion.
3. The above reason helped to increase ICP, CHR and NHRR peaks with CB+3gAP, KB+3gAP blends.
4. The ICP peaks of CB+3gAP, KB+3gAP blends at full load operation has presented them in Figure 5.2_b, 5.2_d respectively.
5. The CB+3gAP, KB+3gAP blends ICP peaks are 72.99, 69.74 bar respectively.
6. The % increase of ICP peaks of CB+3gAP, KB+3gAP blends with Diesel are 14.25, 9.19 % respectively.
7. The CHR peaks of CB+3gAP, KB+3gAP blends at full load operation has presented them in Figure 5.3_b, 5.3_d respectively.
8. The CB+3gAP, KB+3gAP blends CHR peaks are 1.26, 1.25 kJ respectively.
9. The % increase of CHR peaks of CB+3gAP, KB+3gAP blends with Diesel are 36.96, 35.87 % respectively.

10. The smaller CHR difference between fuels described above blends because of their higher and nearly same Viscosity, density.
11. The above blends higher viscosity, density is caused to increase fuel rich zones in the combustion chamber and increased CO, HC, and Smoke emissions.
12. The lower Calorific value and higher densities of MCM particles mixed CB, and KB blends attributed to less NHRR peaks than Diesel fuel though there is higher ICP, CHR peaks.
13. The NHRR peaks of CB+3gAP, KB+3gAP blends are 43.64, 48.31 J/θ respectively
14. The % NHRR decrease of CB+3gAP blend 6.43% and % increase of KB+3gAP blend 3.58% than Diesel fuel at engine full load operation.
15. The percentage BTE decrease of CB+3gAP blend 11.70% and KB+3gAP blend 11.86% than Diesel fuel at engine full load operation.
16. The reduction in BTE with KB+3gAP blend because of less Calorific value, higher viscosity, density also the occurrence of ICP, CHR and NHRR peaks away from TDC than neat biodiesel fuels.
17. The higher BTE with Diesel fuel than other fuels because of its high Calorific value, lower density, and viscosity.
18. The lack of Oxygen in Diesel fuel caused to increase the CO, HC, & Smoke emissions than all other fuel samples.
19. The absorption heat by MCM particles for evaporation before the explosion has provoked to NOx emissions reduction.

6.3 The effect of IP on engine characteristics with CB+MCM, KB+MCM blends @ 100% load, 17.5 CR, & 1500 rpm

1. The achieved highest ICP peaks with IP variation on CB+1gAP, CB+2gAP, and CB+3gAP are 69.64 bar (@ 250 bar IP), 72.84 bar (@ 230 bar IP) and 72.99 bar (@ 210 bar IP) respectively.
2. The highest ICP peak at 210 bar IP with CB+3gAP blend because of less fuel jet penetration with required cone angle than at 250bar IP.
3. The lower ICP at 250 bar IP with CB+3gAP blend is due to the increasing penetration length and induced to impinge on piston head or cylinder walls.

4. The achieved highest ICP peaks with IP variation on KB+1gAP, KB+2gAP, and KB+3gAP are 69.59 bar (@ 210 bar IP), 70.16 bar (@ 230 bar IP) and 70.65 bar (@ 230 bar IP) respectively.
5. The highest ICP peak at 230 bar IP with KB+3gAP blend because of less fuel jet penetration with required cone angle than at 250bar IP.
6. The 3.28 % ICP increase of CB+3gAP blend than KB+3gAP blend is due to its 30.18 %, 1.14 % lower viscosity, density and available fuel borne Oxygen though it has 1.12% less calorific value.
7. The highest BTE values of CB+1gAP, CB+2gAP, and CB+3gAP blends are observed 28.02 % (@ 250 bar IP), 25.93 % (@ 230 bar IP), 26.14 % (@ 250 bar IP) respectively.
8. In the above presented BTE results the 28.02% has achieved at 250 bar IP with CB+1gAP blend because of its lower viscosity, density, and higher calorific value than other blends.
9. The highest BTE values of KB+1gAP, KB+2gAP, and KB+3gAP blends are observed 26.32 % (@ 210 bar IP), 25.66 % (@ 230 bar IP), 25.83 % (@ 250 bar IP) respectively.
10. The 26.32 % BTE achieved with of KB+1gAP at 210 bar IP because of its lower viscosity, density, and higher calorific value than other KB+MCM blends.
11. The 6.46 % BTE decrease of KB+1gAP blend than CB+1gAP blend because of its higher viscosity, density, lower Cetane number, Oxygen composition also lower ICP peak.
12. The highest NOx emissions of CB+1gAP, CB+2gAP, and CB+3gAP blends are observed 1708 ppm (@ 250 bar IP), 1685 ppm (@ 230 bar IP), 1643 ppm (@ 210 bar IP) respectively.
13. The highest NOx emissions are occurred at 250 bar IP with CB+1gAP blend due to improved atomization, availability of Oxygen, lower density & viscosity than other two blends.
14. The highest NOx emissions of KB+1gAP, KB+2gAP, and KB+3gAP blends has observed 1766 ppm (@ 210 bar IP), 1812 ppm (@ 250 bar IP), 1845 ppm (@ 250 bar IP) respectively.
15. The highest NOx emissions are observed at 250 IP with KB+3gAP blend because of slightly higher Calorific value, lower Cetane number and higher viscosity led to accumulating more fuel in the ID.

16. In portrayed Figure 5.35$_c$the accumulated fuel rapidly combust at 250 bar IP with proper atomization and caused to higher NOx emissions.

6.4 The effect of Lauric acid on engine characteristics @ 100% load & SOPs

1. The ICP peaks of KB+10gLA, KB+20gLA, and KB+30gLA blends at SOPs are 60.12, 49.74 and 47.76 bar respectively.
2. The 33.73% ICP reduction has observed with KB+30gLA blend because of its higher heat capacity, lower Calorific value and higher boiling point.
3. The highest ICP peak with increase IP has achieved with KB+10gLA blend which is 64.23bar at 230bar IP
4. The higher ICP peak has attained with KB+10gLA blend at 230 bar IP more or less same with Diesel.
5. The KB+10gLA blend has accomplished 23.3% BTE which is higher than the other two blends at SOPs.
6. The BTE value with IP variation of KB+10gLA, KB+20gLA, and KB+30gLA blends has achieved at 230 bar IP.
7. At SOPs the NOx emissions of KB+10gLA, KB+20gLA, and KB+30gLA are 1382, 1325, 1294 respectively.
8. The attained NOx emissions with KB+LA blends are lower than Diesel fuel.
9. At engine SOPs the highest NOx emission reduction has achieved with KB+30gLA blend which is 14.2 %.
10. The highest NOx emissions of KB+LA blends has observed at 230bar IP because of improvement in fuel atomization.

6.5 Overall conclusions

1. The increase in ICP peaks of MCM particles contained blends because of improvement in air/fuel mixing due to increased surface area/volume ratio.
2. The improved air/fuel mixing and multilevel explosions of MCM particles are owed to increase BTE than neat CB, KB fuels.
3. Above reasons are greatly influenced to increase BTE of CB+MCM blends than KB+MCM blends due to their lower viscosity, density, and higher Cetane number.
4. The highest achieved BTE with CB+1gAP, KB+1gAP and KB+10gLA are 28.02, 26.32 and 23.03% respectively than neat biodiesels at 250bar injection pressure.

5. The lowest NOx emissions have achieved with KB+30gLA blend than CB+3gAP, KB+3gAP blends due to maximum heat absorption of Lauric acid.
6. The present investigation revealed that the lower level (1g) addition of MCM particles improved the engine performance with a slight penalty in NOx emissions. The higher level addition (3g) of MCM particles has reduced NOx emissions with a slight compromise in Performance.

6.6 The scope of future work

The following suggestions are made as future work to run engine using MCM particles.

1. The optimized particle size needs to be identified for better engine characteristics.
2. The engine characteristics need to be analyzed by adding different blends of MCM particles in Diesel fuel.
3. The testing is required to check the effect of different engine modifications like compressions ratio, injection timing, SCR and DPF for CO, HC and Smoke emissions reduction.
4. All the emission parameters need to be analyzed interms of specific quantities.
5. The engine characteristics optimization needs to be done on an engine to identify better Lauric acid blend quantity.

6.7 List of publications

Journal publications:

1. **Katam Ganesh Babu**, A.Veeresh Babu, K.Madhu Murthy, Ganesh S. Warkhade, **Review on algae for biodiesel fuel production, its characteristics comparison with other and their impact on performance, combustion and emissions of diesel engine**, **World journal of Engineering, DOI: 10.1108/WJE-06-2016-0012**

2. **Katam Ganesh Babu**, A.Veeresh Babu, Ganesh S. Warkhade, **Experimental investigations of Direct Injection Compression Ignition (DI CI) engine by using Coconut, and Karanja biodiesel fuels with emulsions of Microalgae based Antioxidant, International Journal of Ambient Energy, DOI: 10.1080/01430750.2018.1432505.**

3. **Katam Ganesh Babu**, A. Veeresh Babu, K Madhu Murthy, Ganesh S. Warkhade, "The Performance, emissions investigations of Compression Ignition (CI) engine using Algal biomass as an antioxidant additive in Coconut, Karanja methyl esters", **Proceedings of the National Academy of Sciences, India Section A: Physical Sciences, DOI: 10.1007/s40010-019-00623-6**.

4. **Katam Ganesh Babu**, A.Veeresh Babu, K.Madhu Murthy, **A review on Comparison of some Edible, Inedible and Waste oil sources with Algae for biodiesel production**, **Iranica Journal of Energy and Environment,** DOI: **10.5829/idosi.ijee.2016.07.04.01 .**

5. **Katam Ganesh Babu**, A.Veeresh Babu, K. Madhu Murthy, and M.Kiran Kumar "**Mixed Culture Microalgae-Based Coconut Biodiesel as Fuel to Improve DI CI Engine Performance, Emission Characteristics**" **Applied Mechanics and Materials, 10.4028/www.scientific.net/AMM.877.347.**

6. **Katam Ganesh Babu**, A. Veeresh Babu A., K. Madhu Murthy, Investigations of DI CI Engine using Algal particles contained Coconut Biodiesel, **International Journal of Energy Technology** (Accepted on 31st May 2019).

Conference Publications:

1. **Katam Ganesh Babu**, A.Veeresh Babu, Baisa Raghuveer, "**Performance investigation of the IDI diesel engine using Sunflower Oil Methyl Ester**" **Proceedings of International Conference on Energy and Environment** (ICEE2014), **Hyderabad (INDIA)** , 2014.

2. A. Veeresh Babu, M. Vijay Kumar, P. Ravi Kumar and **Katam Ganesh Babu** "Investigation on the Performance and Emission Characteristics of Biodiesel (Animal oil) -Ethanol Blends in a Single Cylinder Diesel Engine, **Proceedings of the Intl. Conf. on Advances in Applied science and Environmental Technology**, (115-119), 2015.

6.8 References:

[1] Zhang W, Huang B, Luo D. Effects of land use and transportation on carbon sources and carbon sinks: A case study in Shenzhen, China. Landsc Urban Plan 2014;122:175–85. doi:10.1016/j.landurbplan.2013.09.014.

[2] Luthra S, Kumar S, Garg D, Haleem A. Barriers to renewable/sustainable energy technologies adoption: Indian perspective. Renew Sustain Energy Rev 2015;41:762–76. doi:10.1016/j.rser.2014.08.077.

[3] Savaliya ML. Recent advancement in production of liquid biofuels from renewable resources : a review. 2015. doi:10.1007/s11164-013-1231-z.

[4] Demirbas A. Progress and recent trends in biodiesel fuels. Energy Convers Manag 2009;50:14–34. doi:10.1016/j.enconman.2008.09.001.

[5] John B. Heywood. Internal Combustion Engine Fundamentals. 1st ed. New York: McGraw-Hill Education; 1988.

[6] Arcoumanis C. Internal Combustion Engines. Acad Press 1988:401.

[7] Ibrahim Aslan Res¸itog lu, Kemal Altinis¸ik Keskin A. The pollutant emissions from diesel-engine vehicles and exhaust aftertreatment systems. Clean Technol Environ Policy 2015;17:15–27. doi:10.1007/s10098-014-0793-9.

[8] Saxena V, Kumar N, Kumar V. A comprehensive review on combustion and stability aspects of metal nanoparticles and its additive e ff ect on diesel and biodiesel fuelled C . I . engine. Renew Sustain Energy Rev 2017;70:563–88. doi:10.1016/j.rser.2016.11.067.

[9] Leading biodiesel producers worldwide in 2017, by country (in billion liters) n.d.

[10] Sharma YC, Singh B. Development of biodiesel: Current scenario. Renew Sustain Energy Rev 2009;13:1646–51. doi:10.1016/j.rser.2008.08.009.

[11] Atabani AE, Silitonga AS, Anjum I, Mahlia TMII, Masjuki HH, Mekhilef S, et al. A comprehensive review on biodiesel as an alternative energy resource and its characteristics. Renew Sustain Energy Rev 2012;16:2070–93. doi:10.1016/j.rser.2012.01.003.

[12] Stamenkovi OS, Veljkovi VB, Bankovi IB, Banković-Ilić IB, Stamenković OS, Veljković VB, et al. Biodiesel production from non-edible plant oils. Renew Sustain Energy Rev 2012;16:3621–47. doi:10.1016/j.rser.2012.03.002.

[13] Kannan GR, Anand R. Biodiesel as an alternative fuel for direct injection diesel engines : A review 2012;012703:1–18. doi:10.1063/1.3687942.

[14] Kumar M, Sharma MP, Kumar M, Sharma MP, Kumar M, Sharma MP, et al. Selection of potential oils for biodiesel production. Renew Sustain Energy Rev 2016;56:1129–38. doi:10.1016/j.rser.2015.12.032.

[15] Chojnacka K, Noworyta A. Evaluation of Spirulina sp . growth in photoautotrophic , heterotrophic and mixotrophic cultures 2004;34:461–5. doi:10.1016/j.enzmictec.2003.12.002.

[16] Mun R, Guieysse B. Algal – bacterial processes for the treatment of hazardous contaminants : A review 2006;40:2799–815. doi:10.1016/j.watres.2006.06.011.

[17] Mata, Teresa M., Anto nio A. Martins Caetano NS. Microalgae for biodiesel production and other applications: A review. Renew Sustain Energy Rev 2010;14:217–32. doi:10.1016/j.rser.2009.07.020.

[18] Singh UB, Ahluwalia AS. Microalgae: A promising tool for carbon sequestration. Mitig Adapt Strateg Glob Chang 2013;18:73–95. doi:10.1007/s11027-012-9393-3.

[19] Delucchi MA. A Lifecycle Emissions Model (LEM): Lifecycle Emissions from Transportation Fuels, Motor Vehicles, Transportation Modes, Electricity Use, Heating and Cooking Fuels, and Materials. 2003.

[20] Ullah K, Ahmad M, Kumar V, Lu P, Harvey A, Zafar M, et al. Algal biomass as a global source of transport fuels : Overview and development perspectives. Prog Nat Sci Mater Int 2014. doi:10.1016/j.pnsc.2014.06.008.

[21] Brennan L, Owende P. Biofuels from microalgae — A review of technologies for production , processing , and extractions of biofuels and co-products 2010;14:557–77. doi:10.1016/j.rser.2009.10.009.

[22] Rashid N, Ur Rehman MS, Sadiq M, Mahmood T, Han JI. Current status, issues and developments in microalgae derived biodiesel production. Renew Sustain Energy Rev 2014;40:760–78. doi:10.1016/j.rser.2014.07.104.

[23] Liu Z, Wang G. Effect of iron on growth and lipid accumulation in Chlorella vulgaris 2008;99:4717–22. doi:10.1016/j.biortech.2007.09.073.

[24] Demirbas A, Fatih Demirbas M, Demirbas MF, Fatih Demirbas M, Demirbas MF, Fatih Demirbas M, et al. Importance of algae oil as a source of biodiesel. Energy Convers Manag 2011;52:163–70. doi:10.1016/j.enconman.2010.06.055.

[25] Baka J. What wastelands? A critique of biofuel policy discourse in South India. Geoforum 2014;54:315–23. doi:10.1016/j.geoforum.2013.08.007.

[26] Patil V, Tran KQ, Giselrød HR. Towards sustainable production of biofuels from

microalgae. Int J Mol Sci 2008;9:1188–95. doi:10.3390/ijms9071188.

[27] Collet P, Lardon L, Hélias A, Bricout S, Lombaert-Valot I, Perrier B, et al. Biodiesel from microalgae - Life cycle assessment and recommendations for potential improvements. Renew Energy 2014;71:525–33. doi:10.1016/j.renene.2014.06.009.

[28] Chandra Y, Singh V. Microalgal biodiesel : A possible solution for India ' s energy security. Renew Sustain Energy Rev 2017;67:72–88. doi:10.1016/j.rser.2016.08.031.

[29] Sheehan J, Dunahay T, Benemann J, Roessler P. Look Back at the U.S. Department of Energy's Aquatic Species Program: Biodiesel from Algae; Close-Out Report. Golden, CO: 1998. doi:10.2172/15003040.

[30] Meher LC, Sagar DV, Naik SN. Technical aspects of biodiesel production by transesterification — a review 2006;10:248–68. doi:10.1016/j.rser.2004.09.002.

[31] Chen L, Liu T, Zhang W, Chen X, Wang J. Biodiesel production from algae oil high in free fatty acids by two-step catalytic conversion. Bioresour Technol 2012;111:208–14. doi:10.1016/j.biortech.2012.02.033.

[32] Yunus TM, Atabani AE, Anjum I, Badarudin A, Khayoon MS, Triwahyono S, et al. Recent scenario and technologies to utilize non-edible oils for biodiesel production. Renew Sustain Energy Rev 2014;37:840–51. doi:10.1016/j.rser.2014.05.064.

[33] Van Gerpen J. Biodiesel processing and production. Fuel Process Technol 2005;86:1097–107. doi:10.1016/j.fuproc.2004.11.005.

[34] Gui MMM, Lee KTTÃ, Bhatia S. Feasibility of edible oil vs. non-edible oil vs. waste edible oil as biodiesel feedstock. Energy 2008;33:1646–53. doi:10.1016/j.energy.2008.06.002.

[35] Verma P, Sharma MP. Review of process parameters for biodiesel production from different feedstocks. Renew Sustain Energy Rev 2016;62:1063–71. doi:10.1016/j.rser.2016.04.054.

[36] Karmakar A, Karmakar S, Mukherjee S. Properties of various plants and animals feedstocks for biodiesel production. Bioresour Technol 2010;101:7201–10. doi:10.1016/j.biortech.2010.04.079.

[37] Soydemir G, Keris-Sen UD, Sen U, Gurol MD, Diler U, Sen KU, et al. Biodiesel production potential of mixed microalgal culture grown in domestic wastewater. Bioprocess Biosyst Eng 2016;39:45–51. doi:10.1007/s00449-015-1487-3.

[38] Scott SA, Davey MP, Dennis JS, Horst I, Howe CJ, Lea-Smith DJ, et al. Biodiesel from algae: challenges and prospects. Curr Opin Biotechnol 2010;21:277–86.

doi:10.1016/j.copbio.2010.03.005.

[39] Hidalgo P, Toro C, Ciudad G, Navia R. Advances in direct transesterification of microalgal biomass for biodiesel production 2013. doi:10.1007/s11157-013-9308-0.

[40] Rosenberg JN, Oyler GA, Wilkinson L, Betenbaugh MJ. A green light for engineered algae : redirecting metabolism to fuel a biotechnology revolution 2008:430–6. doi:10.1016/j.copbio.2008.07.008.

[41] Tobergte DR, Curtis S. Encyclopedia of Food Sciences and Nutrition. J Chem Inf Model 2013;53:1689–99. doi:10.1017/CBO9781107415324.004.

[42] Nielsen S. Food Analysis Laboratory Manual. 2003. doi:10.1007/978-1-4757-5250-2.

[43] Zambiazi RUIC, Przybylski R, Zambiazi MW, Mendonça CB, MENDONÇA RCZRPMWZCB, Zambiazi RUIC, et al. Fatty Acid Composition of Vegetable Oils and Fats. BCeppa Curtiba 2007;25:1–10.

[44] Wong YF, Saad B, Makahleh A. Capillary electrophoresis with capacitively coupled contactless conductivity detection for the determination of cis/trans isomers of octadec-9-enoic acid and other long chain fatty acids. J Chromatogr A 2013;1290:82–90. doi:10.1016/j.chroma.2013.03.014.

[45] Pinzi S, Gandía LM, Arzamendi G, Ruiz JJ, Dorado MP. Influence of vegetable oils fatty acid composition on reaction temperature and glycerides conversion to biodiesel during transesterification. Bioresour Technol 2011;102:1044–50. doi:10.1016/j.biortech.2010.08.029.

[46] Moser BR, Bryan R. Moser, Moser BR, Bryan R. Moser, Moser BR, Bryan R. Moser, et al. Biodiesel production, properties, and feedstocks. Vitr Cell Dev Biol - Plant 2009;45:229–66. doi:10.1007/s11627-009-9204-z.

[47] Siddeeg A, Xia W. Oxidative stability, chemical composition and organoleptic properties of seinat (Cucumis melo var. tibish) seed oil blends with peanut oil from China. J Food Sci Technol 2015;52:8172–9. doi:10.1007/s13197-015-1889-x.

[48] Puhan S, Jegan R, Balasubbramanian K, Nagarajan G. Effect of injection pressure on performance, emission and combustion characteristics of high linolenic linseed oil methyl ester in a DI diesel engine. Renew Energy 2009;34:1227–33. doi:10.1016/j.renene.2008.10.001.

[49] Arbab MI, Masjuki HH, Varman M, Kalam MA, Sajjad H, Imtenan S. Performance and emission characteristics of a diesel engine fueled by an optimum biodiesel-

biodiesel blend. Rsc Adv 2014;4:37122–9. doi:10.1039/c4ra06177b.

[50] Chuah LF, Yusup S, Aziz ARA, Klemeš JJ, Bokhari A, Abdullah MZ, et al. Influence of fatty acids content in non-edible oil for biodiesel properties. Clean Technol Environ Policy 2016;18:473–82. doi:10.1007/s10098-015-1022-x.

[51] Allwayzy SH, Yusaf T, Mccabe B, Pittaway P, Aravinthan V. Microalgae as Alternative Fuel for Compression Ignition (CI) Engines. Srec 2010 2010:1–5.

[52] Issariyakul T, Dalai AK. Biodiesel from vegetable oils. Renew Sustain Energy Rev 2014;31:446–71. doi:10.1016/j.rser.2013.11.001.

[53] Reddy NKÆRP. Evaluation of Methyl Esters of Mahua Oil (Madhuca Indica) as Diesel Fuel 2008:185–8. doi:10.1007/s11746-007-1179-5.

[54] Sarantopoulos I, Chatzisymeon E, Foteinis S, Tsoutsos T. Energy for Sustainable Development Optimization of biodiesel production from waste lard by a two-step transesteri fi cation process under mild conditions. Energy Sustain Dev 2014;23:110–4. doi:10.1016/j.esd.2014.08.005.

[55] Lee JY, Yoo C, Jun SY, Ahn CY, Oh HM. Comparison of several methods for effective lipid extraction from microalgae. Bioresour Technol 2010;101:S75–7. doi:10.1016/j.biortech.2009.03.058.

[56] Ahmad F, Khan AU, Yasar A. Transesterification of oil extracted from different species of algae for biodiesel production. African J Environ Sci Technol 2013;7:358–64. doi:10.5897/AJEST12.167.

[57] Islam MA, Ayoko GA, Brown R, Stuart D, Heimann K. Influence of fatty acid structure on fuel properties of algae derived biodiesel. Procedia Eng 2013;56:591–6. doi:10.1016/j.proeng.2013.03.164.

[58] Wiesman Z. Olive-oil quality biotechnologies. Desert Olive Oil Cultiv., 2009, p. 257–302. doi:10.1016/B978-0-12-374257-5.00011-7.

[59] Savaliya ML, Patel JR, Dholakiya BZ. A Concise Review on Acid , Alkali and Enzyme Catalyzed Transesterification of Fatty Acid Esters of Glycerol (FAEG) to Fatty Acid Methyl Ester (FAME) Fuel. Int J Chem Stud 2013;1:5–19.

[60] Schuchardt U, Sercheli R, Matheus R. Transesterification of Vegetable Oils : a Review. J Braz Chem Soc, 1998;9:199–210. doi:10.1590/S0103-50531998000300002.

[61] Feng, R.O., and Grose T. Modification of vegetable oils VII Alkali catalysed transesterification of peanut oil with ethanol. J Am Oil Chem Soc 1949;26:97–102.

[62] Malins K, Kampars V, Kampare R, Prilucka J, Brinks J, Murnieks R, et al. Properties of rapeseed oil fatty acid alkyl esters derived from different alcohols. Fuel 2014;137:28–35. doi:10.1016/j.fuel.2014.07.091.

[63] Abbaszaadeh A, Ghobadian B, Omidkhah MR, Najafi G. Current biodiesel production technologies: A comparative review. Energy Convers Manag 2012;63:138–48. doi:10.1016/j.enconman.2012.02.027.

[64] Bhatti HN, Hanif MA, Qasim M, Ata-ur-Rehman. Biodiesel production from waste tallow. Fuel 2008;87:2961–6. doi:10.1016/j.fuel.2008.04.016.

[65] Verma P, Sharma MP, Dwivedi G. Impact of alcohol on biodiesel production and properties. Renew Sustain Energy Rev 2016;56:319–33. doi:10.1016/j.rser.2015.11.048.

[66] Hulwan DB, Joshi S V. Performance, emission and combustion characteristic of a multicylinder DI diesel engine running on diesel-ethanol-biodiesel blends of high ethanol content. Appl Energy 2011;88:5042–55. doi:10.1016/j.apenergy.2011.07.008.

[67] Yasin MHM, Yusaf T, Mamat R, Yusop AF. Characterization of a diesel engine operating with a small proportion of methanol as a fuel additive in biodiesel blend. Appl Energy 2014;114:865–73. doi:10.1016/j.apenergy.2013.06.012.

[68] Musa IA. The effects of alcohol to oil molar ratios and the type of alcohol on biodiesel production using transesterification process. Egypt J Pet 2016;25:21–31. doi:10.1016/j.ejpe.2015.06.007.

[69] Jegannathan KR, Eng-Seng C, Ravindra P. Economic assessment of biodiesel production: Comparison of alkali and biocatalyst processes. Renew Sustain Energy Rev 2011;15:745–51. doi:10.1016/j.rser.2010.07.055.

[70] Avhad MR, Marchetti JM. Innovation in solid heterogeneous catalysis for the generation of economically viable and ecofriendly biodiesel: A review. Catal Rev - Sci Eng 2016;58:157–208. doi:10.1080/01614940.2015.1103594.

[71] Abdullah SHYS, Hanapi NHM, Azid A, Umar R, Juahir H, Khatoon H, et al. A review of biomass-derived heterogeneous catalyst for a sustainable biodiesel production. Renew Sustain Energy Rev 2017;70:1040–51. doi:10.1016/j.rser.2016.12.008.

[72] Marwaha A, Dhir A, Mahla SK, Mohapatra SK. An overview of solid base heterogeneous catalysts for biodiesel production. Catal Rev 2018;00:1–35. doi:10.1080/01614940.2018.1494782.

[73] Li Y, Qiu F, Yang D, Li X, Sun P. Preparation, characterization and application of heterogeneous solid base catalyst for biodiesel production from soybean oil. Biomass and Bioenergy 2011;35:2787–95. doi:10.1016/j.biombioe.2011.03.009.

[74] Jamil F, Al-Haj L, Al-Muhtaseb AH, Al-Hinai MA, Baawain M, Rashid U, et al. Current scenario of catalysts for biodiesel production: A critical review. Rev Chem Eng 2018;34:267–97. doi:10.1515/revce-2016-0026.

[75] Lapuerta M, Armas O, Rodríguez-fernández J. Effect of the Degree of Unsaturation of Biodiesel Fuels on NOx and Particulate Emissions 2016;1:1150–8.

[76] Mizushima N, Kawano D, Ishii H, Goto Y, Arai H. Effect of Fuel Properties of Biodiesel on Its Combustion and Emission Characteristics. SAE Pap 2016.

[77] Lin B, Huang J-H, Huang D-Y. Experimental study of the effects of vegetable oil methyl ester on DI diesel engine performance characteristics and pollutant emissions. Fuel 2009;88:1779–85. doi:10.1016/j.fuel.2009.04.006.

[78] İleri E, Koçar G, Ileri E, Koc G. Experimental Investigation of the Effect of Fuel Injection Advance on Engine Performance and Exhaust Emission Parameters Using Canola Oil Methyl Ester in a Turbocharged Direct-Injection Diesel Engine. Energy & Fuels 2009;23:5191–8. doi:10.1021/ef9004434.

[79] Jaichandar S, Annamalai K. Effects of open combustion chamber geometries on the performance of pongamia biodiesel in a di diesel engine. Fuel 2012;98:272–9. doi:10.1016/j.fuel.2012.04.004.

[80] Akar MA. Performance and emission characteristics of compression ignition engine operating with false flax biodiesel and butanol blends. Adv Mech Eng 2016;8:1–7. doi:10.1177/1687814016632677.

[81] Awolu OO, Layokun SK. Optimization of two-step transesterification production of biodiesel from neem (Azadirachta indica) oil. Int J Energy Environ Eng 2013;4:39. doi:10.1186/2251-6832-4-39.

[82] Puhan S, Vedaraman N, Ram BVB, Sankarnarayanan G, Jeychandran K. Mahua oil (Madhuca Indica seed oil) methyl ester as biodiesel-preparation and emission characterstics. Biomass and Bioenergy 2005;28:87–93. doi:10.1016/j.biombioe.2004.06.002.

[83] Ang GT, Ooi SN, Tan KT, Lee KT, Mohamed AR, Tin G, et al. Optimization and kinetic studies of sea mango (Cerbera odollam) oil for biodiesel production via supercritical reaction. Energy Convers Manag 2015;99:242–51. doi:10.1016/j.enconman.2015.04.037.

[84] Rasim Behçet. Evaluation as fuel diesel engine of methyl esters derived from waste animal fats. ENERGY Explor Exploit 2015;33:227–42.

[85] Selvam DJP, Vadivel K. Performance and Emission Analysis of DI Diesel Engine Fuelled with Methyl Esters of Beef Tallow and Diesel Blends. Procedia Eng 2012;38:342–58. doi:10.1016/j.proeng.2012.06.043.

[86] Selvam DJP, Vadivel K. An Experimental Investigation on Performance , Emission , and Combustion Characteristics of a Diesel Engine Fueled with Methyl Esters of Waste Pork Lard and Diesel Blends. Int J Green Energy 2015:37–41. doi:10.1080/15435075.2012.727366.

[87] Canakci M, Gerpen JH Van. Comparison of Engine Performance and Emissions for Petroleum Diesel fuel,Yellow grease Biodiesel, and Soybean oil Biodiesel 2003;46:937–44.

[88] Ashokkumar V, Agila E, Sivakumar P, Salam Z, Rengasamy R, Ani FN. Optimization and characterization of biodiesel production from microalgae Botryococcus grown at semi-continuous system. Energy Convers Manag 2014;88:936–46. doi:10.1016/j.enconman.2014.09.019.

[89] Nabi N, Heimann K, Islam MA, Magnusson M, Brown RJ, Ayoko GA, et al. Microalgal species selection for biodiesel production based on fuel properties derived from fatty acid profiles. Energies 2013;6:5676–702. doi:10.3390/en6115676.

[90] Kawano D. Exhaust Emission Characteristics of Commercial Vehicles Fuelled with Biodiesel. SAE Int 2016.

[91] Jaroonjitsathian S, Sae-ong P, Siangsanorh S, Akarapanjavit N, Noomwongs N, Boonchukosol K. A Study of the Effect of Biodiesel Blended Fuel on Diesel Combustion. SAE Pap 2011:757–71. doi:10.4271/2011-01-1952.

[92] Tsaousis P, Wang Y, Roskilly AP, Caldwell GS. Algae to energy : Engine performance using raw algal oil. Energy Procedia 2014;61:656–9. doi:10.1016/j.egypro.2014.11.936.

[93] Tüccar G, Aydın K. Evaluation of methyl ester of microalgae oil as fuel in a diesel engine. Fuel 2013;112:203–7. doi:10.1016/j.fuel.2013.05.016.

[94] Jitesh Singh Patel, Naveen Kumar, Amar Deep, Abhishek Sharma and DG, Patel JS, Kumar N, Deep A, Sharma A, Gupta D, et al. Evaluation of Emission Characteristics of Blend of Algae Oil Methyl Ester with Diesel in a Medium Capacity Diesel Engine. SAE Tech Pap 2014;2014-01-13:389–93. doi:10.4271/2014-01-1378.Copyright.

[95] Velappan R, Sivaprakasam S. Investigation of Single Cylinder Diesel Engine Using Bio Diesel from Marine Algae 2014;1:399–403.

[96] Velappan R, Sivaprakasam S. An Effect of Injection Timing on Di Diesel Engine Powered By Algae Methyl Ester. Int J Innov Res Creat Technol WwwIjirctOrg 2001;1:443–6.

[97] Jayaprabakar J, Karthikeyan A, K GK, Ganesh A, Prabhu L, Kumar SS, et al. Combustion Characteristics of a Ci Engine Fuelled With Macro and Micro Algae Biodiesel Blends. J Chem Pharm Sci 2015:408–12.

[98] Haik Y, Selim MYE, Abdulrehman T. Combustion of algae oil methyl ester in an indirect injection diesel engine. Energy 2011;36:1827–35. doi:10.1016/j.energy.2010.11.017.

[99] Scragg AH, Morrison J, Shales SW. The use of a fuel containing Chlorella vulgaris in a diesel engine. Enzyme Microb Technol 2003;33:884–9. doi:10.1016/j.enzmictec.2003.01.001.

[100] S. Jaichandar a,* KA b, A, Jaichandar S, Annamalai K, S. Jaichandar a,* KA b, A, et al. Combined impact of injection pressure and combustion chamber geometry on the performance of a biodiesel fueled diesel engine. Energy 2013;55:330–9. doi:10.1016/j.energy.2013.04.019.

[101] Varun, Singh P, Tiwari SK, Singh R, Kumar N. Modification in combustion chamber geometry of CI engines for suitability of biodiesel: A review. Renew Sustain Energy Rev 2017;79:1016–33. doi:10.1016/j.rser.2017.05.116.

[102] Rashedul HK, Masjuki HH, Kalam MA, Ashraful AM, Ashrafur Rahman SM, Shahir SA. The effect of additives on properties, performance and emission of biodiesel fuelled compression ignition engine. Energy Convers Manag 2014;88:348–64. doi:10.1016/j.enconman.2014.08.034.

[103] Shah PR, Ganesh A. A comparative study on influence of fuel additives with edible and non-edible vegetable oil based on fuel characterization and engine characteristics of diesel engine. Appl Therm Eng 2016;102:800–12. doi:10.1016/j.applthermaleng.2016.03.128.

[104] Safafar H, Wagenen J Van, Møller P, Jacobsen C. Carotenoids, phenolic compounds and tocopherols contribute to the antioxidative properties of some microalgae species grown on industrial wastewater. Mar Drugs 2015;13:7339–56. doi:10.3390/md13127069.

[105] World diesel engine demand - by region 2015 | Forecast n.d.

https://www.statista.com/statistics/245357/world-diesel-engine-demand-by-region/ (accessed July 26, 2018).

[106] Reitz RD, Duraisamy G. Review of high efficiency and clean reactivity controlled compression ignition (RCCI) combustion in internal combustion engines. Prog Energy Combust Sci 2015;46:12–71. doi:10.1016/j.pecs.2014.05.003.

[107] Lloyd AC, Cackette TA. Diesel Engines: Environmental Impact and Control. J Air Waste Manag Assoc 2001;51:809–47. doi:10.1080/10473289.2001.10464315.

[108] Stone R. Internal Combustion Engines. MACMILLAN PRESS LTD; n.d.

[109] Hooper PR, Goodwin MJ. Advanced modern low-emission two-stroke cycle engines 2011;225:1531–43. doi:10.1177/0954407011408649.

[110] Senatore A, Buono D, Frosina E, Vittoria M, Valentino G. Performances and Emissions of A 2-Stroke Diesel engine fueled with Biofuel blends 2015;81:918–29. doi:10.1016/j.egypro.2015.12.147.

[111] Guan C, Theotokatos G, Chen H. Analysis of Two Stroke Marine Diesel Engine Operation Including Turbocharger Cut-Out by Using a Zero-Dimensional Model 2015:5738–64. doi:10.3390/en8065738.

[112] Od S. Principles of internal combustion engines n.d.

[113] Combustion V, Taylor F. The Internal-Combustion Engine in Theory and Practice. vol. 11. n.d.

[114] Asthana S, Bansal S, Jaggi S, Kumar N. A Comparative Study of Recent Advancements in the Field of Variable Compression Ratio Engine Technology 2016. doi:10.4271/2016-01-0669.Copyright.

[115] Mohan B, Yang W, Raman V, Sivasankaralingam V, Chou SK. Optimization of biodiesel fueled engine to meet emission standards through varying nozzle opening pressure and static injection timing. Appl Energy 2014:1–8. doi:10.1016/j.apenergy.2014.02.033.

[116] Barik D, Murugan S. Experimental investigation on the behavior of a DI diesel engine fueled with raw biogas e diesel dual fuel at different injection timing. J Energy Inst 2015:1–16. doi:10.1016/j.joei.2015.03.002.

[117] Ganapathy T, Gakkhar RP, Murugesan K. Influence of injection timing on performance, combustion and emission characteristics of Jatropha biodiesel engine. Appl Energy 2011;88:4376–86. doi:10.1016/j.apenergy.2011.05.016.

[118] Gopal KN, Karupparaj RT. Effect of pongamia biodiesel on emission and combustion

characteristics of DI compression ignition engine. AIN SHAMS Eng J 2014;6:1–9. doi:10.1016/j.asej.2014.10.001.

[119] Gonca G, Dobrucali E. engine fueled with diesel-biodiesel blends The effects of engine design and operating parameters on the performance of a diesel engine fueled with diesel-biodiesel blends 2016;025702. doi:10.1063/1.4944457.

[120] Santhosh M, Padmanaban KP. Performance Characteristics of Variable Compression Ratio Engine using COME Biodiesel 2014;985:907–12. doi:10.4028/www.scientific.net/AMR.984-985.907.

[121] Chavan SB, Kumbhar RR, Kumar A, Sharma YC. Study of Biodiesel Blends on Emission and Performance Characterization of a Variable Compression Ratio Engine. Energy Fuels 2015:8–13. doi:10.1021/acs.energyfuels.5b00742.

[122] Datta A, Mandal BK. Effect of compression ratio on the performance, combustion and emission from a diesel engine using palm biodiesel 2016;13:050005. doi:10.1063/1.4958396.

[123] Jindal S. International Journal of Sustainable Experimental investigation of the effect of compression ratio and injection pressure in a direct injection diesel engine running on Karanj methyl 2011;6451:37–41. doi:10.1080/14786451.2011.598936.

[124] Pandian M, Sivapirakasam SP, Udayakumar M. Investigation on the effect of injection system parameters on performance and emission characteristics of a twin cylinder compression ignition direct injection engine fuelled with pongamia biodiesel – diesel blend using response surface methodology. Appl Energy 2011;88:2663–76. doi:10.1016/j.apenergy.2011.01.069.

[125] Channapattana S V., Pawar AA, Kamble PG. Effect of Injection Pressure on the Performance and Emission Characteristics of VCR engine using Honne Biodiesel as a Fuel. Mater Today Proc 2015;2:1316–25. doi:10.1016/j.matpr.2015.07.049.

[126] Otera J. Transesterification. Chem Rev 1993. doi:10.1021/cr00020a004.

[127] Knothe G, Razon LF. Biodiesel fuels. Prog Energy Combust Sci 2017;58:36–59. doi:10.1016/j.pecs.2016.08.001.

[128] Luz GVS, Sousa BASM, Guedes A V., Barreto CC, Brasil LM. Biocides used as additives to biodiesels and their risks to the environment and public health: A review. Molecules 2018;23. doi:10.3390/molecules23102698.

[129] Wyatt VT, Hess MA, Dunn RO, Foglia TA, Haas MJ, Marmer WN. Fuel Properties and Nitrogen Oxide Emission Levels of Biodiesel Produced from Animal Fats

2005;82.

[130] Milina R, Mustafa Z. Gas chromatographic investigations of compositional profiles of biodiesel from different origin. Pet Coal 2013;55:12–9.

[131] Thangaraja J, Rajkumar S. Effect of Saturation and Unsaturation of Fatty Methyl Esters on Biodiesel NOx Emission Characteristics. Appl Mech Mater 2015;787:766–70. doi:10.4028/www.scientific.net/AMM.787.766.

[132] Pinzi S, Rounce P, Herreros JM, Tsolakis A, Dorado MP, Pilar Dorado M. The effect of biodiesel fatty acid composition on combustion and diesel engine exhaust emissions. Fuel 2013;104:170–82. doi:10.1016/j.fuel.2012.08.056.

[133] Gopinath A, Puhan Sukumar NG. Effect of unsaturated fatty acid esters of biodiesel fuels on combustion, performance and emission characteristics of a DI diesel engine. Int J Energy Environ 2010;1:411–30. doi:10.1016/S0031-9384(10)00122-8.

[134] Kumar A, Murugan S. Review on production , characterisation and utilisation of solid fuels in diesel engines. Renew Sustain Energy Rev 2015;51:249–62. doi:10.1016/j.rser.2015.06.018.

[135] Urban CM, Mecredy HE, Ryan TW, Ingalls MN. Coal-Water Slurry Operation in an EMD Diesel Engine. J Eng Gas Turbines Power 1988;110:437–43. doi:10.1115/1.3240140.

[136] Ryan TW. Experiments With Coal Fuels in a High-Temperature Diesel Engine. J Eng Gas Turbines Power 1988;110/445.

[137] Yuchi W, Li B, Li W, Chen H. Effects of coal characteristics on the properties of coal water slurry. Coal Prep 2005;25:239–49. doi:10.1080/07349340500444489.

[138] Zhangqiang, Liukeming, Tiandafeng. Research on diesel-water coal slurry blends combustion on diesel engine of generating unit. Asia-Pacific Power Energy Eng Conf APPEEC 2009:2–5. doi:10.1109/APPEEC.2009.4918681.

[139] Patton R, Steele P, Yu F. Coal vs. charcoal-fueled diesel engines: A review. Energy Sources, Part A Recover Util Environ Eff 2010;32:315–22. doi:10.1080/15567030802612028.

[140] Soloiu V, Lewis J, Yoshihara Y, Nishiwaki K. Combustion characteristics of a charcoal slurry in a direct injection diesel engine and the impact on the injection system performance. Energy 2011;36:4353–71. doi:10.1016/j.energy.2011.04.006.

[141] Qiang Z, Lan-zhu R YT. Effect of fuel supply advance angle on combustion and emission of diesel engine with diesel coal water slurry blend fuel. Renew Sustain

Energy Rev 2015;51:249–262. doi:http://dx.doi.org/10.1016/j.rser.2015.06.018.

[142] Wamankar AK, Murugan S. Experimental investigation of carbon black-water-diesel emulsion in a stationary di diesel engine. Fuel Process Technol 2014;125:258–66. doi:10.1016/j.fuproc.2014.04.009.

[143] Wamankar AK, Murugan S. Combustion, performance and emission of a diesel engine fuelled with diesel doped with carbon black. Energy 2015;86:467–75. doi:10.1016/j.energy.2015.04.012.

[144] Wamankar AK, Murugan S. DI diesel engine operated with carbon-black-water-diesel slurry at different injection timing and nozzle opening pressure. J Energy Inst 2016;89:731–44. doi:10.1016/j.joei.2015.04.003.

[145] Piriou B, Vaitilingom G, Veyssière B, Cuq B, Rouau X. Potential direct use of solid biomass in internal combustion engines. Prog Energy Combust Sci 2013;39:169–88. doi:10.1016/j.pecs.2012.08.001.

[146] Purushothaman K, Nagarajan G. Effect of injection pressure on heat release rate and emissions in CI engine using orange skin powder diesel solution. Energy Convers Manag 2009;50:962–9. doi:10.1016/j.enconman.2008.12.030.

[147] Rohith M, Vinay P. The Effect of Orange Peel Powder Extracts in Diesel Solution on Exhaust Gas Emissions in Compression Ignition engine. Int J Mech Prod Eng 2013;1:16–9.

[148] Vigneshwaran P V., Suresh M. Bio-mass based slurry fuel. Proc 2015 IEEE 9th Int Conf Intell Syst Control ISCO 2015 2015:2–4. doi:10.1109/ISCO.2015.7282363.

[149] Vinukumar K, Azhagurajan A, Vettivel SC, Vedaraman N, Lenin AH. Biodiesel with nano additives from coconut shell for decreasing emissions in diesel engines. Fuel 2018;222:180–4. doi:10.1016/j.fuel.2018.02.129.

[150] Xu Y, Hellier P, Purton S, Baganz F, Ladommatos N. Algal biomass and diesel emulsions : An alternative approach for utilizing the energy content of microalgal biomass in diesel engines. Appl Energy 2016;172:80–95. doi:10.1016/j.apenergy.2016.03.019.

[151] Lewis RS, Deen WM. Kinetics of the Reaction of Nitric Oxide with Oxygen in Aqueous Solutions. Chem Res Toxicol 1994;7:568–74. doi:10.1021/tx00040a013.

[152] Thangaraja J, Kannan C. Effect of exhaust gas recirculation on advanced diesel combustion and alternate fuels - A review High speed Direct Injection Number of Transfer Units Start of Injection. Appl Energy 2016;180:169–84.

doi:10.1016/j.apenergy.2016.07.096.

[153] A.Veeresh Babu, Rajnish K. Calay and PVR. Conversion Efficiencies of Urea –SCR System for Mahua Methyl Ester Fuelled DI Diesel Engine. Iran J Energy Environ 2014;5:42 – 50.

[154] Praveena V, Martin MLJ. A review on various after treatment techniques to reduce NOx emissions in a CI engine. J Energy Inst 2017:1–17. doi:10.1016/j.joei.2017.05.010.

[155] Rashedul HK, Masjuki HH, Kalam MA, Teoh YH, How HG, Fattah IMR. Effect of antioxidant on the oxidation stability and combustion – performance – emission characteristics of a diesel engine fueled with diesel – biodiesel blend 2015;106:849–58. doi:10.1016/j.enconman.2015.10.024.

[156] Jakeria MR, Fazal MA, Haseeb ASMA. Influence of different factors on the stability of biodiesel: A review. Renew Sustain Energy Rev 2014;30:154–63. doi:10.1016/j.rser.2013.09.024.

[157] Sathiyamoorthi R, Sankaranarayanan G. Effect of antioxidant additives on the performance and emission characteristics of a DICI engine using neat lemongrass oil-diesel blend. Fuel 2016;174:89–96. doi:10.1016/j.fuel.2016.01.076.

[158] Knothe G. Some aspects of biodiesel oxidative stability. Fuel Process Technol 2007;88:669–77. doi:10.1016/j.fuproc.2007.01.005.

[159] Sharma YC, Singh B, Upadhyay SN. Advancements in development and characterization of biodiesel: A review. Fuel 2008;87:2355–73. doi:10.1016/j.fuel.2008.01.014.

[160] Varatharajan K, Cheralathan M, Technology FP, Varatharajan K, Cheralathan M. Effect of aromatic amine antioxidants on NOx emissions from a soybean biodiesel powered di diesel engine. Fuel Process Technol 2013;106:526–32. doi:10.1016/j.fuproc.2012.09.023.

[161] Velmurugan K, Sathiyagnanam AP. Impact of antioxidants on NOx emissions from a mango seed biodiesel powered di diesel engine. Alexandria Eng J 2016;55:715–22. doi:10.1016/j.aej.2015.10.004.

[162] Fernando S, Hall C, Jha S. NOx Reduction from Biodiesel Fuels. Energy & Fuels 2006;20:376–82. doi:10.1021/ef050202m.

[163] Ashraful AM, Masjuki HH, Kalam MA, Rizwanul Fattah IM, Imtenan S, Shahir SA, et al. Production and comparison of fuel properties, engine performance, and

emission characteristics of biodiesel from various non-edible vegetable oils: A review. Energy Convers Manag 2014;80:202–28. doi:10.1016/j.enconman.2014.01.037.

[164] Kumar R, Tiwari P, Garg S. Alkali transesterification of linseed oil for biodiesel production. Fuel 2013;104:553–60. doi:10.1016/j.fuel.2012.05.002.

[165] https://pubchem.ncbi.nlm.nih.gov/compound/lauric_acid#section=Top. Physicochemical properties of Lauric acid. New J Chem 2004;28:104–14. doi:10.1039/B307208H.

[166] Molar mass of C12H24O2 - Chemistry Online Education n.d. https://www.webqc.org/mmcalc.php (accessed March 28, 2018).

[167] Shancita I, Masjuki HH, Kalam MA, Reham SS, Ruhul AM, Monirul IM. Advances Evaluation of the characteristics of non-oxidative biodiesels : a FAME composition , thermogravimetric and IR analysis. RSC Adv 2016;6:8198–210. doi:10.1039/C5RA23963J.

[168] Woo C, Kook S, Hawkes ER, Rogers PL, Marquis C. Dependency of engine combustion on blending ratio variations of lipase-catalysed coconut oil biodiesel and petroleum diesel. Fuel 2016;169:146–57. doi:10.1016/j.fuel.2015.12.024.

[169] Kumar, M., Ramesh, A., and Nagalingam, B. Complete Vegetable Oil Fueled Dual Fuel Compression Ignition Engine. SAE Tech Pap 2001. doi:10.4271/2001-28-0067.

[170] Gumus M. A comprehensive experimental investigation of combustion and heat release characteristics of a biodiesel (hazelnut kernel oil methyl ester) fueled direct injection compression ignition engine. Fuel 2010;89:2802–14. doi:10.1016/j.fuel.2010.01.035.

[171] Balamurugan T, Nalini R. Experimental investigation on performance, combustion and emission characteristics of four stroke diesel engine using diesel blended with alcohol as fuel. Energy 2014;78:356–63. doi:10.1016/j.energy.2014.10.020.

[172] Dhinesh B, Isaac JoshuaRamesh Lalvani J, Parthasarathy M, Annamalai K. An assessment on performance, emission and combustion characteristics of single cylinder diesel engine powered by Cymbopogon flexuosus biofuel. Energy Convers Manag 2016;117:466–74. doi:10.1016/j.enconman.2016.03.049.

[173] Balamurugan T, Arun A, Sathishkumar GB. Biodiesel derived from corn oil – A fuel substitute for diesel. Renew Sustain Energy Rev 2018;94:772–8. doi:10.1016/j.rser.2018.06.048.

[174] Kegl B. Influence of biodiesel on engine combustion and emission characteristics. Appl Energy 2011;88:1803–12. doi:10.1016/j.apenergy.2010.12.007.

[175] Yesilyurt MK. The effects of the fuel injection pressure on the performance and emission characteristics of a diesel engine fuelled with waste cooking oil biodiesel-diesel blends. Renew Energy 2019;132:649–66. doi:10.1016/j.renene.2018.08.024.

[176] An H, Yang WM, Maghbouli A, Li J, Chou SK, Chua KJ. Performance, combustion and emission characteristics of biodiesel derived from waste cooking oils. Appl Energy 2013;112:493–9. doi:10.1016/j.apenergy.2012.12.044.

[177] Rao GLN, Prasad BD, Sampath S, Rajagopal K. Combustion analysis of diesel engine fueled with Jatropha oil methy Lester-diesel blends. Int J Green Energy 2007;4:645–58. doi:10.1080/15435070701665446.

[178] Suh, Hyun Kyu, Hyun Gu Roh CSL. Spray and Combustion Characteristics of Biodiesel/Diesel Blended Fuel in a Direct Injection Common-Rail Diesel Engine.pdf. J Eng Gas Turbines Power 2008;130.

[179] Higgins BS, Mueller CJ S. Measurements of fuel effects on liquidphase penetration in DI sprays. SAE Int 1999:01–0519.

[180] Genzale CL, Pickett LM KS. Liquid penetration of diesel and biodiesel sprays at late-cycle post-injection conditions. SAE Int 2010:01–0610.

[181] Ananthakumar S, Jayabal S, Thirumal P. Investigation on performance, emission and combustion characteristics of variable compression engine fuelled with diesel, waste plastics oil blends. J Brazilian Soc Mech Sci Eng 2016. doi:10.1007/s40430-016-0518-6.

[182] Muzio LJ, Quartucy GC, Energy F, Pointe CS, Hills L. Implementing NOx Control : Research to Application. Prog Energy Combust Sci 1997;23:233–66. doi:10.1016/S0360-1285(97)00002-6.

[183] Yehliu K, Boehman AL, Armas O. Emissions from different alternative diesel fuels operating with single and split fuel injection. Fuel 2010;89:423–37. doi:10.1016/j.fuel.2009.08.025.

[184] Medipally SR, Yusoff FM, Banerjee S, Shariff M. Microalgae as sustainable renewable energy feedstock for biofuel production. Biomed Res Int 2015;2015. doi:10.1155/2015/519513.

[185] Ryu K, Oh Y. Combustion Characteristics of an Agricultural Diesel Engine using Biodiesel Fuel 2004;18.

[186] Focke WW, Westhuizen I Van Der, Grobler ABL, Nshoane KT, Reddy JK, Luyt AS. The effect of synthetic antioxidants on the oxidative stability of biodiesel. Fuel 2012;94:227–33. doi:10.1016/j.fuel.2011.11.061.

[187] Lebedevas S, Vaicekauskas A, Lebedeva G. Change in Operational Characteristics of Diesel Engines Running on RME Biodiesel Fuel 2007:3010–6.

[188] Enweremadu CC, Rutto HL. Combustion, emission and engine performance characteristics of used cooking oil biodiesel - A review. Renew Sustain Energy Rev 2010;14:2863–73. doi:10.1016/j.rser.2010.07.036.

[189] Enweremadu CC, Peleowo AN, Rutto HL. Experimental Study of a Diesel Engine Fuelled With Methyl 2013;49:23–8.

[190] Yaliwal VS, Banapurmath NR, Gireesh NM, Hosmath RS, Donateo T, Tewari PG. Effect of nozzle and combustion chamber geometry on the performance of a diesel engine operated on dual fuel mode using renewable fuels. Renew Energy 2016;93:483–501. doi:10.1016/j.renene.2016.03.020.

[191] Lahane S, Subramanian KA. Effect of different percentages of biodiesel-diesel blends on injection, spray, combustion, performance, and emission characteristics of a diesel engine. Fuel 2015;139:537–45. doi:10.1016/j.fuel.2014.09.036.

[192] Sayin C, Gumus M. Impact of compression ratio and injection parameters on the performance and emissions of a di diesel engine fueled with biodiesel-blended diesel fuel. Appl Therm Eng 2011;31:3182–8. doi:10.1016/j.applthermaleng.2011.05.044.

[193] Park SH, Yoon SH, Lee CS. Effects of multiple-injection strategies on overall spray behavior, combustion, and emissions reduction characteristics of biodiesel fuel. Appl Energy 2011;88:88–98. doi:10.1016/j.apenergy.2010.07.024.

[194] Agarwal AK, Dhar A, Gupta JG, Kim W Il, Choi K, Lee CS, et al. Effect of fuel injection pressure and injection timing of Karanja biodiesel blends on fuel spray, engine performance, emissions and combustion characteristics. Energy Convers Manag 2015;91:302–14. doi:10.1016/j.enconman.2014.12.004.

[195] İçıngür Y, Altiparmak D. Effect of fuel cetane number and injection pressure on a DI Diesel engine performance and emissions. Energy Convers Manag 2003;44:389–97. doi:10.1016/S0196-8904(02)00063-8.

[196] Agarwal AK, Dhar A, Gupta JG, Kim W Il, Lee CS, Park S. Effect of fuel injection pressure and injection timing on spray characteristics and particulate size-number distribution in a biodiesel fuelled common rail direct injection diesel engine. Appl Energy 2014;130:212–21. doi:10.1016/j.apenergy.2014.05.041.

[197] Sayin C, Gumus M, Canakci M. Effect of fuel injection pressure on the injection, combustion and performance characteristics of a DI diesel engine fueled with canola oil methyl esters-diesel fuel blends. Biomass and Bioenergy 2012;46:435–46. doi:10.1016/j.biombioe.2012.07.016.

[198] Miyamoto N, Ogawa H, Nururn NM, Obata K, Arima T. Smokeless, Low NOx, High Thermal Efficiency, and Low Noise Diesel Combustion with Oxygenated Agensts as Main Fuel. Sae 1998:980506. doi:10.1098/rstb.2008.0317.

[199] Jayashankara B, Ganesan V. Effect of fuel injection timing and intake pressure on the performance of a di diesel engine - A parametric study using CFD. Energy Convers Manag 2010;51:1835–48. doi:10.1016/j.enconman.2009.11.006.

[200] Wang X, Huang Z, Kuti OA, Zhang W, Nishida K. Experimental and analytical study on biodiesel and diesel spray characteristics under ultra-high injection pressure. Int J Heat Fluid Flow 2010;31:659–66. doi:10.1016/j.ijheatfluidflow.2010.03.006.

[201] Zhang G, Qiao X, Miao X, Hong J, Zheng J. Effects of highly dispersed spray nozzle on fuel injection characteristics and emissions of heavy-duty diesel engine. Fuel 2012;102:666–73. doi:10.1016/j.fuel.2012.07.053.

[202] Zhao J, Hong W, Li X, Xie F, Jue L. Study about effects of EGR and injection parameters on the combustion and emissions of high-pressure common-rail diesel engine. ICIMA 2010 - 2010 2nd Int Conf Ind Mechatronics Autom 2010;1:290–4. doi:10.1109/ICINDMA.2010.5538161.

[203] Gumus M, Sayin C, Canakci M. The impact of fuel injection pressure on the exhaust emissions of a direct injection diesel engine fueled with biodiesel-diesel fuel blends. Fuel 2012;95:486–94. doi:10.1016/j.fuel.2011.11.020.

[204] Lakshminarayanan PA, Nayak N, Dingare S V., Dani AD. Predicting Hydrocarbon Emissions From Direct Injection Diesel Engines. J Eng Gas Turbines Power 2002;124:708. doi:10.1115/1.1456091.

[205] Mueller CJ, Boehman AL, Martin GC. An Experimental Investigation of the Origin of Increased NO_x Emissions When Fueling a Heavy-Duty Compression-Ignition Engine with Soy Biodiesel. SAE Int J Fuels Lubr 2009;2:2009-01-1792. doi:10.4271/2009-01-1792.

[206] Nanthagopal K, Ashok B, Raj RTK, Karuppa Raj RT. Influence of fuel injection pressures on Calophyllum inophyllum methyl ester fuelled direct injection diesel engine. Energy Convers Manag 2016;116:165–73. doi:10.1016/j.enconman.2016.03.002.

[207] Ogunkoya D, Roberts WL, Fang T, Thapaliya N. Investigation of the effects of renewable diesel fuels on engine performance, combustion, and emissions. Fuel 2015;140:541–54. doi:10.1016/j.fuel.2014.09.061.

[208] Of E, Pressure I, The ON, Formation S, Low OF, Rejection H, et al. Effect of Injection Pressure on the Performance and Smoke Formation of Low Heat Rejection 2013;1:108–14.

[209] Man XJ, Cheung CS, Ning Z, Wei L, Huang ZH. Influence of engine load and speed on regulated and unregulated emissions of a diesel engine fueled with diesel fuel blended with waste cooking oil biodiesel. Fuel 2016;180:41–9. doi:10.1016/j.fuel.2016.04.007.

[210] Venkanna BK, Wadawadagi SB, Reddy CV. Effect of Injection Pressure on Performance , Emission and Combustion Characteristics of Direct Injection Diesel Engine Running on Blends of Pongamia Pinnata Linn Oil (Honge oil) and Diesel Fuel. CIGR Ejournal 2009;XI:1–17. doi:10.3965/j.issn.

[211] Basha JS, Sadhik Basha J, Anand RB, Basha JS, Sadhik Basha J, Anand RB, et al. Performance, emission and combustion characteristics of a diesel engine using Carbon Nanotubes blended Jatropha Methyl Ester Emulsions. Alexandria Eng J 2014;53:259–73. doi:10.1016/j.aej.2014.04.001.

[212] Boudy F, Seers P. Impact of physical properties of biodiesel on the injection process in a common-rail direct injection system. Energy Convers Manag 2009;50:2905–12. doi:10.1016/j.enconman.2009.07.005.

[213] Shaafi T, Sairam K, Gopinath A, Kumaresan G, Velraj R. Effect of dispersion of various nanoadditives on the performance and emission characteristics of a CI engine fuelled with diesel, biodiesel and blends—A review. Renew Sustain Energy Rev 2015;49:563–73. doi:10.1016/j.rser.2015.04.086.

[214] Bari S, Yu CW, Lim TH. A comparison of combustion characteristics of waste cooking oil with diesel as fuel in a direct injection diesel engine. Proc Inst Mech Eng Part D J Automob Eng 2004;218:93–104. doi:10.1243/095440704322829209.

[215] Junior C, Dingel O. Experimental Investigation on Effect of Fuel Property on Emissions and Performance of a Light-Duty Diesel Engine. Springer International Publishing; 2018. doi:10.1007/978-3-030-00819-2.

[216] Puhan S, Nagarajan G, Vedaraman N, Ramabramhmam B V. Mahua oil (madhuca indica oil) derivatives as a renewable fuel for diesel engine systems in India: A performance and emissions comparative study. Int J Green Energy 2007;4:89–104. doi:10.1080/15325000601015627.

APPENDIX – A

Uncertainty analysis of instruments used in experimental setup:

Errors and uncertainties in the experiments can arise from instrument selection, condition, calibration, environment, observation, reading and test planning. Uncertainty analysis is needed to prove the accuracy of the experiments (Holman, J.B.1988). The percentage uncertainties of various parameters like brake power and brake thermal efficiency were calculated using the percentage uncertainties of various instruments given in Table 1. The uncertainity analysis was performed using Eq. (1).

Table1: Various used instruments and its range, accuracy and percentage uncertainties

Sl. No.	Instruments	Range	Accuracy	% uncertainties
1.	Pressure transducer (CP)	0 -350 bar	±1bar	±0.1
2.	Crank angle encoder (θ)	0 - 360°	±1°	±0.2
3.	Engine speed (N)	0 – 5000 rpm	±10 rpm	±0.7
4.	Load cell (w)	0 – 50 kg	±0.1 kg	±0.01
5.	Fuel flow transmitter (mf)	0 – 500 mmWC	±1 cc	±0.3
6.	Time measurement (t)	-	±0.2 s	±0.2
7.	Air flow transmitter (af)	0 – 250 mm WC	±1 mm	±0.2
8.	Exhaust gas temperature (EGT)	0 – 1200 °C	±10 °C	±1.7
Five Gas analyzer				
9.	Carbon Monoxide (CO)	0 – 15 % vol	±0.06 %	±0.4
10.	Carbon dioxide (CO_2)	0 – 20 % vol	±0.5 %	±0.5
11.	Oxygen (O_2)	0 – 25 % vol	±0.1 %	±0.4
12.	Unburnt Hydrocarbons (HC)	0 - 10000 ppm	±12 ppm	±0.12
13.	Oxides of Nitrogen (NO_x)	0 – 5000 ppm	±10 ppm	±0.2
14.	Smoke	0 – 100 %	±1.0 %	±1.0%

Percentage uncertainty = $\sqrt{x_1^2 + x_2^2 + ...x_n^2}$ -------- **(1)**

Percentage of uncertainty occurring in the experiments

$$= \sqrt{\begin{pmatrix}(\mathrm{CP})^2 + (\theta)^2 + (\mathrm{n})^2 + (w)^2 + (\mathrm{mf})^2 + (\mathrm{t})^2 + (\mathrm{af})^2 + (EGT)^2 + (CO)^2 + (\mathrm{CO_2})^2 \\ + (\mathrm{O_2})^2 + (HC)^2 + (NOx)^2 + (Smoke)^2\end{pmatrix}}$$

% Uncertainity in experimental measurement =

$$\sqrt{0.1^2 + 0.2^2 + 0.7^2 + 0.01^2 + 0.3^2 + 0.2^2 + 0.2^2 + 1.7^2 + 0.4^2 + 0.5^2 + 0.4^2 + 1.12^2 + 0.2^2 + 1.0^2}$$

= 2.065 %

Determined Physicochemical Properties of Diesel fuel:

Property	Test runs					Average	Standard Deviation	Standard Uncertainty	Equation used	Apparatus used	ASTM standards
	$Test_1$	$Test_2$	$Test_3$	$Test_4$	$Test_5$						
Flash point (˚C)	55	54	52	56	50	53.4	2.41	1.08	-	Pensky Martens	D93
Fire point (˚C)	61	58	57	54	57	57.4	2.51	1.12	-		
Density (kg/m3)	835	829	832	834	831	832.2	2.39	1.07	-	Hydro meter	D792
Kinematic viscosity (mm^2/sec)	3.41	2.83	2.45	2.58	2.84	2.82	0.37	0.16	$\mu=(A*t)-(B/t)$ A=0.247, B=279 t=time (sec)	Red wood viscometer -1	D445
Calorific value (kJ/kg)	43723	43714	43706	43710	43706	43711.8	7.09	3.17	$CV=m*Cp*\Delta T$	SPAM Automatic Bomb Calorimeter	D240

Average $(\bar{x}) = \left(\frac{Test_1 + Test_2 + Test_3 + Test_4 + Test_5}{5}\right)$,

Standard deviation $(\sigma) = \sqrt{\left(\frac{(Test_1 - \bar{x})^2 + (Test_2 - \bar{x})^2 + (Test_3 - \bar{x})^2 + (Test_4 - \bar{x})^2 + (Test_5 - \bar{x})^2}{5-1}\right)}$, Standard uncertainty $(u) = \left(\frac{\sigma}{\sqrt{5}}\right)$

Overall Diesel fuel testing uncertainty $= \sqrt{\left((1.08)^2 + (1.12)^2 + (1.07)^2 + (0.16)^2 + (3.17)^2\right)} = 3.693\ \%$

APPENDIX – B

Fuel	SPEED (N)	Load (kg)	EGT (°C)	Air flow mm WC	Fuel flow in CC
Diesel	1497	12.288	338.709	59.839	21
	1494	12.273	339.849	59.11	20
	1497	12.284	340.158	60.245	20
	1494	12.242	346.708	59.487	20
	1495	12.244	345.738	60.398	19
$\bar{x}$	1495.40	12.266	342.232	59.816	20.00
σ	1.5	0.022	3.699	0.532	0.71
u	0.7	0.010	1.654	0.238	0.32

Sample Performance calculations on Diesel fuel at full load operation:

Fuel consumption in burette (mf) = 20 cc

Time taken for 20cc (Tf) = 60 sec

Calorific value of Fuel (CV) = 43712 kJ/kg

Engine speed (N) = 1495 rpm

Maximum load on engine (w) = 12.27 kg

Arm length = 0.185 m

Density of fuel (ρ) = 832 kg/m^3

Torque (T) = (wt * g * Arm length) = 12.27 * 9.81 * 0.185 = **22.27N-m**

Brake power (BP) $= \left(\frac{2*\pi*N*T}{60000}\right) = \left(\frac{2*\pi*1495*22.27}{60000}\right) =$ **3.49 kW**

Fuel consumption (FC) $= \left(\frac{mf*3600*0.832}{Tf*1000}\right) =$ 0.9984 kg/hr = **$2.77*10^{-4}$ kg/sec**

Brake thermal efficiency (BTE) $= \left(\frac{BP}{FC*CV}\right) = \left(\frac{3.49}{(2.77*10^{-4})*43712}\right) =$ **28.79 %**

Brake specific fuel consumption (BSFC) = (FC/BP)=(0.9984/3.49)= **0.286 kg/kW–hr**

Brake specific Energy consumption (BSEC) = (BSFC*CV) = (0.286*43.712)

= **12.50 MJ/kg – hr**